THE UNIVERSITY
of EDINBURGH

Mechanisms of cohesin protection and removal during meiosis in *Saccharomyces cerevisiae*

Rachael Barton

Thesis submitted for the degree of Doctor of Philosophy

The University of Edinburgh

2018

Declaration

I declare that this thesis was composed by myself, and that the research presented within is my own work except where stated otherwise by reference or acknowledgement. This work has not been submitted, in whole or in part, for any other degree or professional qualification except as specified.

Rachael Barton

2018

Acknowledgements

I would like to first acknowledge the Wellcome Trust for funding my four-year PhD studentship at the Wellcome Trust Centre for Cell Biology. Without this funding I wouldn't have been able to undertake this PhD in the Marston Lab, or the rotation project in the Hardwick and Arulanandam labs, so I am truly grateful.

Firstly, thank you to Adele for making this PhD a fantastic experience. Over six years ago you welcomed me into the lab as an undergraduate with no lab experience, and it was this that really inspired me to come back as a PhD student. You have taught me an incredible amount during my PhD, both in the lab as well as in presenting and writing, so thank you for teaching me to become a scientist!

Thank you to all the members of the Marston lab, as without all of you my PhD would not have been the same. Julie, thank you so much for looking after me as a summer student and having the patience to teach me so many skills I still use today. Bonnie, Colette, Claudia, Beth, and Julie, thank you all so so much for being there throughout the past four years (and more), I always looked forward to our coffee breaks and lunchtime chats, and our after-work Friday night pub trips - you are all amazing and never failed to make me smile!! Vasso, thank you for all of your help and support, and for always being there with words of advice! Thank you to Wera and Flora for being my bench neighbours for the past couple of years, and for putting up with a running commentary about my experiments! Thank you to Stefan for supervising me throughout my rotation project, and for allowing me to contribute to your paper. Thank you also to Josh for helping me with my project through your work on Hos1, and for being a great Honour's student. Sorry to everyone else that I haven't mentioned, thank you all for helping me and being supportive over the last four years.

Dave, thank you for all of your help with microscopy, and for being there in times of need - the microscopes always sensed when I was in the room and purposefully broke!! Thank you also for trusting me to help with the outreach in COIL, hopefully we managed to inspire a few scientists of the future! Thank you to Christos for all of your help with mass spectrometry and the analysis.

Lastly, thank you to all of my friends and family, you have all been amazing. Brad, thank you so much for moving with me to Edinburgh, and for being with me over the last five years. You have been so incredible and supportive, and I couldn't have done it without you!! Mum, Dad, Granny and Garbiggie, thank you all so much for always being so supportive throughout my PhD, for always believing in me, and for being there at the other end of the phone when needed!

Lay summary

Diploid cells have two copies of every chromosome, whereas haploid cells have only one copy. Higher eukaryotes, such as humans, are made up of diploid cells. To sexually reproduce, haploid cells need to be produced from diploid cells, by a process known as meiosis, which in humans results in the production of sperm and eggs. If meiosis does not occur correctly, and the haploid cells receive the incorrect number of chromosomes, then after the egg and sperm fuse, the embryo will also have the wrong number of chromosomes. This causes human genetic disorders such as Down syndrome, infertility or miscarriage. Therefore, it is essential to ensure that each haploid cell has the correct amount of DNA following meiosis.

During meiosis, the DNA of the diploid cell is first copied, and then is divided to form daughter cells in a two-step division. It is important during the first and second meiotic divisions that the correct chromosomes are segregated. A protein complex called cohesin is essential in ensuring that this occurs. Cohesin holds the chromosomes together from DNA replication until the chromosomes are ready to be segregated, however, to allow segregation, cohesin needs to be removed. In meiosis, the most well documented mechanism of cohesin removal is by cleavage. A protein known as shugoshin protects cohesin from cleavage until the correct time in meiosis. I aimed to study how shugoshin is regulated, and which other proteins interact with shugoshin.

There is also another way of removing cohesin from the DNA, through destabilisation rather than cleavage. Only recently has cohesin destabilisation been shown to be important in meiosis. Through carrying out this research in budding yeast, the components of the destabilisation pathway were found to be important for correct chromosome segregation in meiosis. This research may help prompt new avenues of research in other organisms, such as in humans, as these proteins are conserved.

Abstract

Meiosis is a specialised form of cell division which results in the formation of haploid cells from a diploid progenitor, and thus meiosis halves the chromosome content of the parental cell. A tightly controlled sequence of chromosome segregation events is required to ensure that chromosome missegregation does not occur during meiosis. Chromosome missegregation causes aneuploidy, which in humans can result in the genetic disorder Down Syndrome, and is the leading cause of infertility and miscarriage. To avoid this, it is critical that in the first meiotic division homologous chromosomes are segregated, followed by sister chromatid segregation in meiosis II.

Cohesin is a ring-shaped protein complex that holds that sister chromatids together during meiosis, and aids homologue pairing and recombination, as well as ensuring the correct timing of chromosome segregation. In meiosis I, cohesin must be cleaved by separase on the arms of the chromosomes, to allow homologue segregation, whilst at the centromere Sgo1-PP2A protects this pool of cohesin from cleavage and holds sister chromatids together. In meiosis II, the remaining centromeric cohesin is cleaved to allow segregation of sister chromatids. Therefore, correct regulation of Sgo1 and its interaction partners in meiosis is crucial to prevent aneuploidy. In this study I characterise the role of an Sgo1 binding partner, condensin, in meiotic chromosome segregation, and show that condensin is essential for faithful chromosome segregation in both meiosis I and II. Sgo1 is post-translationally modified in meiosis, and in this study Sgo1 phosphomutants were analysed, but were found to have no discernible effects on faithful chromosome segregation. However additional Sgo1 post-translational modifications were identified, leaving the regulation of Sgo1 by post-translational modification open to future study.

Additional to the removal of cohesin by separase cleavage, there is a non-proteolytic pathway for cohesin removal. During mitotic prophase in higher eukaryotes, cohesin is destabilised from replicated sister chromatid arms through the action of Wapl. However, a subset of cohesin is protected from the destabilising effects of Wapl because acetylation of the Smc3 subunit of cohesin allows binding of sororin. Phosphorylation events prevent sororin association with chromosome arms, making cohesin susceptible to removal by Wapl. In contrast, at centromeres, shugoshin counteracts these phosphorylation events, thereby protecting centromeric cohesin from Wapl.

During meiosis, Wapl is important in cohesin destabilisation in mouse, *C. elegans* and *A. thaliana*, and recent evidence suggests that this pathway is also active in budding yeast. However, it is unclear if the acetyltransferase, Eco1, and cohesin acetylation are important in the generation of cohesive cohesin in meiosis to allow faithful chromosome segregation. Additionally it is unclear if the destabilising activity of Wapl only contributes to cohesin removal on chromosome arms, or whether mechanisms are required to protect cohesin from destabilisation activity near centromeres. I aim to address these questions using budding yeast. Previous work showed that deletion of Wapl (Rad61) in meiosis prevents destabilisation of cohesin from the DNA prior to metaphase I. Consistently, I found Rad61 is regulated in meiosis, and has a role in promoting faithful chromosome segregation in tetranucleates. Additionally, Eco1 acetyltransferase is expressed during S phase of meiosis, and this expression coincides with Smc3 acetylation. In meiosis, disruption of Eco1 function and Smc3 acetylation has a detrimental impact on DNA segregation and cell viability. Further findings show that Sgo1 interacts with cohesin in budding yeast meiosis, and Sgo1 localisation to the chromatin is impacted in Eco1 mutants, but the precise interplay between Sgo1 and acetylated cohesin remains to be fully deduced.

Abbreviations

Acronym	Definition
A. thaliana	*Arabidopsis thaliana*
ABC	Ammonium bicarbonate
ACN	Acetonitrile
APC/C	Anaphase promoting complex/Cyclosome
APS	Ammonium persulphate
ATM	Ataxia Telangiectasia mutated protein
ATR	Ataxia Telangiectasia and Rad3 related protein
ATP	Adenosine triphosphate
ATPase	Adenosine triphosphatase
BSA	Bovine serum albumin
C. elegans	*Caenorhabditis elegans*
CDK	Cyclin dependent kinase
ChIP	Chromatin immunoprecipitation
CPC	Chromosomal passenger complex
CTCF	CCCTC-binding factor
D box	Destruction box
D. melanogaster	*Drosophila melanogaster*
DAPI	4',6-diamidino-2-phenylindole
DDK	Dbf4-dependent kinase
DMP	Dimethyl pimelimidate
DMSO	Dimethyl sulphoxide
DNA	Deoxyribonucleic acid
DSB	Double strand break
DSP	Dithiobis(succinimidyl propionate)
DTT	Dithioreitol
E. coli	*Escherichia coli*
ECL	Enhanced chemiluminescence
GAD	*GAL4* activation domain
GBD	*GAL4* DNA binding domain
GFP	Green fluorescent protein
HRP	Horseradish Peroxidase

IPTG	Isopropyl β-D-1-thiogalactopyranoside
KMN	Knl1-Mis12-Ndc80 complex
LB	Luria-Bertani
MBF	Mlu I cell cycle box binding factor
MCAK	Mitotic centromere-associated kinesin
MCC	Mitotic checkpoint complex
MEN	Mitotic exit network
MRX	Mre11/Rad50/Xrs2
OD	Optical density
ORC	Origin recognition complex
PCNA	Proliferating cellular nuclear antigen
PCR	Polymerase chain reaction
Peri	Pericentromere
PP1γ	Protein phosphatase 1 γ
PP2A	Protein phosphatase 2A
qPCR	Quantitative polymerase chain reaction
rDNA	Ribosomal DNA
RNAi	RNA interference
RPA	Replication Protein A
S. cerevisiae	*Saccharomyces cerevisiae*
S. pombe	*Schizosaccharomyces pombe*
SAC	Spindle assembly checkpoint
SBF	Swi4/6 cell cycle box binding factor
SC	Synaptonemal complex
SDS-PAGE	Sodium dodecyl sulphate polyacrylamide gel electrophoresis
SIM	Structural illumination microscopy
SMC	Structural maintenance of chromosomes
SOC	Super Optimal Broth with Catabolite Repression
SPB	Spindle pole body
SPO	Sporulation media
TAD	Topologically associated domain
TCA	Trichloroacetic acid
TEMED	Tetramethylethylenediamine

Contents

Chapter 1. Introduction

1.1 Overview of the cell cycle

All eukaryotes need to grow and divide, and this occurs through cells undergoing the cell cycle. In the mitotic cell cycle one parental cell duplicates to generate two identical daughter cells. This cell division process is divided into discrete stages that are broadly conserved throughout evolution, although cell cycle regulation is in general more complex in higher eukaryotes than lower eukaryotes.

1.1.1 Phases of the cell cycle

During the cell cycle the DNA (Deoxyribonucleic acid) is first replicated during S phase, followed by equal segregation of the chromosomes between two daughter cells in mitosis. These cell cycle stages are separated by intervening gap (G) phases. The first gap phase is G1, and it is in this stage that cells either commit to undergo the next cell division or, if the environment is unfavourable, pause at this stage until the growth conditions become favourable. If the environment remains unfavourable for cell duplication, or if the cell is highly differentiated, then inhibitory signals will prevent entry into the cell cycle and the cell will instead become arrested in a stationary quiescent state, known as G0. Once the cell receives signals to grow and divide then it will proceed out of the G1 phase and into S phase, during which DNA replication will occur. Following DNA replication there is an additional gap phase, G2, which is especially important in higher eukaryotes for allowing repair of DNA damage that occurred during DNA replication. Progression out of G2 permits the cell to enter mitosis, during which time the replicated DNA is segregated equally into two daughter cells. This is followed by separation of the cells through a process known as cytokinesis (reviewed in Morgan 2007).

Mitosis itself is subdivided into several discrete steps known as prophase, prometaphase, metaphase, anaphase and telophase. These individual stages have been documented for several centuries as the chromosome morphology at each step can be clearly visualised by microscopy. DNA replication in S phase produces two identical sister chromatids that are held together by a multi-protein complex called cohesin. After DNA replication and G2, the cells enter into prophase and the sister chromatids condense down to form worm-like structures that are tightly held together. By mitosis, a large multi-subunit protein complex

called the kinetochore is assembled onto a region of DNA known as the centromere. Although the function of the centromere is conserved, the centromeric DNA sequence is highly variable between organisms, and ranges from a small 125 bp DNA sequence in budding yeast, to large arrays of α-satellite repeats that can be thousands of base pairs long in human cells. The kinetochores that have assembled on the sister chromatids are biased to form a back-to-back geometry that predisposes the two sister chromatid kinetochores to capture microtubules emanating from opposite sides of the cell during prometaphase. In metaphase, all of the sister chromatids become aligned along the metaphase plate and the kinetochore-microtubule attachments are under tension due to pulling forces of the spindle, thus biorientation is achieved. In anaphase, the cohesin complex holding the sister chromatids together is cleaved and the sister chromatids separate to opposite poles of the cell (reviewed in Morgan 2007).

1.1.2 Cell cycle regulation

It is essential that the cell cycle proceeds in a unidirectional manner, and therefore this process is exquisitely regulated by a family of proteins known as Cyclin Dependant Kinases (CDKs) and their regulatory subunits, cyclins. The individual CDK-cyclin complexes are restricted to certain periods of the cell cycle and phosphorylate many targets to regulate cell cycle events and timely entry into the next stage. Throughout the cell cycle there are several checkpoints, and once progressed past a checkpoint, the cell is inhibited from re-entering the previous phase (reviewed in (Nasmyth, 1996; Bahler, 2005; Harashima, Dissmeyer and Schnittger, 2013)).

In *Saccharomyces cerevisiae* (*S. cerevisiae*) there is only one CDK, Cdc28, that is regulated by different cyclins to promote progression through the cell cycle. Cyclin Cln3 is responsible for promoting cell division rather than spore formation, although the cell must reach a critical size before *CLN3* is activated. This prevents premature entry into the cell cycle if the cell has only just replicated or is in an unfavourable environment. CDK-Cln3 phosphorylates and inhibits Whi5, which in turn activates the transcription factor SBF (SCB (Swi4/6 cell cycle box) binding factor) to promote expression of the G1/S phase cyclins, Cln1 and Cln2, to initiate budding and spindle pole body (SPB) duplication, and to promote irreversible entry into S phase. Activation of another transcription factor MBF (MCB (Mlu I cell cycle box) binding factor) promotes expression of the S phase cyclins Clb5 and Clb6 to promote

DNA replication. If DNA damage occurs during DNA replication, and is not repaired, then entry into the next stage of the cell cycle is inhibited by DNA damage repair proteins. As cells enter into mitosis the Forkhead family of transcription factors (Mcm1-Fkh1/2-Ndd1) activate transcription of mitotic genes, including the cyclin genes *CLB2* and *CLB1* to initiate irreversible mitotic entry. Destruction of the cyclins and activation of the Anaphase Promoting Complex/Cyclosome (APC/C) at the metaphase to anaphase transition then allows chromosome segregation, mitotic exit, and cytokinesis (reviewed in (Nasmyth, 1996; Bahler, 2005; Harashima, Dissmeyer and Schnittger, 2013)).

1.1.3 Chromosome missegregation during the cell cycle

Faithful chromosome segregation is crucial during the cell cycle to maintain healthy cells, and spindle assembly checkpoint at the metaphase-anaphase transition is one mechanism by which cells ensure that incorrect chromosome segregation does not occur. However, if incorrect chromosome segregation does occur then this will result in aneuploidy. An example of how chromosome missegregation can occur is if incorrect kinetochore-microtubule attachments are made but are not corrected. If both kinetochores attach to the microtubules from the same pole of the cell (syntelic attachment) or one kinetochore attaches to both poles (merotelic attachment), and chromosome segregation is initiated, then this can result in aneuploidy. Another mechanism by which aneuploidy can occur is if the cohesin complex is incorrectly loaded onto the DNA and fails to hold the sister chromatids together, or if cohesin is prematurely removed from the DNA (reviewed in (Marston, 2014; Sansregret and Swanton, 2017)). Additionally, defects in DNA replication or in repair of DNA damage can also result in aneuploidy (reviewed in (Chunduri and Storchova, 2019).

If a cell becomes aneuploid and has either received too many or too few chromosomes, then this often results in cell cycle arrest that is sometimes followed by cell death (reviewed in (Chunduri and Storchova, 2019)). However, up to 80 % of human cancer cells are found to be aneuploid, and this is associated with increased chromosomal instability that leads to daughter cells further gaining or losing chromosomes as the parental cell divides (reviewed in (Chunduri and Storchova, 2019)). These aneuploid cells have altered gene expression patterns that result in changes in protein levels, which can affect the transcriptome of the whole genome (reviewed in (Chunduri and Storchova, 2019)). Aneuploidy in cancer cells, as

in other cell types, leads to increased cell death, but can also promote tumorigenesis and cancer progression. Down syndrome patients, who have trisomy of chromosome 21, have an increased risk of developing leukaemia but an overall lower risk of developing solid tumours, suggesting aneuploidy may promote some cancers (Hasle, Clemmensen and Mikkelsen, 2000). Additionally, aneuploidy not only increases chromosomal instability, but also the frequency of point mutations as cells have defects in DNA replication and DNA repair leading to high variability in the tumour karyotype (reviewed in (Sansregret and Swanton, 2017; Chunduri and Storchova, 2019)). Chromosomal instability in tumours correlates with multidrug resistance, and chromosomally unstable colorectal cancer cell lines have significant multidrug resistance compared to genomically stable cancer cells (Lee *et al.*, 2011; Kuznetsova *et al.*, 2015). Sequencing of human cancer cells revealed that deletions or inactivating mutations occurred in one of the subunits of cohesin, SA2/Scc3, in over a third of cells (Solomon *et al.*, 2011). In human cell lines, inactivation of SA2 resulted in cohesion defects between sister chromatids that resulted in aneuploidy, whereas correction of mutations in SA2 in human cancer cell lines increased chromosomal stability (Solomon *et al.*, 2011).

1.2 The role of the conserved SMC complexes, cohesin and condensin

1.2.1 SMC proteins

Structural Maintenance of Chromosome (SMC) proteins are conserved throughout evolution, and although with diverse functions, all have roles involving DNA. In eukaryotes, SMC proteins are especially well-known for forming the protein complexes cohesin and condensin that are important for chromosome structure and segregation during the cell cycle, as well as the Smc5/6 complex (reviewed in (Hirano, Mitchison and Swedlow, 1995; Marston, 2014)).

SMC proteins have very distinctive domains that are highly conserved even when the primary amino acid sequence is diverged. These proteins are characterised by N- and C-terminal globular domains that contain Walker A and Walker B motifs respectively, and these interact to form separate ATPase (adenosine triphosphatase) head domains (Melby *et al.*, 1998; Lowe, Cordell and van den Ent, 2001; Haering *et al.*, 2002). In the central region of the protein is a small globular domain that forms the "hinge" region that allows dimerisation with another SMC protein (Haering *et al.*, 2002; Gruber, Haering and Nasmyth,

2003). The regions between the N- and C-terminal domains and the hinge region form highly flexible coiled-coils. These two coiled coil regions are 100 nm length and fold back on each other to make an intra-molecular anti-parallel coiled coil (Melby *et al.*, 1998; Haering *et al.*, 2002). The dimerisation of SMC proteins makes a V shaped structure, which can be closed by a kleisin subunit bridging the ATPase head domains to form a ring (reviewed in (Hirano, Mitchison and Swedlow, 1995)).

Budding yeast contains three different SMC complexes, cohesin, condensin and SMC5/6 that all have different functions (Toth *et al.*, 1999; Freeman, Aragon-Alcaide and Strunnikov, 2000; Lehmann, 2005). Cohesin contains Smc1 and Smc3, and was first discovered due to its essential function in promoting faithful chromosome segregation during cell division, as cells with mutations in the cohesin complex prematurely separate sister chromatids and fail to undergo cell division (Strunnikov, Larionov and Koshland, 1993; Michaelis, Ciosk and Nasmyth, 1997; Guacci, Koshland and Strunnikov, 1997; Losada, Hirano and Hirano, 1998; Toth *et al.*, 1999). Cohesin is also important for a diverse range of other functions, including chromosome condensation through chromatin loop formation, transcriptional regulation, DNA damage repair, and homologous recombination. Condensin contains Smc2 and Smc4 and is important in DNA looping and in forming higher-order chromatin structures, which is especially important during mitosis when the chromosomes condense to aid faithful segregation into daughter cells (Strunnikov, Hogan and Koshland, 1995; Freeman, Aragon-Alcaide and Strunnikov, 2000; Lavoie, Hogan and Koshland, 2002; Hirano, 2005; van Ruiten and Rowland, 2018). The Smc5/6 complex is primarily involved in DNA damage repair and in rescuing stalled replication forks but will not be further discussed (reviewed in (Lehmann, 2005; Potts, 2009; Wu and Yu, 2012)).

1.2.2 Cohesin

Cohesin is a highly conserved protein complex throughout eukaryotes that localises to the cell nucleus, and which contains two proteins of the Structural Maintenance of Chromosomes protein family (Strunnikov, Larionov and Koshland, 1993; Michaelis, Ciosk and Nasmyth, 1997; Guacci, Koshland and Strunnikov, 1997; Losada, Hirano and Hirano, 1998; Losada *et al.*, 2000; Sumara *et al.*, 2000). The cohesin tri-partite ring-shaped protein complex is made up of Smc1 and Smc3, and a kleisin subunit, Scc1/Mcd1, which closes the ring (Strunnikov, Larionov and Koshland, 1993; Michaelis, Ciosk and Nasmyth, 1997; Guacci,

Koshland and Strunnikov, 1997; Losada, Hirano and Hirano, 1998; Haering *et al.*, 2002; Gruber, Haering and Nasmyth, 2003). Two accessory subunits are also important for cohesin function - these are known as Pds5 and Scc3 (Figure 1.2.1A) (Toth *et al.*, 1999; Hartman *et al.*, 2000; Losada *et al.*, 2000; Panizza *et al.*, 2000; Sumara *et al.*, 2000).

As with all SMC proteins, Smc1 and Smc3 are coiled-coil proteins that have globular regions at the N- and C-termini, which interact to form separate ATPase head domains (Melby *et al.*, 1998; Lowe, Cordell and van den Ent, 2001; Haering *et al.*, 2002). The Smc1 head domain interacts with the C-terminus of Scc1, and the N-terminus of Scc1 interacts with Smc3 (Haering *et al.*, 2002; Gruber, Haering and Nasmyth, 2003). The crystal structure of the Smc3/Scc1 interface revealed that the N-terminal domain of Scc1 interacts with the coiled-coil of Smc3, and forms a four-helix bundle (Gligoris *et al.*, 2014).

Together, Smc1, Smc3 and Scc1 form a tripartite proteinaceous loop or ring with approximately 40 nm diameter, which is large enough to suggest that cohesin could embrace one or two chromatin fibres (Haering *et al.*, 2002; Gruber, Haering and Nasmyth, 2003; Ivanov and Nasmyth, 2005; Haering *et al.*, 2008; Gligoris *et al.*, 2014). Evidence for cohesin embracing two DNA molecules came from an elegant series of experiments in (Haering *et al.*, 2008). Cohesin was found to interact with circular mini-chromosomes purified from budding yeast, but this interaction was abolished both by cleaving the cohesin ring or by linearisation of the DNA (Ivanov and Nasmyth, 2005). In a later study, cysteine residues were placed at the Smc1-Smc3 and Smc1-Scc1 interfaces, to allow fusion of these interfaces with a chemical cross-linker, and an Smc3-Scc1 fusion protein was synthesised to prevent opening of this interface (Haering *et al.*, 2008). Purification of circular mini-chromosome dimers from metaphase-arrested budding yeast, followed by chemical cross-linking and denaturation, revealed that the chromosome dimers were held together only in the presence of cross-linking reagent (Haering *et al.*, 2008). This dimerisation was abolished by cleavage of the Smc3-Scc1 fusion protein, suggesting that cohesin topologically embraces two DNA molecules (Haering *et al.*, 2008). This was recently shown to also be true *in vivo* in budding yeast, as purification of circular mini-chromosome dimers from live budding yeast pre-treated with cross-linking agents again revealed that even after denaturation the chromosome dimers were held together (Gligoris *et al.*, 2014). Therefore, the cohesin ring embraced the two mini-chromosomes *in vivo* (Gligoris *et al.*, 2014).

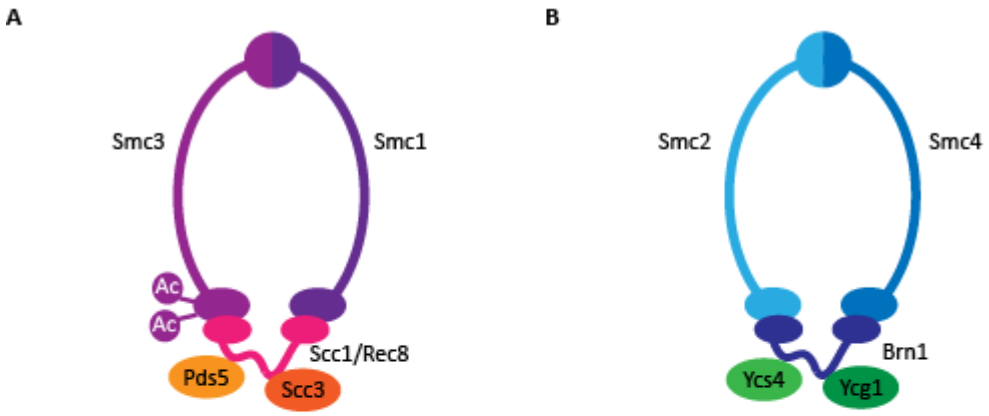

Figure 1.2.1: The SMC complexes cohesin and condensin
A) Schematic of the cohesin complex in *S. cerevisiae*. The SMC proteins, Smc1 and Smc3, form anti-parallel coiled-coil structures with central hinge domains to allow dimerisation. The N- and C-terminal ATPase domains interact to form a head domain. The head domain of Smc3 interacts with the N-terminus of Scc1, and the head domain of Smc1 interacts with the C-terminus of Scc1. The accessory subunits Pds5 and Scc3 interact with Scc1. In meiosis, the Scc1 kleisin subunit is replaced by Rec8. B) Schematic of the condensin complex in *S. cerevisiae*. The Smc2 and Smc4 coiled-coil SMC proteins form a similar structure to the SMC proteins of cohesin, and are similarly bridged by the Brn1 kleisin subunit. The accessory subunits Ycs4 and Ycg1 interact with Brn1, and modulate condensin function.

The Scc1 kleisin subunit that bridges the two SMC proteins provides a binding platform for the cohesin regulatory subunits. One molecule of Scc3 binds to the C-terminus of Scc1, and one molecule of Pds5 binds to the N-terminus of Scc1 (Haering *et al.*, 2002; Chan *et al.*, 2012; Chan *et al.*, 2013; Hara *et al.*, 2014; Lee *et al.*, 2016). Pds5 additionally makes contacts with the Smc3 ATPase domain, close to sites involved in the establishment of cohesion (Chan *et al.*, 2013; Huis in 't Veld *et al.*, 2014). Pds5 itself then forms a binding platform for further regulatory subunits of cohesin, including Wapl and Sororin in higher eukaryotes (Rowland *et al.*, 2009; Shintomi and Hirano, 2009; Chan *et al.*, 2012; Chan *et al.*, 2013; Hara *et al.*, 2014). Thus Scc1 serves as a platform onto which multiple regulatory proteins can bind to cohesin and modulate cohesin activity (Haering *et al.*, 2002; Chan *et al.*, 2012; Chan *et al.*, 2013; Hara *et al.*, 2014; Huis in 't Veld *et al.*, 2014; Lee *et al.*, 2016).

1.2.3 Condensin

Condensin is another highly conserved, essential, five subunit protein complex of the SMC family of proteins, and is important in chromosome structure, condensation, and faithful segregation (Strunnikov, Hogan and Koshland, 1995; Freeman, Aragon-Alcaide and Strunnikov, 2000; Lavoie *et al.*, 2000; Bhalla, Biggins and Murray, 2002; Lavoie, Hogan and Koshland, 2002; Yong-Gonzalez *et al.*, 2007; D'Ambrosio *et al.*, 2008; Johzuka and Horiuchi, 2009). Condensin is also a ring-shaped complex that has a high structural similarity to cohesin (Hirano, Mitchison and Swedlow, 1995). Condensin is made up of the anti-parallel coiled-coil proteins Smc2 and Smc4, the two ATPase head domains of which are bridged by the kleisin subunit Brn1, to form the tripartite protein complex (Strunnikov, Hogan and Koshland, 1995; Freeman, Aragon-Alcaide and Strunnikov, 2000). Accessory subunits Ycg1 and Ycs4 bind to Brn1, and regulate the condensin complex (Figure 1.2.1B) (Freeman, Aragon-Alcaide and Strunnikov, 2000).

As the name suggests, condensin is important in condensation of chromosomes during mitosis in order to form long-range DNA interactions, which is important for maintaining chromosome structure to facilitate faithful chromosome segregation (reviewed in (Hirano, 2005; Cuylen and Haering, 2011; van Ruiten and Rowland, 2018)). Condensin binds to the yeast genome approximately every 10.7 kb and is highly enriched at both the centromeres and rDNA (ribosomal DNA) (Wang *et al.*, 2005). In budding yeast, depletion of condensin causes defects in condensation of the rDNA that results in this region becoming tangled as

cells undergo DNA segregation in anaphase, and therefore condensin mutants have chromosome segregation defects (Strunnikov, Hogan and Koshland, 1995; Freeman, Aragon-Alcaide and Strunnikov, 2000; Lavoie *et al.*, 2000; Bhalla, Biggins and Murray, 2002; Lavoie, Hogan and Koshland, 2002). Additionally, condensin is important at the centromeric region and is important for kinetochore bi-orientation and correct microtubule attachment. In higher eukaryotes there is evidence suggesting that condensin has a role in regulating the elasticity of the pericentromeric heterochromatin (Gerlich *et al.*, 2006; Yong-Gonzalez *et al.*, 2007; Ribeiro *et al.*, 2009; Stephens *et al.*, 2011; Peplowska, Wallek and Storchova, 2014; Verzijlbergen *et al.*, 2014).

1.3 The mitotic cell cycle

To prevent aneuploidy during cell duplication it is crucial that the chromosomes are replicated and the sister chromatids are held together until DNA segregation occurs in anaphase of mitosis (Figure 1.3.1A). Throughout the cell cycle there are multiple steps which ensure this faithful transmission of sister DNA, and these will be described below, with particular focus on the roles of cohesin, condensin, and the pericentromeric adaptor protein, shugoshin. The cell cycle of budding yeast will be described, with differences in vertebrates being highlighted (reviewed in (Marston, 2014)).

1.3.1 Interphase and G1

In budding yeast, cohesin is loaded onto the DNA in late G1, once Scc1 is expressed. Cohesin is loaded through a mechanism that relies on the conserved Scc2/Scc4 (Nipbl/Mau2) complex and ATP (adenosine triphosphate) hydrolysis by cohesin (Michaelis, Ciosk and Nasmyth, 1997; Ciosk *et al.*, 2000; Arumugam *et al.*, 2003; Weitzer, Lehane and Uhlmann, 2003; Tonkin *et al.*, 2004; Watrin *et al.*, 2006; Murayama and Uhlmann, 2014). How DNA enters the cohesin ring is still disputed, although it is thought that DNA enters the cohesin ring through the Smc3-Scc1 interface near to where Scc2/Scc4 is bound, although there is also evidence for opening of the Smc1-Smc3 hinge domains to allow DNA entry (Gruber *et al.*, 2006; Buheitel and Stemmann, 2013; Murayama and Uhlmann, 2015). In budding yeast, the sites of Scc2/Scc4 binding to the DNA are distinct from the sites of cohesin enrichment, due to cohesin translocating from the site of loading along the DNA via a mechanism that is thought to be dependent on transcription

A

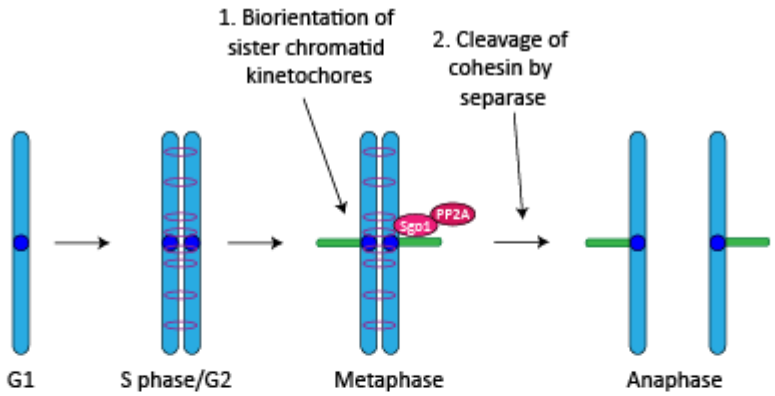

Figure 1.3.1: Chromosome segregation during mitosis in *S. cerevisiae*

A) Schematic of chromosome segregation during mitosis in budding yeast. A stationary cell enters into the cell cycle in G1 in response to signals to divide. The DNA is replicated during S phase of the cell cycle, and cohesin (purple loops in the diagram) embraces the duplicated DNA strands to establish cohesion between the two sister chromatids. This cohesion is maintained along the entire length of the sister chromatids throughout S phase and G2. The sister chromatid kinetochores biorient (1) and stably attach to microtubules, resulting in generation of tension due to cohesion. At the centromeres Sgo1 localises, and recruits PP2A, as well as condensin and Ipl1 (Aurora B) that aid kinetochore biorientation and stable microtubule attachment. By metaphase, all kinetochore-microtubule attachments are correct and under tension, which results in silencing of the spindle assembly checkpoint and activation of the anaphase promoting complex. Activation of the APC/C-Cdc20 complex results in degradation of securin and activation of separase that cleaves cohesin in anaphase (2). Cohesin cleavage allows segregation of the two sister chromatids to opposite poles in anaphase, and two nuclei are generated. The cell cycle is completed during cytokinesis when the daughter bud is separated.

(Ciosk *et al.*, 2000; Lengronne *et al.*, 2004; Hu *et al.*, 2011; Davidson *et al.*, 2016). Cohesin enrichment therefore is not random along the chromosomes, but is enhanced at specific arm loci, and at the centromere and surrounding pericentromeric region (Tanaka *et al.*, 1999; Megee *et al.*, 1999; Kiburz *et al.*, 2005). Although Scc2/Scc4 is also required for cohesin loading at the centromere, the mechanism by which this occurs is slightly different, at least in budding yeast (Hinshaw *et al.*, 2015; Hinshaw *et al.*, 2017). At the centromere the multi-protein kinetochore complex assembles, and this includes the CTF19 complex that is made up of several subunits, including Ctf3 and Ctf19. Dbf4-dependent kinase (DDK) binds to Ctf3 and phosphorylates the N-terminus of Ctf19, thus recruiting Scc2/Scc4 to the centromeres to load cohesin onto the DNA (Hinshaw *et al.*, 2017). The phospho-null mutant of Ctf19, *ctf19-9A*, loses centromeric enrichment of Scc2/Scc4 and, consequently, the centromere-specific enrichment of cohesin (Hinshaw *et al.*, 2017).

During interphase and G1 of the cell cycle cohesin is not stably bound to the DNA, and this is due to the actions of Wapl (Rad61 in *S. cerevisiae*) (Gandhi, Gillespie and Hirano, 2006; Kueng *et al.*, 2006; Chan *et al.*, 2012; Lopez-Serra *et al.*, 2013). After Scc2/Scc4 loading of cohesin onto the DNA, the Scc2/Scc4 complex exchanges for Pds5, which binds to Scc1 of cohesin (Petela *et al.*, 2018). Wapl binds to Pds5, and destabilises the cohesin from the DNA through opening of the Scc1-Smc3 interface of cohesin, resulting in cohesin dynamically interacting with the DNA (Rowland *et al.*, 2009; Shintomi and Hirano, 2009; Sutani *et al.*, 2009; Chan *et al.*, 2012; Lopez-Serra *et al.*, 2013; Huis in 't Veld *et al.*, 2014; Murayama and Uhlmann, 2015; Bloom, Koshland and Guacci, 2018).

In mammalian cells, cohesin is loaded onto the DNA in telophase of the previous cell cycle, and this mechanism of loading by the Scc2/Scc4 (Nipbl/Mau2) complex is conserved with budding yeast. Once cohesin is loaded, it is thought that a small DNA loop forms, and that cohesin translocation along the DNA increases this loop size until convergent CTCF (CCCTC-binding factor) sites are encountered, thus a chromatin loop is formed (Davidson *et al.*, 2016; Haarhuis *et al.*, 2017; Rao *et al.*, 2017; Wutz *et al.*, 2017; van Ruiten and Rowland, 2018). The length of time that cohesin resides on the DNA is thought to be important for regulating the length of chromatin loops, therefore the balance of Scc2/Scc4 and Wapl activity is crucial. In Wapl mutants the size of the chromatin loops were found to be larger, as cohesin could bind to the DNA for longer, and thus increase the size of the loops

(Haarhuis *et al.*, 2017; Rao *et al.*, 2017; Wutz *et al.*, 2017). Through this mechanism, Wapl controls DNA loop size through regulating cohesin stability on the chromatin.

In mammalian cells, prior to DNA replication, the chromosomes are organised into an open three-dimensional structure that is thought of as transcriptionally active state. The chromatin is organised into a high-order structure of discreet domains, known as topologically associated domains (TADs), within which the chromatin has a high frequency contacts. The TADs themselves are made up of smaller chromatin domains or loops, for example Insulated Neighbourhoods that are chromatin loops which are held together at the base by CTCF. CTCF proteins bind to repeats of the CCCTA DNA sequence, and cohesin enrichment also coincides with these sites to form boundaries (Lobanenkov *et al.*, 1990; Parelho *et al.*, 2008; Wendt *et al.*, 2008). Together, cohesin and CTCF are important in transcriptional regulation and all genes within one Insulated Neighbourhood are similarly expressed due to the boundaries defining the region within which enhancer-gene interactions occur - disruption of the boundary regions therefore disrupts gene expression (reviewed in (Pombo and Dillon, 2015; Hnisz, Day and Young, 2016; Zhao, Rivera-Mulia and Gilbert, 2017)). DNA replication timing also coincides with the three-dimensional organisation of the genome, and individual replicons correspond to individual TADs, which can be early or late replicating.

1.3.2 S phase

As cells progress into S phase, the DNA is replicated and the resulting sister chromatids need to be entrapped and held together by the cohesin complex. Prior to S phase, distinct regions known as replication origins are bound by a highly conserved pre-replication complex made up of ORC1-6 (origin recognition complex) and Cdc6. Cdt1 then recruits the DNA helicase Mcm2-7 to the ORC-Cdc6 complex, followed by Cdc45 and GINS replacing Cdc6 to form the helicase that will ultimately allow unwinding of the DNA. Recruitment of DDK and Cdk-cyclin complexes to the pre-replication complex then allows recruitment of DNA polymerase, initiation of DNA unwinding and Replication Protein A (RPA) binding. Once DNA replication has been initiated by DNA polymerase ε, the clamp loader (Replication Factor C) is loaded to recruit the sliding clamp, PCNA (Proliferating cellular nuclear antigen), resulting in DNA polymerase α and δ loading to initiate replication elongation (reviewed in (Remus and Diffley, 2009; O'Donnell, Langston and Stillman, 2013)).

At the replication fork, an acetyltransferase known as Eco1 closely associates with the components of RFC-Ctf18 and PCNA (Lengronne *et al.*, 2006; Moldovan, Pfander and Jentsch, 2006; Lopez-Serra *et al.*, 2013). As the replication fork progresses, cohesin on the DNA encounters the replication fork and embraces the two newly replicated sister chromatids to hold them together (Haering *et al.*, 2008). Eco1 acetylates the Smc3 subunit of the cohesin complex on the ATPase head domain at the highly conserved residues K112 and K113 (K105 and K106 in humans and *Schizosaccharomyces pombe* (*S. pombe*)), which locks the cohesin ring shut at the Smc3-Scc1 interface and prevents ATPase activity, thereby preventing Rad61-driven cohesin unloading (Rolef Ben-Shahar *et al.*, 2008; Unal *et al.*, 2008; Zhang *et al.*, 2008b; Rowland *et al.*, 2009; Sutani *et al.*, 2009; Chan *et al.*, 2012; Lopez-Serra *et al.*, 2013; Guacci *et al.*, 2015; Murayama and Uhlmann, 2015). As cohesin now embraces the two sister chromatids, this acetylation establishes cohesion between them. Upon completion of DNA replication, phosphorylation of Eco1 by Cdk1 targets Eco1 for degradation by the proteasome (Lyons and Morgan, 2011).

In vertebrates, the acetylation of cohesin on Smc3-K105, and Smc3-K106 is carried out by two homologues of Eco1, Esco1 and Esco2 (Hou and Zou, 2005). Esco1 acetylates cohesin throughout the cell cycle, and this is thought to be important for cohesin function in DNA loop formation, whereas Esco2 activity is restricted to S phase and is essential for the establishment of cohesion between sister chromatids (Hou and Zou, 2005; Zhang *et al.*, 2008b; Song *et al.*, 2012; Ladurner *et al.*, 2016; Alomer *et al.*, 2017). Similarly to Eco1 in budding yeast, Esco2 localises to the DNA replication fork and was recently shown to interact with several proteins of the MCM complex by cross-linking mass spectrometry (Ivanov *et al.*, 2018).

Acetylation of Smc3 in vertebrates promotes sororin binding to the Pds5 subunit of cohesin through FGF motifs, and this displaces Wapl from Pds5 (Rankin, Ayad and Kirschner, 2005; Shintomi and Hirano, 2009; Lafont, Song and Rankin, 2010; Nishiyama *et al.*, 2010; Song *et al.*, 2012; Ladurner *et al.*, 2016). Therefore, sororin binding stabilises the acetylated cohesin on the DNA, and prevents opening of the Smc3-Scc1 interface (Rankin, Ayad and Kirschner, 2005; Schmitz *et al.*, 2007; Lafont, Song and Rankin, 2010; Nishiyama *et al.*, 2010; Song *et al.*, 2012; Buheitel and Stemmann, 2013; Huis in 't Veld *et al.*, 2014; Ladurner *et al.*, 2016).

Wapl is however still weakly associated with the cohesin ring through interactions with SA2/Scc3 of cohesin (Hara *et al.*, 2014). There is no known sororin homologue in budding yeast. Instead, acetylation of cohesin appears to be sufficient for establishment of cohesion.

In humans, mutations in Esco2 result in an extremely rare genetic disease known as Robert's syndrome (Vega *et al.*, 2005). Robert's syndrome results in severe growth retardation, and many other developmental defects such as microcephaly and cleft palate (Vega *et al.*, 2005). At a cellular level the mutations in Esco2 cause premature loss of sister chromatid centromere cohesion that results in aneuploidy and decreased cell proliferation, which has been proposed to contribute to the disease outcome (Vega *et al.*, 2005).

In chicken DT40 cells, depletion of Esco2 also results in loss of centromeric cohesion between sister chromatids, and together with Esco1, is crucial for proliferation and for promoting sister chromatid cohesion (Kawasumi *et al.*, 2017). However, the sister chromatid cohesion defects of Esco1 and Esco2 double depletion are neither rescued by the further depletion of Wapl nor the expression of an acetyl-mimic mutant of Smc3, Smc3-K105Q,K106Q. Additionally, the acetyl-null mutant of Smc3, Smc3-K105R,K106R, is viable. Depletion of Esco1 and Esco2 causes a further increase of cohesin on interphase chromatin in Wapl mutants, and results in altered gene expression (Kawasumi *et al.*, 2017). Together these results suggest that Esco1 and Esco2 acetyltransferases may have multiple targets in addition to Smc3 (Kawasumi *et al.*, 2017).

1.3.3 DNA repair by Eco1 in *S. cerevisiae*

In *S. cerevisiae*, Eco1 is essential for establishment of cohesion between sister chromatids through acetylating Smc3-K112,K113. However, Eco1 is also important in cohesin-mediated DNA double-strand break repair through generation of additional cohesion between sister chromatids to aid the DNA repair (Strom *et al.*, 2004; Unal *et al.*, 2004; Strom *et al.*, 2007; Unal, Heidinger-Pauli and Koshland, 2007). In response to DNA damage, the Scc1 subunit of cohesin is phosphorylated by Chk1 kinase, which has been activated by the DNA damage repair complex Mre11/Rad50/Xrs2 (MRX) (Unal, Heidinger-Pauli and Koshland, 2007; Strom *et al.*, 2007; Heidinger-Pauli *et al.*, 2008). This phosphorylation of Scc1 then promotes acetylation of Scc1 by Eco1 acetyltransferase, and this promotes genome-wide

establishment of cohesion (Heidinger-Pauli, Unal and Koshland, 2009). Mutation of two Eco1 acetylation sites on Scc1, K84 and K210, results in reduced cohesion establishment in response to DNA damage, suggesting Scc1 is the target of Eco1 (Heidinger-Pauli, Unal and Koshland, 2009). Therefore, in *S. cerevisiae*, in circumstances of DNA damage, cohesion can be established between sister chromatids after S phase.

1.3.4 G2

In budding yeast, upon completion of DNA replication, cells progress into mitosis without any delay. However, in most eukaryotic cells between S phase and mitosis there is an additional intervening gap phase known as G2. This gap phase is important for protein synthesis and cell growth as the cell prepares to divide into two daughter cells in mitosis. After DNA replication it is essential that any unreplicated DNA or DNA damage is repaired to ensure that both daughter cells receive identical and correct copies of the genome during mitosis. In G2, unrepaired sites of DNA damage are bound by the conserved Serine/Threonine protein kinases, ATR (Ataxia Telangiectasia and Rad3 related protein) and ATM (Ataxia Telangiectasia mutated protein), that respond to various types of DNA damage including replication fork blockages and DNA double strand breaks. Once bound, ATM and ATR kinases initiate a signalling cascade through the phosphorylation and activation of the Chk1 and Chk2 effector protein kinases. These kinases in turn amplify the DNA damage signal to trigger a cell cycle arrest through the G2/M checkpoint and to initiate transcription of genes that encode DNA damage repair proteins. Only once the DNA damage is repaired can the G2/M checkpoint be silenced and the cells progress into prophase of mitosis.

1.3.5 Prophase

In *S. cerevisiae*, S phase established cohesion is maintained along the entire length of the sister chromatids until anaphase, when separase-dependent cohesin cleavage occurs. However, in mammalian cells, cohesin removal occurs in two stages (Figure 1.3.2A). The first step of cohesin removal is through a destabilisation pathway known as the "prophase pathway", and the second step is by cohesin cleavage in anaphase (reviewed in (Haarhuis, Elbatsh and Rowland, 2014)). Currently it is not fully understood why budding yeast do not have a destabilisation step of cohesin removal prior to anaphase of mitosis, but it is possible that the removal pathway may be active, but that cohesin removal is simply hard to detect due to cells progressing immediately from S phase into mitosis without an

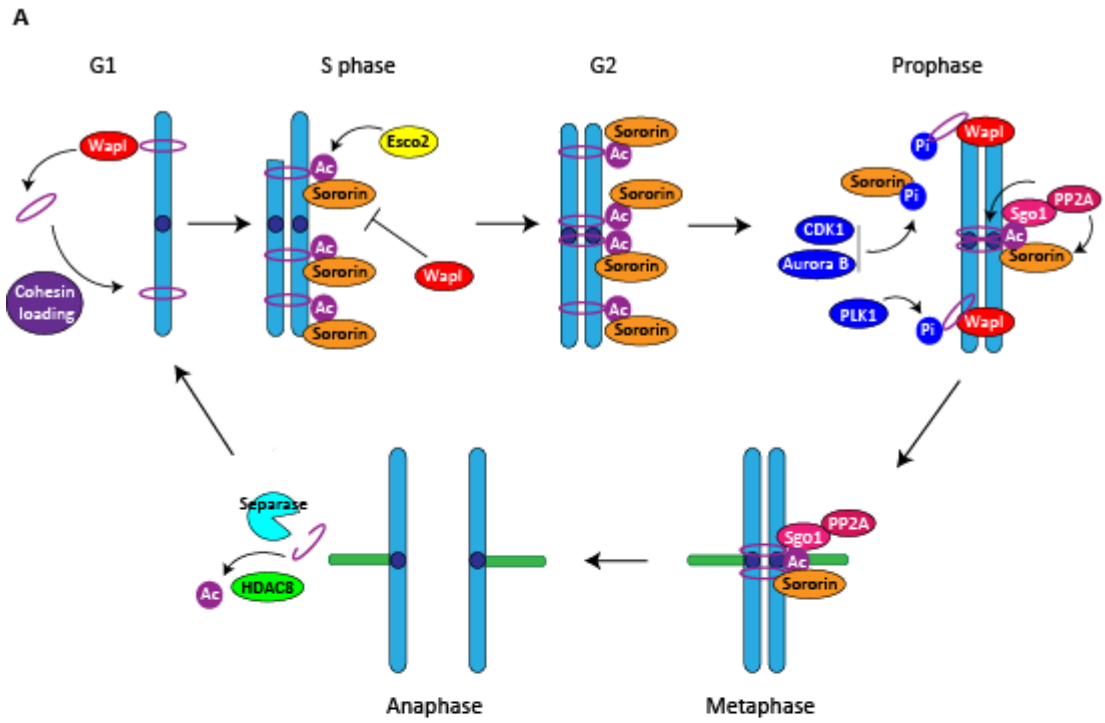

Figure 1.3.2: The prophase pathway of cohesin removal in vertebrates

A) Schematic of cohesin loading and removal in vertebrates. During G1 of the cell cycle, cohesin is loaded onto the DNA through interactions with the Scc2/Scc4 complex (Nipbl/Mau2). The interaction between cohesin and the DNA is dynamic due to the destabilisation of chromatin-bound cohesin by Wapl. In S phase, cohesion is formed between the two newly replicated sister chromatids. The Esco2 acetyltransferase travels with the replication fork and acetylates cohesin, thereby generating cohesion between the two DNA strands. The acetylation of cohesin at Smc3-K105,K106 promotes binding of sororin to cohesin. In G2 acetylated cohesin is stabilised along the entire length of the sister chromatids. In prophase, Cdk1 and Aurora B phosphorylate sororin and destabilise it from Pds5 to allow binding of Wapl and destabilisation of cohesin. Additionally Plk1 phosphorylates cohesin, and this aids removal of cohesin from the chromosome arms. At the centromeres Sgo1-PP2A dephosphorylates and protects sororin and cohesin from removal, and this centromeric cohesin maintains cohesion between the sister chromatids in metaphase. The bioriented sister chromatid kinetochores attach to microtubules emanating from opposite poles in metaphase, and once all of the attachments are correct and under tension, the spindle assembly checkpoint is silenced. In anaphase, cohesin is cleaved by separase, and the Smc3 subunit is deacetylated by HDAC8 to allow recycling during the next cell cycle.

intervening G2. Accompanying the loss of cohesion in prophase is the condensation activity of condensin which aids sister chromatid resolution and promotes faithful sister chromatid segregation.

As cells enter prophase in mammalian cells, the acetylated cohesin on the chromosome arms is associated with Pds5 which interacts with sororin, and Scc3 that is bound by Wapl (Rankin, Ayad and Kirschner, 2005; Schmitz *et al.*, 2007; Shintomi and Hirano, 2009; Lafont, Song and Rankin, 2010; Nishiyama *et al.*, 2010; Song *et al.*, 2012; Hara *et al.*, 2014; Ladurner *et al.*, 2016). Progression into prophase of mitosis causes activation of Cdk1 and Aurora B kinase which both phosphorylate sororin on multiple residues that triggers the dissociation of sororin from Pds5, allowing Wapl to re-associate with Pds5 (Rankin, Ayad and Kirschner, 2005; Shintomi and Hirano, 2009; Nishiyama *et al.*, 2010; Dreier, Bekier and Taylor, 2011; Nishiyama *et al.*, 2013). Additionally, Plk1 phosphorylates the SA2 (Scc3) subunit of cohesin, and this along with Wapl association with Pds5, promotes opening of the Smc3-Scc1 interface and cohesin dissociation from the chromatin (Sumara *et al.*, 2002; Hauf *et al.*, 2005; McGuinness *et al.*, 2005; Kueng *et al.*, 2006; Shintomi and Hirano, 2009; Nishiyama *et al.*, 2013; Buheitel and Stemmann, 2013; Huis in 't Veld *et al.*, 2014). As a result, the sister chromatid arms have less cohesion between them, and thus are more loosely connected (Losada, Hirano and Hirano, 1998; Losada *et al.*, 2000; Sumara *et al.*, 2000; Waizenegger *et al.*, 2000; Losada, Hirano and Hirano, 2002).

At kinetochores, a protein of the spindle assembly checkpoint (SAC), Bub1, phosphorylates Histone H2A-Thr120, creating the binding site for Sgo1, of the shugoshin family (Tang *et al.*, 2004; Kitajima *et al.*, 2005; Kawashima *et al.*, 2010; Liu, Jia and Yu, 2013). Additionally, RNA polymerase II is important for Sgo1 centromeric localisation (Liu *et al.*, 2015). Sgo1 is phosphorylated at Thr346 by Cdk1 during prophase, allowing Sgo1 to bind to the SA2/Scc1 subunits of cohesin (Liu, Rankin and Yu, 2013). Binding of Sgo1 to cohesin displaces Wapl completely from the sororin-bound acetylated cohesin, and therefore protects cohesin from Wapl (Hara *et al.*, 2014). The key mediator of Sgo1 protective function is Protein Phosphatase 2A (PP2A) that is recruited by Sgo1 to the centromere, where PP2A then dephosphorylates both sororin and SA2 (Kitajima *et al.*, 2006; Tang *et al.*, 2006; Xu *et al.*, 2009; Dreier, Bekier and Taylor, 2011; Nishiyama *et al.*, 2013). Dephosphorylation of sororin at the centromere prevents Wapl binding to Pds5, protecting centromeric cohesin from

destabilisation by the prophase pathway (Salic, Waters and Mitchison, 2004; Kitajima *et al.*, 2005; McGuinness *et al.*, 2005; Kitajima *et al.*, 2006; Kueng *et al.*, 2006; Nishiyama *et al.*, 2010; Nishiyama *et al.*, 2013; Ladurner *et al.*, 2016).

There is no evidence that the prophase pathway of cohesin removal from chromosome arms prior to metaphase exists in budding yeast (Indjeian, Stern and Murray, 2005; Rowland *et al.*, 2009; Sutani *et al.*, 2009). Nevertheless, the prophase pathway components do still exist in budding yeast (Indjeian, Stern and Murray, 2005; Rowland *et al.*, 2009; Sutani *et al.*, 2009). Pds5 associates with the cohesin complex after loading onto the DNA, and although there is no active prophase-like pathway, Pds5 is important for maintaining and protecting cohesion after S phase and prevents premature deacetylation of cohesin that would result in destabilisation from the sister chromatids (Hartman *et al.*, 2000; Panizza *et al.*, 2000; Sutani *et al.*, 2009; Chan *et al.*, 2012; Chan *et al.*, 2013; Tong and Skibbens, 2014; Bloom, Koshland and Guacci, 2018).

Deletion of *ECO1* or mutation of *SMC3-K112,K113* to non-acetylatable residues is lethal in budding yeast due to loss of sister chromatid cohesion, but can be rescued by deletion of *RAD61* or mutation of the Rad61-binding site on Pds5 (Rolef Ben-Shahar *et al.*, 2008; Unal *et al.*, 2008; Rowland *et al.*, 2009; Sutani *et al.*, 2009; Chan *et al.*, 2012; Guacci and Koshland, 2012; Lopez-Serra *et al.*, 2013; Guacci *et al.*, 2015). This shows that in the absence of Smc3 acetylation by Eco1, cohesin is susceptible to Rad61-dependent removal after S phase that results in a complete loss of cohesion that results in aneuploidy and cell death. So, although there is no detectable destabilisation pathway in budding yeast, the unacetylated pool of cohesin is still susceptible to removal by Rad61. But, deletion of *RAD61* in *ECO1* mutants does not fully rescue the cohesion defects of *ECO1* mutants, and instead rescues the chromosome condensation defects in these cells (Rolef Ben-Shahar *et al.*, 2008; Rowland *et al.*, 2009; Sutani *et al.*, 2009; Guacci and Koshland, 2012; Lopez-Serra *et al.*, 2013; Guacci *et al.*, 2015; Bloom, Koshland and Guacci, 2018). Overall, in the absence of Eco1 and the destabilising activity of Rad61, unacetylated cohesin can at least partially hold sister chromatids together from S phase until mitosis to allow at least a proportion of chromatids to segregate faithfully. Rad61 also promotes DNA damage repair and correct cohesion between sister chromatids, and so overall has both positive and negative roles in cohesin regulation (Rolef Ben-Shahar *et al.*, 2008; Rowland *et al.*, 2009; Sutani *et al.*, 2009;

Guacci and Koshland, 2012; Lopez-Serra *et al.*, 2013; Guacci *et al.*, 2015; Bloom, Koshland and Guacci, 2018). The interplay between cohesin acetylation, Pds5, Scc3 and Rad61 is still not fully understood and remains an open avenue of research.

1.3.6 Condensation of sister chromatids during prophase

One important event of prophase is chromosome condensation. Condensin complexes are important for this step through looping of the DNA to induce compaction. Mutations in the condensin complex are lethal during budding yeast cell division, as the rDNA of the sister chromatids become tangled during DNA segregation resulting in aneuploidy and cell death (Strunnikov, Hogan and Koshland, 1995; Freeman, Aragon-Alcaide and Strunnikov, 2000; Lavoie *et al.*, 2000; Bhalla, Biggins and Murray, 2002; Lavoie, Hogan and Koshland, 2002). The looping function of condensin is mediated by the accessory subunit Ycg1, promoting binding of the kleisin subunit Brn1 to the DNA. This in turn stimulates the ATPase activity of the SMC proteins that could allow entrapment of another region of DNA *in cis* to the first within the SMC proteins. Through the ATPase activity of condensin, the second *in cis* region of DNA could be "reeled" through the condensin complex to generate a DNA loop (van Ruiten and Rowland, 2018). Through this mechanism condensin forms DNA loops and the chromosomes become condensed, aiding chromosome segregation (reviewed in (Cuylen and Haering, 2011)).

In vertebrates, removal of cohesin during prophase promotes loosening of the sister chromatid arms. It is important that this occurs with the concomitant condensation of the arms of the sister chromatids to prevent tangling of the DNA. In vertebrates there are two main condensin complexes: condensin I and condensin II (Hirano, 2005). Condensin II is present in the nucleus throughout the cell cycle and interacts with the DNA, but only in prophase does condensin II stably bind the DNA to promote sister chromatid disentanglement and chromosome condensation (Hirano, 2005; Gerlich *et al.*, 2006). Condensin I is cytoplasmic and therefore only associates with and condenses the DNA after nuclear envelope breakdown (between prometaphase and anaphase), and also has additional roles in structuring the centromeric chromatin (Hirano, 2005; Gerlich *et al.*, 2006; Ribeiro *et al.*, 2009; Stephens *et al.*, 2011). The presence of condensin II in the nucleus throughout the cell cycle allows large chromatin loops of around 450 kb in size to form, and the activity of condensin I in prophase then further loops the chromatin into smaller 70 kb

domains to further condense the mitotic chromosomes (Hirano, 2005; van Ruiten and Rowland, 2018). Condensin is therefore important in mitotic chromosome structure from yeasts to vertebrates.

1.3.7 Metaphase

As cells progress into mitosis microtubules emanating from opposite sides of the cell, known as spindle poles in budding yeast, must correctly attach to the sister chromatid kinetochores to form stable amphitelic attachments that generate tension. This state is known as sister kinetochore biorientation. Shugoshin is important in promoting kinetochore biorientation and for sensing kinetochore-microtubule tension through interactions with the adaptor proteins Ipl1 (Aurora B) and condensin. Only once all of the kinetochores are correctly attached and under tension can the APC/C be activated to degrade securin (Pds1 in *S. cerevisiae*) to permit separase activation (Esp1 in *S. cerevisiae*) and cohesin cleavage. The spindle assembly checkpoint (SAC) is a cell cycle checkpoint at the metaphase-to-anaphase transition that is essential in preventing premature separation of the sister chromatids in the absence of correct kinetochore-microtubule attachments. This checkpoint therefore guards against aneuploidy during anaphase.

1.3.8 Shugoshin as a pericentromeric adaptor protein

In *S. cerevisiae* there is one shugoshin, Sgo1, that localises to the centromeric and pericentromeric regions through binding to phosphorylated Histone H2A-S121 (Kawashima *et al.*, 2010). As in vertebrates, Bub1 kinase is responsible for this phosphorylation. However, Bub1 has additional unknown targets that promotes Sgo1 kinetochore recruitment, as *bub1Δ* mutants lose centromeric Sgo1 enrichment even when the phospho-mimetic *H2A-S121D* mutant is expressed (Fernius and Hardwick, 2007; Kawashima *et al.*, 2010; Nerusheva *et al.*, 2014). Unlike in vertebrates, Sgo1 does not protect centromeric cohesin in mitosis as there is no prophase pathway of cohesin removal prior to anaphase, and *sgo1Δ* mutants do not prematurely separate sister chromatids (Katis *et al.*, 2004a; Indjeian, Stern and Murray, 2005; Kiburz *et al.*, 2005; Verzijlbergen *et al.*, 2014). However, Sgo1 is important in kinetochore biorientation and tension sensing in budding yeast mitosis, and in this way promotes faithful chromosome segregation (Indjeian, Stern and Murray, 2005; Fernius and Hardwick, 2007; Indjeian and Murray, 2007; Storchova *et al.*, 2011; Eshleman and Morgan, 2014; Nerusheva *et al.*, 2014; Peplowska, Wallek and Storchova,

2014; Verzijlbergen *et al.*, 2014). Sgo1 also interacts with PP2A-Rts1 in mitosis through directly binding to the regulatory subunit Rts1 through an N-terminal coiled-coil domain (Xu *et al.*, 2009). Many experiments have been carried out to establish the importance of PP2A-Rts1 in kinetochore biorientation and tension sensing, but the results are inconclusive (Storchova *et al.*, 2011; Eshleman and Morgan, 2014; Peplowska, Wallek and Storchova, 2014; Verzijlbergen *et al.*, 2014).

1.3.9 Biorientation of sister chromatid kinetochores

Sister chromatid kinetochores have an intrinsic bias to form a back-to-back geometry, which means that the two kinetochores on the newly replicated sister chromatids face away from each other (Indjeian and Murray, 2007). This biases the kinetochores to capture microtubules emanating from the spindle pole bodies at each end of the cell in yeast, or centrosomes in animal and plant cells, so that biorientation can be established. Sgo1 recruits condensin to the pericentromeric and centromeric region, which aids the formation of the back-to-back geometry of the sister chromatid kinetochores (Freeman, Aragon-Alcaide and Strunnikov, 2000; Wang *et al.*, 2005; Yong-Gonzalez *et al.*, 2007; Bachellier-Bassi *et al.*, 2008; D'Ambrosio *et al.*, 2008; Stephens *et al.*, 2011; Peplowska, Wallek and Storchova, 2014; Verzijlbergen *et al.*, 2014). It is not known if shugoshin in higher eukaryotes can recruit condensin to the centromeric region. However, condensin I also localises to the centromeres in vertebrates, and is important for strengthening the centromeric heterochromatin so that it can act in a spring-like fashion to withstand microtubule pulling forces (Gerlich *et al.*, 2006; Ribeiro *et al.*, 2009). This has been found to be important for correct microtubule attachment and faithful chromosome segregation (Cuylen and Haering, 2011).

1.3.10 Tension sensing and the spindle assembly checkpoint

The bias of sister kinetochores to form a back-to-back geometry is important for promoting correct kinetochore-microtubule attachments. But incorrect kinetochore-microtubule attachments frequently occur, and it is essential that these are destabilised and corrected to prevent aneuploidy. The highly conserved chromosomal passenger complex (CPC) is made up of four proteins, Ipl1 (Aurora B), Bir1 (Survivin), Sli15 (INCENP) and Nbl1 (Borealin) and is important for both kinetochore biorientation and sensing tension (reviewed in (Krenn and Musacchio, 2015)). In mitosis, Ipl1 localises to unattached kinetochores in a

manner dependent on Sgo1, although in vertebrates, the localisation of Sgo1 itself is also dependent on Aurora B (Kawashima *et al.*, 2007; Pouwels *et al.*, 2007; Lee *et al.*, 2014; Nerusheva *et al.*, 2014; Peplowska, Wallek and Storchova, 2014; Verzijlbergen *et al.*, 2014). In vertebrates, the Sgo2 homologue of Sgo1 is important in mitosis for faithful mitotic chromosome segregation through interactions with PP2A-B56 and MCAK (mitotic centromere-associated kinesin), which are promoted by Aurora B kinase phosphorylation of Sgo2 (Huang *et al.*, 2007; Lee *et al.*, 2008; Tanno *et al.*, 2010; Rattani *et al.*, 2017).

The main function of Ipl1 localisation to the kinetochores is to destabilise incorrect kinetochore-microtubule interactions and, as a consequence, activate the spindle assembly checkpoint (SAC). To destabilise incorrect kinetochore-microtubule attachments, Ipl1 phosphorylates multiple kinetochore components, including the Ndc80 and Dam1 complexes, to induce the release of microtubules (Cheeseman *et al.*, 2002; Pinsky *et al.*, 2006; Akiyoshi *et al.*, 2009; Demirel *et al.*, 2012; Krenn and Musacchio, 2015). The presence of an unattached kinetochore recruits Mps1 kinase to the kinetochore, to initiate SAC activation. Mps1 binding to phosphorylated Ndc80 of the KMN (Knl1-Mis12-Ndc80) complex then results in phosphorylation of Knl1, which in turn recruits Bub1-Bub3 complexes. A dimer of the Mad1 checkpoint protein localises to the kinetochores with the active Mad2 checkpoint protein (Mad2-closed), and this recruits inactive Mad2 (Mad2-open) that is subsequently converted into the active closed state. The activated Mad2 protein then forms the MCC (mitotic checkpoint complex) with Mad3 and Cdc20, that binds to and inhibits the APC/C. This prevents premature degradation of Clb2 and securin, and thus blocks progression through anaphase, until all kinetochore-microtubule attachments are under tension (reviewed in (Musacchio, 2015)).

1.3.11 Completion of biorientation

Upon correct kinetochore-microtubule attachments, the two bioriented kinetochores come under spindle-generated tension that pulls the sister chromatid centromeres apart (Tanaka *et al.*, 2000). This removes Sgo1 from the pericentromeric region, and therefore also delocalises Ipl1 and condensin (Bachellier-Bassi *et al.*, 2008; Nerusheva *et al.*, 2014). In higher eukaryotes this tension results in Sgo1-T346 being dephosphorylated and Sgo1 is re-distributed from centromeric cohesin back to phosphorylated Histone H2A-Thr120 at kinetochores (Liu, Jia and Yu, 2013). Once removed, Sgo1 is then targeted for degradation

by the APC/C (Fu *et al.*, 2007; Karamysheva *et al.*, 2009; Eshleman and Morgan, 2014). In budding yeast, stabilisation of Sgo1 protein by mutation of a C-terminal KEN box, to create the *sgo1-Δdb* mutant, does not cause any defects in cell cycle progression, therefore it is removal of Sgo1 from the centromeric region, rather than its degradation, that is important in inactivating Sgo1 (Eshleman and Morgan, 2014).

The spindle assembly checkpoint is also turned off in response to tension, although it is still not clear exactly how this happens. The MCC is disassembled, allowing Cdc20 to bind to and activate the APC/C. Activation of the APC/C results in poly-ubiquitination of numerous targets, including Clb2, to allow transition into anaphase, and securin to allow activation of separase (reviewed in (Musacchio, 2015)).

1.3.12 Metaphase-Anaphase transition

Activation of the APC/C by Cdc20 results in poly-ubiquitination of securin (Pds1) that leads to its degradation (Cohen-Fix *et al.*, 1996; Yamamoto, Guacci and Koshland, 1996; Ciosk *et al.*, 1998). This releases separase to cleave the cohesin Scc1 kleisin subunit, which allows sister chromatids to be pulled towards opposite poles and segregated into two daughter nuclei (Uhlmann, Lottspeich and Nasmyth, 1999; Uhlmann *et al.*, 2000). Although separase can cleave unmodified Scc1, phosphorylation of Scc1 by Cdc5 increases the efficiency of the cleavage reaction and aids proficient progression through anaphase (Alexandru *et al.*, 2001; Mishra *et al.*, 2016). In mammalian cells, the majority of the arm cohesin is destabilised by Wapl in prophase, so in anaphase only the remaining arm cohesin, as well as all of the centromeric cohesin, is cleaved by separase to allow segregation (Hauf, Waizenegger and Peters, 2001).

After cohesin cleavage, the acetylated Smc3 is deacetylated by Hos1 in budding yeast (HDAC8 in mammals) to allow recycling of unacetylated Smc3 for the next cell cycle (Beckouet *et al.*, 2010; Borges *et al.*, 2010; Xiong, Lu and Gerton, 2010; Deardorff *et al.*, 2012; Li, Yue and Tanaka, 2017). The deacetylation of cohesin also aids the release of the DNA from the cohesin ring, and so promotes sister chromatid segregation in anaphase (Li, Yue and Tanaka, 2017).

Additionally, activation of the APC/C results in inactivation of Cdc28-cyclin complexes and the activation of the Mitotic Exit Network (MEN). Release of Cdc14 phosphatase from the nucleolus results in dephosphorylation and activation of many Cdc28-cyclin substrates, including Cdh1 and Swi5. This process drives spindle elongation, progression through anaphase and exit from mitosis (reviewed in Morgan 2007).

1.3.13 Cytokinesis

In budding yeast progression through anaphase results in two nuclei, with one in the mother cell and one in the daughter cell. The daughter bud is separated from the mother cell during cytokinesis by contraction of an actin-myosin ring at the bud-neck and therefore the two cells are generated. In animals and plants, the nuclear envelope is broken down during prophase, therefore this has to re-generate after anaphase (during telophase) in addition to cytokinesis of the cell membrane to divide the two daughter cells (reviewed in Morgan 2007).

1.3.14 Cornelia de Lange syndrome

Cohesin is involved in many processes during the cell cycle, and although is most well-known for cohesion of sister chromatids, is also important for a range of other processes including for chromatin structure and transcriptional regulation, and for DNA damage repair. Perturbation of cohesin through mutation of the loading complex, cohesin itself, or cohesin modifying proteins can result in a group of genetic diseases known as cohesinopathies (reviewed in (Liu and Krantz, 2008). As previously mentioned, mutation in Esco2 can result in Robert's syndrome (Vega *et al.*, 2005). Cornelia de Lange syndrome is a group of rare genetic diseases caused by mutations in SMC1, SMC3 or HDAC8, although the majority of cases are due to mutation in the Scc2 homologue NIPBL (Tonkin *et al.*, 2004; Liu and Krantz, 2008; Deardorff *et al.*, 2012). It is thought that these mutations in cohesin result in dis-regulation of transcription, which leads to the clinical phenotype. Therefore, furthering the knowledge of cohesin and its regulation in mammals may lead to increased knowledge about this developmental disorder, and aid therapy generation.

1.4 Overview of meiosis

Meiosis is a specialised form of cell division in which one diploid progenitor cell divides to generate haploid progeny, in contrast to mitotic cell division in which two genetically identical daughter cells are generated from one parental cell (Figure 1.4.1A). As in the mitotic cell cycle, during meiotic cell division, the DNA is replicated in S phase and the sister chromatids are held together by cohesin. However, there are then several adaptations to the meiotic cell division programme to ensure that the chromosomes are faithfully segregated during two consecutive rounds of DNA segregation.

The first major difference is that after S phase of meiosis the homologous chromosomes undergo pairing, and programmed double strand breaks then occur which initiates repair by recombination between the homologous chromosomes. This results in DNA crossovers between the homologous chromosomes being formed, known as chiasmata, that hold the two pairs of sister chromatids together in a bivalent state. This is in contrast to the mitotic cell cycle in which there is no programmed DNA double strand breaks, and any DNA damage is repaired using the sister chromatid. The formation of bivalents in prophase of meiosis is important for holding the homologous chromosomes together so that these can be correctly segregated away from each other in the first meiotic division. Prior to meiosis I, a second major change occurs as the sister chromatid kinetochores are no longer biased to biorient and capture microtubules from opposite poles of the cell. Instead the sister chromatid kinetochores are biased to mono-orient to face towards the same pole, promoting biorientation of the homologous chromosomes. During the first meiotic division, the chiasmata are resolved and the DNA damage repaired, and the homologous chromosomes are segregated in a reductional chromosomal division. It is essential that during the first meiotic division the sister chromatids are not segregated, as this would result in aneuploidy. For this to occur, a third major change is made to the meiotic program, and only the cohesin on the arms of the sister chromatids must be cleaved in meiosis I. Shugoshin localisation to the centromeric region is essential in protecting this pool of cohesin to hold the sister chromatids together. Only in the second meiotic division is the centromeric cohesin cleaved by separase to allow equational chromosome segregation to occur, and the sister chromatids are separated (reviewed in (Marston, 2014)).

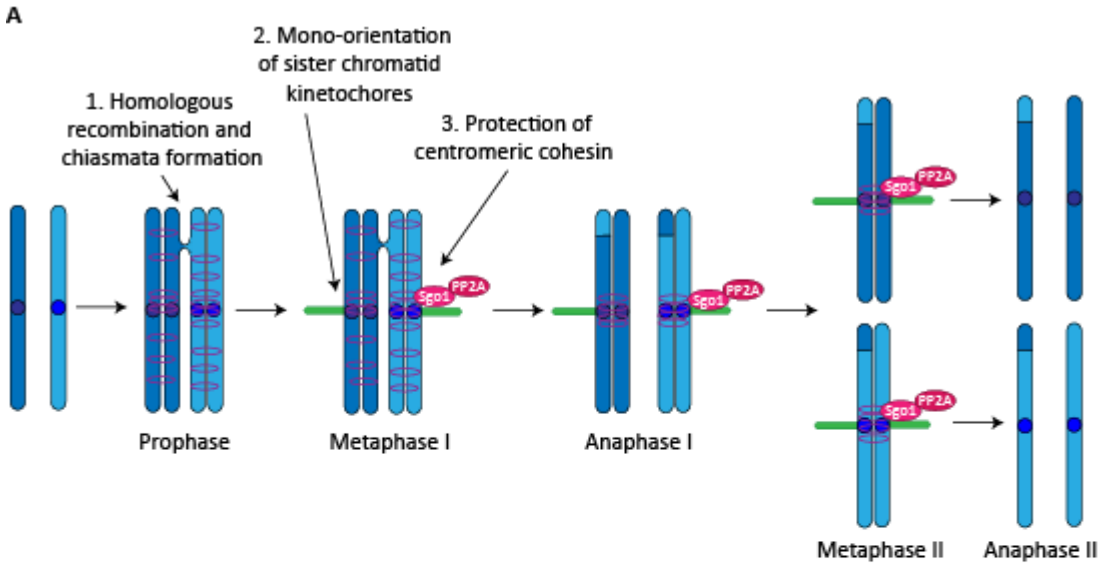

Figure 1.4.1: Chromosome segregation during meiosis in *S. cerevisiae*

A) Schematic of chromosome segregation during meiosis in budding yeast. A diploid cell enters meiosis and undergoes DNA replication and the resulting sister chromatids are held together by cohesin. During prophase homologous recombination takes place to form chiasmata that link the two homologous chromosomes (1). The monopolin complex fuses the sister chromatid kinetochores to promote mono-orientation by metaphase I and allow attachment of the homologous chromosomes to microtubules emanating from opposite poles (2). Sgo1-PP2A localises to the centromeric region of the chromosomes to protect centromeric cohesin in meiosis I (3). Prior to anaphase I, cohesin on the arms of the chromosomes is phosphorylated. Activation of separase in anaphase I allows cohesin cleavage on the arms of the chromosomes, and the homologous chromosomes are segregated into two nuclei. In metaphase II, the sister chromatid kinetochores biorient and attach to microtubules from opposite poles. The remaining centromeric cohesin is cleaved in anaphase II, and the sister chromatids are segregated into four daughter nuclei.

1.4.1 Meiosis in *S. cerevisiae* and humans

Budding yeast can exist stably in the haploid state, with two different mating types: a and α. Both haploid states can undergo cell division and replicate, however, diploid cells can be formed upon mating between a and α. Under starvation conditions or introduction into a stressful environment, the diploid budding yeast cells are induced to undergo meiosis that results in the formation of four haploid germ cells (spores), which are held together in an ascus and form a tetrad. Meiosis is an efficient survival mechanism, as the tetrads are stable and highly resistant to environmental stress. Upon the return of nutrients the budding yeast spores will germinate and once again form haploid cells that can undergo cell division (reviewed in Morgan 2007).

In humans, meiotic cell division is important for the generation of haploid gametes for sexual reproduction. In male meiosis, one diploid primary spermatocyte undergoes meiosis I and meiosis II in an analogous process to budding yeast, thus generating four haploid spermatids. In human females, the oocyte progenitor cells in the three-month old foetus undergo meiotic DNA replication and homologous recombination to stably hold the two pairs of homologous sister chromatids together with chiasmata: this state is known as a bivalent. The bivalent is arrested until maturation occurs ready for ovulation, which in humans can be decades after bivalent formation. Upon maturation, the bivalent exits from the late prophase (dictyate) arrest and undergoes the first meiotic chromosome division, half of the chromosomes are extruded into a polar body, and the secondary oocytes arrest in metaphase II. Upon fertilisation by a sperm, the secondary oocyte resumes meiosis and undergoes the final round of chromosome segregation, extruding half of the chromosomes into a second polar body. Therefore, one haploid ovum is generated from one diploid oocyte.

1.4.2 Aneuploidy in human meiosis

Incorrect chromosome segregation in meiosis also results in aneuploidy, as in mitosis. In humans, aneuploidy in gametes is thought to be the leading cause of infertility and miscarriages and is also the cause of several genetic diseases, such as Down syndrome and Edwards syndrome caused by trisomy of chromosome 21 and 18 respectively (Hassold and Hunt, 2001). It is calculated that approximately one third of miscarriages are due to aneuploidy, although this is possibly an underestimate as miscarriages very early in

pregnancy are never detected (Hassold and Hunt, 2001). Down syndrome accounts for approximately 0.1 % of live births every year world-wide, and although it is difficult to assess due to abortion rates and improved medical care, overall the number of Down syndrome pregnancies is thought to be increasing (Weijerman and de Winter, 2010). This is hypothesised to be due to an overall increase in the average maternal age, which is especially prevalent in more developed countries (Hassold and Hunt, 2001).

Human oocytes are arrested in the bivalent state for many decades, and as women age the frequency of oocytes which undergo premature separation of sister chromatids in meiosis I increases (Hassold and Hunt, 2001). One cause of this premature separation is thought to be decreased levels of cohesin on the chromosomes, which has been termed "cohesin fatigue" (Nagaoka, Hassold and Hunt, 2012). Cohesin fatigue occurs as the cohesin that is established onto the chromosomes in meiotic S phase is not replenished over time and, as oocytes age, levels of both cohesin, and the cohesin-protector shugoshin, are seen to decrease (Chiang *et al.*, 2010; Lister *et al.*, 2010; Tachibana-Konwalski *et al.*, 2010). The precise cause of this weakening of sister chromatid cohesion has yet to be determined, and it is unknown if it is due to destabilisation of cohesin or cleavage of cohesin, or simply the cohesin ring falling apart.

1.5 Meiotic cell division in *S. cerevisiae*

1.5.1 Entry into meiosis and meiotic S phase

In response to starvation, diploid budding yeast initiate meiosis through a mechanism that relies on a change in the transcriptional program of the cell. Ime1 is the transcription factor that activates the regulatory genes to promote entry into meiosis, and meiotic DNA replication and recombination. One of the targets of Ime1 is the kinase Ime2 that promotes meiotic S phase through activation of Cdc28-Clb5/6. Therefore, Ime1 and Ime2 together promote meiotic DNA replication, which occurs as in the mitotic cell cycle, and results in duplicated sister chromatids that are held together by cohesin (reviewed in Morgan 2007).

1.5.2 Prophase and homologous recombination

After meiotic DNA replication, meiotic prophase takes place during which time homologue pairing and recombination occurs. In mitotic cell division there is no programmed DNA

breaks after S phase, and any DNA damage is repaired using the sister chromatid. In meiosis, repair of programmed double-strand DNA breaks through inter-homologue recombination generates chiasmata that hold the homologous chromosomes together. In meiosis, the switch to DNA damage repair using the homologous chromosome, that results in chiasmata formation, holds the homologues together, and is crucial in ensuring faithful reductional segregation in meiosis I. Prophase is divided into morphologically distinguishable steps known as leptotene, zygotene, pachytene, diplotene and diakinesis (entry in meiosis I).

In leptotene, the newly replicated chromosomes undergo condensation and homologue pairing, resulting in two parallel chromosome axes forming that are slightly separated and not yet linked together. The nuclease Spo11 catalyses DNA double strand breaks (DSBs) in both of the sister chromatids of the homologue pair. The DSBs are resected back to form single stranded DNA that are subsequently coated by Dmc1 and Rad51 to promote initiation of recombination and allow invasion of the homologous chromosome by the single stranded DNA to form a "D loop". In zygotene the "D loops" are designated to either form a non-crossover, in which the single-stranded DNA goes back into the original homologue and is repaired, or a crossover, in which a single-end invasion is formed. This decision is coordinated with the initiation of synaptonemal complex (SC) formation only at the sites of crossovers. The SC is made up of lateral elements that are formed from the original homolog axis, and a central element that forms the central core of the SC. Bridging the central and lateral elements are the traverse filaments that includes proteins such as Zip1. Therefore, the SC forms a rail-road like structure between the two homologous chromosomes. Completion of SC formation along the length of the two homologues occurs by pachytene, and this coincides with extension of the single end invasion, interaction with the second strand of single-stranded DNA, and ultimately formation of a stable Holliday Junction. By the end of pachytene the SC is disassembled and entry into diplotene coincides with stable chiasmata and formation of the bivalent structure (reviewed in Morgan 2007).

Cohesin is an important component of the chromosome axes in early prophase, and consequently is important for chromosome pairing and synaptonemal complex formation (Brar *et al.*, 2009). Additionally cohesin is important for faithful double-strand break repair and chiasmata formation at the end of prophase (Klein *et al.*, 1999). Therefore, in addition

to cohesion of the sister chromatids, cohesin is also important for faithful meiotic recombination. Condensin also has a role in meiotic recombination in budding yeast, and localises to the rDNA early in meiosis where it is important for suppressing DSB formation (Yu and Koshland, 2003; Yu and Koshland, 2005; Li, Jin and Yu, 2014). This suppression of DSB formation and regulation of rDNA repair is important to maintain rDNA stability and ensure faithful segregation of this region of the genome (Li, Jin and Yu, 2014). In mouse oocytes, condensin I and II both localise to the longitudinal axes of bivalents (Houlard *et al.*, 2015). Depletion in oocytes revealed that the condensin II complex is important for the longitudinal condensation of the chromosomes during prophase of meiosis, and for ensuring that the bivalent chromosomes have a compact and rigid structure, that ultimately ensures the correct biorientation of the bivalent and faithful homologue segregation in meiosis I (Houlard *et al.*, 2015).

1.5.3 Exit from prophase

In budding yeast, the pachytene checkpoint prevents entry into the meiotic nuclear divisions with unrepaired DNA double-strand breaks. Satisfaction of this checkpoint results in expression of *NDT80* that encodes the transcription factor Ndt80, which activates transcription of numerous genes to initiate entry into the meiotic nuclear divisions. These genes include cyclin Clb1 to promote entry into meiosis I, as well as the polo-like kinase Cdc5 to promote mono-orientation and cohesin removal (reviewed in Morgan 2007).

1.5.4 Mono-orientation

Sister chromatid kinetochores have an intrinsic bias to form a back-to-back geometry that, in mitosis and meiosis II, promotes the kinetochores to capture of microtubules from opposite spindle pole bodies. However, in meiosis I, it is important that the homologous chromosomes are segregated in a reductional division, and that the sister chromatids co-segregate into the daughter nuclei. This faithful segregation of homologous chromosomes requires the sister chromatid kinetochores to become mono-oriented in meiosis I, and thus face towards the same spindle pole body. The monopolin complex is a four-subunit protein complex composed of Mam1, Csm1, Lrs4 and Hrr25 (casein kinase 1) (Toth *et al.*, 2000; Rabitsch *et al.*, 2003; Petronczki *et al.*, 2006). The monopolin complex bridges the two sister chromatid kinetochores and fuses them together resulting in kinetochore co-orientation and attachment to one microtubule (Corbett *et al.*, 2010; Sarangapani *et al.*, 2014). Fusion

of sister chromatid kinetochores was shown by comparison of the microtubule binding strength of purified kinetochores from mitotic or meiosis I-arrested cells by employment of a laser-trap assay, which revealed that monopolin-bound meiosis I kinetochores have stronger microtubule binding (Sarangapani *et al.*, 2014). In meiosis I, each mono-oriented pair of sister chromatids attaches to a microtubule emanating from opposite poles, and therefore the homologues reductionally segregate into two daughter nuclei. Similar to in mitosis, the condensin complex is thought to be important for kinetochore geometry in meiosis I, and condensin mutants have defects in monopolin localisation to the centromeric region, and thus have chromosome segregation defects in meiosis I (Yu and Koshland, 2003; Brito, Yu and Amon, 2010; Li, Jin and Yu, 2014).

A meiosis-specific protein known as Spo13 also localises to the centromeric region during meiosis I and is crucial for mono-orientation of sister chromatid kinetochores (Hugerat and Simchen, 1993; Shonn, McCarroll and Murray, 2002; Lee, Kiburz and Amon, 2004; Katis *et al.*, 2004b; Matos *et al.*, 2008; Mehta *et al.*, 2018). Spo13 interacts with Cdc5 kinase through a conservation Polo-box binding domain, and so localises Cdc5 to the centromeric region (Matos *et al.*, 2008). This localisation of Cdc5 is crucial for maintenance of the monopolin complex at kinetochores and for promoting mono-orientation, possibly through phosphorylation of Lrs4 by Cdc5 (Shonn, McCarroll and Murray, 2002; Lee and Amon, 2003; Lee, Kiburz and Amon, 2004; Katis *et al.*, 2004b; Monje-Casas *et al.*, 2007; Matos *et al.*, 2008; Attner *et al.*, 2013). Additionally, DDK is also important for mono-orientation in meiosis I (Matos *et al.*, 2008).

1.5.5 Meiosis I and centromeric cohesin protection

In meiosis, the mitosis-specific kleisin subunit of cohesin (Scc1) is replaced by a meiosis-specific kleisin subunit known as Rec8 (Klein *et al.*, 1999; Watanabe and Nurse, 1999; Buonomo *et al.*, 2000). Phosphorylation of the Rec8 subunit of cohesin on multiple residues by the protein kinases Hrr25, Cdc5 and DDK prior to meiosis I is crucial for cleavage of Rec8 by separase (Lee and Amon, 2003; Brar *et al.*, 2006; Ishiguro *et al.*, 2010; Katis *et al.*, 2010; Attner *et al.*, 2013). However, in meiosis I the centromeric cohesin must be protected from cleavage in order to maintain cohesion between the sister chromatids until meiosis II. Therefore, Rec8 at the centromeres must be maintained in a dephosphorylated state and protected in meiosis I (reviewed in (Marston, 2015).

The shugoshin family of proteins are essential for centromeric cohesin protection in meiosis I throughout evolution (Kerrebrock *et al.*, 1995; Katis *et al.*, 2004a; Kitajima, Kawashima and Watanabe, 2004; Marston *et al.*, 2004; Rabitsch *et al.*, 2004; Salic, Waters and Mitchison, 2004; McGuinness *et al.*, 2005). Sgo1-PP2A localises to the centromeric region from late prophase of meiosis, and is crucial for dephosphorylating centromeric Rec8, and therefore protecting the centromeric cohesin from cleavage (Katis *et al.*, 2004a; Kitajima, Kawashima and Watanabe, 2004; Marston *et al.*, 2004; Kiburz *et al.*, 2005; Brar *et al.*, 2006; Riedel *et al.*, 2006; Xu *et al.*, 2009; Katis *et al.*, 2010). Deletion of *SGO1* results in random segregation of sister chromatids in meiosis II due to loss of the centromeric cohesion (Lee and Amon, 2003; Katis *et al.*, 2004a; Kitajima, Kawashima and Watanabe, 2004; Marston *et al.*, 2004; Riedel *et al.*, 2006). In mouse, the Sgo2 member of the shugoshin family is essential for centromeric cohesin protection, and Sgo2-null mice are infertile due to premature loss of centromeric cohesin (Lee *et al.*, 2008; Llano *et al.*, 2008). Additionally, in budding yeast, Sgo1 is also important in kinetochore orientation in meiosis (as in mitosis), although this has a minor role in promoting faithful chromosome segregation (Katis *et al.*, 2004a; Kiburz, Amon and Marston, 2008; Mehta *et al.*, 2018). Similarly, condensin mutants also have gross DNA segregation defects in both meiosis I and II, therefore suggesting that condensin may have a role in meiotic kinetochore geometry, as well as in condensing and detangling the DNA to allow faithful segregation (Yu and Koshland, 2003; Yu and Koshland, 2005; Brito, Yu and Amon, 2010; Li, Jin and Yu, 2014; Houlard *et al.*, 2015).

However, it is not just Sgo1-PP2A that is important for centromeric cohesin protection. In addition to a role in mono-orientation of sister chromatid kinetochores, Spo13 is important for protection of centromeric cohesin in meiosis I (Shonn, McCarroll and Murray, 2002; Lee, Kiburz and Amon, 2004; Katis *et al.*, 2004b). Diploid cells lacking *SPO13* undergo one meiotic division to form dyads during which chromosomes segregate both reductionally and equationally due to a loss of both sister kinetochore mono-orientation and centromeric cohesin (Klapholz and Esposito, 1980; Wang *et al.*, 1987; Hugerat and Simchen, 1993; Shonn, McCarroll and Murray, 2002). The mechanism by which Spo13 protects centromeric cohesin is still debated. But the role of Spo13 is conserved throughout evolution, and in mouse Meikin interacts with Plk1 and is important in both mono-orientation and protection of centromeric cohesin, and in *S. pombe* this role is carried out by Moa1 (Kim *et al.*, 2015).

As in mitosis, correct attachment of microtubules to the mono-oriented sister chromatid kinetochores results in the generation of tension, and silencing of the spindle assembly checkpoint. This results in the destruction of securin and activation of separase to cleave Rec8 along the arms of the chromosomes and allow homologue segregation into two daughter nuclei in anaphase I (Buonomo *et al.*, 2000; Salah and Nasmyth, 2000; Marston, 2014).

1.5.6 Meiosis II

Segregation of the homologous chromosomes in anaphase I results in a binucleate cell with pairs of cohered sister chromatids in each nuclei. In mitosis, chromosome segregation is always followed by DNA replication before another round of chromosome segregation occurs. However, sister chromatid segregation in meiosis II must occur after meiosis I, without an intervening round of DNA replication. At the end of meiosis I, activation of the FEAR network results in Cdc14 release from the nucleolus, that causes reversal of CDK-dependent phosphorylation, spindle disassembly and spindle pole body re-duplication (Buonomo *et al.*, 2003; Marston, Lee and Amon, 2003; Fox *et al.*, 2017). However, the MEN is not activated and therefore there is no replication origin licensing and entry into DNA replication is not initiated. Therefore, the action of Cdc14 phosphatase allows a second round of chromosome segregation on a new pair of spindles (reviewed in (Marston, 2014)).

In meiosis II, the sister chromatids undergo a mitosis-like division. The sister kinetochores biorient and attach to microtubules emanating from opposite poles, which causes the centromeric region to come under tension. However, unlike in mitosis, centromeric cohesin must be de-protected, as Rec8 phosphorylation is required for cleavage by separase. In meiosis II, Mps1 kinase is responsible for localisation of Sgo1-PP2A to the centromeric region in budding yeast (Arguello-Miranda *et al.*, 2017). To allow deprotection, Mps1 kinase is degraded by the APC/C, resulting in Sgo1-PP2A delocalisation from the centromeric region (Arguello-Miranda *et al.*, 2017; Jonak *et al.*, 2017). Sgo1 is then also degraded by the activity of the APC/C (Jonak *et al.*, 2017). This removes PP2A from the centromeric region, allowing Hrr25 to phosphorylate Rec8 and thus promote cleavage by separase (Arguello-Miranda *et al.*, 2017). Stabilisation of Mps1 and Sgo1 in meiosis II by mutation of the degradation boxes (D-boxes) of these proteins prevents nuclear division in meiosis II due to

prolonged protection of centromeric Rec8 (Arguello-Miranda *et al.*, 2017). As anaphase II occurs, the sister chromatids are segregated into four nuclei. In budding yeast, the four nuclei are packaged into spores and a tetrad is formed.

1.6 The role of the prophase pathway components in meiosis

1.6.1 Wapl is important for meiotic recombination and for removal of cohesin prior to meiosis I

In budding yeast meiosis, cohesin is removed from the chromosomes in two consecutive steps through cleavage of Rec8 by separase, however there is increasing evidence for a period of cohesin destabilisation prior to meiosis I (Yu and Koshland, 2005; Challa *et al.*, 2019). In late prophase, phosphorylation of Rec8 by Cdc5 and DDK promotes cohesin destabilisation by Rad61, which is itself activated through phosphorylation by Cdc5 and DDK (Challa *et al.*, 2019). In mouse spermatocytes, Wapl is present in prophase and removes a pool of cohesin (including sororin) from the chromosomes prior to meiosis I (Kuroda *et al.*, 2005; Zhang *et al.*, 2008a; Brieno-Enriquez *et al.*, 2016). To destabilise cohesin, Wapl must be maintained in the dephosphorylated state by protein phosphatase 1γ (PP1γ), which itself has to be activated by phosphorylation by NEK1 kinase (Brieno-Enriquez *et al.*, 2016). Thus Wapl is differentially regulated by phosphorylation in budding yeast and mouse. Interestingly, in *Caenorhabditis elegans* (*C. elegans*), WAPL-1 does not destabilise cohesin containing the Rec8 kleisin subunit in meiosis, but instead only destabilises cohesin which contains the alternative kleisin subunits COH-3 or COH-4 (Crawley *et al.*, 2016).

Wapl also has additional roles in meiosis aside from destabilisation of cohesin. In *C. elegans*, during prophase, WAPL-1 is important for the timing of axial element formation and morphogenesis, as well as for DSB repair (Crawley *et al.*, 2016). This is similar to in budding yeast meiosis, in which Rad61 is important for timely DSB repair and processing of Holliday Junction intermediates (Challa *et al.*, 2016).

1.6.2 Eco1 homologues have diverse functions in meiosis

The role of Eco1 has not been studied in budding yeast meiosis, although there is some evidence of Smc3-K112,K113 acetylation in meiotic chromatin fractionation experiments (Challa *et al.*, 2019). In *S. pombe*, Eso1 acetylates the Smc3 homologue, Psm3, at the

conserved sites Psm3-K105,K106, and mutation of these sites to non-acetylatable arginine results in premature loss of chromatid cohesion (Kagami *et al.*, 2011). Eso1 was found to have a further role in promoting mono-orientation of sister chromatid kinetochores in meiosis I through acetylation of a so-far-undefined target (Kagami *et al.*, 2011). Therefore, in *S. pombe*, Eso1 acetylates at least two different targets to promote faithful chromosome segregation.

In higher eukaryotes, Esco1 and Esco2 acetylate cohesin in mitosis, however, neither of these acetyltransferases have been directly shown to acetylate cohesin in mammalian meiosis (Hou and Zou, 2005; Zhang *et al.*, 2008b; Song *et al.*, 2012; Ladurner *et al.*, 2016; Alomer *et al.*, 2017). Both Esco1 and Esco2 are important for faithful meiotic chromosome segregation through acetylation of α-Tubulin-K40 and Histone H4-K16 respectively (Lu *et al.*, 2017; Lu *et al.*, 2018). Acetylated Smc3 has been detected in mouse oocytes, and co-localises with Rec8-cohesin on the chromosome axes of bivalents in prometaphase I by immunostaining (Reichmann *et al.*, 2017). The germline genome defence gene, Tex19.1, protects chromatin-associated acetylated Smc3 in mouse oocytes, potentially by inhibiting the activity of Ubr2 E3 ubiquitin ligase (Reichmann *et al.*, 2017). Tex19.1 maintains arm cohesion through specifically protecting acetylated cohesin, which promotes faithful homolog segregation and maintenance of sister chromatid cohesion, and so prevents aneuploidy (Reichmann *et al.*, 2017).

In meiosis I and meiosis II, sororin localises to the centromeric regions of chromosomes in a PP2A-dependent manner, and loss of sororin results in precocious separation of sister chromatids, suggesting that sororin may be protecting centromeric acetylated cohesin (Gomez *et al.*, 2016; Huang *et al.*, 2017). Sororin is also present in prophase of mouse spermatocyte meiosis and localises to the lateral and central elements of synapsed chromosomes independently of cohesin, suggesting that sororin may also have a meiosis-specific, cohesin-independent role (Gomez *et al.*, 2016; Jordan *et al.*, 2017).

1.7 Aims of this study

Aim 1: Define the interaction between Sgo1 and condensin, and characterise the role of condensin in meiosis

In mitosis, condensin is important in chromosome condensation and global DNA segregation. Sgo1 recruits the condensin complex to the centromeric and pericentromeric regions. This is important for kinetochore biorientation, and promotes faithful sister chromatid segregation. During meiosis, condensin is also important for faithful DNA segregation. However, it is unknown if condensin also localises to the centromeric region in an Sgo1-dependent manner in meiosis I and II, and if this has a role in kinetochore orientation. In this study, I aimed to further characterise the chromosome segregation defects of condensin mutants in meiosis and to address the role of condensin at the centromeres through generation of a Sgo1 allele to specifically disrupt the interact with condensin.

Aim 2: Characterise the role of Sgo1 phosphorylation in meiosis

Post-translational modification of shugoshin throughout evolution is important for both promoting and inhibiting shugoshin function, and for its correct localisation to the pericentromeric region. Recently, Hrr25 has been shown to regulate Sgo1 removal from centromeres in meiosis II in budding yeast to allow cohesin deprotection and cleavage. Mass spectrometry analysis of Sgo1 purified from budding yeast revealed numerous phosphorylation sites on Sgo1, some of which were only found in meiosis I. I aimed to determine the functional importance of these phosphorylation sites for the Sgo1 cohesin-protection function in meiosis.

Aim 3: Determine the role of the conserved prophase pathway components in budding yeast meiosis

In mammalian mitosis, cohesin from the chromosome arms is removed through destabilisation by Wapl in prophase, whilst shugoshin protects the centromeric cohesin until anaphase, when the kleisin subunit is cleaved by separase. In budding yeast mitosis, there is no known cohesin destabilisation step prior to metaphase. However, in meiosis there is increasing evidence for cohesin destabilisation during prophase I by the Wapl homologue, Rad61. I aimed to characterise the role of cohesin acetylation by Eco1 and the function of Rad61 in chromosome segregation in budding yeast meiosis. Additionally, I

aimed to determine whether the cohesin protectors, Sgo1 and Spo13, protect the centromeric pool of cohesin from the destabilisation pathway.

Chapter 2. The function of the interaction between Sgo1 and condensin in budding yeast meiosis

2.1 Introduction

In budding yeast, *Saccharomyces cerevisiae*, there is one shugoshin protein, Sgo1, that has roles in chromosome segregation in both mitosis and meiosis (Katis *et al.*, 2004a; Kitajima, Kawashima and Watanabe, 2004; Marston *et al.*, 2004; Rabitsch *et al.*, 2004). Sgo1 was first identified as the protector of centromeric cohesin in meiosis I in budding yeast (Katis *et al.*, 2004a; Kitajima, Kawashima and Watanabe, 2004; Marston *et al.*, 2004; Rabitsch *et al.*, 2004; Kiburz *et al.*, 2005). In meiosis, the cohesin complex is made up of two SMC proteins, Smc1 and Smc3, and the meiosis-specific kleisin subunit, Rec8. Prior to the first meiotic division, Rec8 is phosphorylated by Dbf4-dependent kinase (DDK), Casein kinase (Hrr25) and Polo kinase (Cdc5), which makes Rec8 susceptible to cleavage by separase in meiosis I (Lee and Amon, 2003; Brar *et al.*, 2006; Ishiguro *et al.*, 2010; Katis *et al.*, 2010; Attner *et al.*, 2013). Sgo1 localises to a 50 kb centromeric and pericentromeric region of the chromosomes (Katis *et al.*, 2004a; Kitajima, Kawashima and Watanabe, 2004; Marston *et al.*, 2004; Kiburz *et al.*, 2005), and recruits PP2A-Rts1 to this region to dephosphorylate Rec8 (Brar *et al.*, 2006; Riedel *et al.*, 2006; Katis *et al.*, 2010). Loss of Sgo1 function in meiosis, either by deletion of *SGO1,* or by meiosis specific depletion through placing *SGO1* under the mitosis specific *CLB2* promoter (*pCLB2-SGO1*), results in all cohesin being cleaved in meiosis I, and random sister chromatid segregation occurring in meiosis II (Lee and Amon, 2003; Katis *et al.*, 2004a; Kitajima, Kawashima and Watanabe, 2004; Marston *et al.*, 2004; Brar *et al.*, 2006; Riedel *et al.*, 2006). The *SGO1* allele, *sgo1-3A*, has three point mutations in the N-terminal coiled-coil domain that specifically disrupts binding to PP2A-Rts1, resulting in random meiosis II chromosome segregation due to loss of the centromeric phosphatase (Xu *et al.*, 2009).

The cohesin protection function of Sgo1 is not conserved in budding yeast mitosis (Katis *et al.*, 2004a; Indjeian, Stern and Murray, 2005; Kiburz *et al.*, 2005; Verzijlbergen *et al.*, 2014). In mitosis, cohesin is loaded onto the sister chromatids as the DNA is replicated. This coheres the sister chromatids together until anaphase, when all of the cohesin holding the sister chromatids together is cleaved by separase, allowing chromosome segregation into two daughter cells. In mitosis, the kleisin subunit of cohesin is Scc1, and although phosphorylation of Scc1 by Cdc5 does enhance the efficiency of cleavage by separase, it is

not essential, as in the case of phosphorylation of Rec8 (Alexandru *et al.*, 2001). It was found that Sgo1-PP2A-Rts1 had no discernible cohesin-protection function in mitosis, and no premature loss of cohesion was observed prior to anaphase in *SGO1* mutants (Katis *et al.*, 2004a; Indjeian, Stern and Murray, 2005; Kiburz *et al.*, 2005; Verzijlbergen *et al.*, 2014).

However, Sgo1 does have functions in kinetochore biorientation and tension sensing in mitosis (Indjeian, Stern and Murray, 2005; Fernius and Hardwick, 2007; Indjeian and Murray, 2007; Storchova *et al.*, 2011; Eshleman and Morgan, 2014; Nerusheva *et al.*, 2014; Peplowska, Wallek and Storchova, 2014; Verzijlbergen *et al.*, 2014). After DNA replication, the kinetochores on sister chromatids need to attach to microtubules emanating from opposite spindle pole bodies, called sister kinetochore biorientation. This is facilitated because sister kinetochores are intrinsically biased to form a back-to-back geometry, thus predisposing them to capture microtubules from opposite poles (Indjeian and Murray, 2007). *SGO1* mutants have defects in this bias to biorient, since sister kinetochores attach to microtubules from the same pole more frequently than wild type cells after treatment with microtubule depolymerising drugs such as nocodazole (Indjeian, Stern and Murray, 2005; Fernius and Hardwick, 2007; Indjeian and Murray, 2007; Storchova *et al.*, 2011; Eshleman and Morgan, 2014; Nerusheva *et al.*, 2014; Peplowska, Wallek and Storchova, 2014; Verzijlbergen *et al.*, 2014). This role of Sgo1 in correct kinetochore orientation also operates in meiosis (Kiburz, Amon and Marston, 2008), and this is a conserved function carried out by Sgo2 in fission yeast (Vaur *et al.*, 2005).

In addition to biorientation defects, *SGO1* mutants have increased syntelic attachments due to defective tension sensing (Indjeian, Stern and Murray, 2005; Fernius and Hardwick, 2007; Indjeian and Murray, 2007; Storchova *et al.*, 2011; Eshleman and Morgan, 2014; Nerusheva *et al.*, 2014; Peplowska, Wallek and Storchova, 2014; Verzijlbergen *et al.*, 2014). When biorientation is achieved, microtubules from opposite poles attach to the kinetochores, and exert a pulling force on them. The pericentromeric cohesin counteracts this pulling force, thus generating tension that separates the centromeres of the sister chromatids (Tanaka *et al.*, 2000). If both kinetochores attach to the same spindle pole body (syntelic attachment) then there is no tension generated, and Aurora B kinase (Ipl1), a component of the Chromosomal Passenger Complex (CPC), destabilises these incorrect attachments through phosphorylation (Cheeseman *et al.*, 2002; Pinsky *et al.*, 2006; Akiyoshi *et al.*, 2009; Demirel

et al., 2012; Krenn and Musacchio, 2015). Sgo1 is important for Ipl1 maintenance at centromeres, and for ensuring Ipl1 is removed once kinetochores are under tension to prevent disruption of correct attachments (Nerusheva *et al.*, 2014; Peplowska, Wallek and Storchova, 2014; Verzijlbergen *et al.*, 2014). In *SGO1* mutants, Ipl1 is not maintained at centromeres, and incorrect kinetochore-microtubule attachments that fail to come under tension are not released so syntelic attachments are not corrected, resulting in aneuploidy (Peplowska, Wallek and Storchova, 2014; Verzijlbergen *et al.*, 2014).

PP2A-Rts1 may also contribute to kinetochore biorientation and tension sensing in mitosis, however its exact function is unclear as some data in the literature is contradictory (Storchova *et al.*, 2011; Eshleman and Morgan, 2014; Peplowska, Wallek and Storchova, 2014; Verzijlbergen *et al.*, 2014). Deletion of *RTS1* was found to not cause biorientation defects (Eshleman and Morgan, 2014; Verzijlbergen *et al.*, 2014), however *rts1Δ* is lethal in mutants which have increased levels of syntelic attachments, suggesting that it may have a role (Peplowska, Wallek and Storchova, 2014). Interestingly, *sgo1-3A*, the shugoshin allele that disrupts the interaction with PP2A-Rts1 (Xu *et al.*, 2009), has impaired kinetochore biorientation (Eshleman and Morgan, 2014; Verzijlbergen *et al.*, 2014), and this is rescued by tethering Rts1 back to kinetochores (Eshleman and Morgan, 2014). A possible explanation may be that the *sgo1-3A* mutant delocalises all PP2A from centromeres, including both PP2A-Rts1 and PP2A-Cdc55, whereas *rts1Δ* will only delocalise the PP2A-Rts1 pool. *CDC55* mutants do not have biorientation defect (Storchova *et al.*, 2011), but this could be due to PP2A-Rts1 being present at centromeres. Furthermore, the dependence of Ipl1 localisation on PP2A-Rts1 is unclear, and subtle variations in experimental conditions may cause differing results (Peplowska, Wallek and Storchova, 2014; Verzijlbergen *et al.*, 2014).

Condensin is a highly conserved member of the SMC family of proteins, and is comprised of two SMC proteins, Smc2 and Smc4, a kleisin subunit, Brn1, and two accessory subunits, Ycg1 (Ycs5) and Ycs4 (Freeman, Aragon-Alcaide and Strunnikov, 2000). Mutants of the condensin complex have major defects in DNA condensation and chromosome segregation during mitosis, and lagging chromosomes that form anaphase bridges due to the rDNA becoming tangled (Strunnikov, Hogan and Koshland, 1995; Freeman, Aragon-Alcaide and Strunnikov, 2000; Lavoie *et al.*, 2000; Bhalla, Biggins and Murray, 2002; Lavoie, Hogan and

Koshland, 2002). In *S. cerevisiae* and *S. pombe*, condensin is localised to the rDNA throughout the cell cycle, and this is dependent on Csm1 and Lrs4 (Pcs1 and Mde4 respectively in *S. pombe*) (Freeman, Aragon-Alcaide and Strunnikov, 2000; Bhalla, Biggins and Murray, 2002; Lavoie, Hogan and Koshland, 2002; Wang *et al.*, 2005; Bachellier-Bassi *et al.*, 2008; Johzuka and Horiuchi, 2009; Tada *et al.*, 2011).

In addition to the role of condensin in chromosome condensation, throughout evolution there is evidence for the importance of condensin at the centromere. In higher eukaryotes, condensin I localises to the centromeric region from prometaphase until anaphase, and stabilises the centromeric chromatin structure to withstand the pulling forces of the spindle, by increasing the "stiffness" of the chromatin (Gerlich *et al.*, 2006; Ribeiro *et al.*, 2009). This means that when the microtubules correctly attach to the bioriented kinetochores, these can act in a spring-like manner, and withstand the tension forces (Ribeiro *et al.*, 2009; Stephens *et al.*, 2011). In *S. pombe* the centromeric localisation of condensin depends on the Pcs1-Mde4 complex and H2A (or H2AZ), and delocalisation of condensin results in sensitivity to microtubule depolymerising drugs and in lagging chromosomes (Tada *et al.*, 2011).

Purification and mass spectrometry analysis of Sgo1 from budding yeast arrested in metaphase of mitosis, identified the condensin complex as a binding partner (Verzijlbergen *et al.*, 2014). Sgo1 was found to be required to localise condensin to the centromeric region prior to metaphase, until it delocalises from this region once kinetochores come under tension (Freeman, Aragon-Alcaide and Strunnikov, 2000; Wang *et al.*, 2005; Yong-Gonzalez *et al.*, 2007; Bachellier-Bassi *et al.*, 2008; D'Ambrosio *et al.*, 2008; Stephens *et al.*, 2011; Tada *et al.*, 2011; Peplowska, Wallek and Storchova, 2014; Verzijlbergen *et al.*, 2014; Leonard *et al.*, 2015). This release has been proposed to be Cdc5-dependent (Leonard *et al.*, 2015). Similar to *SGO1* mutants, condensin mutants have severe biorientation defects and lose the intrinsic bias to form a back-to-back geometry (Yong-Gonzalez *et al.*, 2007; Peplowska, Wallek and Storchova, 2014; Verzijlbergen *et al.*, 2014). Therefore the role of condensin in forming a rigid DNA structure to withstand the pulling forces once the microtubules attach to kinetochores during metaphase appears to be conserved (Gerlich *et al.*, 2006; Yong-Gonzalez *et al.*, 2007; D'Ambrosio *et al.*, 2008; Ribeiro *et al.*, 2009; Stephens

et al., 2011; Tada *et al.*, 2011; Peplowska, Wallek and Storchova, 2014; Verzijlbergen *et al.*, 2014).

Condensin is also important in budding yeast meiosis, as condensin mutants have gross DNA missegregation during meiosis, and fail to form viable spores (Yu and Koshland, 2003). As in mitosis, condensin localises to the rDNA early in meiosis. In metaphase, condensin disperses in a Cdc5-dependent manner, before re-localising to the rDNA in anaphase (Yu and Koshland, 2003; Yu and Koshland, 2005; Li, Jin and Yu, 2014). At the rDNA, condensin is important in suppressing double-strand break formation during meiotic recombination, and also in preventing rDNA missegregation during anaphase I (Li, Jin and Yu, 2014). Additional to this role at the rDNA, condensin mutants have defects in meiotic recombination throughout the genome, with a reduction in DSB formation, and a decrease in the bias to form Holliday Junction's between homologous chromosomes rather than sister chromatids (Hong, Choi and Kim, 2015). This results in a defect in synaptonemal complex formation, a reduction in homologue pairing, and resultant homologue segregation defects (Yu and Koshland, 2003; Yu and Koshland, 2005; Brito, Yu and Amon, 2010; Li, Jin and Yu, 2014; Hong, Choi and Kim, 2015).

Condensin mutants have defects in localisation of the monopolin complex to the centromeric region that results in meiosis I segregation defects, and in addition, these mutants also have defects in meiosis II DNA segregation (Yu and Koshland, 2003; Brito, Yu and Amon, 2010; Li, Jin and Yu, 2014). Therefore these data have led to the hypothesis that condensin may play a role at centromeres in meiosis, as in mitosis. In this chapter my aim was to analyse chromosome segregation in condensin mutants in comparison to *SGO1* mutants, and to determine if condensin localises to the centromeric region in a Sgo1-dependent manner. To address the role of condensin specifically at centromeres, I initially also aimed to determine the interacting regions of Sgo1 and condensin, with a view to generation of an Sgo1 mutant that would specifically disrupt condensin association with centromeres.

2.2 Results

2.2.1 Sgo1 is required for faithful chromosome segregation in meiosis I and II

SGO1 was identified as a gene, which when deleted, resulted in random segregation of sister chromatids during meiosis II due to complete loss of centromeric cohesin in meiosis I (Katis *et al.*, 2004a; Kitajima, Kawashima and Watanabe, 2004; Marston *et al.*, 2004; Rabitsch *et al.*, 2004). I first aimed to reproduce the results from the microscopy screen of non-essential genes carried out by Marston 2004 that identified *SGO1*, to ensure that I could visualise the same chromosome missegregation phenotype, to allow later comparison to condensin mutants.

Chromosome missegregation in meiosis can be evaluated by using a microscopy assay to analyse the segregation of chromosome V. To visualise chromosome V, 224 *tetO* sequences are integrated at the centromere. The cells constitutively express TetR-GFP, which binds to the *CEN5 tetO* array, producing a fluorescently labelled section of the DNA that can be visualised by fluorescence microscopy, and will hereafter be described as a *CEN5 tetO*/TetR-GFP dot (Figure 2.2.1.1A) (Michaelis, Ciosk and Nasmyth, 1997). As diploid cells homozygous for *CEN5 tetO*/TetR-GFP dots undergo meiosis I, one GFP (Green Fluorescent Protein) dot will be visualised in each nucleus of the binucleate cell, due to the homologues segregating to opposite poles (Figure 2.2.1.1B). During the second meiotic division the sister chromatids segregate, resulting in one GFP foci in each nucleus of the tetranucleate (Figure 2.2.1.1B).

I first compared chromosome segregation of wild type with *sgo1Δ* and *pCLB2-3HA-SGO1* cells. The *pCLB2-3HA-SGO1* construct allows specific depletion of Sgo1 during meiosis, by preventing *SGO1* expression through placing *SGO1* under the *CLB2* promoter that is inactive during meiosis but is active in mitosis (Lee, Kiburz and Amon, 2004). Due to premature loss of centromeric cohesin during meiosis I in *SGO1* mutants, random segregation of sister chromatids in meiosis II occurs, resulting in an increase in tetranucleates with GFP dots in three out of four nuclei (Figure 2.2.1.2A) (Katis *et al.*, 2004a; Kitajima, Kawashima and Watanabe, 2004; Marston *et al.*, 2004; Rabitsch *et al.*, 2004; Riedel *et al.*, 2006; Brar *et al.*, 2006).

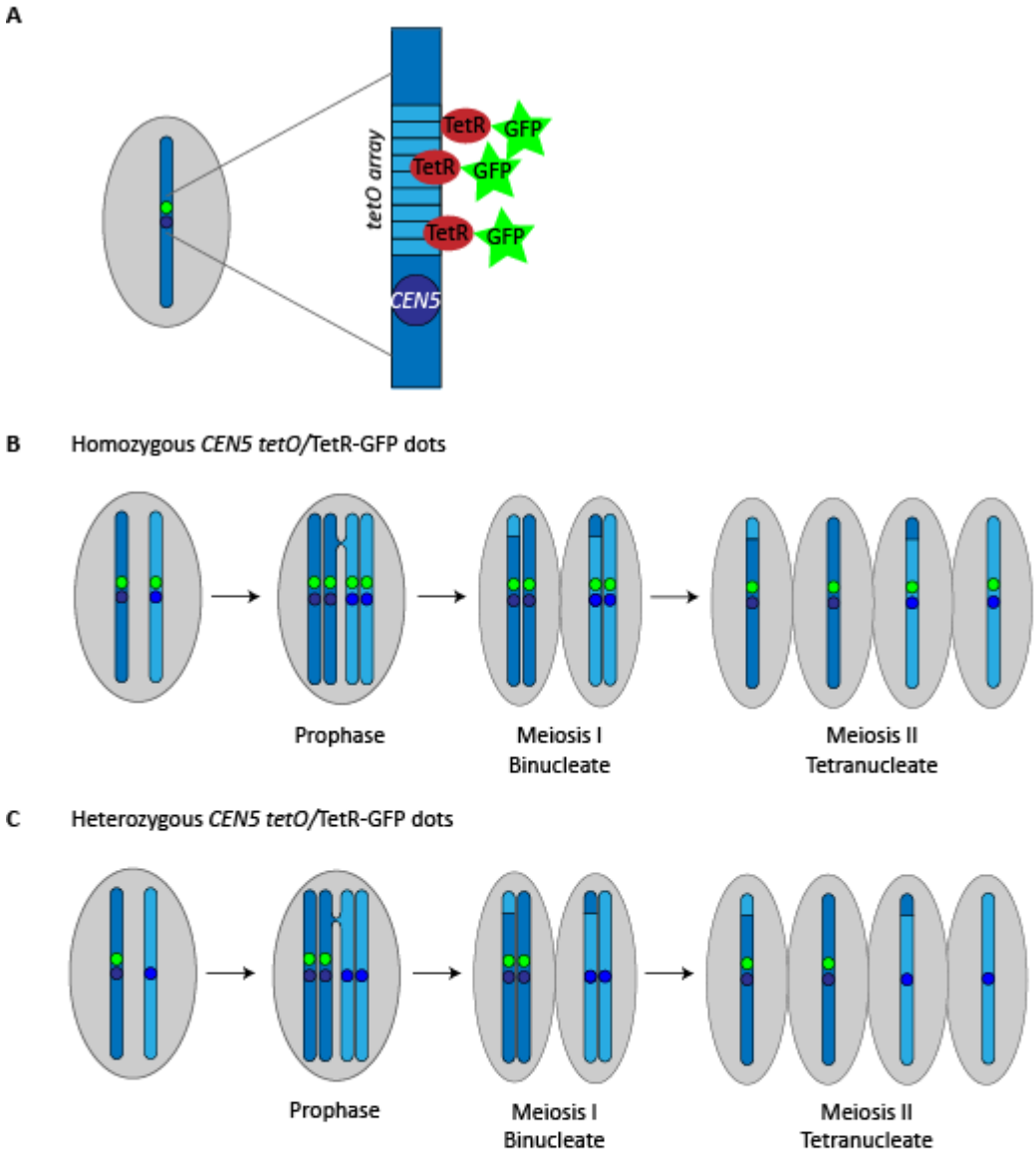

Figure 2.2.1.1: Schematic of homozygous and heterozygous GFP dot segregation in meiosis
Schematic of homozygous and heterozygous *CEN5 tetO*/TetR-GFP dot segregation in meiosis. A) A diploid cell has 224 *tetO* arrays integrated at *CEN5* of chromosome V. The cells constitutively express TetR-GFP that binds to the *tetO* arrays, and produces a GFP dot. During meiosis, the fluorescent dots can be visualised by fluorescence microscopy, thus providing information on the segregation of chromosome V. B) Schematic of a diploid cell undergoing meiosis with *tetO* arrays integrated at both copies of *CEN5* to produce homozygous GFP dots. The resulting tetranucleates contain one GFP dot in each nuclei. This assay allows homologous chromosome bi-orientation to be assesssed in the binucleates, and for precocious loss of sister chromatid cohesion and loss of sister chromatid bi-orientation to be assessed in the tetranucleates. C) Schematic of a diploid cell undergoing meiosis with *tetO* arrays integrated at one copy of *CEN5* to produce heterozygous GFP dots. The resulting tetranucleates contain one GFP dot in two of the nuclei, with two nuclei remaining empty. This assay allows premature separation of sister chromatids, due to a loss of mono-orientationand premature loss of centromeric cohesion between sister chromatids, to be assessed in the binucleates, and for defective bi-orientation of sister chromatids to be assessed in the tetranucleates.

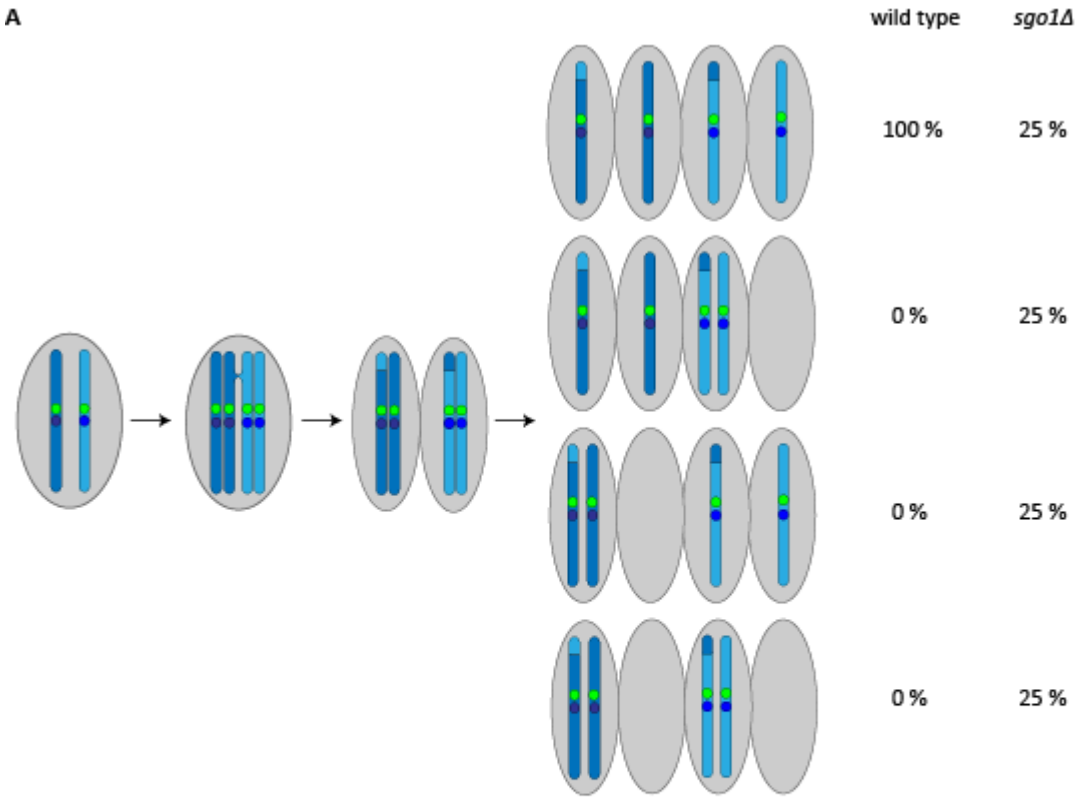

Figure 2.2.1.2: Schematic of random homozygous GFP dot segregation in meiosis in *SGO1* mutants
A) Schematic of homozygous *CEN5 tetO/*TetR-GFP dot segregation in meiosis in wild type and *sgo1Δ*. In a diploid cell homozygous for *CEN5 tetO/*TetR-GFP dots, after meiosis I one GFP dot will be in each half of the binucleate cell. After meiosis II in a wild type cell, one GFP dot will segregate into each of the four nuclei of the tetranucleate. In *sgo1Δ*, all of the cohesin is cleaved in the first meiotic division, therefore the sister chromatids segregate randomly in meiosis II. This results in, theoretically, 25 % of cells containing one GFP dot in all nuclei of the tetranucleate, 50 % of cells containing GFP dots in three out of four nuclei, and 25 % of cells containing GFP dots in two out of four nuclei.

Diploid wild type, *sgo1Δ* and *pCLB2-3HA-SGO1* strains, homozygous for *CEN5 tetO*/TetR-GFP dots, were placed in sporulation media and meiotic progression followed by DAPI staining. The *pCLB2-3HA-SGO1* diploids formed tetranucleates to a wild type level of 75 %, but *sgo1Δ* were less efficient in undergoing meiosis with only 50 % cells forming tetranucleates (Figure 2.2.1.3A). This decrease in tetranucleate formation in *sgo1Δ* diploids is likely due aneuploidy having occurred during vegetative growth that results in increased sickness of the cells, which prevents entry into meiosis. After 10 h in sporulation media *CEN5 tetO*/TetR-GFP dot segregation was analysed by fluorescence microscopy (Figure 2.2.1.3B). The wild type cells faithfully segregated chromosome V in 96 % of cells, compared to *sgo1Δ* that had under 40 % correct chromosome segregation, consistent with previously published results (Katis *et al.*, 2004a; Kitajima, Kawashima and Watanabe, 2004; Marston *et al.*, 2004; Rabitsch *et al.*, 2004; Riedel *et al.*, 2006; Brar *et al.*, 2006). *CEN5 tetO*/TetR-GFP dot segregation was also analysed in *pCLB2-3HA-SGO1*, and showed that 45 % of tetranucleates had missegregated chromosome V, therefore confirming that the meiosis specific depletion of *SGO1* also caused random segregation of sister chromatids (Figure 2.2.1.3B).

Sgo1 may also have a role in faithful homologue segregation in the first meiotic division due to additional roles in kinetochore orientation and tension sensing (Katis *et al.*, 2004a; Kiburz, Amon and Marston, 2008; Mehta *et al.*, 2018), although this is debated (Marston *et al.*, 2004). To clarify the role of Sgo1 in homologue segregation, I analysed the segregation of the homozygous *CEN5 tetO*/TetR-GFP dots at the binucleate stage. After meiosis I in a wild type binucleate there should be one GFP dot in each nucleus (Figure 2.2.1.1B). Analysis of *sgo1Δ* and *pCLB2-3HA-SGO1* binucleate cells showed that a high percentage contained two GFP dots in one or both nuclei, due to the premature loss of centromeric Rec8 in anaphase I. However, interestingly, in both *sgo1Δ* and *pCLB2-3HA-SGO1* mutants, 10 % and 17 % of binucleates respectively, had one nucleus that did not contain a *CEN5 tetO*/TetR-GFP dot (Figure 2.2.1.3C). Therefore Sgo1 may have a role in correct biorientation of homologous chromosomes, or a role in sensing the tension of correct kinetochore-microtubule attachments (Katis *et al.*, 2004a; Kiburz, Amon and Marston, 2008).

2.2.2 Condensin is required for faithful chromosome segregation in meiosis

In meiosis, condensin is essential for faithful DNA segregation, as condensin mutants have

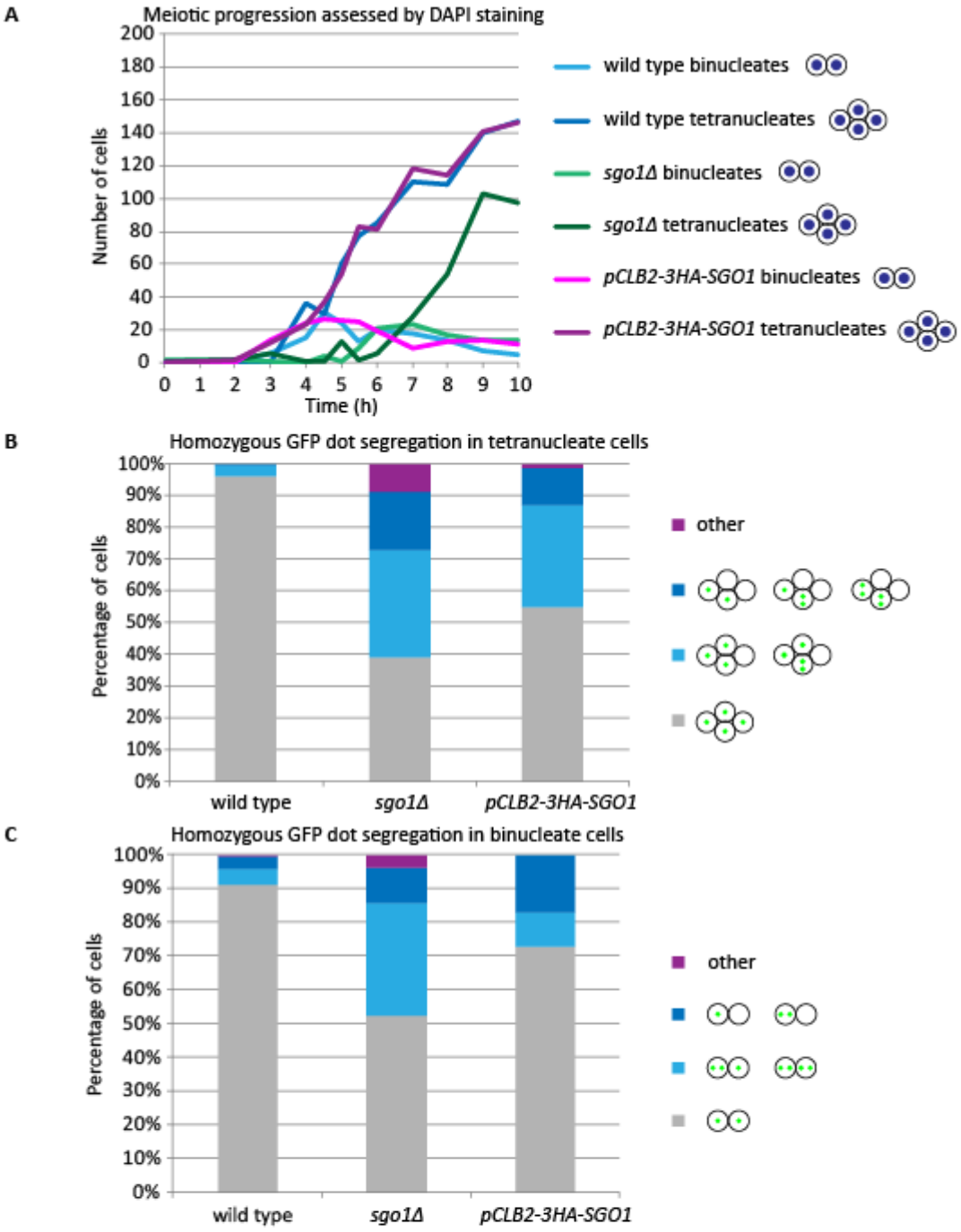

Figure 2.2.1.3: Sgo1 is required for faithful meiosis I and meiosis II chromosome segregation
Diploid strains homozygous for *CEN5 tetO*/TetR-GFP dots, were placed in sporulation media to induce meiosis. A) DAPI scoring of the number of binucleate and tetranucleate cells at each timepoint of the asynchronous meiotic time course. Strains used were wild type (9968, n=200), *sgo1Δ* (877, n=200), and *pCLB2-3HA-SGO1* (11668, n=200). B) Homozygous *CEN5 tetO*/TetR-GFP dot segregation in tetranucleate cells. Diploid strains were placed in sporulation media to induce meiosis, and after 10 h GFP dot segregation was counted in tetranucleates by fluorescence microscopy. Graph shown is the percentage of each phenotype. Average from 3 repeats for wild type (9968, n=300), *sgo1Δ* (877, n=311), and *pCLB2-3HA-SGO1* (11668, n=301). C) Homozygous *CEN5 tetO*/TetR-GFP dot segregation in binucleate cells after 7 h in sporulation media. Graph shown is the percentage of each phenotype. Average from 3 repeats for wild type (9968, n=300), *sgo1Δ* (877, n=299), and *pCLB2-3HA-SGO1* (11668, n=300).

fragmented DNA and very low spore viability (Yu and Koshland, 2003). This is partly due to the role of condensin at the rDNA. However condensin also has a more global role in meiosis I and meiosis II chromosome segregation (Yu and Koshland, 2003; Li, Jin and Yu, 2014; Hong, Choi and Kim, 2015). I investigated this in more detail by employing the *CEN5 tetO*/TetR-GFP dot assay (Figure 2.2.1.1B).

Condensin is essential, therefore two previously published condensin alleles were used to investigate the role of condensin in meiotic chromosome segregation in this study: *ycg1-2*, and *ycs4S*. The condensin mutant *ycg1-2* is a temperature sensitive allele of Ycg1, which causes severe chromosome condensation defects in mitosis (Lavoie, Hogan and Koshland, 2002), and has gross DNA missegregation and low spore viability in meiosis at the restrictive temperature (Yu and Koshland, 2003). Meiotic progression of *ycg1-2* was followed by DAPI staining for 10 h after induction of sporulation at 34 ^{o}C, resulting in under 17 % tetranucleate formation (Figure 2.2.2.1A). However, wild type diploids sporulated at 34 ^{o}C only achieved 17 % tetranucleate formation after 10 h (Figure 2.2.2.1A), compared to 63 % at 30 ^{o}C (Figure 2.2.2.1B), therefore the higher temperature greatly reduced sporulation efficiency. The *ycs4S* allele is a meiosis-specific condensin hypomorph, which is due to a C-terminal 12xMYC tag on Ycs4 (Yu and Koshland, 2003). In meiosis, *ycs4S* has normal chromosome condensation and spores do not contain fragmented DNA, but there are defects in synaptonemal complex formation and chromosome segregation (Yu and Koshland, 2003). The meiotic progression of *ycs4S* was followed by DAPI staining, and after 10 h in sporulation media 70 % of cells had formed tetranucleates (Figure 2.2.2.1B), as in wild type.

Homozygous *CEN5 tetO*/TetR-GFP dot segregation was analysed in the condensin mutants. Over 20 % of *ycg1-2* and *ycs4S* diploids exhibited missegregation of chromosome V in the tetranucleate cells (Figure 2.2.2.2A), showing that condensin is essential for sister chromatid segregation in meiosis II. Analysis of *CEN5 tetO*/TetR-GFP dot segregation at the binucleate stage, revealed that 17 % and 22 % of *ycg1-2* and *ycs4S* cells had one nucleus in the binucleate that did not contain chromosome V, suggesting that condensin mutants have defects in homologue segregation in meiosis I (Figure 2.2.2.2B).

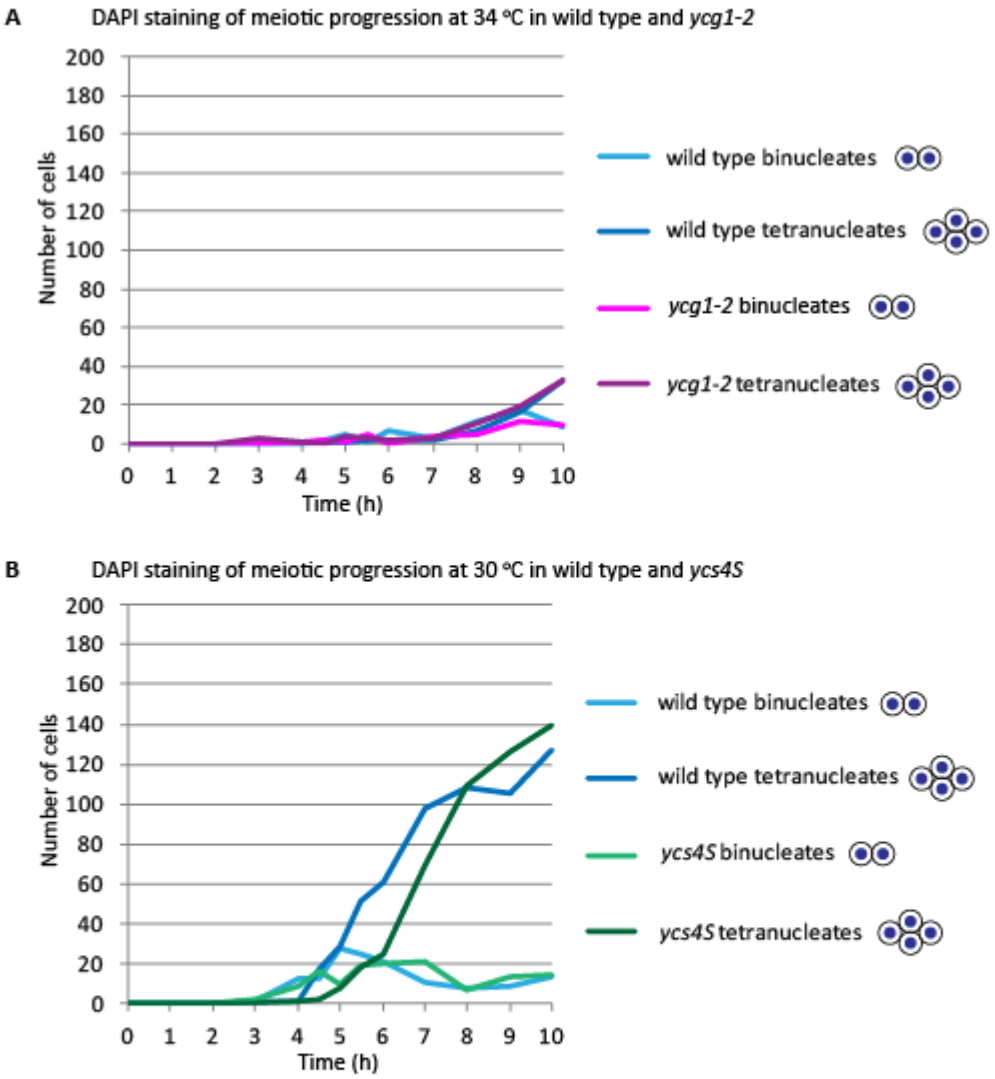

Figure 2.2.2.1: Meiotic progression of condensin mutants *ycg1-2* and *ycs4S*
Wild type or condensin mutants were placed in sporulation media and meiotic progression assessed by DAPI staining for binucleate and tetranucleate cells through an asynchronous meiotic time course. A) Graph of DAPI staining of wild type (9968, n=200) and *ycg1-2,* (16640, n=200) meiotic progression at 34 °C. B) Graph of DAPI staining of wild type (9968, n=200) and *ycs4S* (17113, n=200) meiotic progression at 30 °C.

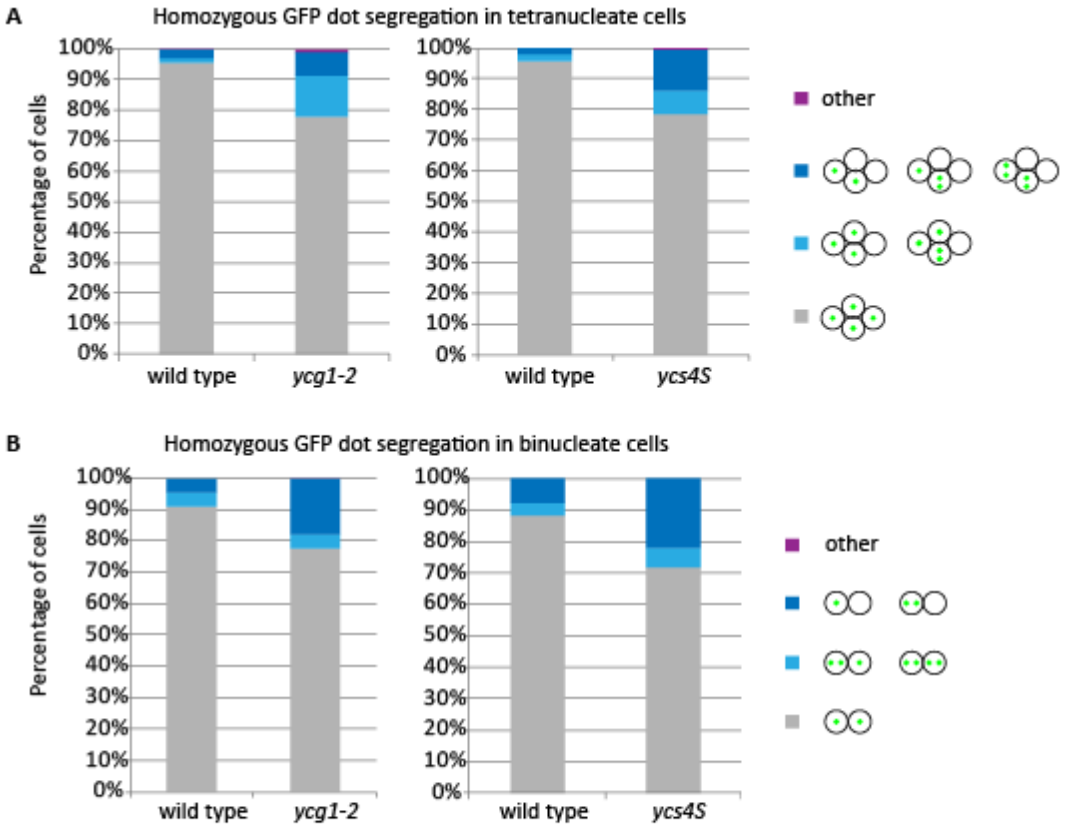

Figure 2.2.2.2: Condensin is required for faithful meiosis I and meiosis II chromosome segregation
A) Homozygous *CEN5 tetO*/TetR-GFP dot segregation in tetranucleate cells. Diploid strains were placed in sporulation media to induce meiosis, and after 10 h GFP dot segregation was counted in tetranucleates by fluorescence microscopy. Graph shown is the percentage of each phenotype. Average from 3 repeats for wild type (9968, n=300) and *ycg1-2* (16640, n=300) with cells grown at 34 °C. Average from 3 repeats for wild type (9968, n=300) and *ycs4S* (17113, n=300) with cells grown at 30 °C. B) Homozygous *CEN5 tetO*/TetR-GFP dot segregation in binucleate cells. Diploid strains were placed in sporulation media to induce meiosis, and after 5.5-9 h GFP dot segregation was counted in binucleates by fluorescence microscopy. Graph shown is the percentage of each phenotype. Average from 2 repeats for wild type (9968, n=200) and 3 repeats for *ycg1-2* (16640, n=300) with cells grown at 34 °C. Average from 3 repeats for wild type (9968, n=300) and *ycs4S* (17113, n=300) with cells grown at 30 °C.

Centromeric condensin has previously been implicated in sister kinetochore mono-orientation (Brito, Yu and Amon, 2010). To determine whether mono-orientation defects can be observed in cells with impaired condensin function, I used diploids heterozygous for *CEN5 tetO*/TetR-GFP, so that just one copy of chromosome V is labelled with a GFP dot. In wild type strains, after meiosis I, the binucleate cell will contain one GFP dot in one half of the binucleate (Figure 2.2.2.1C). In cells that have mono-orientation defects, one GFP dot will segregate into each half of the binucleate, as the sister chromatids separate. Heterozygous *CEN5 tetO*/TetR-GFP dot segregation was assayed in *ycg1-2* and *ycs4S* tetranucleates after 10 h in sporulation media, and no severe chromosome missegregation was seen (Figure 2.2.2.3A). However, analysis of heterozygous *CEN5 tetO*/TetR-GFP dot segregation in binucleates showed a minor mono-orientation defect of 6.7 % in *ycg1-2*, but not in *ycs4S* (Figure 2.2.2.3B).

The missegregation of chromosome V in meiosis in *ycg1-2* and *ycs4S* condensin mutants may be due to defective homologous recombination (Yu and Koshland, 2003; Li, Jin and Yu, 2014; Hong, Choi and Kim, 2015). As *ycg1-2* is a temperature sensitive allele the cells have functional condensin at 25 ^{o}C (Lavoie, Hogan and Koshland, 2002), therefore this allele could be used to analyse the role of condensin in chromosome segregation independently of homologous recombination, by shifting to the restrictive temperature only once this has occurred.

Homologous recombination occurs during prophase of meiosis. At the end of prophase, expression of a gene encoding the transcription factor, Ndt80, is activated, allowing progression out of prophase and into meiosis I. By placing *NDT80* under the inducible *GAL1-10* promoter (*pGAL-NDT80*) cells can be arrested in late prophase, and then induced to exit prophase with very high cell synchronisation. However, SK1 budding yeast are unable to sense galactose, so addition of galactose does not induce the *GAL1-10* promoter. Instead the cells, in addition to *pGAL-NDT80*, also contain a Gal4 transcription factor that is fused to the Estrogen Receptor (Gal4.ER). The Gal4.ER fusion is present in the cytoplasm until the addition of β-estradiol, which causes the Estrogen receptor to enter the nucleus, allowing the Gal4 transcription factor to bind to the *GAL* promoter and activate transcription. Therefore through addition of β-estradiol, *NDT80* transcription is induced and

Figure 2.2.2.3: Condensin has a minor role in mono-orientation during meiosis I

A) Heterozygous *CEN5 tetO*/TetR-GFP dot segregation in tetranucleate cells. Diploid strains were placed in sporulation media to induce meiosis, and after 10 h GFP dot segregation was counted in tetranucleates by fluorescence microscopy. Graph shown is the percentage of each phenotype. Average from 3 repeats for wild type (359, n=300), and *ycg1-2* (17529, n=300) with cells grown at 34 °C. Average from 3 repeats for wild type (359, n=300), and *ycs4S* (17528, n=300) with cells grown at 30 °C. B) Homozygous *CEN5 tetO*/TetR-GFP dot segregation in binucleate cells. Diploid strains were placed in sporulation media to induce meiosis, and after 6-10 h GFP dot segregation was counted in binucleates by fluorescence microscopy. Graph shown is the percentage of each phenotype. Average from 3 repeats for wild type (359, n=300), and *ycg1-2* (17529, n=300) with cells grown at 34 °C. Average from 3 repeats for wild type (359, n=300), and *ycs4S* (17528, n=300) with cells grown at 30 °C.

cells then progress synchronously into meiosis I and meiosis II (Figure 2.2.2.4A) (Carlile and Amon, 2008). In a wild type meiosis, the timing of metaphase I, anaphase I, metaphase II, and anaphase II can be followed by analysing spindle morphology by tubulin immunofluorescence (Figure 2.2.2.4B).

Wild type and *ycg1-2* strains containing the *pGAL-NDT80* block/release construct, and which were homozygous for *CEN5 tetO*/TetR-GFP dots, were placed into sporulation media and grown at the permissive temperature, 25 ^{o}C, for 6 h into the prophase arrest to allow homologous recombination to occur with functional condensin. The cells were then shifted to the restrictive temperature of 34 ^{o}C to inactivate condensin, and induced to proceed into the meiotic divisions by addition of β-estradiol. Cell cycle progression was monitored by DAPI staining for the formation of binucleate and tetranucleate cells, which in the wild type cells began to occur at 1 h and 2 h respectively after release (Figure 2.2.2.5A). However, analysis of *ycg1-2* meiotic progression showed that, although binucleate cells were forming at the same time as wild type, the process was less efficient, and by the time of tetranucleate formation in wild type, in *ycg1-2* a high number of cells with fragmented nuclei (other) appeared, and a lower level of tetranucleate formation was scored (Figure 2.2.2.5B). Therefore, allowing cells to progress through recombination at the permissive temperature increased the proportion of wild type and *ycg1-2* that underwent meiotic divisions compared to at 34 ^{o}C (Figure 2.2.2.1A), but gross chromosome missegregation occurred after prophase when condensin function was impaired.

Analysis of *CEN5 tetO*/TetR-GFP dot segregation in the wild type and *ycg1-2* tetranucleates after 6 h at 34 ^{o}C showed that there was missegregation of chromosome V in nearly 40 % *ycg1-2* cells, compared to 7.5 % wild type cells (Figure 2.2.2.6A). This is a much greater proportion than the 22 % missegregation phenotype in *ycg1-2* when cells were incubated at 34 ^{o}C for all of meiosis (Figure 2.2.2.2A), and may be because fewer cells arrest in prophase due to recombination defects. Analysis of *CEN5 tetO*/TetR-GFP dot segregation in binucleate cells, however, was comparable in both wild type and *ycg1-2* cells released from the prophase I arrest (Figure 2.2.2.6B). This data indicates that inhibiting condensin function after prophase mainly affects meiosis II chromosome segregation. However, only a small fraction of cells were correctly undergoing meiosis II and forming clear tetranucleates,

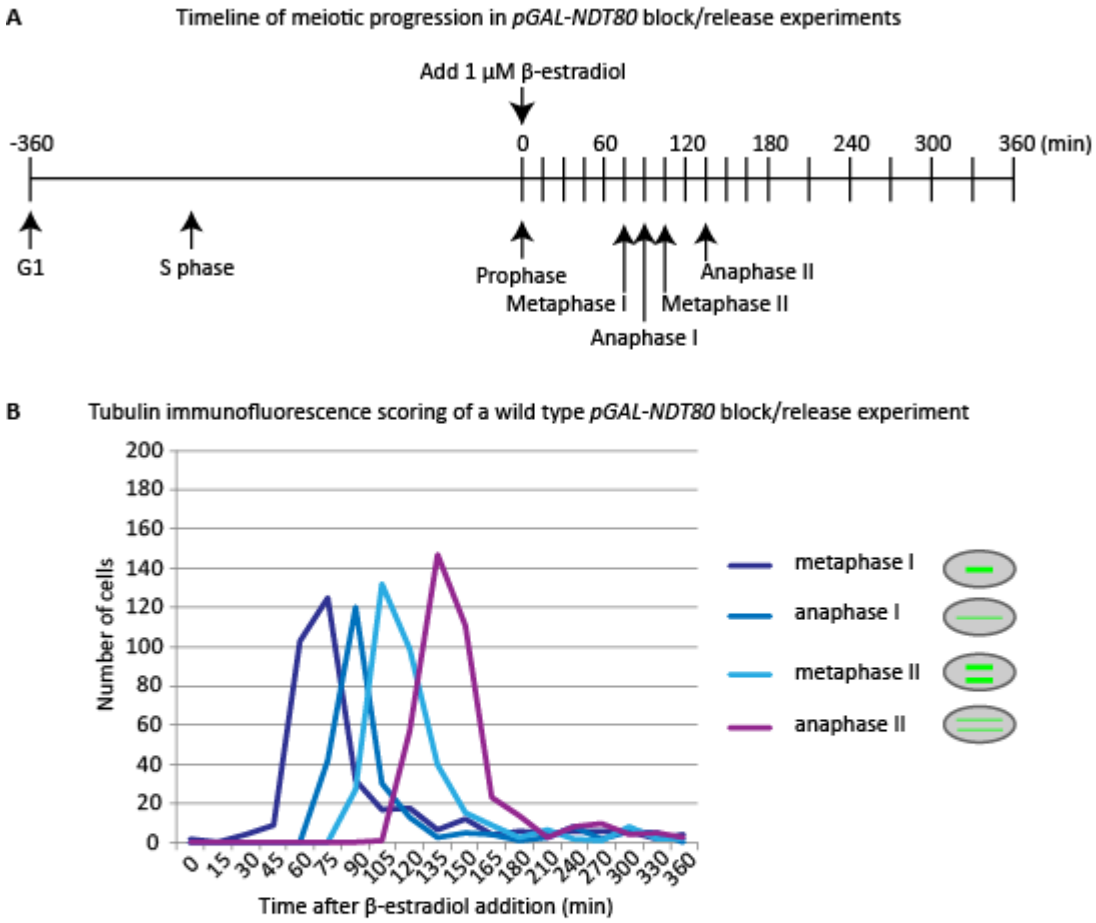

Figure 2.2.2.4: Schematic of the *pGAL-NDT80* block/release time course experiment protocol
A) Schematic of *pGAL-NDT80* block/release experiment with timing in minutes. Cells are placed into sporulation media and grown for 6 h to allow progression through S phase and homologous recombination. After 6 h, 1 µM β-estradiol is added to the culture to induce *NDT80* expression and allow progression through meiosis I and meiosis II. Samples are usually taken every 15 min for 3 h, then every 30 min for 3 h. B) After release from the *NDT80* arrest cells are collected at each timepoint indicated and immunofluorescence against tubulin carried out to assess cell cycle stage. Typical meiotic progression of a wild type strain shown (16180, n=200 cells/timepoint). Example schematic of tubulin immunofluorescence at each cell cycle stage shown.

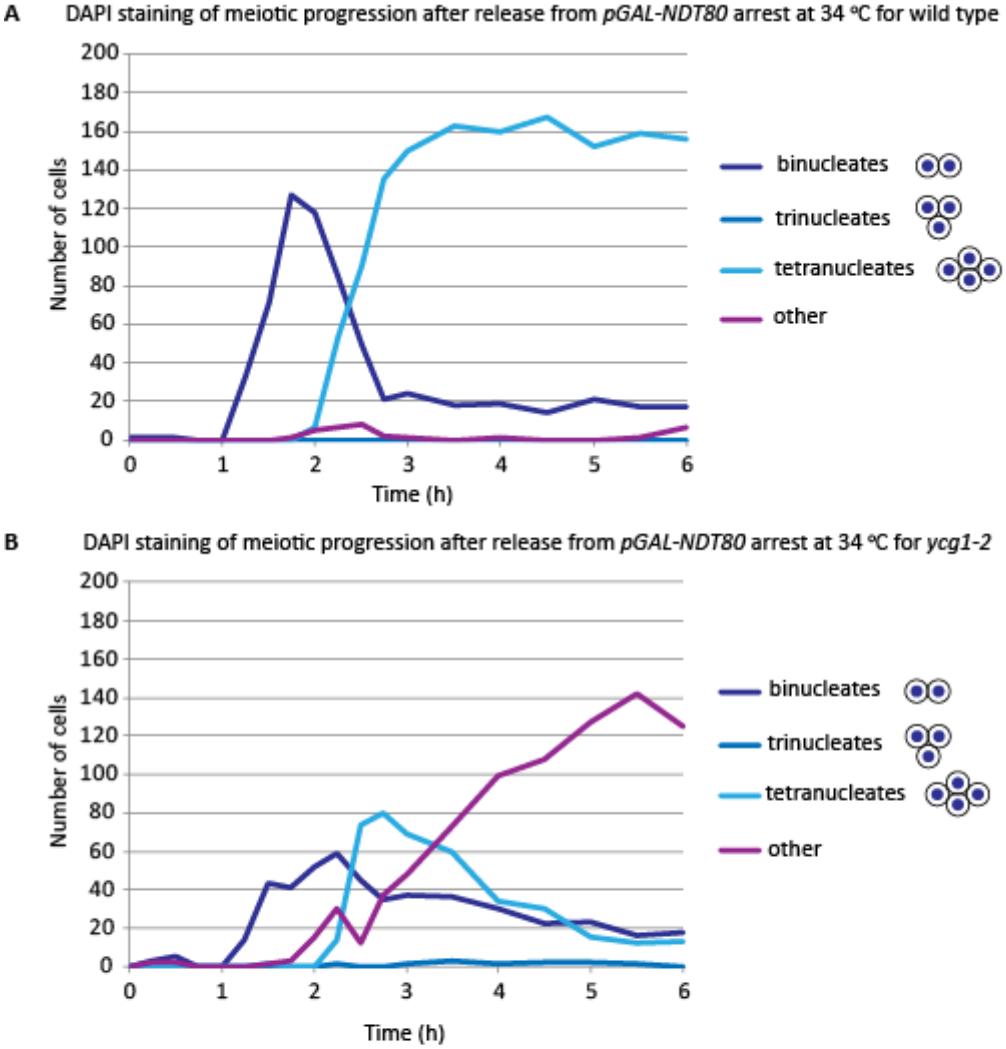

Figure 2.2.2.5: Meiotic progression of wild type and *ycg1-2* after release from *pGAL-NDT80* arrest
Wild type or *ycg1-2* cells containing *pGAL-NDT80* were placed in sporulation media at 25 ºC for 6 h, to arrest cells in prophase. Cells were shifted to 34 ºC and induced to express *NDT80* by addition of 1 µM β-estradiol, and meiotic progression followed by DAPI staining. A) Graph showing DAPI scoring of wild type (11358, n=200) as cells progress through meiosis I and meiosis II at 34 ºC. B) Graph showing DAPI scoring of *ycg1-2* (19055, n=200) as cells progress through meiosis I and meiosis II at 34 ºC. Other represents cells with fragmented DNA.

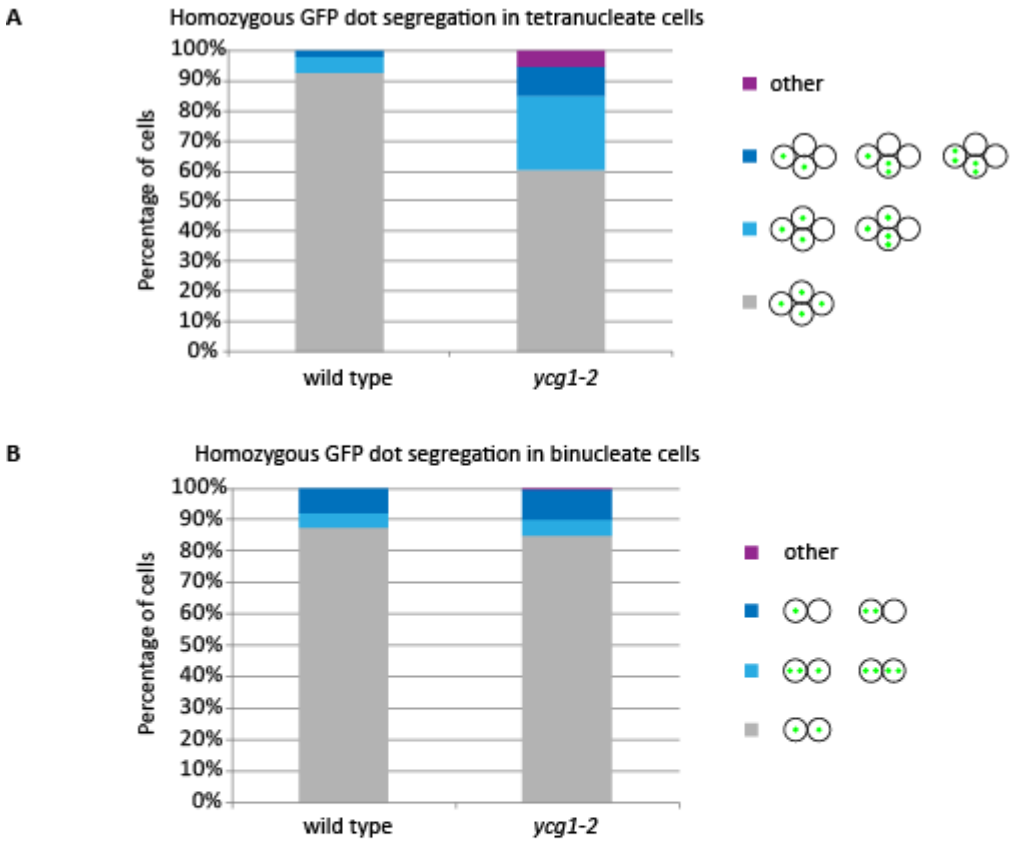

Figure 2.2.2.6: Condensin is required for faithful meiosis II chromosome segregation independently of it's role in homologous recombination

A) Homozygous *CEN5 tetO*/TetR-GFP dot segregation in tetranucleate cells. Strains were placed in sporulation media at 25 °C for 6 h, to arrest cells in prophase. Cells were shifted to 34 °C and induced to express *NDT80* by addition of 1 µM β-estradiol, and after 6 h GFP dot segregation was counted in tetranucleates with four clear DNA masses by fluorescence microscopy. Graph shown is the percentage of each phenotype. Average from 2 repeats for wild type (11358, n=200) and *ycg1-2* (19055, n=200). B) Homozygous *CEN5 tetO*/TetR-GFP dot segregation in binucleate cells. Strains were placed in sporulation media at 25 °C for 6 h, to arrest cells in prophase. Cells were shifted to 34 °C and induced to express *NDT80* by addition of 1 µM β-estradiol, and after 1.5-2 h GFP dot segregation was counted in binucleates by fluorescence microscopy. Graph shown is the percentage of each phenotype. Average from 2 repeats for wild type (11358, n=200) and *ycg1-2* (19055, n=200).

therefore masking the defects of the population of cells which failed to undergo meiosis I and II divisions.

2.2.3 Shugoshin and condensin interact in metaphase I of meiosis

In mitosis condensin localises to the centromeric region, where it is important for kinetochore biorientation (Freeman, Aragon-Alcaide and Strunnikov, 2000; Wang *et al.*, 2005; Yong-Gonzalez *et al.*, 2007; Bachellier-Bassi *et al.*, 2008; D'Ambrosio *et al.*, 2008; Stephens *et al.*, 2011; Tada *et al.*, 2011; Peplowska, Wallek and Storchova, 2014; Verzijlbergen *et al.*, 2014; Leonard *et al.*, 2015). However, it is unknown if condensin localises to the pericentromeric region in meiosis, although there is evidence for condensin influencing the kinetochore protein composition through a decrease in binding of the monopolin complex in condensin mutants (Brito, Yu and Amon, 2010). Therefore I aimed to determine whether condensin binds to the centromeric region in metaphase I of meiosis.

Meiotic cells containing Brn1-6HA were arrested in metaphase I of meiosis using the *pCLB2-CDC20* construct. Cdc20 is an activator of the Anaphase Promoting Complex/Cyclosome (APC/C), and is essential for progression into anaphase I of meiosis. By placing *CDC20* under the control of mitosis-specific *CLB2* promoter, Cdc20 expression is repressed in meiosis and cells arrest in metaphase I (Lee and Amon, 2003). Chromatin Immunoprecipitation (ChIP) of Brn1-6HA followed by quantitative-PCR (qPCR) in metaphase I arrested cells showed that Brn1-6HA was enriched at the centromeric and pericentromeric (Peri) regions in wild type cells (Figure 2.2.3.1A).

In mitosis the centromeric localisation of Brn1-6HA depends on Sgo1 (Peplowska, Wallek and Storchova, 2014; Verzijlbergen *et al.*, 2014). To determine if this was also the case in meiosis, Sgo1 was depleted using the *pCLB2-3HA-SGO1* construct, and ChIP-qPCR for Brn1 carried out. Upon Sgo1 depletion, Brn1-6HA was significantly decreased at the centromeric sites, but not significantly at a test pericentromeric site (Figure 2.2.3.1A). At an arm site, condensin was also modestly, though significantly decreased upon Sgo1 depletion (Figure 2.2.3.1.A), however western blotting showed that whole cell protein levels of condensin were not decreased (Figure 2.2.3.1B), and that the metaphase I arrest was equal in all strains as evaluated by tubulin immunofluorescence (Figure 2.2.3.1C). The decrease at this arm site may be due to defective condensin loading due to loss of Sgo1 at centromeres and

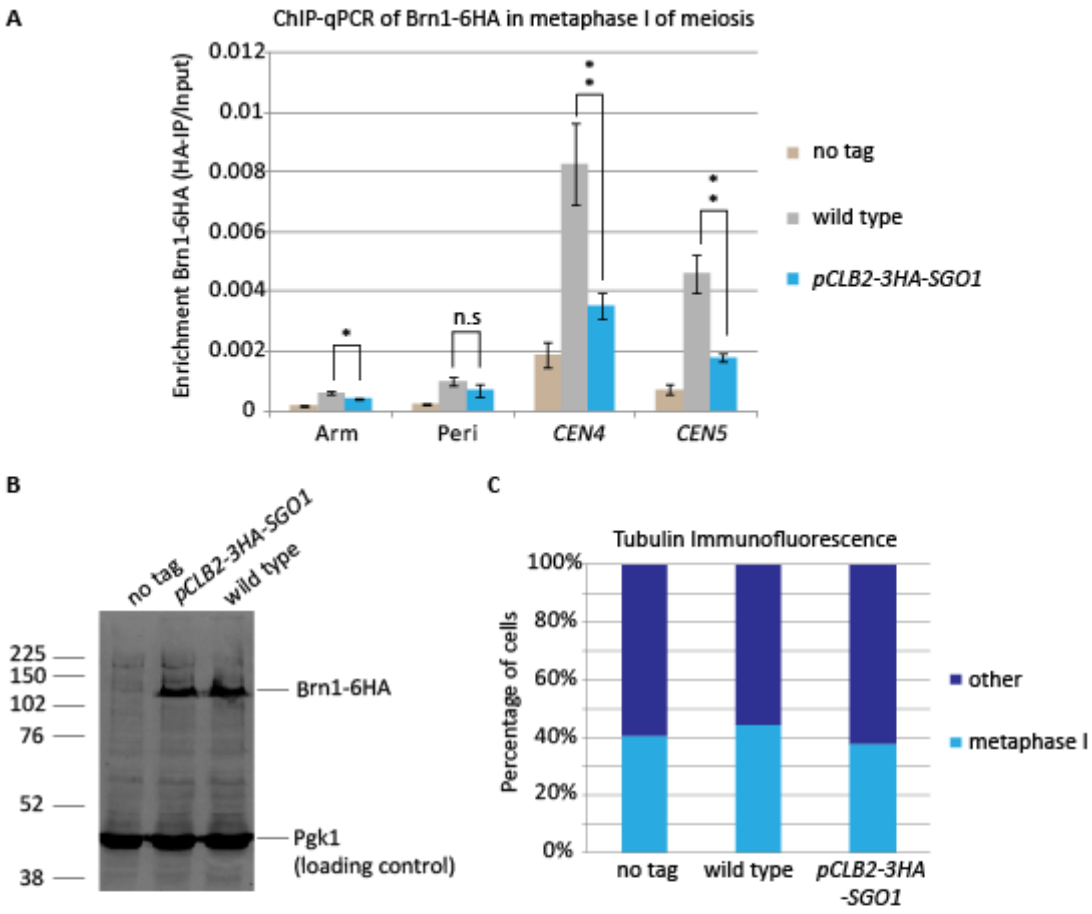

Figure 2.2.3.1: Condensin localisation to the centromeric region in metaphase I of meiosis depends on Sgo1

ChIP-qPCR of condensin in metaphase I meiosis shows condensin is enriched at the centromere in a Sgo1-dependent manner. A) Diploid strains containing Brn1-6HA were placed sporulation media and grown for 6 h into a *pCLB2-CDC20* metaphase I arrest, before harvesting for ChIP-qPCR. ChIP for Brn1-6HA was carried out in wild type (11625) and in *pCLB2-3HA-SGO1* (11624), as well as in a no tag background (8067), using 12CA5 antibody against 6HA. Average of 6 repeats for Arm, Peri and *CEN4*, and average of 5 repeats for *CEN5*. Error bars show standard error. Unpaired Student T-test gave p values of Arm= 0.013, Peri=0.274, *CEN4*=0.0075, and *CEN5*=0.0031. B) Western blotting for Brn1-6HA and a loading control (Pgk1) in the strains used for ChIP-qPCR. Western blot developed by LICOR, using 12CA5 to probe against Brn1-6HA, and homemade rabbit anti-PGK1 for the loading control. No tag (8067), wild type (11625) and *pCLB2-3HA-SGO1* (11624) samples shown. C) Tubulin immunofluorescence for the metaphase I arrest of no tag (8067), wild type (11625) and *pCLB2-3HA-SGO1* (11624). Average of 6 repeats, n=200.

therefore less spreading of condensin to the arm loci, however, further sites would need to be tested to determine if this is a global effect.

The dependence of condensin binding to centromeres in metaphase I of meiosis on Sgo1, suggests that Sgo1 and condensin may interact, as in mitosis (Peplowska, Wallek and Storchova, 2014; Verzijlbergen *et al.*, 2014). Purification of Sgo1-6HIS-3FLAG was carried out from metaphase I arrested meiotic cells (Figure 2.2.3.2A). Cells expressing Sgo1-6HIS-3FLAG were grown for 6 h into the *pCLB2-CDC20* metaphase I arrest (Figure 2.2.3.2B). After grinding to break open cells, the lysate was treated with benzonase to degrade DNA, to ensure that interactions observed were not mediated through proteins binding to the same stretch of DNA. Sgo1-6HIS-3FLAG was immunoprecipitated from the cell lysate, and a sample of the resulting eluate was run on a SDS-PAGE gel and silver-staining carried out (Figure 2.2.3.2A). The remaining sample was digested with trypsin and analysed by mass spectrometry to identify binding partners (Figure 2.2.3.2C, D).

Sgo1-6HIS-3FLAG was successfully identified by mass spectrometry (Figure 2.2.3.2C), and was found to be phosphorylated (Figure 2.2.3.2D) and acetylated (Figure 2.2.3.2E). The presence of phosphorylated Histone H2A-S121 indicated that some of the Sgo1 isolated by immunoprecipitation corresponded to functional kinetochore-bound Sgo1 (Figure 2.2.3.2D) (Kawashima *et al.*, 2010). The known Sgo1 binding partner PP2A-Rts1 was also present in high abundance (Kitajima *et al.*, 2006; Riedel *et al.*, 2006; Tang *et al.*, 2006; Xu *et al.*, 2009; Tanno *et al.*, 2010; Eshleman and Morgan, 2014), as well as the cohesin complex, suggesting that Sgo1 may interact with cohesin in budding yeast as in mammalian cells (Liu, Rankin and Yu, 2013) (Figure 2.2.3.2C). Importantly, three condensin subunits, Brn1, Smc2 and Ycs4, were purified with Sgo1-6HIS-3FLAG, suggesting that Sgo1 may interact with condensin in budding yeast meiosis, as in mitosis.

To verify the interaction between Sgo1 and condensin in budding yeast meiosis, co-immunoprecipitation of Sgo1-SZZ-TAP and Brn1-6HA was carried out (Figure 2.2.3.3A). Cells were arrested in metaphase I (Figure 2.2.3.3B), before cross-linking with DSP (Dithiobis(succinimidyl propionate)) to preserve weak interactions between Sgo1-SZZ-TAP and interacting partners during the immunoprecipitation experiment. The resulting eluate

A

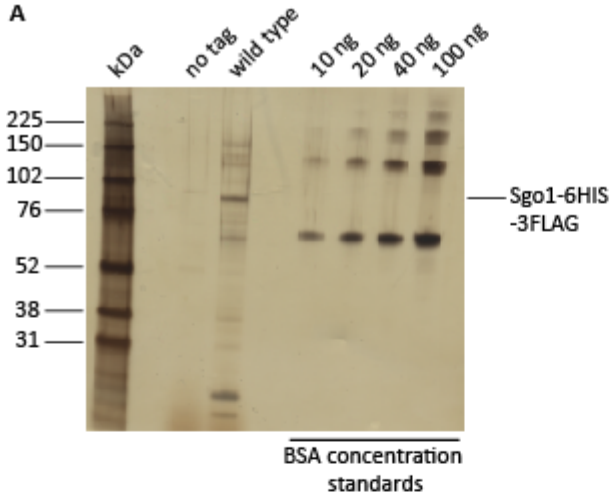

B

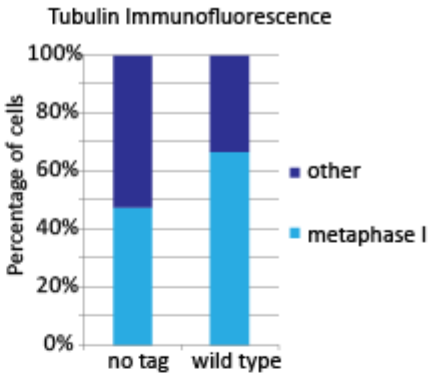

C

		Number of peptides		% coverage
Protein group	Protein	no tag	wild type	wild type
Sgo1	Sgo1	2	45	57.8
PP2A	Rts1	0	18	27.6
	Tpd3	0	15	27.9
	Pph22	0	10	34.2
	Pph21	0	8	29.8
Cohesin	Pds5	0	23	23.8
	Smc3	0	19	16.7
	Smc1	0	14	14.2
	Rec8	0	14	23.2
	Scc3	0	6	9.2
Condensin	Brn1	0	5	8.1
	Smc2	0	2	2.8
	Ycs4	0	2	1.6
Other	Spt16	0	42	48.2
	Isw1;Isw2	0	27	25.5
	Pob3	0	20	44.9
	Ioc3	0	10	12.3

D

Protein	Phosphorylation site
Cdc28	T169
Hho1	S174
Hta2	S122
Rts1	T257, T272
Sgo1	S151, S173, S364, S421, S423, S426, S482, S486, S487, S518, T444, T523

E

Protein	Acetylation site
Sgo1	K71, K85, K124, K420, K485, K531

Figure 2.2.3.2: Sgo1 interacts with PP2A-Rts1, cohesin and condensin in metaphase I of meiosis
A) Sgo1-6HIS-3FLAG was immunoprecipitated from metaphase I arrested meiotic cells, using M2-FLAG coupled dynabeads. A silver stained 4-12 % Bis-Tris protein gel of the eluate from the purification of no tag (3560) and wild type (18039) was used to visualise the immunoprecipitate (10 % total eluate). BSA concentration standards of 10 ng, 20 ng, 40 ng and 100 ng were used. B) Tubulin immunofluorescence for the metaphase I arrest of no tag (3560, n=196) and wild type (18039, n=200). C) Results of mass spectrometry after trypin digestion of the Sgo1-6HIS-3FLAG immunoprecipitate. Results were analysed using MAXQUANT. Shown is the number of peptides for each protein identified in either no tag (3560) or wild type (18039), and the percentage of sequence coverage for each protein identified in wild type (18039). D) Examples of phosphorylated Serine (S) and Threonine (T) residues identified by mass spectrometry of Sgo1-6HIS-3FLAG immunoprecipitation from wild type (18039). E) Acetylation sites on Sgo1 identified by mass spectrometry of Sgo1-6HIS-3FLAG immunoprecipitation from wild type (18039).

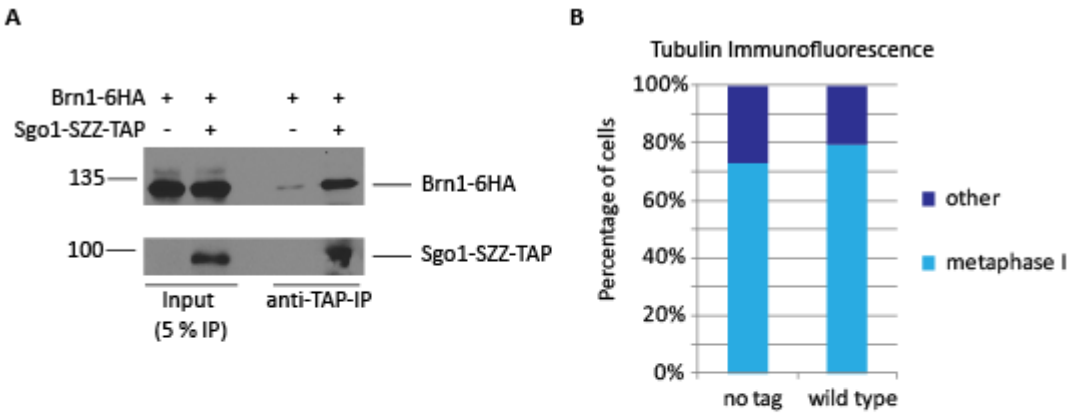

Figure 2.2.3.3: Sgo1 co-immunoprecipitates with condensin in metaphase I of meiosis
A) Co-immunoprecipitation of Brn1-6HA and Sgo1-SZZ-TAP from cells arrested in metaphase I of meiosis. Sgo1-SZZ-TAP was immunoprecipitated from 3 mg cell lysate of no tag (11625) and wild type (18103) containing Brn1-6HA, using rabbit IgG coupled to epoxy-activated dynabeads. After boiling, all eluate and 5 % INPUT were loaded onto a 10 % SDS-PAGE gel. Western blotting using HA11 and TAP antibody showed that Brn1-6HA co-immunoprecipitated with Sgo1-SZZ-TAP in metaphase I of meiosis. (B) Tubulin immunofluorescence for the metaphase I arrest of no tag (11625, n=200) and wild type (18103, n=200).

was run on an SDS-PAGE gel and western blotting carried out, showing that Sgo1-SZZ-TAP and Brn1-6HA interact in metaphase I of meiosis (Figure 2.2.3.3A).

2.2.4 Identification of the binding site for condensin on Sgo1

As condensin has multiple roles in meiosis including in chromosome condensation, homologous recombination and in detangling the rDNA during anaphase, this makes interpretation of the phenotypes of condensin mutants complex (Yu and Koshland, 2003; Yu and Koshland, 2005; Brito, Yu and Amon, 2010; Li, Jin and Yu, 2014; Hong, Choi and Kim, 2015). As I have shown that Sgo1 is required for condensin enrichment at the meiotic kinetochore, I aimed to identify the region of Sgo1 to which condensin binds, to ultimately generate an allele of Sgo1 to specifically deplete condensin from the meiotic centromeric region.

These Sgo1 mutants could also be employed to specifically deplete condensin from the mitotic centromeres. Therefore, for simplicity, I aimed to identify the interacting regions of Sgo1 and condensin in mitosis, before extending this work to meiosis. Sgo1 is highly enriched on kinetochores that are not under tension, therefore, in the presence of nocodazole, Sgo1 is stably associated with the centromeric region as cells lack microtubules and therefore tension is absent. Co-immunoprecipitation of Sgo1-SZZ-TAP and Brn1-6HA in mitotic nocodazole-arrested cells was carried out, followed by western blot analysis for both Sgo1-SZZ-TAP and Brn1-6HA. This showed that Brn1-6HA co-immunoprecipitated with Sgo1-SZZ-TAP from metaphase-arrested cells, as in previously published work (Figure 2.2.4.1A) (Peplowska, Wallek and Storchova, 2014; Verzijlbergen *et al.*, 2014).

To identify the region of Sgo1 to which condensin binds, I made use of a series of Sgo1 truncations that had been previously made in the Marston lab (C. Schaffner, unpublished). Sgo1 is predicted to be largely unstructured, other than an N-terminal coiled-coil and C-terminal basic region. In the absence of clear domains, we therefore constructed truncations of consecutive 100 residue regions of Sgo1 (Figure 2.2.4.2A). These truncations were TAP-tagged to allow co-immunoprecipitation with Brn1-6HA, to screen for loss of the interaction and thereby determine the site to which condensin binds to on Sgo1. Strains containing Brn1-6HA and Sgo1-SZZ-TAP truncations were arrested in nocodazole in metaphase of mitosis, before cross-linking with DSP. The eluate and input samples were

A

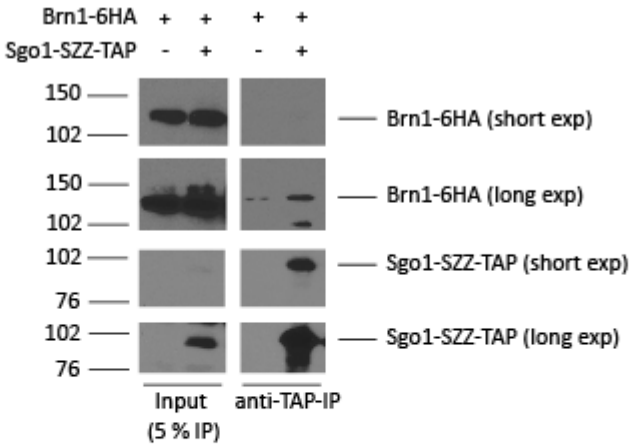

Figure 2.2.4.1: Sgo1 co-immunoprecipitates with condensin in nocodazole-arrested mitotic cells
A) Co-immunoprecipitation of Brn1-6HA and Sgo1-SZZ-TAP from cells arrested in metaphase of mitosis in the presence of nocodazole. Sgo1-SZZ-TAP was immunoprecipitated from 3 mg cell lysate of no tag (5708) and wild type (9266) containing Brn1-6HA, using rabbit IgG coupled to epoxy-activated dynabeads. After boiling, all eluate and 5 % INPUT were loaded onto a 10 % SDS-PAGE gel. Western blotting using HA11 and TAP antibody showed that Brn1-6HA co-immunoprecipitated with Sgo1-SZZ-TAP in metaphase of mitosis.

A

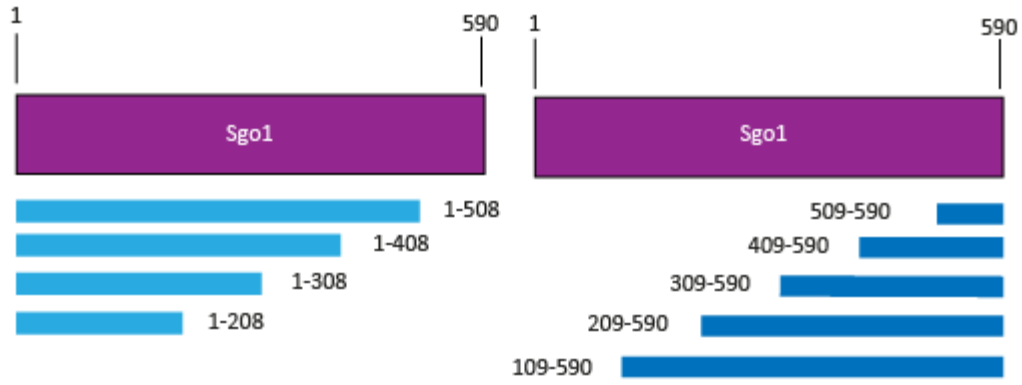

Figure 2.2.4.2: Schematic of Sgo1 truncations
A) Schematic of N-terminal and C-terminal truncations of Sgo1 (C. Schaffner). All trunctions were TAP-tagged to allow immunoprecipitation experiments to be carried out with Brn1-6HA.

run on an SDS-PAGE gel, and western blotting carried out. All of the C-terminal truncations of Sgo1 co-immunoprecipitated with Brn1-6HA (Figure 2.2.4.3A), suggesting that the N-terminus of Sgo1 is important for the interaction with condensin. However, all of the N-terminal truncations of Sgo1 also co-immunoprecipitated with Brn1-6HA (Figure 2.2.4.3B). Therefore no conclusions could be made about the region of Sgo1 to which condensin binds in metaphase of mitosis.

Brn1-6HA could potentially interact with the TAP tag on Sgo1 causing a false-positive result. Therefore a control co-immunoprecipitation experiment was carried out between Hst1-SZZ-TAP and Brn1-6HA (Figure 2.2.4.4A). Hst1 is a component of the Set3 histone deacetylase complex, and is in close proximity with the DNA, and potentially, therefore, condensin. Strains containing Hst1-SZZ-TAP and Brn1-6HA were grown into a metaphase nocodazole arrest, before cross-linking with DSP and immunoprecipitation of Hst1-SZZ-TAP carried out. Western blotting showed that Hst1-SZZ-TAP was successfully immunoprecipitated from cell lysate, and there was a faint Brn1-6HA background band in the eluate, but this was greatly reduced in comparison to the Sgo1-SZZ-TAP pull-down of Brn1-6HA (Figure 2.2.4.4A). Therefore it is inconclusive as to why all of the Sgo1 N- and C-terminal truncations interacted with Brn1-6HA by co-immunoprecipitation, but may be due to there being multiple binding sites for condensin on Sgo1.

2.2.5 Identification of the subunit of condensin that binds Sgo1

The yeast-two-hybrid assay has long been used to detect and map protein-protein interactions *in vivo* (James, Halladay and Craig, 1996). I therefore employed this technique to determine which of the subunits of the condensin complex binds to Sgo1 (Figure 2.2.5.1A). In the yeast-two-hybrid assay two reporter genes are placed under the control of the *GAL* promoter: in this case *HIS3* and *ADE2*. One protein of interest is fused to the p*GAL*-DNA binding domain (GBD) and thus binds to the *GAL* promoter upstream of the reporter gene. This is the "bait". The other protein of interest is fused to the p*GAL* activation domain (GAD), and this is the "prey". Only if the two proteins interact is the GAD brought to the *GAL*-containing promoter and transcription activated, allowing yeast to grow on selective media (Figure 2.2.5.1A).

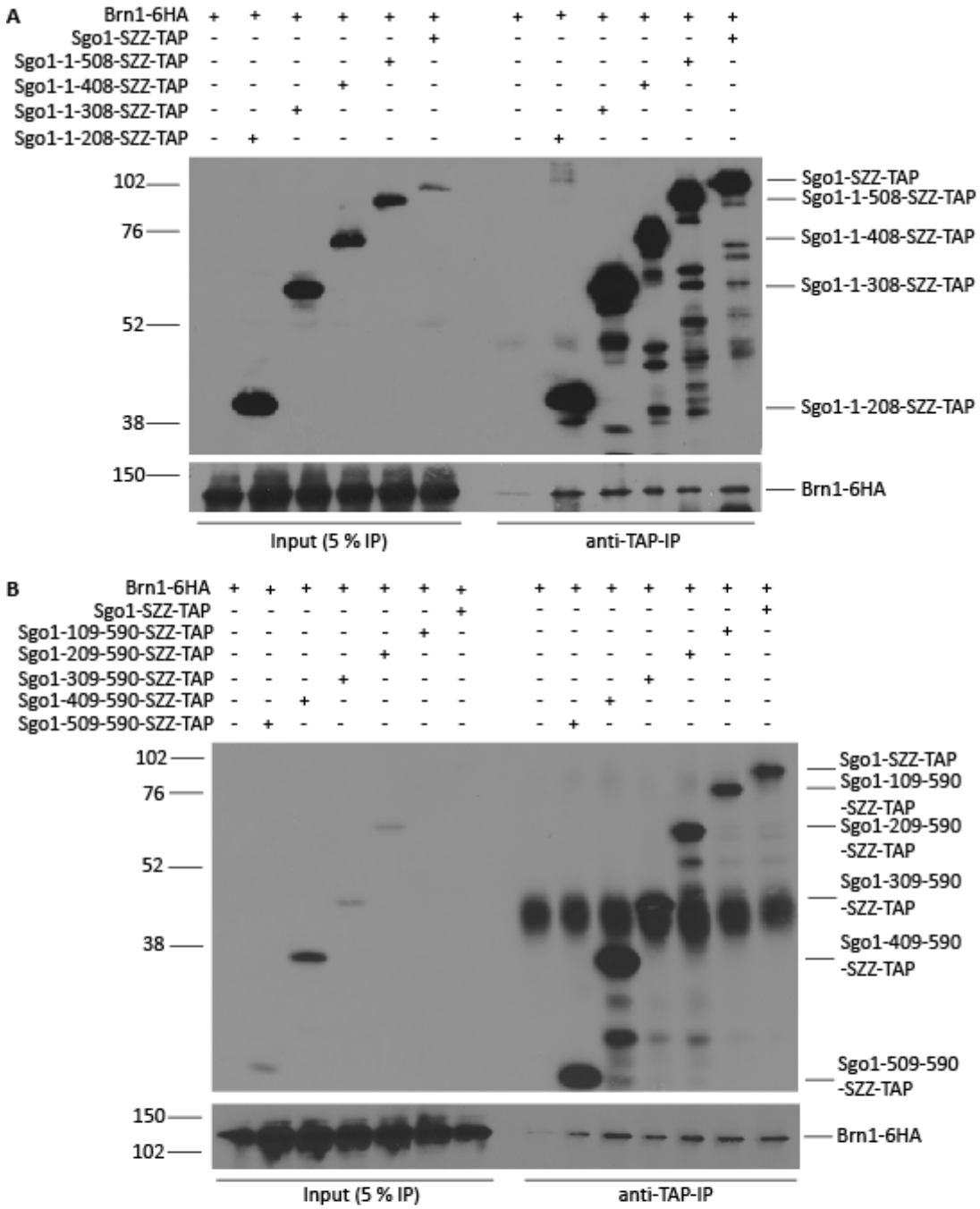

Figure 2.2.4.3: All Sgo1 C- and N-terminal trunctions interact with condensin in nocodazole arrested mitotic cells.

Co-immunoprecipitation of Brn1-6HA with C-terminal and N-terminal truncations of Sgo1-SZZ-TAP in cells arrested in metaphase of mitosis in the presence of nocodazole. Sgo1-SZZ-TAP was immunoprecipitated from 3 mg of cell lysate using rabbit IgG coupled to epoxy-activated dynabeads. After boiling all eluate and 5 % INPUT were loaded onto a 10 % SDS-PAGE gel, and western blotting carried out using HA11 and TAP antibodies. A) Western blot of C-terminal Sgo1 truncations and Brn1-6HA, using no tag (5708), wild type (9266), Sgo1-1-508-SZZ-TAP (17559), Sgo1-1-408-SZZ-TAP (18106), Sgo1-1-308-SZZ-TAP (17213), and Sgo1-1-208-SZZ-TAP (17214). B) Western blot of N-terminal Sgo1 truncations and Brn1-6HA using no tag (5708), wild type (9266), Sgo1-109-590-SZZ-TAP (20255), Sgo1-209-590-SZZ-TAP (17720), Sgo1-309-590-SZZ-TAP (17558), Sgo1-409-590-SZZ-TAP (17439) and Sgo1-509-590-SZZ-TAP (17840).

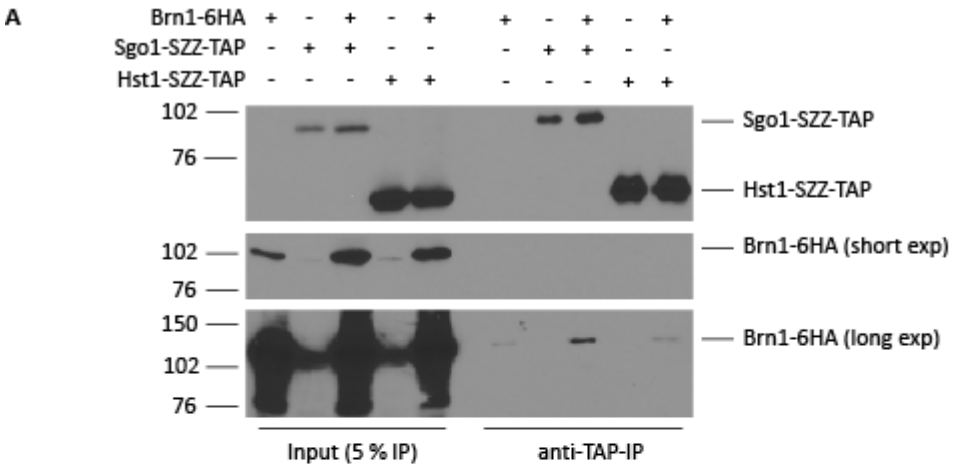

Figure 2.2.4.4: The interaction between Sgo1 and condensin is not an artifact of the co-immunoprecipitation protocol

A) Both Sgo1-SZZ-TAP or Hst1-SZZ-TAP were immunoprecipitated with Brn1-6HA from cells arrested in metaphase mitosis in the presence of nocodazole. Either Sgo1-SZZ-TAP or Hst1-SZZ-TAP were immunoprecipitated from 3 mg cell lysate of Brn1-6HA alone (5708), Sgo1-SZZ-TAP alone (7509), Hst1-SZZ-TAP alone (8892), Sgo1-SZZ-TAP with Brn1-6HA (9266), or Hst1-SZZ-TAP with Brn1-6HA (20188) using rabbit IgG coupled to epoxy-activated dynabeads. After boiling all eluate and 5 % INPUT were loaded onto a 10 % SDS-PAGE gel. Western blotting using HA11 and TAP antibody showed that Brn1-6HA co-immunoprecipitated with Sgo1-SZZ-TAP in metaphase of mitosis, and did not co-immunoprecipitate with Hst1-SZZ-TAP.

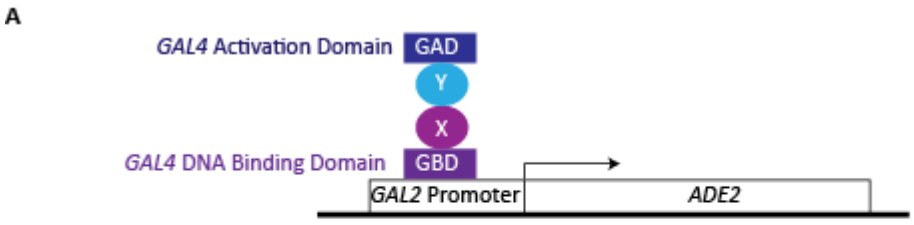

Figure 2.2.5.1: Schematic of the Yeast-two-Hybrid reporter system

A)Schematic of the yeast-two-hybrid reporter system. Proteins X and Y are tagged with the *GAL4* DNA binding domain (GBD) or the *GAL4* activation domain (GAD) respectively. If proteins X and Y interact, this brings the GAD to the GBD at the *GAL2* promoter, activating transcription, thus allowing the yeast-2-hybrid strain (strain 2584) to grow on -adenine signalling a strong interaction, or -histidine signalling a weak interaction (James, 1996).

GAD-Sgo1 and the known binding partner, GBD-Rts1, were tested for interaction using the yeast-two-hybrid system, and only a weak interaction detected through slow growth on -ADE and strong growth on -HIS (Figure 2.2.5.2A). However, the interaction between Sgo1 and Rts1 is known to be direct, therefore a strong interaction on -ADE would be expected (Kitajima *et al.*, 2006; Riedel *et al.*, 2006; Tang *et al.*, 2006; Xu *et al.*, 2009; Tanno *et al.*, 2010). Nevertheless, Sgo1 was also tested for a yeast-two-hybrid interaction with Ycs4, Ycs5 and Brn1, but no interaction detected using GAD-Sgo1 (Figure 2.2.5.2A). A weak interaction between GBD-Sgo1 and GAD-Ycs4 was detected, but this was not reproducible, and as GBD-Sgo1 and GAD-Rts1 did not show a robust positive signal (Figure 2.2.5.2B), this is likely to be a false-positive interaction due to GAD-Ycs4 binding to the DNA independently of an interaction with Sgo1, as part of the endogenous condensin complex.

As an alternative approach, cross-linking mass spectrometry could be used to identify the interacting regions of Sgo1 and condensin (Rappsilber, 2011). However, Sgo1 is relatively low abundance in budding yeast, and therefore to purify the quantities required for cross-linking mass spectrometry is difficult. Therefore I aimed to purify recombinant GST-Sgo1 from *Escherichia coli* (*E. coli*) (Figure 2.2.5.3A) that could then be incubated with yeast condensin to identify the interacting regions. GST-Sgo1 expression was induced with 1 mM IPTG in *E. coli* at 25 ^{o}C for 3 h, followed by lysis and centrifugation. Samples of the resulting pellet and supernatant were run on an SDS-PAGE gel and coomassie stained (Figure 2.2.5.3B). Expression of GST-Sgo1 could be visualised in both the pellet and supernatant, however levels of expression were very low. Therefore the expression of GST-Sgo1 was confirmed by western blotting using homemade anti-Sgo1 antibody (C. Schaffner, unpublished) (Figure 2.2.5.3C).

As GST-Sgo1 was successfully expressed, a small scale induction was carried out, and GST-Sgo1 lysate incubated with glutathione resin. Half of the glutathione resin was boiled and the eluate loaded onto an SDS-PAGE gel before coomassie staining, which showed that low amounts of GST-Sgo1 had been purified (Figure 2.2.5.3D). The remaining half of the glutathione resin with GST-Sgo1 was incubated with yeast lysate from asynchronous cultures containing Brn1-6HA. After incubation with yeast lysate, the glutathione resin was boiled and the resulting eluate loaded onto an SDS-PAGE gel and western blotting carried out for Brn1-6HA (Figure 2.2.5.3E). This showed that yeast condensin was binding

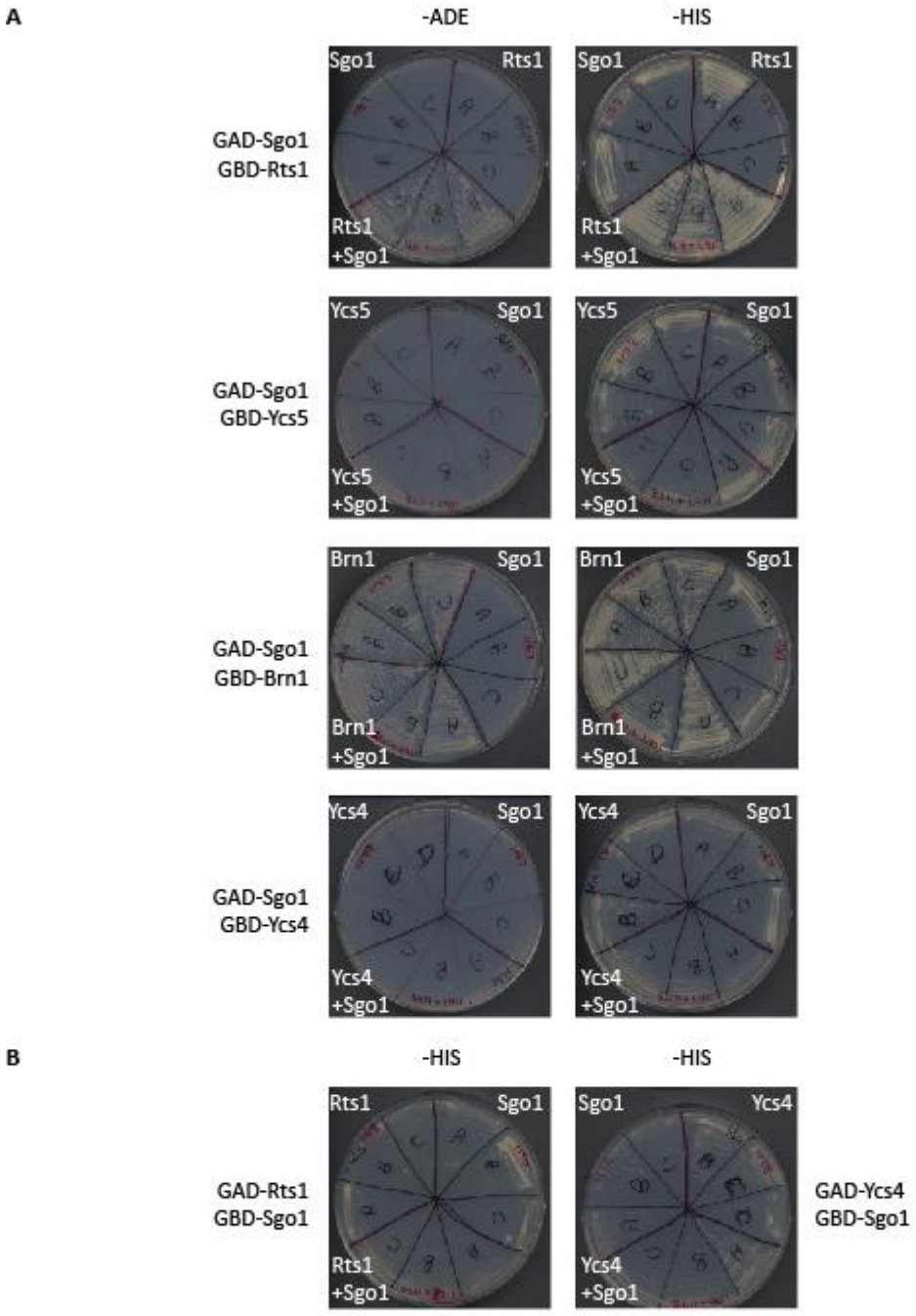

Figure 2.2.5.2: Sgo1 interacts with Rts1 by Yeast-two-Hybrid assay, but not with condensin subunits

Yeast-two-hybrid assay for interaction between Sgo1 and the known binding partner, Rts1, and subunits of the condensin complex. A) Strain 2584 was transformed with *GAD-SGO1* (AMp1167) alone and in combination with *GBD-RTS1* (AMp1171), *GBD-YCS5* (AMp1172), *GBD-BRN1* (AMp1177), or *GBD-YCS4* (AMp1179), and transformants selected for on selective media. Strains were then streaked to single colonies on either -HIS, to detect weak interactions, or on -ADE to detect strong interactions. Interaction between *GAD-SGO1* and *GBD-RTS1* was detected, but no interaction was detected between any of the GBD-tagged condensin subunits and *GAD-SGO1*. B) Strain 2584 was transformed with *GBD-SGO1* (AMp1170) alone or in combination with *GAD-RTS1* (AMp1168) or *GAD-YCS4* (AMp1178). A weak interaction was detected on -HIS with Ycs4, but not Rts1, suggesting this was a false-positive interaction.

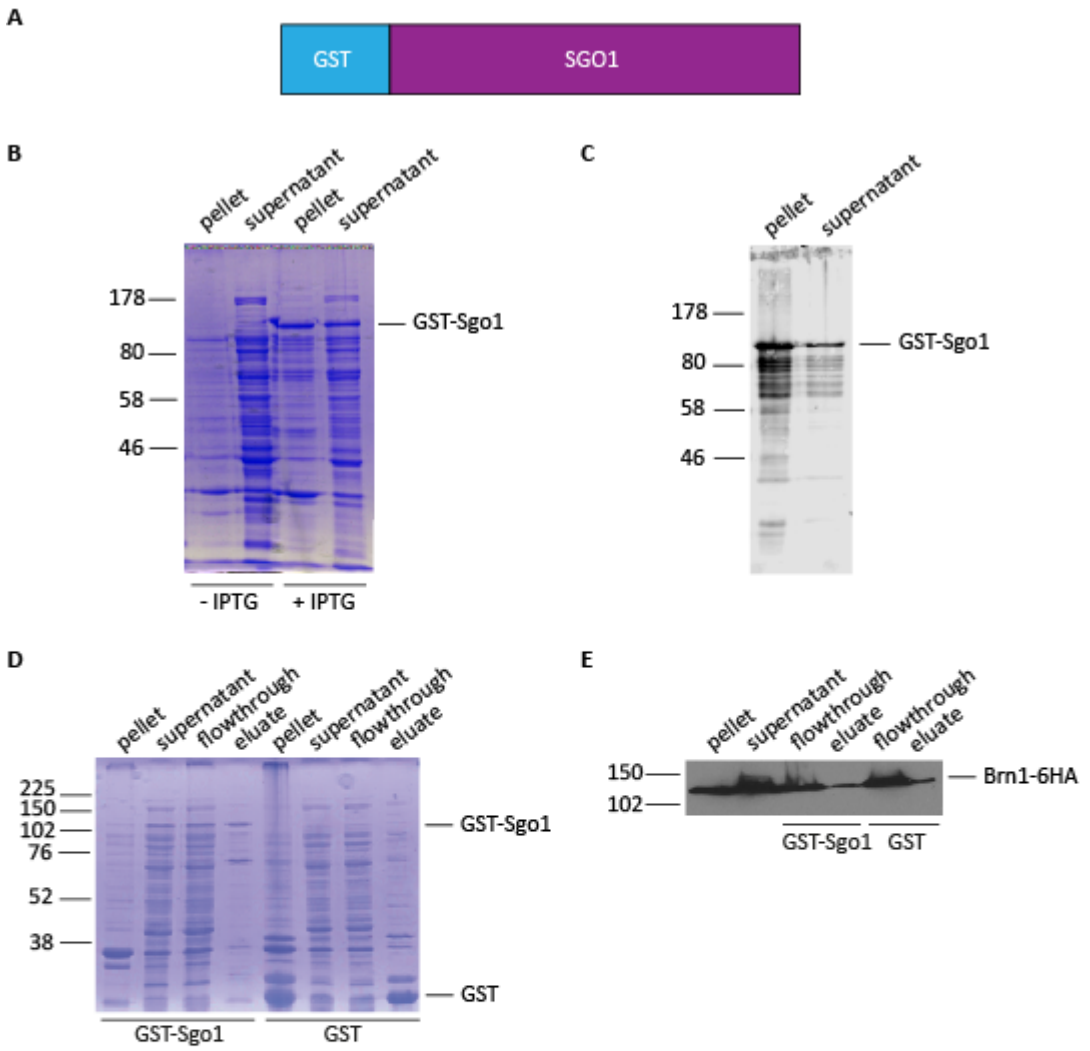

Figure 2.2.5.3: Recombinant GST-Sgo1 does not bind to *S. cerevisiae* condensin
A) Schematic of GST-Sgo1 in AMp1050. B) BL21 *E. coli* containing GST-SGO1 were grown at 37 °C before shifting to 25 °C for 30 min. One culture was induced with 1 mM IPTG to express GST-Sgo1, and one culture was left un-induced, and both cultures were grown for a further 3 h to allow GST-Sgo1 expression. Cells were lysed, before samples of pellet and supernatant were boiled in sample buffer and loaded onto a 10 % SDS-PAGE gel. This was coomassie stained to reveal GST-Sgo1 expression. C) *E. coli* containing GST-Sgo1 were grown and lysed as in B), and samples of pellet and supernatant run on a 10 % SDS-PAGE gel before western blotting using anti-Sgo1 rabbit antibody to reveal GST-Sgo1 expression. D) Small scale induction of GST-Sgo1 and GST at 25 °C for 3 h was carried out as described. After lysis, half of the supernatant was incubated with glutathione resin, followed by boiling in sample buffer. Samples of pellet, supernatant, flowthrough and eluate were run on a 10 % SDS-PAGE gel and coomassie stained. E) The other half of the GST-Sgo1 and GST lysate from D) was incubated with glutathione resin, then incubated with yeast lysate containing Brn1-6HA from asynchronous yeast culture (5708). The glutathione resin was washed and boiled in sample buffer, and run on a 10 % SDS-PAGE gel before western blotting for Brn1-6HA using HA11 antibody.

non-specifically to the glutathione resin, independently of GST-Sgo1, and that there was no further enrichment of Brn1-6HA binding in the presence of GST-Sgo1. Therefore, this approach would be unsuitable for cross-linking mass spectrometry.

2.2.6 The interaction between Sgo1 and condensin in mitosis does not require localisation to the centromeric region or PP2A-Rts1

Sgo1 and condensin interact in both mitosis and meiosis, but it is unknown if the interaction requires the presence of the centromeric chromatin. I carried out a co-immunoprecipitation experiment to clarify if centromeric localisation of Sgo1 is required for the interaction to condensin. Bub1 phosphorylates H2A-S121, and this in turn recruits Sgo1 to the centromeric region (Kawashima *et al.*, 2010). Therefore *bub1Δ* mutants containing Sgo1-SZZ-TAP and Brn1-6HA were arrested in mitosis in the presence of nocodazole, and cross-linked with DSP. The resulting eluate was run on an SDS-PAGE gel, and western blotting carried out for the presence of Brn1-6HA (Figure 2.2.6.1A). This showed that the interaction between Sgo1 and condensin was maintained in *bub1Δ*, and therefore the interaction is independent of the centromeric localisation of Sgo1.

In the literature there have been several discrepancies as to the importance of PP2A-Rts1 in promoting the interacting between Sgo1 and condensin. The localisation of condensin to the centromeres is reduced in *rts1Δ* suggesting PP2A-Rts1 is important for this (Peplowska, Wallek and Storchova, 2014). However the Sgo1-condensin interaction is maintained in the *sgo1-3A* mutant that abolishes the Sgo1-Rts1 interaction (Xu *et al.*, 2009; Verzijlbergen *et al.*, 2014), and the phosphatase activity of PP2A is not required for condensin localisation to the centromeres (Peplowska, Wallek and Storchova, 2014). I therefore set out to clarify the importance of PP2A-Rts1 in the interaction between Sgo1 and condensin.

First I co-immunoprecipitated Sgo1-SZZ-TAP and Brn1-6HA in *rts1Δ* nocodazole arrested mitotic cells. Western blotting showed that the interaction between Sgo1 and Brn1 was maintained in *rts1Δ* (Figure 2.2.6.1A). Additionally ChIP-qPCR of Brn1-6HA in both *rts1Δ* and *sgo1-3A* mutants showed that condensin was enriched at the centromeres in these mutants, but was absent in *sgo1Δ* (Figure 2.2.6.2A). Whole cell levels of Brn1-6HA was equal across all mutant backgrounds (Figure 2.2.6.2B), and the cells had not bypassed the metaphase arrest (Figure 2.2.6.2C). Therefore my data indicates that Rts1 may play a role,

A

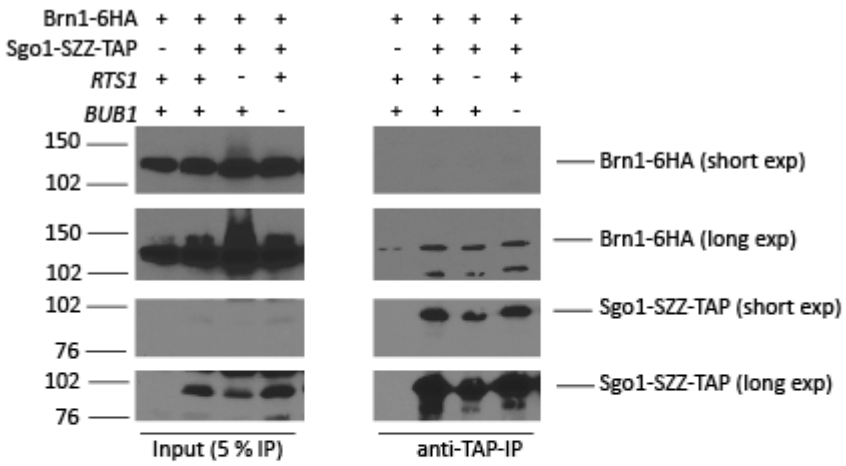

Figure 2.2.6.1: The interaction between Sgo1 and condensin does not require Bub1 or Rts1
A) Co-immunoprecipitation of Brn1-6HA and Sgo1-SZZ-TAP from cells arrested in metaphase of mitosis in the presence of nocodazole. Sgo1-SZZ-TAP was immunoprecipitated from 3 mg cell lysate of no tag (5708), wild type (9266), *bub1Δ* (17215), and *rts1Δ* (18305) containing Brn1-6HA, using rabbit IgG coupled to epoxy-activated dynabeads. After boiling, all eluate and 5 % INPUT were loaded onto an 10 % SDS-PAGE gel. Western blotting using HA11 and TAP antibody showed that Brn1-6HA co-immunoprecipitated with Sgo1-SZZ-TAP in metaphase of mitosis, and the interaction is maintained in both *rts1Δ* and *bub1Δ*.

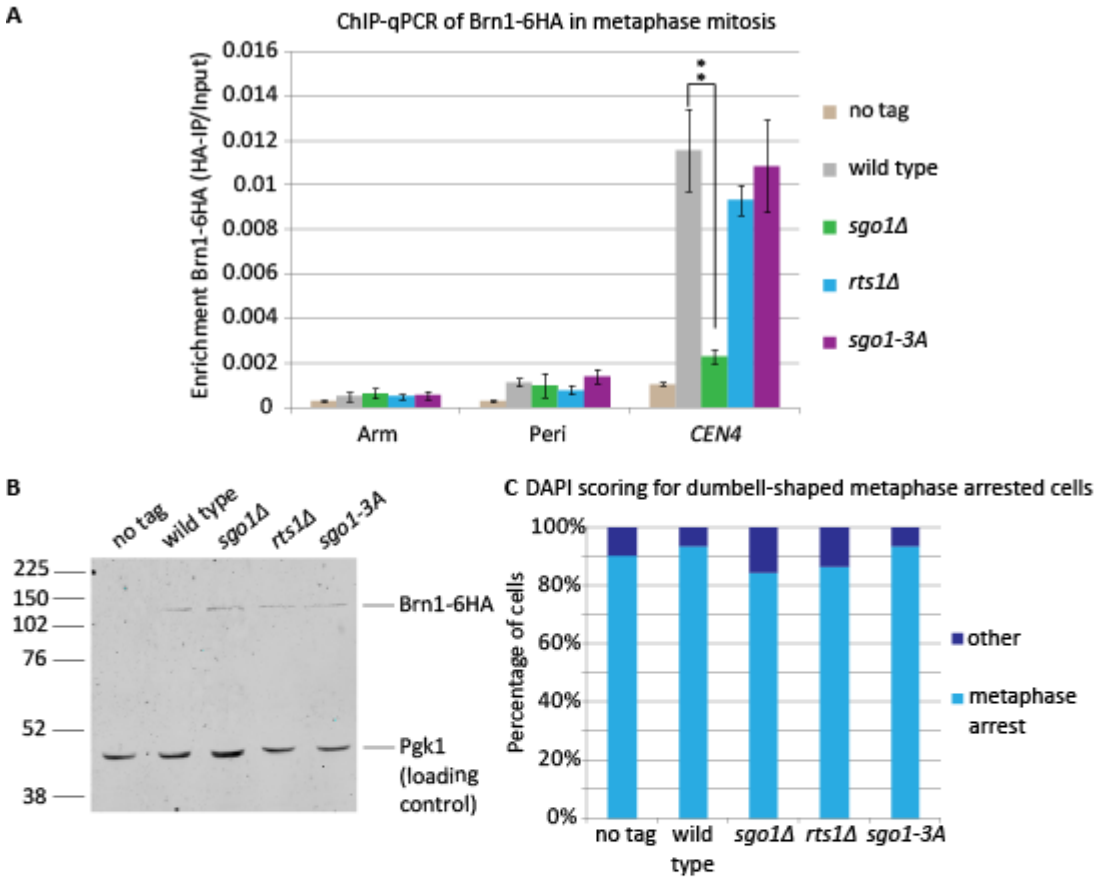

Figure 2.2.6.2: Condensin localisation to the centromeres in metaphase of mitosis is dependent on Sgo1, but not Rts1.

ChIP-qPCR of condensin in nocodazole arrested mitotic cells, shows condensin enrichment at the centromere depends on Sgo1, but not on Rts1. A) Strains containing Brn1-6HA were arrested in metaphase of mitosis in the presence of nocodazole, before harvesting for ChIP-qPCR. ChIP for Brn1-6HA was carried out in wild type (5708), *sgo1Δ* (8834), *rts1Δ* (9218) and *sgo1-3A* (9276), as well as in a no tag background (1176), using 12CA5 antibody against 6HA. *Sgo1-3A* allele specifically abolishes the interaction between Sgo1 and Rts1 (Xu 2009). Average of 4 repeats for Arm, Peri and *CEN4*. Error bars show standard error. Paired student T test gave a p value=0.0099 for *sgo1Δ* at *CEN4*. No other site or mutant was significantly decreased in Brn1-6HA enrichment compared to wild type. B) Western blotting for Brn1-6HA and a loading control (Pgk1) in the strains used for ChIP-qPCR. Western blot developed by LICOR, using 12CA5 to probe against Brn1-6HA, and homemade rabbit anti-PGK1 for the loading control. No tag (1176), wild type (5708), *sgo1Δ* (8834), *rts1Δ* (9218) and *sgo1-3A* (9276) samples shown. C) DAPI scoring of dumbell-shaped metaphase arrested cells, for no tag (1176), wild type (5708), *sgo1Δ* (8834), *rts1Δ* (218) and *sgo1-3A* (9276). Average of 4 repeats, n=100.

but is not essential, for the interaction between Sgo1 and condensin, or for the localisation of Brn1 to the DNA.

2.4 Discussion

2.4.1 Condensin is important for faithful chromosome segregation in meiosis I and II

The condensin complex binds throughout the yeast genome, with a frequency of around 1 condensin complex per 10.7 kb DNA (Wang *et al.*, 2005). However, condensin is highly enriched at both the rDNA and the centromeres, and has essential roles at both of these loci (Freeman, Aragon-Alcaide and Strunnikov, 2000; Bhalla, Biggins and Murray, 2002; Lavoie, Hogan and Koshland, 2002; Wang *et al.*, 2005; Yong-Gonzalez *et al.*, 2007; Bachellier-Bassi *et al.*, 2008; D'Ambrosio *et al.*, 2008; Johzuka and Horiuchi, 2009; Stephens *et al.*, 2011; Tada *et al.*, 2011; Peplowska, Wallek and Storchova, 2014; Verzijlbergen *et al.*, 2014; Leonard *et al.*, 2015). Condensin function at the rDNA has been well documented in both mitosis and meiosis in ensuring that the rDNA does not become tangled in anaphase, and that double strand break formation is suppressed in meiosis (Strunnikov, Hogan and Koshland, 1995; Freeman, Aragon-Alcaide and Strunnikov, 2000; Lavoie *et al.*, 2000; Bhalla, Biggins and Murray, 2002; Lavoie, Hogan and Koshland, 2002; Yu and Koshland, 2003; Li, Jin and Yu, 2014). However, there are several lines of evidence that indicate that the role of condensin at the centromere in kinetochore biorientation during mitosis is important for correct chromosome segregation (Gerlich *et al.*, 2006; Yong-Gonzalez *et al.*, 2007; Ribeiro *et al.*, 2009; Stephens *et al.*, 2011; Tada *et al.*, 2011; Peplowska, Wallek and Storchova, 2014; Verzijlbergen *et al.*, 2014; Leonard *et al.*, 2015). In this study I have shown that in metaphase I of meiosis, as in mitosis, Sgo1 interacts with condensin, and is essential for the recruitment of the condensin complex to this region. Thus suggesting that the function of condensin in centromeric chromatin structure may be conserved between mitosis and meiosis.

After I performed the experiments with the condensin mutant, *ycs4S*, a recent study revealed that the meiosis-specific phenotypes of this allele are not due to the disruption of Ycs4 itself (Markowitz *et al.*, 2017). A mutation in the promoter of the *RED1* gene, that resides just downstream of *YCS4*, is linked to the tagged Ycs4-12xMYC, which causes a 75 % reduction in *RED1* expression, reducing Red1 protein levels to 20 % of wild type (Markowitz *et al.*, 2017). This results in a failure to activate the meiotic checkpoint network in response

to unrepaired DSBs, so cells progress through meiosis without fully repairing DSBs (Markowitz *et al.*, 2017). Therefore only the effect of depleting condensin through using the *ycg1-2* condensin allele with be discussed.

By analysis of chromosome segregation during meiosis in the condensin mutant, *ycg1-2*, this revealed that the condensin complex may have a more general role in chromosome segregation, rather than just segregation of the rDNA. Analysis of homozygous *CEN5 tetO*/TetR-GFP dots in tetranucleates revealed that over 20 % of condensin mutants missegregated *CEN5*: consistent with the DNA missegregation phenotype of condensin mutants previously described (Yu and Koshland, 2003; Li, Jin and Yu, 2014).

Global defects in meiotic recombination occur in condensin mutants, which could lead to reduced homologue pairing, and thus be the cause of both the homologue and sister chromatid segregation defects seen by analysis of homozygous *CEN5 tetO*/TetR-GFP dots (Li, Jin and Yu, 2014; Hong, Choi and Kim, 2015). However, my data suggests that condensin could play a role in chromosome segregation subsequent to the function in meiotic recombination. By allowing *ycg1-2* to undergo prophase at the permissive temperature, before shifting to the restrictive temperature, nearly 40 % of tetranucleate cells missegregated *CEN5 tetO*/TetR-GFP dots. This confirms that condensin has a role in meiotic chromosome segregation independent of its role in recombination. The meiosis II segregation defect of condensin mutants is less pronounced than that of cells lacking *SGO1*, which randomly segregate sister chromatids in meiosis II due to cleavage of centromeric Rec8 in anaphase I. However, Sgo1 is also important for kinetochore orientation, and condensin may contribute to this function of Sgo1 at centromeres. Based on the data from mitotic cells, I suggest that condensin has a role in strengthening the pericentromeric chromatin region of the chromosomes in meiosis, to promote correct kinetochore orientation and withstand tension forces.

Analysis of homozygous *CEN5 tetO*/TetR-GFP dot segregation in cells lacking *SGO1* at the binucleate stage, after meiosis I, showed that 10-17 % of cells had missegregated homologous chromosomes. Therefore Sgo1 contributes towards correct biorientation of homologues in meiosis I, in an analogous way to promoting kinetochore biorientation in budding yeast mitosis (Katis *et al.*, 2004a; Indjeian, Stern and Murray, 2005; Fernius and

Hardwick, 2007; Indjeian and Murray, 2007; Kiburz, Amon and Marston, 2008; Storchova *et al.*, 2011; Eshleman and Morgan, 2014; Nerusheva *et al.*, 2014; Peplowska, Wallek and Storchova, 2014; Verzijlbergen *et al.*, 2014). In asynchronous meiotic time course experiments, 17 % of *ycg1-2* binucleate cells had partitioned homozygous GFP foci to the same pole, suggestive of homologous chromosome non-disjunction during meiosis I. However, when synchronised and allowed to undergo meiotic recombination at the permissive temperature before shifting to the restrictive temperature, *ycg1-2* binucleate cells failed to show any meiosis I defect. Therefore there was a discrepancy between results of the two differing experimental protocols. In an asynchronous meiotic time course, it is possible that the binucleate cells had actually undergone meiosis II and failed to segregate the DNA into four masses, thus the higher percentage of missegregation could be due to observation of abortive meiosis I. On the other hand, a caveat of the synchronised experimental protocol is that functional condensin could persist even 90 min after shifting to the restrictive temperature. Live cell imaging with cell cycle stage markers, such as Pds1 (securin), may help to clarify the importance of condensin in meiosis I chromosome segregation. Overall, Sgo1 has a minor role in homologue biorientation in meiosis I, but it is unclear if condensin contributes to this function.

Condensin mutants had been previously described to have defects in meiosis I kinetochore orientation (Brito, Yu and Amon, 2010). When *ycg1-2* mutants containing heterozygous *CEN5 tetO*/TetR-GFP dots underwent meiosis I, I found that only 6.6 % of binucleates had a mono-orientation defect and segregated sister chromatids. This is in contrast to (Brito, Yu and Amon, 2010) where a much stronger phenotype of 15 % sister chromatid segregation was observed upon meiotic depletion of *BRN1*. Therefore condensin may have a minor role in mono-orientation in meiosis I, with the defect differing depending on the allele used for assessment (Brito, Yu and Amon, 2010). In the future, further experiments will need to be carried out to clarify the mono-orientation defects of condensin mutants. A recent investigation also revealed a potential role for Sgo1 in mono-orientation through promoting Ipl1-dependent localisation of Mam1 (Mehta *et al.*, 2018). Overall however, the available evidence is consistent with both Sgo1 and condensin playing a minor role in meiosis I kinetochore structure and tension sensing, and a more prominent role in meiosis II sister chromatid segregation.

2.4.2 The interaction between Sgo1 and condensin may be partially mediated through additional components

In budding yeast mitosis Sgo1 recruits condensin specifically to the centromeric region, independently of its recruitment to the rDNA and other chromosomal loci (Peplowska, Wallek and Storchova, 2014; Verzijlbergen *et al.*, 2014). An aim of this project was to identify the subunit of condensin that bound to Sgo1, in order to generate an allele of *SGO1* that would specifically disrupt the interaction with condensin, much like the *sgo1-3A* mutant that prevents PP2A-Rts1 localisation to centromeres (Xu *et al.*, 2009). This would then allow condensin function at centromeres in both mitosis and meiosis to be fully dissected, without the disruption of global condensin function.

To identify the subunit of condensin that binds to Sgo1 a yeast-two-hybrid assay was undertaken (James, Halladay and Craig, 1996). An interaction between GAD-Sgo1 and GBD-Rts1 was detected, but no interaction observed with GBD-Brn1, GBD-Ycs4 or GBD-Ycs5. This failure to detect an interaction between the condensin subunits and Sgo1 may be due to the N-terminal tag on Sgo1 disrupting the protein folding, or obstructing the N-terminal coiled-coil domain, as the interaction with Rts1 was seen to be very weak. Additional yeast-two-hybrid experiments with increased linker length in the region between the GAD tag and Sgo1 were carried out with Rts1, but did not improve the strength of the interaction detected. Therefore this approach did not shed any light on the subunit of condensin that bound to Sgo1.

Cross-linking mass spectrometry is a technique that allows interactions between two proteins to be mapped by mass spectrometry (Rappsilber, 2011). This technique requires high quantities of protein, therefore purification of native Sgo1 from yeast cells would be unsuitable due to the low yield obtained. Therefore recombinant GST-Sgo1 was expressed in *E. coli*, and small scale purifications carried out with glutathione resin. But the GST-Sgo1 failed to efficiently bind to the resin, and did not bind to Rts1 or to condensin. The presence of GST-Sgo1 in the pellet, and the failure to bind to the resin and to Rts1, suggested that GST-Sgo1 may have aggregated or misfolded. Sgo1 is post-translationally modified in budding yeast, and therefore these modifications may be important for correct protein folding and protein:protein interactions. In the future, over-expression of Sgo1 from yeast or recombinant Sgo1 from insect cells may allow higher quantities of Sgo1 to be purified for cross-linking experiments with condensin.

The failure of the yeast-two-hybrid and recombinant protein assays may be due to additional factors playing a role in the interaction between Sgo1 and condensin. In the literature there are some inconsistencies as to the role of PP2A-Rts1 in the interaction, therefore I tried to address these in this study. In Peplowska 2014, GFP-tagged condensin is absent from centromeres in *rts1Δ*, and the interaction of Sgo1 and condensin is abolished by co-immunoprecipitation. However, inconsistent with this, it was shown that the phosphatase activity of PP2A is not required for the interaction (Peplowska, Wallek and Storchova, 2014). Published experiments from the Marston Lab showed that the interaction between Sgo1 and condensin is maintained in the *sgo1-3A* mutant (Verzijlbergen *et al.*, 2014). I carried out a co-immunoprecipitation experiment of Sgo1-SZZ-TAP and Brn1-6HA in metaphase of mitosis in *rts1Δ,* and the interaction was maintained. By ChIP, condensin also localised to kinetochores in both *sgo1-3A* and *rts1Δ*, again suggesting that PP2A-Rts1 may not have a role in condensin recruitment. However, Sgo1 levels are increased at centromeres in *rts1Δ*, therefore condensin levels should also be increased (Nerusheva *et al.*, 2014). As they are not, this suggests that PP2A-Rts1 may have a minor role in localisation of condensin to centromeres, and this defect in localisation may be amplified under specific experimental conditions.

I next tried to determine the region of Sgo1 that interacts with condensin. The interaction between Sgo1 and condensin is disrupted in the *sgo1-700* mutant (Indjeian, Stern and Murray, 2005). However, the *sgo1-700* mutant has reduced localisation to the centromeric region (Verzijlbergen *et al.*, 2014), therefore if the interaction between Sgo1 and condensin is mediated by the centromeric chromatin this would explain the loss of interaction. However, co-immunoprecipitation of Sgo1 and condensin in *bub1Δ*, in which Sgo1 is delocalised from the centromere (Kitajima, Kawashima and Watanabe, 2004; Tang *et al.*, 2004; Kiburz *et al.*, 2005; Kitajima *et al.*, 2005; Riedel *et al.*, 2006; Fernius and Hardwick, 2007; Kawashima *et al.*, 2010; Nerusheva *et al.*, 2014), showed that the interaction was maintained and did not rely on the presence of centromeric chromatin.

The mutations in *sgo1-700* are two single residue substitutions (Indjeian, Stern and Murray, 2005), suggesting that the interaction with condensin is through a specific region of Sgo1. Therefore truncations of Sgo1 were used to pull-down condensin, with the prediction that

Sgo1 truncations Sgo1-1-208 and Sgo1-1-308, which lacked the regions mutated in *sgo1-700*, would lose the interaction with condensin. However, they did not, and all of the Sgo1 truncations interacted with condensin. The explanation for this is unclear, however it may be due to inefficient cleavage of the centromeric DNA by benzonase due to the tight compaction of this region.

One caveat with all of the experiments carried out to characterise the interaction between Sgo1 and condensin, is that these relied on the assumption that the interaction is direct. However, in *S. pombe* the localisation of condensin to the centromeric region relies on the Lrs4 and Csm1 homologues, as well as on Histone H2A (and H2A.Z) (Tada *et al.*, 2011). In *S. cerevisiae* Sgo1 binds to centromeric region via H2A-Ser121 phosphorylation (Kawashima *et al.*, 2010), and so interacts directly with histones. A possibility is that condensin may not directly interact with Sgo1, but instead may bind to histones or kinetochore proteins in close proximity to Sgo1 that would result in co-purification with the Sgo1-PP2A-Rts1 complex. An alternative explanation may be that several proteins could act cooperatively to recruit and maintain condensin at the centromeric region.

A potential hypothesis may be that condensin transiently interacts with Sgo1 in the cytoplasm to allow recruitment to the centromeric region, followed by stabilisation at this loci by binding to other proteins, such as histones. This would explain why the interaction between Sgo1 and condensin is captured in *bub1Δ,* when Sgo1 is delocalised from the centromeric region, but also why there is a residual amount of condensin remaining at centromeres in Sgo1 mutants. In depth characterisation of the *sgo1-700* mutant, and the single Pro390His and Asp519Asn point mutants by mass spectrometry and by co-immunoprecipitation with condensin may reveal which residue, if not both, is essential for the interaction. Pro390 is at the C-terminal end of the basic region of Sgo1 that binds to H2A-S121 phosphorylation (Kawashima *et al.*, 2010), therefore mutation of this residue may disrupt this interaction, and also consequently disrupt the deposition of condensin onto the chromatin.

Overall the goal to create an allele of *SGO1* that disrupted the interaction with condensin was not achieved. However, this study has revealed that condensin localisation to the centromeric region in metaphase I of meiosis is Sgo1-dependent and PP2A-Rts1

independent. Once localised to this region, condensin has a crucial role in chromosome segregation in meiosis I and meiosis II, most likely through stabilising the centromeric chromatin to form a rigid platform for microtubule attachment to either mono-oriented or bioriented kinetochores.

Chapter 3. Characterisation of the role of Sgo1 phosphorylation in meiosis

3.1 Introduction

Shugoshin proteins are pericentromeric adaptor proteins that have roles in cohesion protection in both mitosis and meiosis (Kerrebrock *et al.*, 1995; Katis *et al.*, 2004a; Kitajima, Kawashima and Watanabe, 2004; Marston *et al.*, 2004; Rabitsch *et al.*, 2004; Tang *et al.*, 2004; Kitajima *et al.*, 2005; Kiburz *et al.*, 2005; McGuinness *et al.*, 2005; Llano *et al.*, 2008; Lee *et al.*, 2008; Katis *et al.*, 2010; Ishiguro *et al.*, 2010; Liu, Rankin and Yu, 2013), and are also important for tension sensing and biorientation of sister chromatid kinetochores (Salic, Waters and Mitchison, 2004; Indjeian, Stern and Murray, 2005; Tang *et al.*, 2006; Fernius and Hardwick, 2007; Kawashima *et al.*, 2007; Indjeian and Murray, 2007; Pouwels *et al.*, 2007; Vanoosthuyse, Prykhozhij and Hardwick, 2007; Kiburz, Amon and Marston, 2008; Lee *et al.*, 2008; Verzijlbergen *et al.*, 2014; Peplowska, Wallek and Storchova, 2014; Nerusheva *et al.*, 2014; Eshleman and Morgan, 2014). Although these functions have been well-characterised, the regulation of shugoshins varies significantly between species, however, what they all have in common is the involvement of kinases and phosphatases.

A well-documented example of shugoshin phospho-regulation is the CDK-dependent phosphorylation of Sgo1 on Thr346 during prophase of mammalian mitosis to allow binding to cohesin (Liu, Rankin and Yu, 2013). Phosphorylated Sgo1 is recruited to the kinetochores through Histone H2A-T120 phosphorylation by Bub1, to which Sgo1 binds to through a C-terminal basic region (Tang *et al.*, 2004; Kitajima *et al.*, 2005; Kawashima *et al.*, 2010; Liu, Jia and Yu, 2013). This, along with phosphorylation of Sgo1 by Aurora B/C kinase, specifically localises Sgo1 to kinetochores (Pouwels *et al.*, 2007; Kawashima *et al.*, 2007; Lee *et al.*, 2014). Once localised, the phosphorylation of Sgo1-T346 allows Sgo1, with its binding partner PP2A-B56, to directly bind to, and dephosphorylate, cohesin at the centromeric region (Kitajima *et al.*, 2006; Liu, Rankin and Yu, 2013; Liu, Jia and Yu, 2013). Only in metaphase, when the bioriented kinetochores come under tension, is Sgo1 dephosphorylated leading to its redistribution away from cohesin at the centromeres, and re-association with H2A-T120p at kinetochores (Lee *et al.*, 2008; Liu, Jia and Yu, 2013). This deprotects cohesin, and allows cleavage by separase during anaphase. Therefore a Sgo1 phosphorylation cycle plays an essential role in mitotic cohesin protection; without Sgo1-T346 phosphorylation and cohesin binding there is chromosome missegregation, but

without Sgo1 dephosphorylation and redistribution to kinetochores in metaphase, lagging chromosomes will ensue (Liu, Rankin and Yu, 2013; Liu, Jia and Yu, 2013).

In higher vertebrates a second shugoshin family member, Sgo2, is the main meiotic shugoshin, as sgo2-null mice are viable but infertile (Llano *et al.*, 2008). However, Sgo2 may also function in mitotic chromosome segregation and have complementary roles to Sgo1 (Tanno *et al.*, 2010). Sgo2 localises to centromeres in an Aurora B/C kinase phosphorylation-dependent manner, where it recruits both PP2A-B56 and MCAK to facilitate centromeric cohesin protection and chromosome alignment (Huang *et al.*, 2007; Lee *et al.*, 2008; Tanno *et al.*, 2010; Rattani *et al.*, 2017). Phosphorylation of Sgo2 N-terminus by Aurora B allows PP2A-B56 binding, and Sgo2 mid-region phosphorylation, most likely at residues T537 and T620, allows MCAK binding (Tanno *et al.*, 2010). This mechanism of Sgo2 phospho-regulation by Aurora B is conserved in the mouse germ line, and is essential for faithful chromosome segregation in meiosis (Tanno *et al.*, 2010; Rattani *et al.*, 2017).

In *Drosophila melanogaster* (*D. melanogaster*), the function and localisation of the shugoshin homologue MEI-S332 is also regulated by both kinases and phosphatases (Clarke *et al.*, 2005; Resnick *et al.*, 2006; Nogueira *et al.*, 2014; Pinto and Orr-Weaver, 2017). In both mitosis and meiosis, the centromeric localisation of MEI-S332 in prophase relies on INCENP and Aurora B (Resnick *et al.*, 2006; Nogueira *et al.*, 2014). *In vitro* Aurora B directly phosphorylates MEI-S332, and phosphomutants of MEI-S332 have reduced centromere localisation *in vivo* (Resnick *et al.*, 2006; Nogueira *et al.*, 2014). Interestingly, PP2A is also essential for centromeric MEI-S332 localisation during metaphase I of meiosis (Pinto and Orr-Weaver, 2017). MEI-S332 is subsequently removed from centromeres at the metaphase to anaphase transition of mitosis in a POLO kinase dependent manner (Clarke *et al.*, 2005; Nogueira *et al.*, 2014). POLO kinase directly binds to a phosphorylated POLO binding domain on MEI-S332 and subsequently phosphorylates MEI-S332 itself (Clarke *et al.*, 2005). POLO kinase was also found to antagonise MEI-S332 function in meiosis, although the exact mechanism by which this occurs is unknown (Clarke *et al.*, 2005). This regulation may be conserved, as Sgo1 in HeLa cell mitosis is regulated by Plk1 and PP2A-Aα (Kitajima *et al.*, 2006; Tang *et al.*, 2006). In PP2A-Aα-RNAi experiments, Sgo1 is delocalised from centromeres, and this results in chromosome missegregation (Kitajima *et al.*, 2006;

Tang *et al.*, 2006). However, this defect is rescued by co-depletion of Plk1 by RNAi (RNA interference) (Tang *et al.*, 2006), suggesting that in human cells Plk1 also negatively regulates Sgo1 localisation to centromeres.

Therefore in higher eukaryotes members of the shugoshin family are regulated by CDKs, the Aurora B/C family of proteins, and by Polo kinase. Although these phosphorylation events do differ significantly in the kinase responsible, and the outcome that this has on shugoshin localisation and protein:protein interactions, the common feature is that disruption of these phosphorylation events abrogates shugoshin function.

However the story is less clear in budding yeast, as Sgo1 has not yet been shown to be directly regulated by phosphorylation, although there is evidence for regulation by kinases and phosphatases. Budding yeast Sgo1 interacts with PP2A-Rts1 and the CPC, including Aurora B (Ipl1), in both mitosis and meiosis, therefore bringing Sgo1 into close proximity with potential phosphoregulators (Riedel *et al.*, 2006; Yu and Koshland, 2007; Clift, Bizzari and Marston, 2009; Xu *et al.*, 2009; Verzijlbergen *et al.*, 2014; Peplowska, Wallek and Storchova, 2014; Eshleman and Morgan, 2014).

In budding yeast mitosis, Sgo1 localises to the pericentromere prior to metaphase, then is removed upon sister kinetochore biorientation during metaphase, followed by degradation in anaphase (Katis *et al.*, 2004a; Marston *et al.*, 2004; Indjeian, Stern and Murray, 2005; Nerusheva *et al.*, 2014; Eshleman and Morgan, 2014). Sgo1 localisation to centromeres is dependent on phosphorylation of Histone H2A-S121 by Bub1 kinase (Kawashima *et al.*, 2010). However, Bub1 kinase carries out other functions required for retention of Sgo1 at centromeres, as *BUB1* deletion removes Sgo1 from the pericentromere even in the presence of the phospho-mimetic H2A-S121D mutation (Nerusheva *et al.*, 2014). Additionally Mps1 kinase activity is also required for correct Bub1 and Sgo1 kinetochore localisation, and Sgo1 fails to localise to kinetochores in the absence of Mps1 (Storchova *et al.*, 2011). Deletion of *RTS1*, a PP2A regulatory subunit and known binding partner of Sgo1, increases Sgo1 levels at the pericentromere significantly in metaphase-arrested cells lacking tension (Nerusheva *et al.*, 2014).

In meiosis, Sgo1 localisation to the centromeres is essential for protecting centromeric cohesin from cleavage during anaphase I. This localisation of Sgo1 depends on Bub1, as in mitosis (Kiburz *et al.*, 2005; Riedel *et al.*, 2006). However, depletion of *IPL1* (Aurora B) kinase also causes a decrease in Sgo1 levels at centromeres, and mislocalises Rts1 from centromeres in telophase I, resulting in chromosome missegregation in meiosis II (Monje-Casas *et al.*, 2007; Yu and Koshland, 2007). In wild type cells, Sgo1 is maintained at centromeres until anaphase II when it is removed and subsequently degraded: this removal of Sgo1 was found to depend on Hrr25 kinase activity, and is essential for allowing timely centromeric Rec8 cleavage in anaphase II (Arguello-Miranda *et al.*, 2017; Jonak *et al.*, 2017). This suggests that Sgo1 localisation to centromeres is positively regulated by Bub1, Mps1 and Ipl1 in meiosis I, and is negatively regulated by Hrr25 in meiosis II, strongly suggesting that Sgo1 may be phosphoregulated.

Previously in the Marston lab, Sgo1 was purified from both mitotic and meiotic budding yeast, and mass spectrometry carried out on the immunoprecipitates. This revealed that Sgo1 was indeed a phosphoprotein, and identified several specific phosphorylation sites, further enhancing the hypothesis that Sgo1 may be regulated by phosphorylation, as in higher eukaryotes. Therefore my aim was to determine whether phosphorylation of Sgo1 at these specific sites is important for accurate chromosome segregation.

3.2 Results

3.2.1 Mass spectrometry identifies Sgo1 phosphorylation sites

Previously, in the Marston lab, Sgo1 was purified from cells either undergoing mitosis or meiosis, and mass spectrometry was carried out to identify phosphorylation sites (A. Marston and S. Galander). To identify Sgo1 phosphorylation sites that may play a role in mitosis, Sgo1-SZZ-TAP was immunoprecipitated from cells either arrested in metaphase of mitosis in tension-free conditions using the *tub2-401* cold-sensitive tubulin allele (Huffaker, Thomas and Botstein, 1988), or from asynchronous mitotic cells (A. Marston). Mass spectrometry was then carried out on the purified Sgo1-SZZ-TAP. Two phosphorylated residues, S151 and S487, were identified in both the asynchronous and metaphase-arrested samples, and additionally S421 was identified in the metaphase-arrested sample alone (Figure 3.2.1.1A). The S421 phosphorylation may be metaphase-specific as this region of Sgo1 was covered in the purification of Sgo1-SZZ-TAP from asynchronous cells.

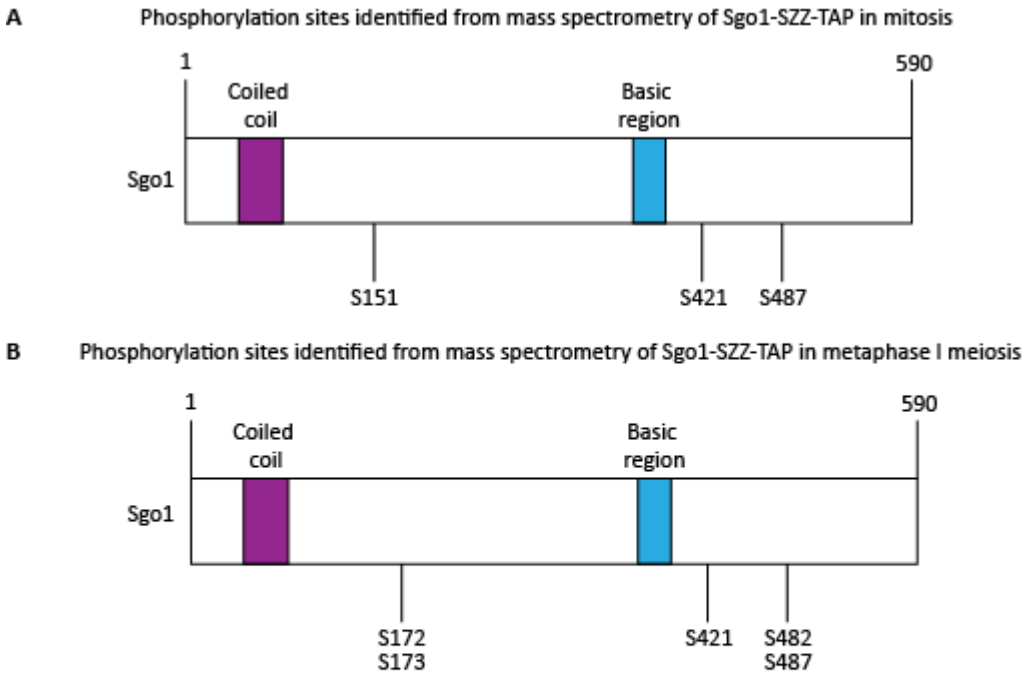

Figure 3.2.1.1 Sgo1 phosphorylation sites identified by mass spectrometry
A) Sgo1-SZZ-TAP was immunoprecipitated from mitotic asynchronous cycling and *tub2-401* metaphase-arrested budding yeast, and mass spectrometry carried out (A. Marston). Sgo1 phosphorylation on residues S151, S421 and S487 identified. B) Sgo1-SZZ-TAP was immunoprecipitated from meiotic *pCLB2-CDC20* metaphase I arrested budding yeast, and mass spectrometry carried out (S. Galander). Sgo1 phosphorylation on residues S172, S173, S421, S482 and S487 identified.

During meiosis Sgo1 has an additional role in protecting centromeric cohesin from cleavage by separase during anaphase I (Katis *et al.*, 2004a; Kitajima, Kawashima and Watanabe, 2004; Marston *et al.*, 2004; Riedel *et al.*, 2006; Brar *et al.*, 2006; Xu *et al.*, 2009; Katis *et al.*, 2010), and additional phosphorylation sites might be important for this meiosis specific function. To identify sites on Sgo1 that are phosphorylated during meiosis I, Sgo1-SZZ-TAP was immunoprecipitated from *pCLB2-CDC20* metaphase I arrested meiotic cells (Lee and Amon, 2003) (S. Galander). Mass spectrometry revealed that Sgo1 was phosphorylated on residues S172, S173, S421, S482 and S487 (Figure 3.2.1.1B). Therefore six phosphorylated residues on Sgo1 were identified in total, with three of these being meiosis specific (A. Marston and S. Galander).

3.2.2 A screen of Sgo1 phosphomutants in budding yeast meiosis

To determine the importance of Sgo1 phosphorylation on the identified sites for accurate chromosome segregation, mutant versions of Sgo1 were generated. The relevant phosphorylated residues were mutated, either individually or in groups of two to four residues, to the phospho-null Alanine or phospho-mimetic Aspartate residues (C. Barnard). To analyse the effects of these mutations on chromosome segregation during meiosis, I employed the homozygous *CEN5 tetO*/TetR-GFP dot assay (Figure 2.2.2.1A, B, C) (Michaelis, Ciosk and Nasmyth, 1997). Wild type cells or the Sgo1 phosphomutants carrying the *CEN5 tetO*/TetR-GFP dots were induced to undergo meiosis, and the pattern of GFP foci was scored in the tetranucleate cells after 10 h (Figure 3.2.2.1A).

In wild type cells, following meiosis, each of the four nuclei will inherit chromosome V and therefore will carry a *CEN5 tetO*/TetR-GFP dot (Figure 2.2.1.1B). In contrast, in cells lacking (*sgo1Δ*), or depleted for (*pCLB2-3HA-SGO1*), Sgo1 both meiosis I and meiosis II chromosome segregation defects are observed due to both defective kinetochore orientation and cohesion protection (Figures 2.2.1.2A, 2.2.1.3B, C and 3.2.2.1A) (Katis *et al.*, 2004a; Kitajima, Kawashima and Watanabe, 2004; Marston *et al.*, 2004; Riedel *et al.*, 2006; Kiburz, Amon and Marston, 2008; Mehta *et al.*, 2018). Therefore any loss of Sgo1 function in the twenty-two Sgo1 phosphomutants generated would be detected using this assay.

Although 100 % of wild type tetranucleates are expected to have one GFP dot in each nuclei, only 92 % were observed to have this pattern (Figure 3.2.2.1A). This could be due to

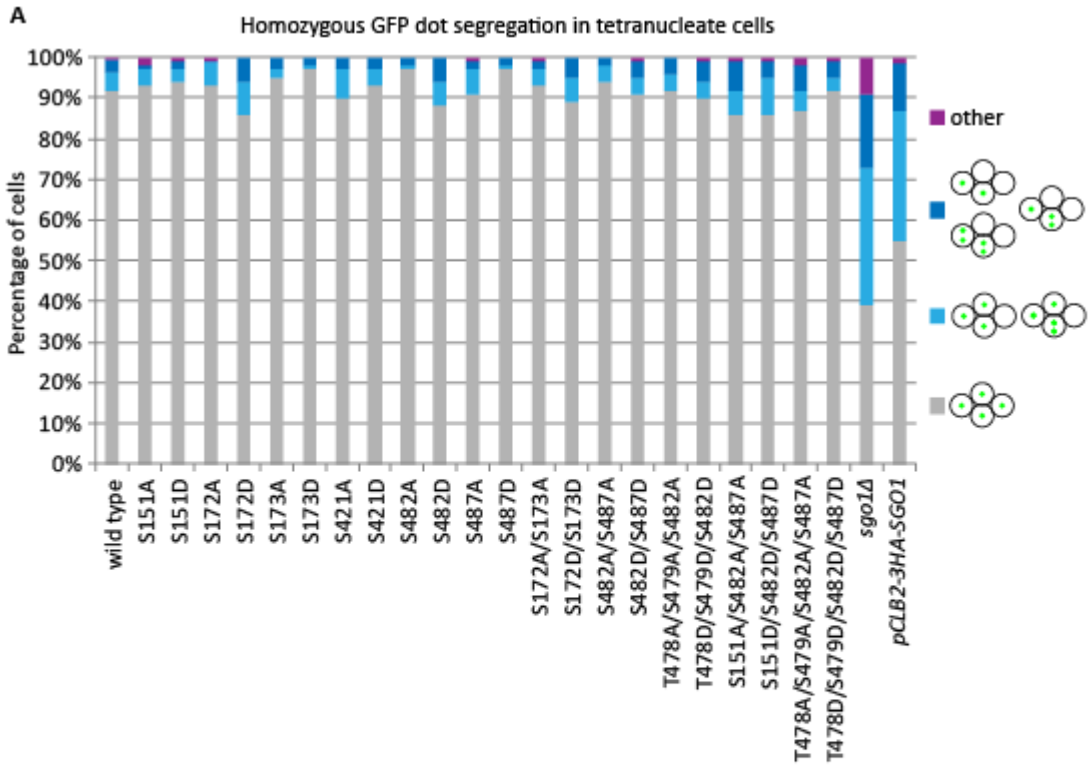

Figure 3.2.2.1 Sgo1 phosphomutants do not have severe meiotic chromosome segregation defects
A) Homozygous *CEN5 tetO*/TetR-GFP dot segregation in Sgo1 wild type and Sgo1 phosphomutant tetranucleates, with data for *sgo1Δ* and *pCLB2-3HA-SGO1* shown for comparison. Diploid strains were placed in sporulation media to induce meiosis, and after 10 h GFP dot segregation was counted in tetranucleates by fluorescence microscopy. Average of 6 repeats for wild type (strain 14441, n=600), and of one repeat for each Sgo1 phosphomutant (strains 14440, 14414, 16713, 16967, 14480, 14218, 12953, 14451, 17115, 17347, 14563, 16984, 14541, 14223, 17458, 14479, 14245, 14222, 17864, 18217, 17714, 18403, n=100). Average from 3 repeats for *sgo1Δ* (strain 877, n=311), and *pCLB2-3HA-SGO1* (strain 11668, n=301) as shown previously in Figure 2.2.1.3. Graph shown is the percentage of each phenotype.

difficultly with detection of the GFP foci or incomplete complementation of *SGO1*. This is due to the construction of the wild type strain by replacement of *sgo1Δ* with *SGO1* carrying a downstream marker, to be consistent with the phosphomutants that were made in the same way. Analysis of chromosome segregation in the Sgo1 phosphomutants revealed over 86 % wild type *CEN5* GFP dot segregation in all mutants, compared to 39 % in *sgo1Δ*, as described in Chapter 2 (Figures 2.2.1.3B and 3.2.2.1A). Therefore none of the Sgo1 phosphomutants analysed had a severe meiotic chromosome segregation defect, suggesting that none of the phosphorylation sites identified were required for Sgo1 function in meiosis.

3.2.3 Sgo1 is both phosphorylated and acetylated in budding yeast meiosis

The screen of the twenty-two Sgo1 phosphomutants showed that none of the phosphorylation sites previously identified were essential for Sgo1 function in budding yeast meiosis. However, because it seemed likely that the previous mass spectrometry did not identify all Sgo1 phosphorylation sites, I decided to repeat this experiment. Mass spectrometry of Sgo1-6HIS-3FLAG immunoprecipitated from metaphase I arrested meiotic cells (Figure 2.2.3.2A, C, D) revealed that Sgo1 was also phosphorylated on additional residues in meiosis to those mutated above. Previously identified phosphorylation of Sgo1 on residues S151, S173, S421, S482 and S487 were again identified, but in addition to these sites, residues S364, S423, S426, T444, S486, S518 and S523 were also phosphorylated (Figure 3.2.3.1A). In addition to the phosphorylated residues identified, acetylation of Sgo1 was also identified on residues K75, K81, K124, K420, K485 and K531 (Figure 2.2.3.2E and 3.2.3.1B). Therefore, Sgo1 is post-translationally modified by both phosphorylation and acetylation during metaphase I of meiosis, suggesting that regulation of Sgo1 in budding yeast is more complex than originally thought.

3.3 Discussion

Shugoshin proteins are regulated by phosphorylation in higher eukaryotes, by both kinases and phosphatases (Clarke *et al.*, 2005; Kitajima *et al.*, 2006; Resnick *et al.*, 2006; Tang *et al.*, 2006; Pouwels *et al.*, 2007; Tanno *et al.*, 2010; Liu, Rankin and Yu, 2013; Lee *et al.*, 2014; Nogueira *et al.*, 2014; Pinto and Orr-Weaver, 2017; Rattani *et al.*, 2017). This regulation differs between species, but in all cases is important for accurate localisation of Sgo1 to

A Phosphorylation sites identified from mass spectrometry of Sgo1-6HIS-3FLAG in metaphase I meiosis

B Acetylation sites identified from mass spectrometry of Sgo1-6HIS-3FLAG in metaphase I meiosis

Figure 3.2.3.1 Additional Sgo1 post-translational modifications identified by mass spectrometry
Sgo1-6HIS-3FLAG was immunoprecipitated from meiotic *pCLB2-CDC20* metaphase I arrested budding yeast, followed by trypsin digestion of the immunoprecipitate and mass spectrometry (Figure 2.2.3.2) A) Sgo1 phosphorylation on residues S151, S173, S364, S421, S423, S426, T444, S482, S486, S487, S518, T523 identified. The region of Sgo1 185-276 was not covered by mass spectrometry due to an absence of Lys residues in this region preventing trypsin digestion. B) Acetylation sites were also identified on immunoprecipitated Sgo1-6HIS-3FLAG from (A) on residues K71, K85, K124, K420, K485 and K531.

centromeres and pericentromeres, and for maintenance of correct protein:protein interactions.

Until recently there was no evidence for direct phosphorylation of Sgo1 in budding yeast, although there was evidence for phospho-regulation (Yu and Koshland, 2007; Storchova *et al.*, 2011; Nerusheva *et al.*, 2014; Arguello-Miranda *et al.*, 2017; Jonak *et al.*, 2017). Bub1, Mps1 and Aurora B kinase are important for correct Sgo1 localisation to centromeres, and PP2A-Rts1 phosphatase and Hrr25 kinase have been shown to negatively regulate Sgo1 localisation to this region in different cell cycle stages (Kiburz *et al.*, 2005; Riedel *et al.*, 2006; Fernius and Hardwick, 2007; Monje-Casas *et al.*, 2007; Yu and Koshland, 2007; Storchova *et al.*, 2011; Nerusheva *et al.*, 2014; Arguello-Miranda *et al.*, 2017; Jonak *et al.*, 2017). These observations prompted analysis of Sgo1 purified from both mitotic and meiotic budding yeast by mass spectrometry, and this revealed six phosphorylation sites. Mutation of these residues and subsequent analysis for chromosome segregation in meiosis using the *CEN5 tetO*/TetR-GFP dot assay showed that none of these sites were essential for Sgo1 function in cohesin protection budding yeast meiosis I.

However, after immunoprecipitation of Sgo1-6HIS-3FLAG from metaphase I arrested meiotic budding yeast using an updated protocol, seven further phosphorylation sites and six acetylation sites were identified. Analysis of the peptide coverage of Sgo1-6HIS-3FLAG revealed that region 185-276 of Sgo1 had not been covered during the mass spectrometry experiment. Closer inspection revealed that this region does not contain any Lysine residues, and therefore was not digested by trypsin to the shorter peptide lengths required for analysis by mass spectrometry. Digestion of Sgo1 with the alternative proteases Endoproteinase GluC and Proteinase K failed to improve Sgo1 sequence coverage in this region. Further trouble-shooting of Sgo1 protease digestion may improve sequence coverage in this region, and yield yet more post-translational modifications on Sgo1.

As the original screen of Sgo1 phosphomutants did not encompass all of the phosphorylated residues on Sgo1, this may explain why no meiotic phenotype was observed. Further screening of the new sites identified may reveal residues important for Sgo1 function in meiosis. However, the *CEN5 tetO*/TetR-GFP dot assay carried out relies on complete, or significant, loss of Sgo1 function that would result in gross chromosome

missegregation due to random segregation of sister chromatids in meiosis II. But, in higher eukaryotes shugoshin phosphorylation is carried out by multiple kinases, and can have both positive and negative effects on shugoshin function and localisation. Therefore it is likely that this may also be the case in budding yeast, and some phosphorylation events may promote Sgo1 function, whilst others abrogate it. Mass spectrometry of purified Sgo1 in *bub1-kd* (kinase dead allele of *BUB1*) and *rts1Δ* from metaphase arrested mitotic cells, and from cells containing *pCLB2-IPL1* and inhibited Mps1 and Hrr25 in meiosis, may yield mutant-specific differences in Sgo1 post-translational modification. Therefore more targeted mutation of Sgo1 phosphorylation sites could be carried out, and localisation of Sgo1, as well as chromosome segregation defects assayed for.

Similarly, identification of the acetyltransferase responsible for Sgo1 acetylation may yield information as to the function of the acetylation. Mutation of these acetylated residues and analysis of Sgo1 localisation and cohesin protection function in meiosis should be carried out in the future.

Several of the newly-identified sites of Sgo1 post-translational modifications may have a direct impact on Sgo1 function. Two of the acetylation sites, K71 and K85, lie in the coiled-coil domain that is the binding site for PP2A-Rts1 (Xu *et al.*, 2009; Eshleman and Morgan, 2014; Verzijlbergen *et al.*, 2014), and therefore post-translational modification of these residues may be important for correct Rts1 interaction with Sgo1. In a similar manner S364 lies in the C-terminal basic region of Sgo1 important for H2A-S121p binding (Kawashima *et al.*, 2010). As this residue is phosphorylated in metaphase, potentially dephosphorylation of this residue could delocalise Sgo1 from the centromeric region. Lastly, Sgo1 is important in correct kinetochore biorientation and tension sensing in mitosis and meiosis (Katis *et al.*, 2004a; Indjeian, Stern and Murray, 2005; Fernius and Hardwick, 2007; Indjeian and Murray, 2007; Kiburz, Amon and Marston, 2008; Storchova *et al.*, 2011; Eshleman and Morgan, 2014; Nerusheva *et al.*, 2014; Peplowska, Wallek and Storchova, 2014; Verzijlbergen *et al.*, 2014). This function of Sgo1 is disrupted in the *sgo1-700* allele that carried the Asp519-Asn mutation (Indjeian, Stern and Murray, 2005). This site is next to two newly identified phosphorylation sites at S518 and T523, therefore mutation of these sites may disrupt the tension-sensing function of Sgo1.

In conclusion, the screen of Sgo1 phosphomutants in budding yeast meiosis did not reveal any evidence for regulation of Sgo1 by phosphorylation. However, the position of newly identified post-translational modifications on Sgo1 suggests that it is highly likely that some of these sites may be important for Sgo1 regulation. Mutation of these, followed by analysis in both mitosis and meiosis, may give important insight into regulation of Sgo1 in budding yeast.

Chapter 4. The prophase pathway components have conserved expression and function in budding yeast meiosis

4.1 Introduction

4.1.1 Cohesin regulation in mitosis

In mammalian mitosis, cohesin regulation is highly important for correct mitotic chromosome behaviour. Cohesin transiently associates with the DNA until S phase, when the Smc3 subunit then undergoes post-translational modification that generates cohesion between the sister chromatids (Zhang *et al.*, 2008b; Ladurner *et al.*, 2016; Alomer *et al.*, 2017). This holds the sister chromatids together until mitosis, when there is a two-step removal of cohesin from the DNA (Losada, Hirano and Hirano, 1998; Losada *et al.*, 2000; Waizenegger *et al.*, 2000). The first step is destabilisation of the cohesin ring from the DNA through the "prophase pathway", which removes the majority of the cohesin from the arms of the sister chromatids. The second step follows at the metaphase to anaphase transition, when the remaining cohesin is cleaved by separase (Losada, Hirano and Hirano, 1998; Losada *et al.*, 2000; Sumara *et al.*, 2000; Waizenegger *et al.*, 2000; Losada, Hirano and Hirano, 2002; Hauf, Waizenegger and Peters, 2001).

The rapid destabilisation and re-loading of cohesin onto the DNA in telophase and G1 is due to the opposing action of Wapl and the cohesion loader complex Nipbl/Mau2 (Tonkin *et al.*, 2004; Gandhi, Gillespie and Hirano, 2006; Kueng *et al.*, 2006; Watrin *et al.*, 2006). During S phase, Esco2 associates with cohesin and acetylates Smc3 on two conserved lysine residues, K105 and K106, as DNA replication occurs (Hou and Zou, 2005; Zhang *et al.*, 2008b; Song *et al.*, 2012; Alomer *et al.*, 2017). This acetylation in the Smc3-ATPase domain locks the cohesin ring shut at the Smc3-Scc1 exit gate, thus preventing dissociation from the DNA, and this is hypothesised to occur due to a change in ATPase activity (Zhang *et al.*, 2008b; Buheitel and Stemmann, 2013; Ladurner *et al.*, 2016). Esco1 also contributes to cohesin acetylation, however, this occurs throughout the cell cycle and may promote cohesin function in structuring the DNA and regulating chromatin loops, rather than in establishing cohesion (Hou and Zou, 2005; Zhang *et al.*, 2008b; Song *et al.*, 2012; Alomer *et al.*, 2017). Co-depletion of Esco1 and Esco2 in chicken DT40 cells revealed that not only are these acetyltransferases important in promoting sister chromatid cohesion after S phase, but are also important for interphase chromatin territory structure and gene expression

through negatively regulating cohesin association with interphase chromatin (Kawasumi *et al.*, 2017).

As cohesin is acetylated during replication, sororin binds to the Pds5 subunit of cohesin via FGF motifs on sororin (Rankin, Ayad and Kirschner, 2005; Lafont, Song and Rankin, 2010; Nishiyama *et al.*, 2010; Ladurner *et al.*, 2016). This displaces Wapl from Pds5, as both sororin and Wapl compete for the same binding site, although Wapl still remains bound to cohesin through SA2/Scc1 (Shintomi and Hirano, 2009; Nishiyama *et al.*, 2010; Hara *et al.*, 2014). Sororin binding to Pds5 stabilises the acetylated pool of cohesive cohesin on the DNA to hold the sister chromatids together (Rankin, Ayad and Kirschner, 2005; Schmitz *et al.*, 2007; Lafont, Song and Rankin, 2010; Nishiyama *et al.*, 2010; Song *et al.*, 2012; Ladurner *et al.*, 2016). Interestingly, in HeLa cells Smc3-K105R,K106R mutants interact with sororin and stably bind to the chromatin in G2, suggesting that the acetylation of these residues is not essential, but that it is the conformational change in Smc3 during DNA replication that subsequently allows sororin binding and cohesion establishment (Nishiyama *et al.*, 2010; Ladurner *et al.*, 2016). Acetyl-null mutants of Smc3 (Smc3-K105R,K106R or Smc3-K105A,K106A) have no defects when expressed as the sole source of Smc3 in chicken DT40 cells, and the acetyl-mimic Smc3-K105Q,K106Q mutant does not rescue the sister chromatid cohesion defects of Esco1 and Esco2 co-depletion, suggesting Smc3 acetylation is not as crucial as previously thought (Kawasumi *et al.*, 2017).

As cells progress into mitotic prophase, the prophase pathway of cohesin removal becomes active. Cdk1 and Aurora B phosphorylate sororin on multiple sites, triggering its dissociation from Pds5, and allowing Wapl to re-associate with Pds5, and consequently destabilise acetylated cohesin on chromosome arms (Gandhi, Gillespie and Hirano, 2006; Kueng *et al.*, 2006; Shintomi and Hirano, 2009; Nishiyama *et al.*, 2010; Dreier, Bekier and Taylor, 2011; Nishiyama *et al.*, 2013; Hara *et al.*, 2014; Huis in 't Veld *et al.*, 2014). At kinetochores, Sgo1-PP2A is recruited through phosphorylation of H2A-Thr120 by Bub1, promoting centromeric cohesin protection (Salic, Waters and Mitchison, 2004; Tang *et al.*, 2004; Kitajima *et al.*, 2005; McGuinness *et al.*, 2005; Kitajima *et al.*, 2006; Tang *et al.*, 2006; Liu, Jia and Yu, 2013). Phosphorylation of Sgo1 on Thr346 by Cdk1 allows direct binding of Sgo1-PP2A to the SA2/Scc1 subunits of cohesin, thus PP2A can dephosphorylate sororin, protecting sororin, and thus cohesin, from destabilisation by Wapl (Nishiyama *et al.*, 2010; Liu, Rankin and Yu,

2013; Nishiyama *et al.*, 2013; Hara *et al.*, 2014). Additionally the SA2 subunit of cohesin is phosphorylated by Plk1 in prophase, which contributes to cohesin destabilisation (Losada *et al.*, 2000; Losada, Hirano and Hirano, 2002; Sumara *et al.*, 2002; Hauf *et al.*, 2005; McGuinness *et al.*, 2005; Kitajima *et al.*, 2006; Kueng *et al.*, 2006). The protected pool of centromeric cohesin is maintained until the kinetochores biorient and attach to microtubules, leading to the tension-dependent redistribution of Sgo1-PP2A from centromeres to kinetochores in metaphase (Pouwels *et al.*, 2007; Liu, Jia and Yu, 2013). Once biorientation has been successfully achieved, and the spindle assembly checkpoint is satisfied, the APC/C becomes active, and separase cleaves the centromeric cohesin allowing sister chromatid segregation (Waizenegger *et al.*, 2000; Hauf, Waizenegger and Peters, 2001).

The acetylation of cohesin during S phase by Esco2, and the resulting protection of this centromeric pool of cohesive cohesin by sororin and Sgo1-PP2A, is essential for cell viability, as depletion of any of these proteins results in complete loss of sister chromatid cohesion in prophase (Salic, Waters and Mitchison, 2004; Tang *et al.*, 2004; Hou and Zou, 2005; Kitajima *et al.*, 2005; McGuinness *et al.*, 2005; Rankin, Ayad and Kirschner, 2005; Kitajima *et al.*, 2006; Tang *et al.*, 2006; Schmitz *et al.*, 2007; Zhang *et al.*, 2008b; Nishiyama *et al.*, 2010; Dreier, Bekier and Taylor, 2011; Alomer *et al.*, 2017). Phospho-null mutants of sororin and SA2, or depletion of Wapl, results in an over-cohesion phenotype whereby the sister chromatids remain cohesed along the entire length of the chromosome arms in prometaphase (Hauf *et al.*, 2005; Gandhi, Gillespie and Hirano, 2006; Kueng *et al.*, 2006; Shintomi and Hirano, 2009; Dreier, Bekier and Taylor, 2011; Liu, Rankin and Yu, 2013; Nishiyama *et al.*, 2013). Although all of the cohesin is cleaved by separase in circumstances where there is over-cohesion, upon Wapl depletion there is an increase in SAC activation, possibly due to the excess cohesin hindering kinetochore biorientation (Gandhi, Gillespie and Hirano, 2006; Kueng *et al.*, 2006). Therefore, the prophase pathway of cohesin removal is important for faithful chromosome segregation in mammalian mitosis.

In budding yeast, the components of the prophase pathway are largely conserved. The yeast homologue of Esco1 and Esco2, called Eco1, is similar to the C-terminal region of the mammalian proteins that contains the acetyltransferase domain and zinc finger region, but does not have the N-terminal domain that is important for the specific chromatin targeting

of Esco1 and Esco2 (Skibbens *et al.*, 1999; Toth *et al.*, 1999; Ivanov *et al.*, 2002; Brands and Skibbens, 2005; Hou and Zou, 2005; Zhang *et al.*, 2008b; Unal *et al.*, 2008). Eco1 is expressed during S phase, and acetylates cohesin at the replication fork on Smc3-K112,K113, allowing establishment of cohesive cohesin (Skibbens *et al.*, 1999; Toth *et al.*, 1999; Rolef Ben-Shahar *et al.*, 2008; Unal *et al.*, 2008; Zhang *et al.*, 2008b; Rowland *et al.*, 2009; Sutani *et al.*, 2009; Beckouet *et al.*, 2010; Lyons and Morgan, 2011; Lopez-Serra *et al.*, 2013; Guacci *et al.*, 2015). Eco1 and Smc3-K112,K113 are both essential for viability in budding yeast, therefore it is solely this pool of acetylated cohesin which holds sister chromatids together and allows faithful chromosome segregation (Skibbens *et al.*, 1999; Toth *et al.*, 1999; Brands and Skibbens, 2005; Haering *et al.*, 2008; Rolef Ben-Shahar *et al.*, 2008; Unal *et al.*, 2008; Rowland *et al.*, 2009; Sutani *et al.*, 2009; Chan *et al.*, 2012; Guacci *et al.*, 2015). Interestingly, there is no evidence for a prophase-pathway like dissociation of cohesin from the DNA prior to anaphase in budding yeast (Indjeian, Stern and Murray, 2005; Rowland *et al.*, 2009; Sutani *et al.*, 2009). Therefore, the acetylated pool of cohesin remains along the entire length of the sister chromatids from S phase until anaphase, when separase becomes active to cleave Scc1 (Uhlmann, Lottspeich and Nasmyth, 1999; Uhlmann *et al.*, 2000; Unal *et al.*, 2008; Rowland *et al.*, 2009; Sutani *et al.*, 2009; Chan *et al.*, 2012; Lopez-Serra *et al.*, 2013). As Scc1 is cleaved, Smc3 is deacetylated by Hos1, promoting cohesin release from the DNA, thus allowing sister chromatid segregation and Smc3 to be recycling, ready for the next cell cycle (Beckouet *et al.*, 2010; Borges *et al.*, 2010; Xiong, Lu and Gerton, 2010; Li, Yue and Tanaka, 2017).

As in mammalian cells, the Smc1-Smc3-Scc1 trimeric cohesin complex is bound by the accessory subunits, including Pds5 and Scc3, which are intrinsic to cohesin behaviour (Toth *et al.*, 1999; Chan *et al.*, 2013). However, unlike in mammals, there is no identified sororin homologue in budding yeast; acetylation of cohesin itself appears sufficient to promote cohesion (Rankin, Ayad and Kirschner, 2005; Rolef Ben-Shahar *et al.*, 2008; Unal *et al.*, 2008; Zhang *et al.*, 2008b; Rowland *et al.*, 2009; Sutani *et al.*, 2009; Lopez-Serra *et al.*, 2013). Nevertheless, Pds5 itself is important for the cohesive behaviour of cohesin, as disruption of Pds5 activity causes severe cohesion defects that can result in inviability (Hartman *et al.*, 2000; Panizza *et al.*, 2000; Sutani *et al.*, 2009; Chan *et al.*, 2013; Tong and Skibbens, 2014). Although the precise role of Pds5 is disputed, it appears that Pds5: aids cohesion establishment through promoting Smc3 acetylation by Eco1; maintains and

protects cohesin in G2; and prevents premature deacetylation by Hos1 (Sutani *et al.*, 2009; Beckouet *et al.*, 2010; Chan *et al.*, 2012; Chan *et al.*, 2013; Bloom, Koshland and Guacci, 2018). However, Pds5 also has negative influences on cohesion in mitosis, and was one of several "anti-establishment factors" identified in screens for suppressors of an *eco1-1* temperature sensitive allele (Rowland *et al.*, 2009; Sutani *et al.*, 2009; Chan *et al.*, 2012). Mutations in the N-terminal domain of Pds5 suppress the lethality of *eco1Δ*, and of *eco1-1* mutations, suggesting that Pds5 has a cohesin-destabilisation function (Rowland *et al.*, 2009; Sutani *et al.*, 2009; Chan *et al.*, 2012; Bloom, Koshland and Guacci, 2018). These mutations were found to be in the binding site on Pds5 for Rad61, the budding yeast homologue of Wapl (Sutani *et al.*, 2009; Chan *et al.*, 2012; Bloom, Koshland and Guacci, 2018).

Rad61 binds to cohesin via Pds5 and Scc3, and in G1 this interaction destabilises cohesin from the DNA through the opening of the cohesin ring at the Smc3-Scc1 interface (Rowland *et al.*, 2009; Sutani *et al.*, 2009; Chan *et al.*, 2012; Lopez-Serra *et al.*, 2013; Huis in 't Veld *et al.*, 2014; Bloom, Koshland and Guacci, 2018). After acetylation of cohesin in S phase, Rad61 is unable to destabilise this minor pool of stabilised acetylated cohesin (Chan *et al.*, 2012; Lopez-Serra *et al.*, 2013). *RAD61* mutants have decreased cohesin turnover in G2, presumably due to stabilisation of the pool of unacetylated cohesin (Chan *et al.*, 2012; Bloom, Koshland and Guacci, 2018), and *rad61Δ* rescues the lethality of *eco1Δ* and *smc3-K112R,K113R* mutants (Rolef Ben-Shahar *et al.*, 2008; Unal *et al.*, 2008; Rowland *et al.*, 2009; Sutani *et al.*, 2009; Guacci and Koshland, 2012; Chan *et al.*, 2012; Lopez-Serra *et al.*, 2013). Therefore, Rad61 is a negative regulator of cohesion, acting to destabilise unacetylated cohesin from the DNA.

One major caveat of this hypothesis is that *rad61Δ* mutants alone have cohesion defects in mitosis, and reduced levels of cohesin on the DNA (Rolef Ben-Shahar *et al.*, 2008; Rowland *et al.*, 2009; Sutani *et al.*, 2009; Guacci and Koshland, 2012; Murayama and Uhlmann, 2015; Guacci *et al.*, 2015; Bloom, Koshland and Guacci, 2018). The *eco1Δ rad61Δ* double mutants are extremely sick with more severe cohesion and DNA repair defects than *rad61Δ* alone (Rolef Ben-Shahar *et al.*, 2008; Rowland *et al.*, 2009; Sutani *et al.*, 2009; Guacci and Koshland, 2012; Lopez-Serra *et al.*, 2013; Guacci *et al.*, 2015; Bloom, Koshland and Guacci, 2018). Deletion of *RAD61* rescues the viability of *eco1Δ* by suppressing condensation

defects, rather than cohesion defects (Guacci and Koshland, 2012; Lopez-Serra *et al.*, 2013; Guacci *et al.*, 2015; Bloom, Koshland and Guacci, 2018). Therefore the exact role of Rad61 in mitosis is not fully understood, as Rad61 has anti-establishment activity and inhibits chromosome condensation, but also promotes DNA damage repair, correct cohesion and faithful sister chromatid segregation (Rolef Ben-Shahar *et al.*, 2008; Rowland *et al.*, 2009; Sutani *et al.*, 2009; Guacci and Koshland, 2012; Lopez-Serra *et al.*, 2013; Bloom, Koshland and Guacci, 2018).

In summary, although there is not a clear prophase pathway of cohesin removal in budding yeast mitotic cell division, the complex interplay of the prophase pathway components is crucial for chromosome segregation though the role of each protein remains to be fully deciphered.

4.1.2 Cohesin regulation in meiosis

Recently, several investigations have highlighted a variety of functions for the prophase pathway components in meiosis. Wapl is highly expressed in mouse testes and ovaries, and is localised to the synaptonemal complex of chromosomes in zygotene and pachytene of prophase (Kuroda *et al.*, 2005; Zhang *et al.*, 2008a), corresponding with localisation of Pds5B to the synaptonemal complex (Fukuda and Hoog, 2010). In a recent study, NEK1 kinase was found to phosphorylate Protein Phosphatase 1γ (PP1γ) in early prophase, which led to the dephosphorylation of Wapl, allowing Wapl association with chromatin (Brieno-Enriquez *et al.*, 2016). Untimely phosphorylation of Wapl led to retention of cohesin on the DNA, implicating Wapl in cohesin release during prophase of meiosis (Brieno-Enriquez *et al.*, 2016). A complementary study in *C. elegans* revealed WAPL-1 expression during prophase is important for removal of cohesin complexes containing the kleisin subunits COH-3/COH-4, but not for removal of REC-8-containing cohesin complexes from the DNA, and that condensin protects cohesin from this destabilisation activity (Crawley *et al.*, 2016; Hernandez *et al.*, 2018). Additionally, *WAPL1* and *WAPL2* in *Arabidopsis thaliana* (*A. thaliana*) destabilise cohesin from chromosomes in prophase of meiosis, which, in an undisrupted meiosis, aids faithful chromosome segregation but causes infertility of Eco1 homologue mutants (Bolanos-Villegas *et al.*, 2013; De *et al.*, 2014).

The role of Esco1/Esco2 has not been investigated in early meiosis in higher eukaryotes, although both Esco1 and Esco2 are expressed by prophase I in oocytes, and have roles in promoting faithful chromosome segregation through acetylation of α-Tubulin-K40 and Histone H4-K16 respectively (Lu *et al.*, 2017; Lu *et al.*, 2018). Although neither Esco1 or Esco2 have been directly shown to acetylate cohesin in meiosis, acetylated Smc3 co-localises with Rec8-cohesin to the meiotic chromosome axes in prometaphase I mouse oocytes (Reichmann *et al.*, 2017). Sororin is expressed throughout prophase of spermatogenesis, and localises to the central region of the synaptonemal complex, with a distinct localisation pattern to cohesin, suggesting sororin has a novel cohesin-independent role in prophase (Gomez *et al.*, 2016; Jordan *et al.*, 2017). However, from late prophase until metaphase II sororin localises to centromeres in a PP2A-dependent manner in spermatocytes, and depletion in oocytes results in loss of sister chromatid cohesion in meiosis II, suggesting that sororin protects centromeric cohesin (Gomez *et al.*, 2016; Huang *et al.*, 2017). Whether sororin is protecting acetylated cohesin at centromeres remains to be determined. However, expression of Rec8-STAG3 in somatic cells revealed that meiotic cohesin is shielded from prophase pathway removal by Wapl through protection by sororin and Sgo2 (Wolf *et al.*, 2018).

The homologues of the prophase pathway components have been extensively studied in budding yeast mitosis, but there is only limited evidence for the role of these proteins in meiosis. A recent study implicated Rad61 in the formation and repair of double strand breaks during homologous recombination, and in chromosome compaction in meiosis, similar to the mitotic function of Rad61 (Guacci and Koshland, 2012; Lopez-Serra *et al.*, 2013; Challa *et al.*, 2016; Bloom, Koshland and Guacci, 2018). This is comparable to the role of WAPL-1 in *C. elegans* in axial element morphogenesis and DSB repair (Crawley *et al.*, 2016). In budding yeast mitosis there is no identified destabilisation pathway of cohesin removal, however in meiosis condensin promotes Cdc5-dependent cohesin removal between prophase and metaphase I (Yu and Koshland, 2005). This finding was corroborated in a recent paper in which phosphorylation of Rec8 by both DDK and Cdc5 promoted the removal of cohesin in a separase-independent manner in late prophase (Challa *et al.*, 2019). In *RAD61* mutants, cohesin persists for longer on the DNA after disassembly of the chromosome axis at the end of prophase, providing evidence for a destabilisation pathway similar to that in higher eukaryotes (Challa *et al.*, 2019). Although there is no known role for

Eco1 in budding yeast meiosis, in *S. pombe* the Eco1 homologue, Eso1, acetylates cohesin during meiotic S phase, and this, along with other targets of Eso1, is essential for mono-orientation of sister chromatid kinetochores in meiosis I, and thus chromosome segregation (Kagami *et al.*, 2011).

Therefore, evidence in the literature points to a role of the prophase pathway components in budding yeast meiosis. In this chapter I aimed to characterise the timing of expression of Rad61, Eco1, and Hos1 during meiosis, and to determine if cohesin was acetylated during S phase. I also aimed to determine the importance of *RAD61* and *HOS1* for chromosome segregation during meiosis.

4.2 Results

4.2.1 Rad61 expression is regulated in meiosis

During the mitotic cell cycle, destabilisation of cohesin by Rad61 is thought to promote DNA repair and sister chromatid cohesion, and to restrict condensation (Rolef Ben-Shahar *et al.*, 2008; Rowland *et al.*, 2009; Sutani *et al.*, 2009; Chan *et al.*, 2012; Guacci and Koshland, 2012; Lopez-Serra *et al.*, 2013; Bloom, Koshland and Guacci, 2018). Rad61 is important in budding yeast meiosis for efficient meiotic recombination, DNA condensation and for cohesin removal prior to metaphase I (Challa *et al.*, 2016; Challa *et al.*, 2019). I decided to further characterise the role of Rad61 in meiosis.

To determine the timing of Rad61 protein expression in meiosis, time course experiments followed by western blotting were carried out. Synchronisation of cells at meiotic entry was carried out by placing the genes for the transcription factor, Ime1, and the mRNA methyltransferase, Ime4, under the inducible *CUP1* promoter (*pCUP1-IME1*/*IME4*) (Berchowitz *et al.*, 2013). After 2 h in sporulation media the cells arrest prior to meiotic S phase, and induction with 25 µM $CuSO_4$ allows cells to synchronously progress through S phase and prophase, and into meiosis I and II (Figure 4.2.1.1).

A diploid strain containing *RAD61-6HA* under the endogenous *RAD61* promoter and the *pCUP1-IME1*/*IME4* block/release construct was placed in sporulation media for 2 h, before induction with 25 µM $CuSO_4$ to allow meiotic progression. At regular time points 5 ml of cell culture was collected, and TCA fixation carried out to prevent protein degradation. The cell

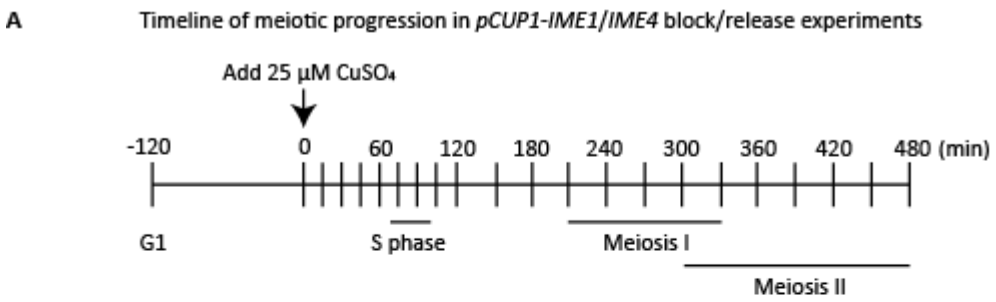

Figure 4.2.1.1: Schematic of the *pCUP1-IME1/IME4* block/release time course experiment protocol
A) Schematic of *pCUP1-IME1/IME4* block/release experiment with timing in minutes. Cells are placed into sporulation media and grown for 2 h to allow induction of meiosis, before arresting prior to S phase. After 2 h, 25 µM $CuSO_4$ is added to the culture to induce *IME1* and *IME4* expression and allow progression through meiotic S phase and into meiosis I and meiosis II. Samples are usually taken every 15 min for 2 h, then every 30 min for 6 h. Progression through S phase is monitored by flow cytometry, and through meiosis I and II by DAPI.

pellets were lysed and boiled in SDS sample buffer, before running on an SDS-PAGE gel and western blotting carried out (Figure 4.2.1.2A). Western blotting revealed that Rad61 protein was present from the start of meiosis but underwent gradual post-translational modification from 45 min after release, and then was degraded at 210-240 min. Progression through S phase was monitored by flow cytometry, showing that S phase occurred around 75-90 min after release, therefore Rad61 post-translational modification occurred at the beginning of DNA replication (Figure 4.2.1.2B). The meiosis I and II nuclear divisions were monitored by DAPI staining which revealed that binucleate formation occurred at 240-270 min and tetranucleate formation at 300 min (Figure 4.2.1.2C), and therefore degradation of Rad61 corresponded with metaphase I.

Analysis of the Rad61 amino acid sequence revealed that Rad61 contained a similar sequence to the Destruction Box (D box) motif (RxxLxxxN rather than RxxLxxxxN), and two KEN Box motifs, suggesting that Rad61 may be a target of the APC/C (Figure 4.2.1.3A) (Glotzer, Murray and Kirschner, 1991; Pfleger and Kirschner, 2000). Additionally, Rad61 also contained five (D/E)xxR putative separase cleavage motifs (Figure 4.2.1.3A) (Sullivan *et al.*, 2004). The presence of these various destruction sequences suggests that Rad61 degradation in meiosis I may be either by the APC/C or separase.

As cells progress through the *pCUP1-IME1*/*IME4* block/release time course, the cells lose synchrony as they enter meiosis I and II, therefore the exact timing of Rad61 degradation was difficult to elucidate. The *pGAL-NDT80* block/release time course system was employed to determine *RAD61-6HA* expression during nuclear division stages, as cells synchronously progress from late prophase through metaphase I and anaphase I, into meiosis II (Figure 2.2.2.4). Cells containing *RAD61-6HA* and *pGAL-NDT80* were grown for 6 h, before release from the prophase arrest. Samples were taken at the indicated times, protein extracts prepared, and Rad61-6HA expression was analysed by anti-HA immunoblot (Figure 4.2.1.3B). This revealed that Rad61 was degraded around 105-120 min after β-estradiol addition, corresponding to anaphase I, as deduced by scoring of spindle morphology after tubulin immunofluorescence (Figure 4.2.1.3C).

Rad61 degradation occurred around anaphase I, corresponding to the time of separase (Esp1) activation (Buonomo *et al.*, 2000). To clarify if the degradation occurred in a

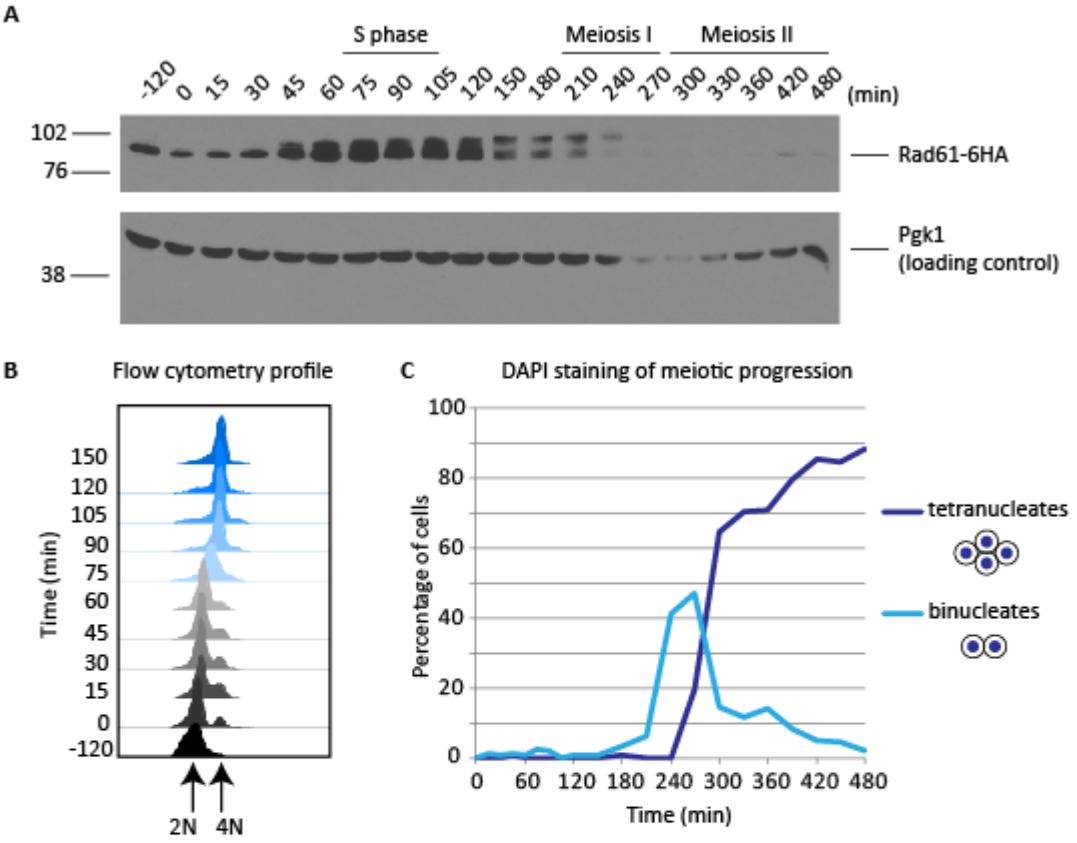

Figure 4.2.1.2: Rad61 undergoes post-translational modification during early meiosis
A diploid strain containing *RAD61-6HA* and the *pCUP1-IME1/IME4* block/release genetic background (strain 20916) was placed in sporulation media. After 2 h, 25 µM $CuSO_4$ was added to the culture to induce *IME1* and *IME4* expression, and allow progression through meiotic S phase and into meiosis I and meiosis II. Samples were removed at the timepoints indicated for protein extracts, flow cytometry and DAPI staining. A) Protein extracts were run on an 10 % SDS-PAGE gel and western blotting carried out. The western blot was developed by ECL using HA11 to probe against Rad61-6HA and homemade rabbit anti-PGK1 for the loading control. B) Flow cytometry samples were taken at -120 min and then between timepoints 0-150 min to monitor progression through S phase. Cells were fixed in ethanol before treatment with RNase and Proteinase K, then stained with Propridium Iodide and flow cytometry carried out (20916, n=20000 cells/timepoint). C) Graph showing DAPI scoring of the Rad61-6HA timecourse in the *pCUP1-IME1/IME4* block/release genetic background (20916, n=200) as cells progress through meiosis I and meiosis II.

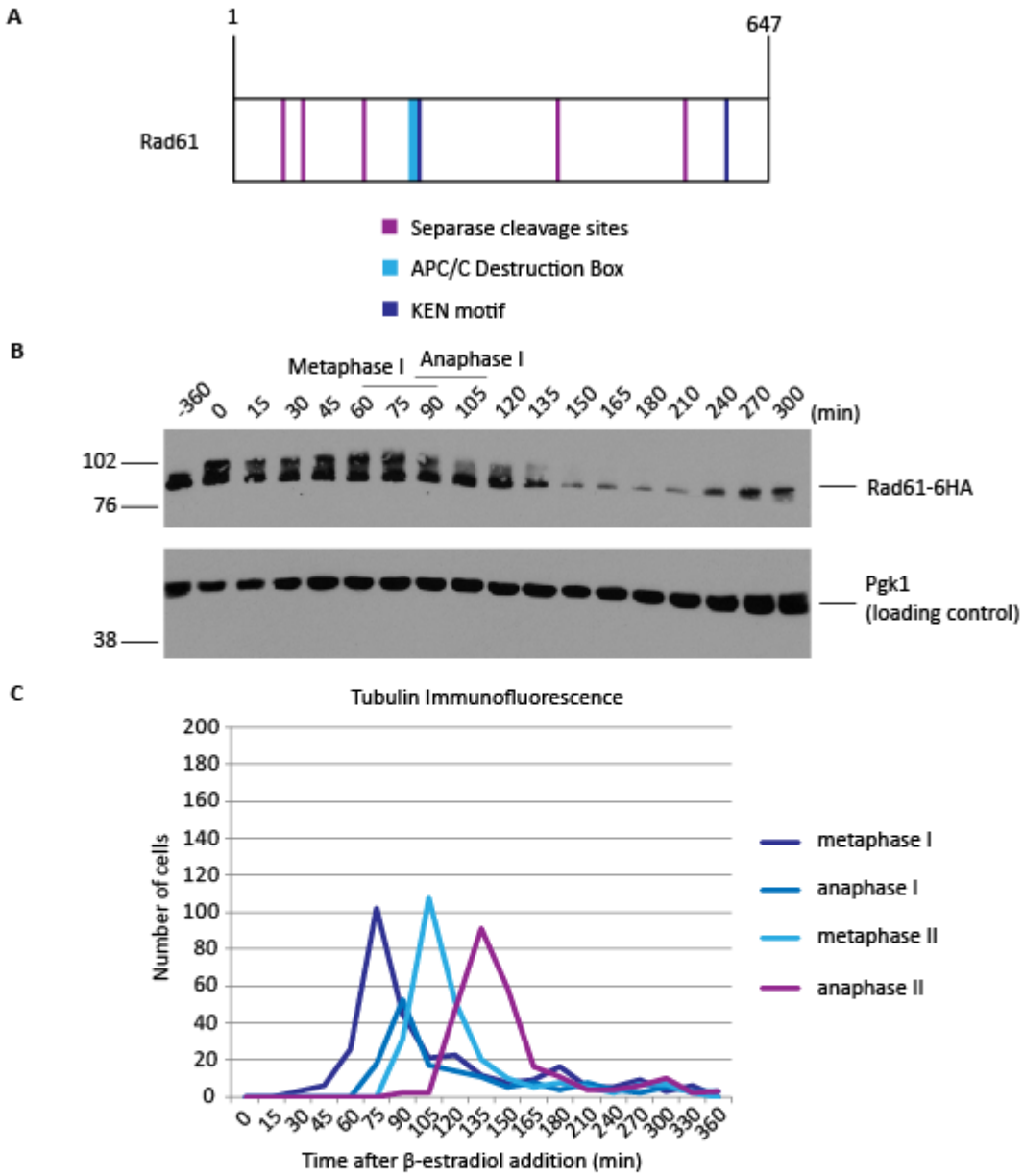

Figure 4.2.1.3: Rad61 is degraded as cells progress through meiosis I

A) Rad61 contains five putative separase cleavage consensus sites ((D/E)xxR), two KEN destruction motifs, and one putative APC/C destruction box consensus site (RxxLxxxN). B, C) A diploid strain containing Rad61-6HA and the *pGAL-NDT80* block/release genetic background (strain 20953) was placed in sporulation media. After 6 h, 1 µM β-estradiol was added to the culture to induce *NDT80* expression, and allow progression through late prophase and into meiosis I and meiosis II. Samples were removed at the timepoints indicated for protein extracts and tubulin immunofluorescence. B) Protein extracts were run on an 10 % SDS-PAGE gel and western blotting carried out. The western blot was developed by ECL using 12CA5 to probe against Rad61-6HA and homemade rabbit anti-PGK1 for the loading control. C) After release from the *NDT80* arrest cells were collected at each timepoint for tubulin immunofluorescence to assess cell cycle stage (20953, n=200 cells/timepoint).

separase dependent manner, the temperature sensitive allele *esp1-2* was utilised (Buonomo *et al.*, 2000). A diploid strain containing *RAD61-6HA*, the *pGAL-NDT80* block/release construct and *esp1-2*, was grown at the restrictive temperature of 30 ^{o}C for 6 h, to inactivate separase and arrest cells in late prophase. Following release of the cells from the prophase block, samples were extracted for analysis of Rad61-6HA expression by western blotting. This revealed that degradation of Rad61 occurred in a timely fashion in the *esp1-2* mutant (Figure 4.2.1.4A). The *esp1-2* mutant strains arrest as mononucleate cells with short metaphase I-like spindles at the restrictive temperature, due to the inhibition of cohesin cleavage preventing homologue segregation, despite APC-Cdc20 activation. Confirming the arrest, I found that the majority of cells had short metaphase I-like spindles (Figure 4.2.1.4B). The same *pGAL-NDT80* block/release experimental protocol was repeated with a diploid strain containing the *pCLB2-CDC20* construct that arrests cells in metaphase I, and Rad61-6HA expression examined by western blotting (Figure 4.2.1.4C). Again, Rad61-6HA was degraded despite the arrest of cells in metaphase I, as visualised by spindle morphology, thus showing Rad61 degradation occurs between prophase and metaphase I (Figure 4.2.1.4D).

Strains arrested in the *pGAL-NDT80* prophase arrest contain two distinctly migrating forms of Rad61 on an SDS-PAGE gel, suggesting that Rad61 may be post-translationally modified. Although the western blots showing Rad61-6HA degradation varied, the slower-migrating band of Rad61 appeared to decrease in intensity prior to the faster-migrating band (Figure 4.2.1.3B). To identify post-translational modifications on Rad61, Rad61 was purified from cells in S phase and prophase, and mass spectrometry was carried out on the immunoprecipitate (Figure 4.2.1.5A). Diploid no tag or *RAD61-6HIS-3FLAG* strains containing the *pCUP1-IME1*/*IME4* block/release construct were grown for 2 h, before releasing through S phase. Cells were harvested 45 min after release from the arrest, which, by flow cytometry analysis of the DNA content of the cells, corresponded to early S phase of meiosis (Figure 4.2.1.5B). Diploid no tag or *RAD61-6HIS-3FLAG* strains were harvested in a *pGAL-NDT80* prophase arrest, 6 h after induction of sporulation. Rad61-6HIS-3FLAG was immunoprecipitated from the cell lysate, and a fraction of the eluates were run on an SDS-PAGE gel and visualised by silver-staining (Figure 4.2.1.5A). Following trypsin digest, the remainder of each sample was analysed by mass spectrometry, however, no Rad61 phosphorylation or acetylation was detected.

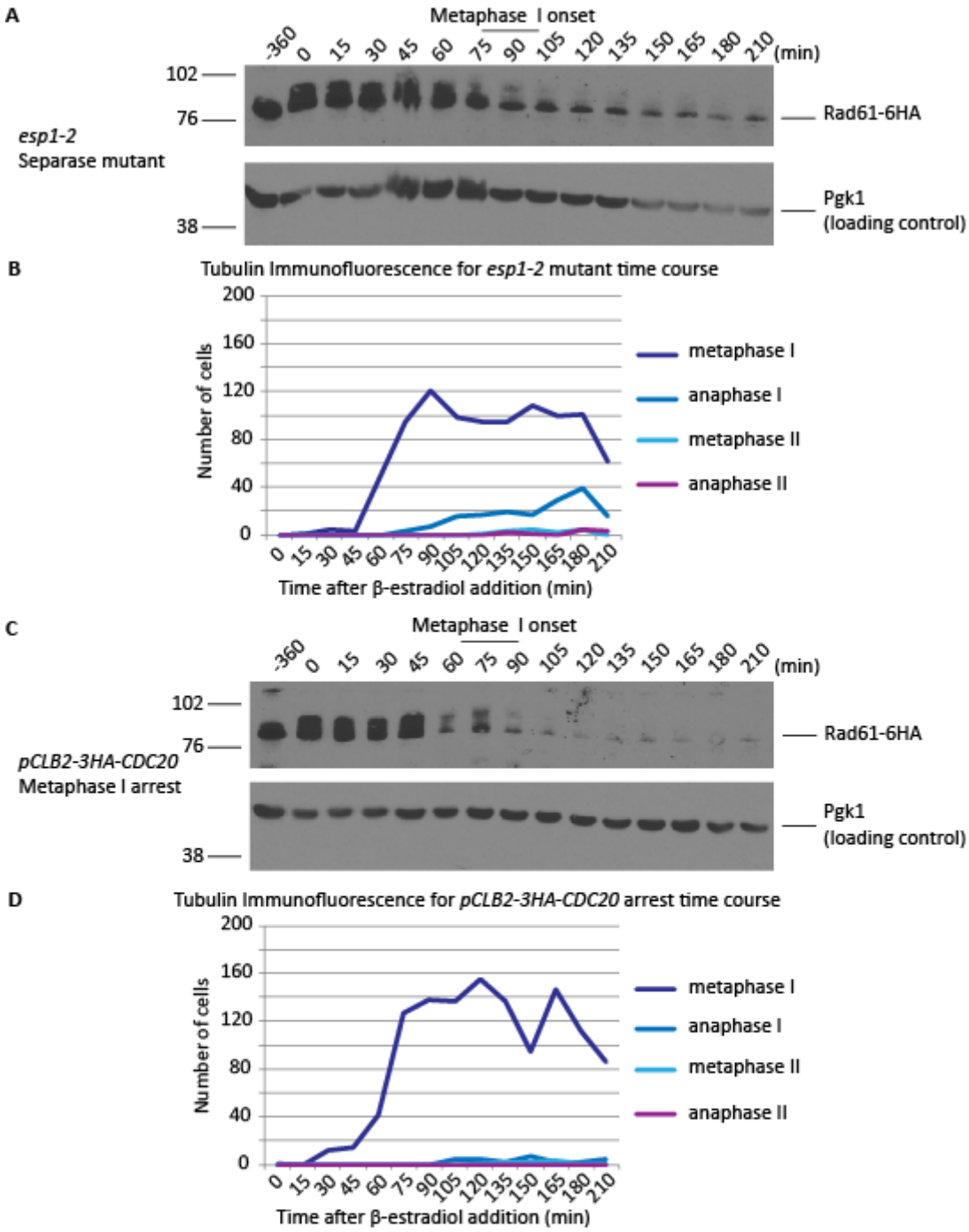

Figure 4.2.1.4: Rad61 is degraded independently of separase activity, prior to metaphase I
Diploid strains containing Rad61-6HA and the *pGAL-NDT80* block/release genetic background were placed in sporulation media at 30 °C. After 6 h, 1 µM β-estradiol was added to induce *NDT80* expression, and allow progression into meiosis I. Samples were removed at the timepoints indicated for protein extracts and tubulin immunofluorescence. Western blotting was carried out by ECL using HA11 to probe against Rad61-6HA and anti-PGK1 for the loading control A) Rad61-6HA expression time course in the *esp1-2* mutant (21904). Protein extracts were run on an 10 % SDS-PAGE gel and western blotting carried out. B) After release from the *NDT80* arrest, cells were collected at each timepoint for tubulin immunofluorescence (21904, n=200 cells/timepoint). C) Rad61-6HA expression time course into the *pCLB2-3HA-CDC20* metaphase I arrest (21903). Protein extracts were run on an 10 % SDS-PAGE gel and western blotting carried out. D) After release from the *NDT80* arrest, cells were collected at each timepoint for tubulin immunofluorescence (21903, n=200 cells/timepoint).

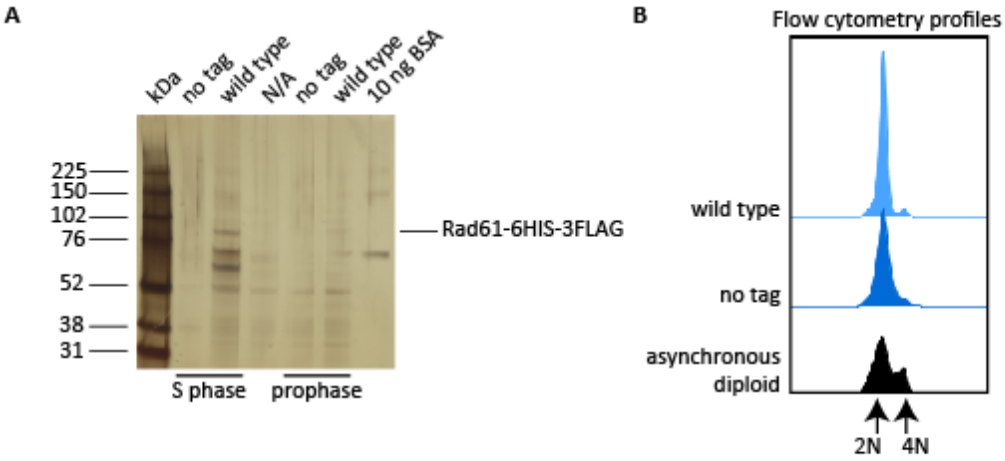

C

		S phase			Prophase		
		Number of peptides		% coverage	Number of peptides		% coverage
Protein group	Protein	no tag	wild type	wild type	no tag	wild type	wild type
Rad61	Rad61	0	51	66.6	0	40	61.7
Cohesin	Pds5	0	45	42.0	0	33	33.0
	Smc3	0	33	34.0	0	19	23.1
	Smc1	0	25	25.1	0	16	18.4
	Rec8	0	21	35.1	0	11	19.1
	Scc3	0	14	17.7	0	6	6.3
	Mcd1	0	3	7.2	0	0	0
	Scc2	0	0	0	0	2	1.7
PP2A	Tpd3	0	1	1.9	1	4	7.1
	Cdc55	0	0	0	0	4	8.4
	Rts1	0	1	1.5	0	1	1.7
Kinases	Cdc28	0	4	14.4	5	11	43.6
	Mek1	0	0	0	0	7	13.5
	Sit4	0	0	0	0	3	13.2
	Ypk2	0	5	9.0	0	6	10.3
	Ypk1	0	0	0	0	5	8.5
	Ipl1	0	0	0	0	5	14.4
	Mck1	0	1	2.4	0	5	16.0
	Cka2	0	2	10.0	0	2	7.4
Recombination	Red1	0	1	1.8	0	9	13.4
	Hop1	0	1	2.1	0	4	9.1

Figure 4.2.1.5: Rad61 interacts with cohesin in both S phase and prophase

Rad61-6HIS-3FLAG was immunoprecipitated from meiotic cells in S phase and prophase. The meiotic S phase samples for no tag (12145) and wild type (21663) were obtained from inducing *pCUP1-IME1/IME4* arrested cells with 25 µM $CuSO_4$ followed by harvesting 45 min after induction. The meiotic prophase samples for no tag (11189) and wild type (21328) were obtained from growing cells for 6 h into a *pGAL-NDT80* arrest. Cells were lysed, followed by Rad61-6HIS-3FLAG purificaton by M2-FLAG immunoprecipitation. A) A silver stained 4-12 % Bis-Tris protein gel of the eluate from the purification was used to visualise the immunoprecipitate (10 % total eluate). B) Flow cytometry samples for the S phase no tag (12145) and wild type (21663) cultures, and for an asynchronous diploid mitotic culture (1835) were taken. Cells were fixed in ethanol before treatment with RNase and Proteinase K, then stained with Propridium Iodide and flow cytometry carried out (n=20000 cells/timepoint). C) Results of mass spectrometry after trypsin digestion of Rad61-6HIS-3FLAG immunoprecipitate from cells in S phase and prophase of meiosis. Results were analysed using MAXQUANT. Shown is the number of peptides for each protein identified in S phase in no tag (12145) and wild type (21663), and for each protein identified in prophase in no tag (11189) and wild type (21328). The percentage of sequence coverage for each protein identified in wild type in S phase (21663) and prophase (21328) samples is also shown.

Rad61 peptides were detected in both meiotic stages and expected binding partners also co-purified (Figure 4.2.1.5C). In both S phase and prophase, Rad61-6HIS-3FLAG co-immunoprecipitated with the cohesin complex, including Pds5, the known binding partner of Rad61 (Rowland *et al.*, 2009; Sutani *et al.*, 2009; Chan *et al.*, 2012; Bloom, Koshland and Guacci, 2018). In prophase, many kinases co-purified with Rad61, the most abundant being Mek1 and Ypk2, and several of these were also detected in the S phase sample. Additionally, proteins such as Red1 and Hop1 that are involved in recombination and form part of the chromosome axis were also detected.

4.2.2 Rad61 is not essential for faithful chromosome segregation in meiosis

In meiosis, homozygous *rad61Δ* mutants have decreased spore viability, loss of homolog pairing and defective sister chromatid cohesion early in prophase (Challa *et al.*, 2016). However, Rec8 ChIP-qPCR revealed that deletion of *RAD61* had variable effects on cohesin levels on the DNA (Challa *et al.*, 2016), whereas in mitosis *RAD61* mutants have reduced chromosomal cohesin due to defects in cohesin maintenance (Rowland *et al.*, 2009; Sutani *et al.*, 2009). I aimed to clarify the effect of deletion of *RAD61* on cohesin levels and chromosome segregation during the meiotic nuclear divisions.

Rec8 ChIP was carried out in wild type and *rad61Δ* cells arrested in metaphase I of meiosis using the *pCLB2-CDC20* construct. Rec8 association with one arm site and two centromeric sites, where cohesin is known to be enriched in wild type cells, was measured by qPCR (Figure 4.2.2.1A). At all of the loci tested, Rec8 was significantly enriched on the DNA in *RAD61* mutants compared to wild type (Figure 4.2.2.1A). This increase was not due to differences in protein levels, as whole cell levels of Rec8 were comparable in all strains by western blotting, and a similar percentage of cells were arrested in metaphase I, as judged by spindle morphology (Figures 4.2.2.1B, C).

Deletion of *RAD61* caused a significant increase of cohesin on the DNA in metaphase I of meiosis. Decreased removal of cohesin from chromosomes prior to meiosis I increases the percentage of paired homolog telomeres in anaphase I, leading to missegregation (Yu and Koshland, 2005). Therefore, an increase of cohesin on the DNA might be expected to decrease the viability of *RAD61* mutants after meiosis. To test this hypothesis, the viability of the products of meiosis, i.e. the haploid spores, was scored. Compared to 98.5 % for wild

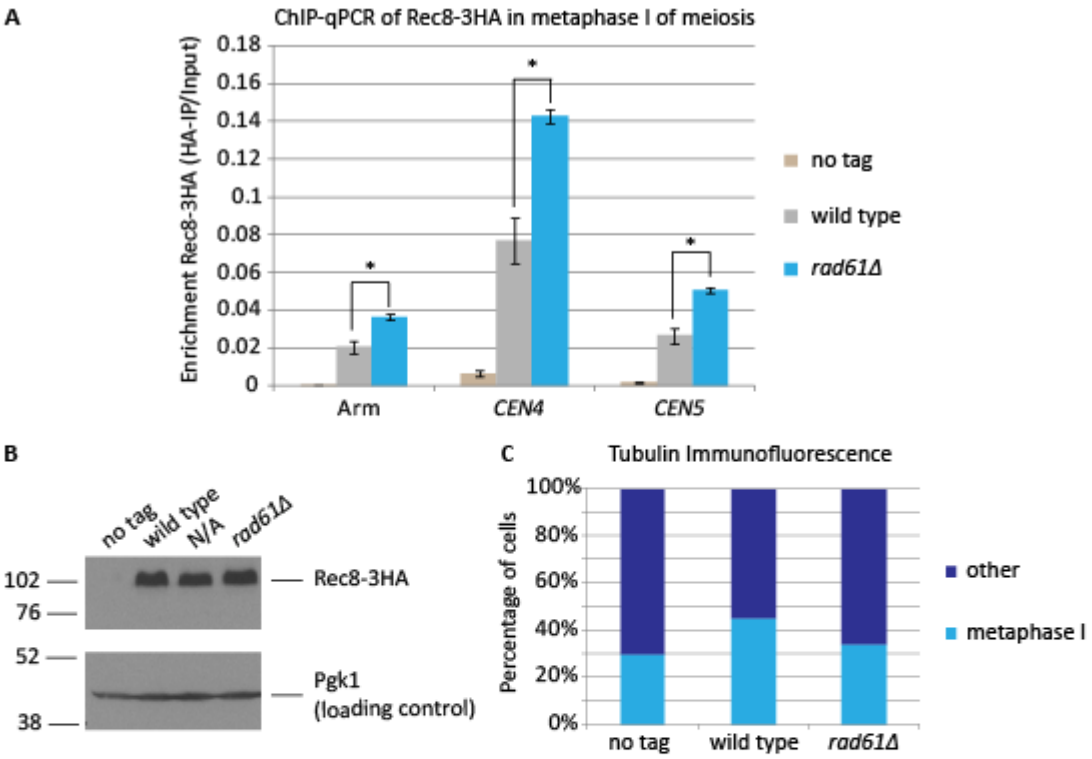

Figure 4.2.2.1: Cohesin has increased association with both centromeric and arm regions in *rad61Δ*
ChIP-qPCR of Rec8-3HA in metaphase I of meiosis shows cohesin is enriched on the DNA in *rad61Δ* A) Diploid strains containing Rec8-3HA were placed sporulation media and grown for 6 h into a *pCLB2-3HA-CDC20* metaphase I arrest, before harvesting for ChIP-qPCR. ChIP for Rec8-3HA was carried out in wild type (3375) and *rad61Δ* (21260), as well as in a no tag background (3560), using 12CA5 antibody against 3HA. Average of 4 repeats for Arm, *CEN4*, and *CEN5*. Error bars show standard error. Paired Student T-test gave p values of Arm= 0.0272, *CEN4*=0.0114, and *CEN5*=0.0109. B) Western blotting for Rec8-3HA and a loading control (Pgk1) in the strains used for ChIP-qPCR. Western blot developed by ECL using HA11 to probe against Rec8-3HA, and homemade rabbit anti-PGK1 for the loading control. No tag (3560), wild type (3375) and *rad61Δ* (21260) samples shown. C) Tubulin immunofluorescence for the metaphase I arrest of no tag (3560), wild type (3375) and *rad61Δ* (21260). Average of 4 repeats, n=200.

type meiosis, I found that spore viability was decreased to 91.25 % for *rad61Δ* (Figure 4.2.2.2A, B).

A decrease in spore viability is often indicative of chromosome missegregation in meiosis. Therefore, meiotic progression and homozygous *CEN5 tetO*/TetR-GFP dot segregation was analysed in the *rad61Δ* diploid after 10 h in sporulation media. As had previously been reported, the timing of binucleate formation was delayed in *rad61Δ*, and tetranucleate formation in *RAD61* mutants was decreased to under 25 % compared to 67 % in wild type (Figure 4.2.2.3A) (Challa *et al.*, 2016). Fluorescence microscopy analysis of the homozygous *CEN5 tetO*/TetR-GFP dot segregation in tetranucleate cells showed that 95 % of wild type cells had one GFP dot in each nuclei, corresponding to accurate chromosome segregation, whereas *rad61Δ* had over 14 % of tetranucleates with other GFP dot morphologies (Figure 4.2.2.3.B). Therefore, Rad61 is important for accurate chromosome segregation during meiosis.

In meiosis I, mono-orientation is essential for faithful segregation of the homologous chromosomes, although cohesin is not required for this process, at least in budding yeast (Monje-Casas *et al.*, 2007). Therefore deletion of *RAD61* should not affect mono-orientation even if cohesin behaviour is altered. Live cell imaging of heterozygous *CEN5 tetO*/TetR-GFP dots can be used to analyse if there are cohesion defects or mono-orientation defects in meiosis I due to the distance that the GFP dots separate in anaphase I (Figures 4.2.2.4A, B). In a wild type situation, the centromeric cohesin is protected in anaphase I, therefore the GFP dots will remain close together (0 μM). However, in a situation of loss of mono-orientation in meiosis I, the GFP dots will separate slightly (0-2 μM), as the kinetochores will biorient and thus be pulled apart, but not separated in anaphase I due to the centromeric cohesin. If centromeric cohesin is additionally lost in mono-orientation-defective cells, then the GFP dots will separate in anaphase I (>2 μM) (Figure 4.2.2.4A, B). Live cell imaging of heterozygous GFP dots in wild type and *rad61Δ* showed that there was no defect in mono-orientation, and no sister chromatid segregation in *RAD61* mutants in meiosis I (Figure 4.2.2.5A).

4.2.3 Eco1 expression coincides with Smc3 acetylation in meiosis

The acetyltransferase, Eco1, is essential for cell viability of budding yeast due to acetylation

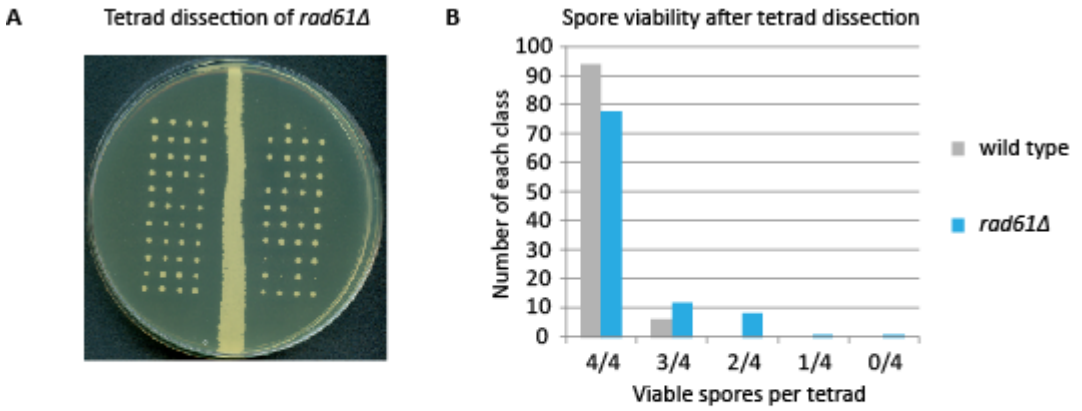

Figure 4.2.2.2: *RAD61* mutants have slightly reduced spore viability

Dissection of wild type and *rad61Δ* tetrads to assess spore viability. Diploid wild type (9968) and *rad61Δ* (5572) were patched onto sporulation media and placed at 30 °C to sporulate, before digestion with zymolyase and dissection of tetrads onto YPD. A) Example YPD plate containing *rad61Δ* (5572) tetrad dissection. B) Graph showing viable spores per tetrad after dissection of 100 tetrads for wild type (9968) and *rad61Δ* (5572), resulting in 98.5 % and 91.25 % viability respectively.

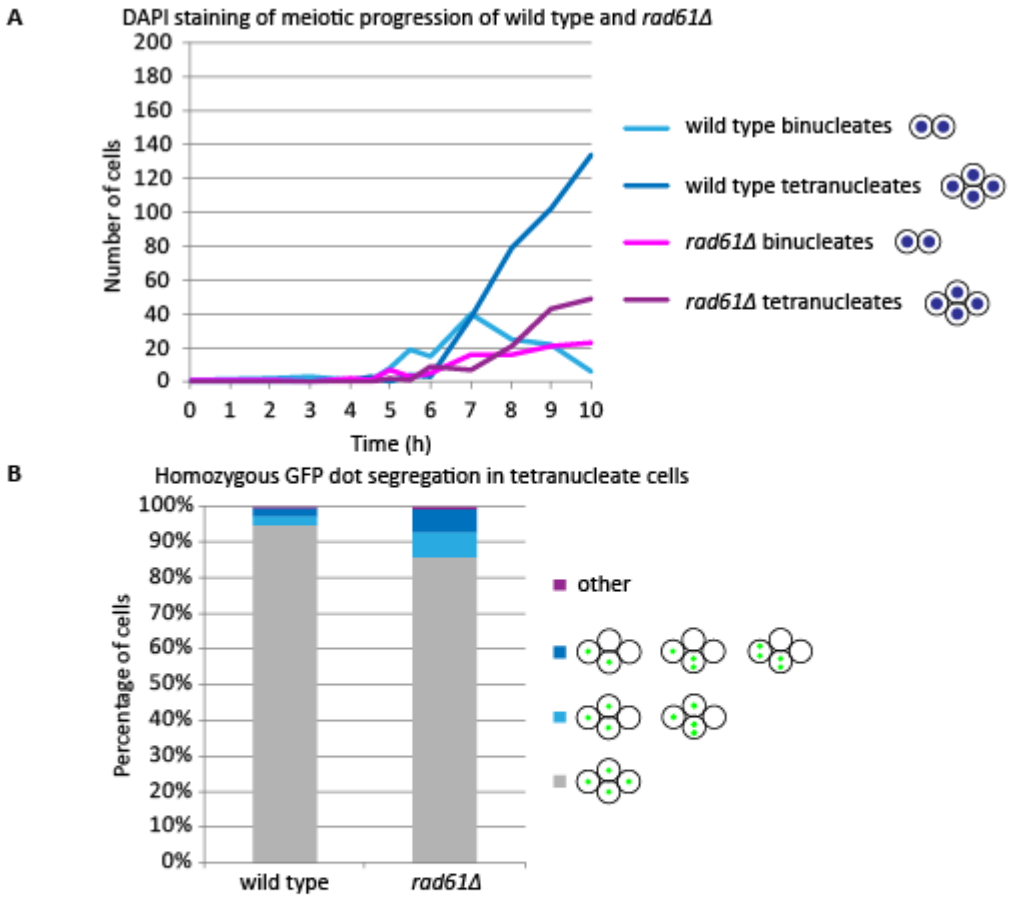

Figure 4.2.2.3: *RAD61* mutants have chromosome segregation defects in meiosis
A) Wild type (9968, n=200) and *rad61Δ* (5572, n=200) were placed in sporulation media and meiotic progression assessed by DAPI staining for binucleate and tetranucleate cell formation throughout the asynchronous meiotic time course. B) Homozygous *CEN5 tetO*/TetR-GFP dot segregation in tetranucleate cells. Diploid strains were placed in sporulation media to induce meiosis at 30 °C, and after 10 h GFP dot segregation was analysed in tetranucleate cells by fluorescence microscopy. Graph shown is the percentage of each phenotype. Average from 3 repeats for wild type (9968, n=300) and *rad61Δ* (5572, n=300).

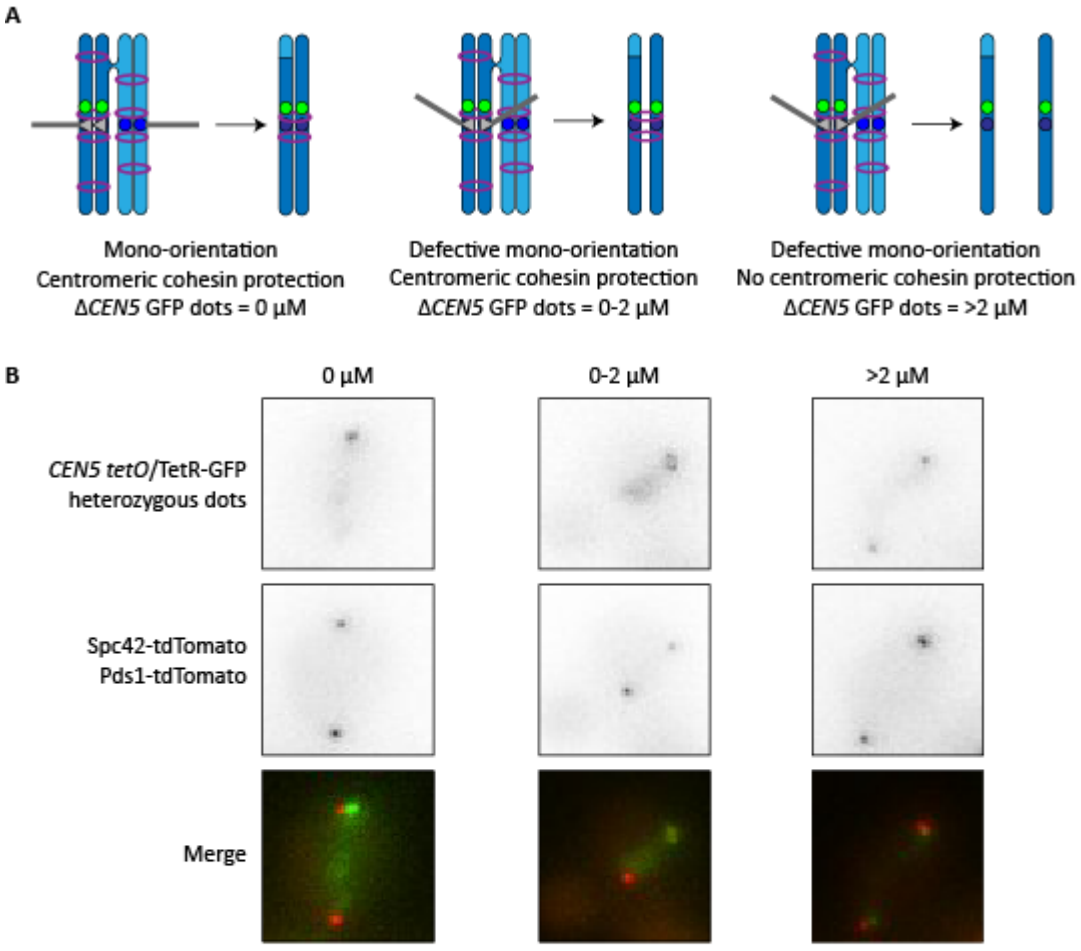

Figure 4.2.2.4: Live cell imaging of heterozygous GFP dot segregation in anaphase I of meiosis
A) Live cell imaging of cells containing *CEN5* heterozygous *tetO*/TetR-GFP dots allows sister chromatid segregation during the metaphase I to anaphase I transition to be visualised. In a wild type situation the sister chromatids mono-orient and remain cohesed, thus the GFP dots do not separate (0 µM). In a situation where there is a defect in mono-orientation, the sister chromatid kinetochores biorient and separate under tension, although remain cohesed, thus separating slightly (0-2 µM). In a situation where there is a defect in mono-orientation and a loss of cohesin protection, all of the cohesin is cleaved at anaphase I, thus allowing sister chromatid separation (>2 µM). B) Live cell imaging of *CEN5 tetO*/TetR-GFP dots is carried out in diploid strains containing Spc42-tdTomato, to label spindle pole bodies, and Pds1-tdTomato to allow cell cycle progression to be determined by securin degradation. After live cell imaging was carried out for 12 h, the distances between the *CEN5 tetO*/TetR-GFP dots were measured in anaphase I after using ImageJ. Example images shown for 0 µM, 0-2 µM, and >2 µM (strains 20146 (0 µM and >2 µM) and 21358 (0-2 µM).

A

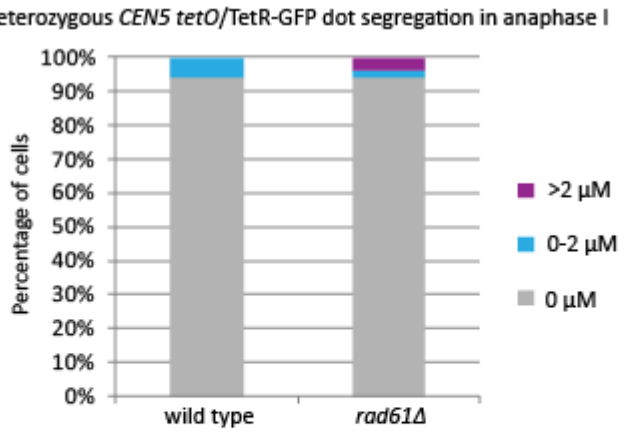

Figure 4.2.2.5: *RAD61* mutants do not have defects in mono-orientation in meiosis I
A) Measuring heterozygous *CEN5 tetO*/TetR-GFP dot separation by live cell imaging in anaphase I of meiosis. Diploid strains were placed in sporulation media to induce meiosis, and live cell imaging carried out for 12 h, with Z-stack images taken every 15 min. Separation of *CEN5 tetO*/TetR-GFP dots was then measured using ImageJ. Percentage of each category shown for wild type (15190, n=50) and *rad61Δ* (21068, n=50).

of cohesin on Smc3-K112,K113 to generate cohesion between sister chromatids (Rolef Ben-Shahar *et al.*, 2008; Unal *et al.*, 2008; Zhang *et al.*, 2008b; Rowland *et al.*, 2009; Sutani *et al.*, 2009). In meiosis, the *S. pombe* homologue Eso1 is crucial for mono-orientation in meiosis I, and Esco1 and Esco2 both promote faithful chromosome segregation in mouse oocyte meiosis (Kagami *et al.*, 2011; Lu *et al.*, 2017; Lu *et al.*, 2018). However, the role of Eco1 and cohesin acetylation has not been investigated in budding yeast meiosis.

Eco1 expression peaks during S phase of mitosis, therefore I aimed to determine if Eco1 was also expressed in S phase of meiosis by employing the *pCUP1-IME1*/*IME4* block/release time course protocol (Toth *et al.*, 1999; Lyons and Morgan, 2011). A diploid strain containing *ECO1-6HA* under the endogenous promoter was arrested prior to meiotic S phase, before induction with copper sulphate to allow progression through meiosis. At regular intervals, samples were extracted for analysis of Eco1-6HA expression by western immunoblot. This revealed that Eco1-6HA protein was expressed and degraded in the early stages of meiosis, between 45-105 min, which by flow cytometry corresponded to the duration of meiotic S phase (Figure 4.2.3.1A, B). However, DAPI staining revealed that binucleate cells accumulated as the time course progressed, with very little tetranucleate formation at 480 min: 39 % of *ECO1-6HA* cells underwent meiosis compared to 88.5 % in the *RAD61-6HA* time course (Figures 4.2.1.2C and 4.2.3.1C).

The absence of tetranucleate cells at the end of the *pCUP1-IME1*/*IME4* block/release time course suggests that Eco1-6HA may not be fully functional. To confirm this, the efficiency of tetranucleate formation was compared in strains containing either *ECO1-6HA* or *ECO1-6HIS-3FLAG* to a diploid wild type, 24 h after induction of meiosis. Fluorescence microscopy of DAPI stained cells revealed that in wild type and *ECO1-6HIS-3FLAG* strains, 79.5 % and 72 % of cells formed tetranucleates respectively, compared to only 32 % of *ECO1-6HA* cells (Figure 4.2.3.2A). Over 50 % of *ECO1-6HA* cells had fragmented or diffuse/faint DNA staining, suggesting that DNA segregation in meiosis had failed, or that the cells had died (Figure 4.2.3.2A). Dissection of sporulated diploids confirmed that Eco1-6HIS-3FLAG was functional, and had 97 % spore viability, compared to the strain expressing Eco1-6HA, which had 7 % viability (Figure 4.2.3.2B, C).

As Eco1-6HA is non-functional in meiosis, the expression pattern of Eco1-6HA previously

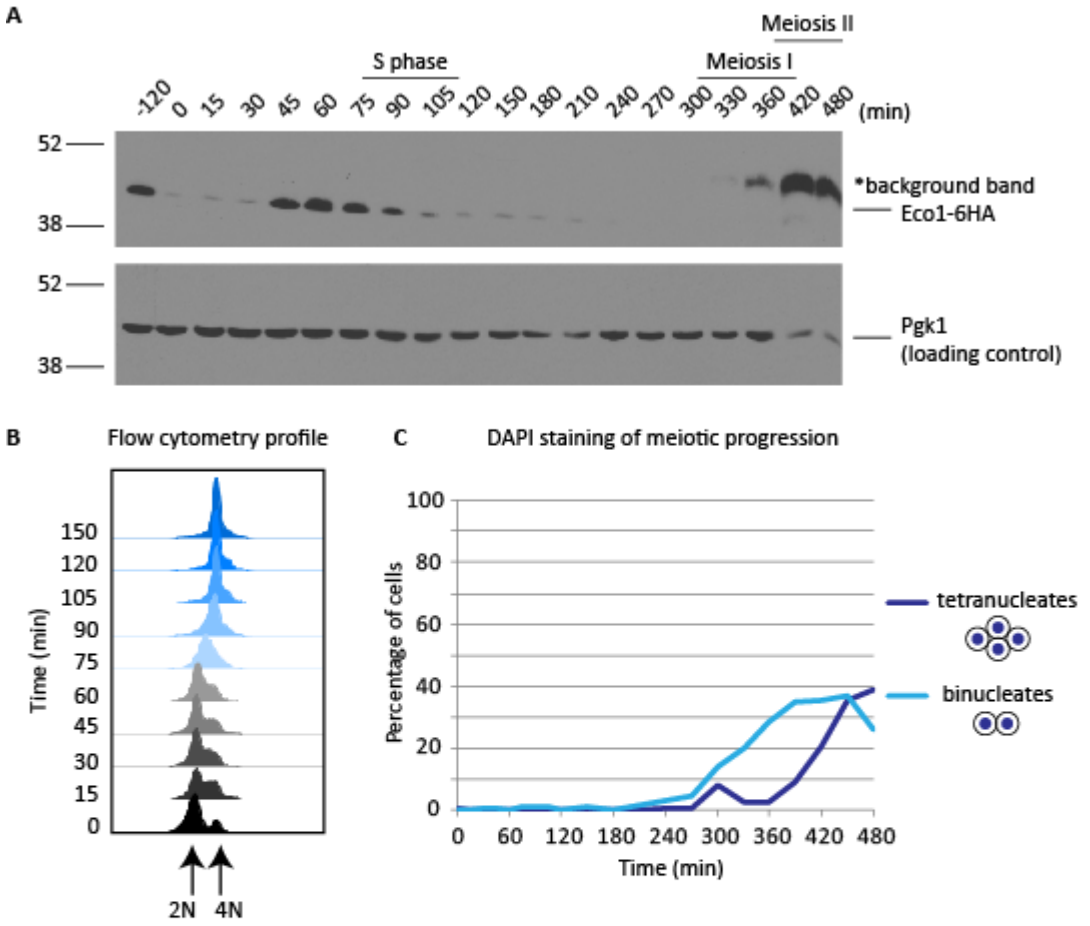

Figure 4.2.3.1: Eco1-6HA is expressed in S phase of meiosis, but cells do not sporulate
A diploid strain containing *ECO1-6HA* and the *pCUP1-IME1/IME4* block/release genetic background (strain 20912) was placed in sporulation media. After 2 h, 25 µM $CuSO_4$ was added to the culture to induce *IME1* and *IME4* expression, and allow progression through meiotic S phase and into meiosis I and meiosis II. Samples were removed at the timepoints indicated for protein extracts, flow cytometry and DAPI staining. A) Protein extracts were run on an 10 % SDS-PAGE gel and western blotting carried out. The western blot was developed by ECL using HA11 to probe against Eco1-6HA and homemade rabbit anti-PGK1 for the loading control. B) Flow cytometry samples were taken between timepoints 0-150 min to monitor progression through S phase. Cells were fixed in ethanol before treatment with RNase and Proteinase K, then stained with Propridium Iodide and flow cytometry carried out (20912, n=20000 cells/timepoint). C) Graph showing DAPI scoring of the Eco1-6HA timecourse in the *pCUP1-IME1/IME4* block/release genetic background (20912, n=200) as cells progress through meiosis I and meiosis II.

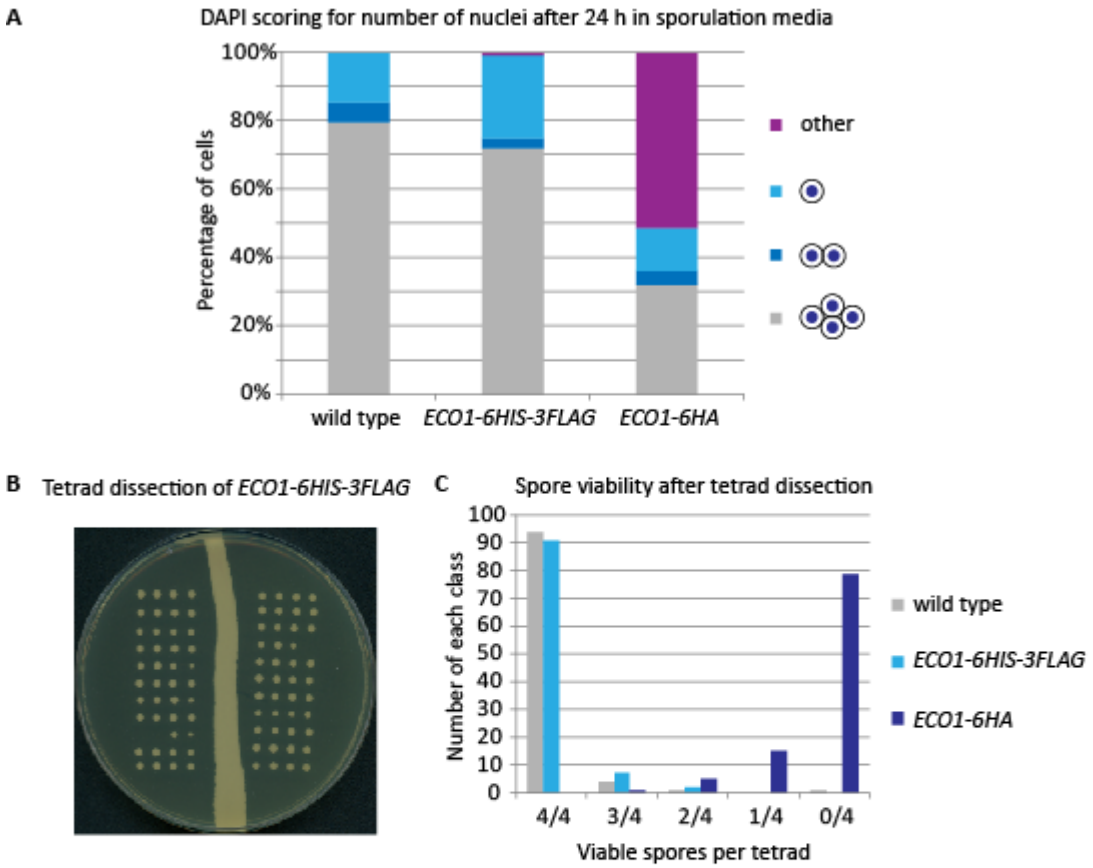

Figure 4.2.3.2: *ECO1-6HA* has low sporulation and decreased viability in comparison to *ECO1-6HIS-3FLAG*

A) Diploid wild type (1835), *ECO1-6HIS-3FLAG* (25844), and *ECO1-6HA* (25926) strains were placed in sporulation media and grown for 24 h at 30 °C, before fixation in 80 % EtOH, and DAPI staining carried out. Graph shows number of nuclei as scored by fluorescence microscopy (n=200 cells/strain). B, C) Dissection of wild type, *ECO1-6HIS-3FLAG* and *ECO1-6HA* tetrads to assess spore viability. Diploid wild type (1835), *ECO1-6HIS-3FLAG* (25844) and *ECO1-6HA* (25926) were patched onto sporulation media and placed at 30 °C to sporulate, before digestion with zymolyase and dissection of tetrads onto YPD. B) Example YPD plate containing *ECO1-6HIS-3FLAG* (25844) tetrad dissection. C) Graph showing viable spores per tetrad after dissection of 100 tetrads for wild type (1835), *ECO1-6HIS-3FLAG* (25844), and *ECO1-6HA* (25926), resulting in 97.5 %, 97.25 % and 7 % viability respectively.

visualised by western blotting may be incorrect (Figure 4.2.3.1A), as the tag may promote premature degradation of Eco1. Therefore the *pCUP1-IME1*/*IME4* block/release time course was repeated, as previously described, with the strain containing *ECO1-6HIS-3FLAG*. Western blotting revealed that Eco1-6HIS-3FLAG was visualised between 60-120 min after release with copper sulphate, which by flow cytometry, corresponded to the time of DNA replication (Figure 4.2.3.3A, B). DAPI staining of fixed cell samples, followed by analysis by fluorescence microscopy, showed that 70 % of cells had undergone meiosis and formed tetranucleates by 420 min (Figure 4.2.3.3C).

The expression of Eco1-6HIS-3FLAG during the DNA replication prior to meiosis suggests that Eco1 may acetylate Smc3-K112,K113, as in mitosis. If Eco1 acetylates cohesin in S phase, and the proteins stably interact, then the Eco1-cohesin interaction should be detectable by mass spectrometry (Figure 4.2.3.4A). A diploid strain containing *ECO1-6HIS-3FLAG* and the *pCUP1-IME1*/*IME4* block/release construct was arrested at meiotic entry, before cells were released and grown into early S phase (Figure 4.2.3.4B). Eco1-6HIS-3FLAG was immunoprecipitated from the cell lysate, and trypsin digestion carried out followed by mass spectrometry. Although Eco1 could not be visualised by silver-staining after a fraction of the immunoprecipitate was run on an SDS-PAGE gel (Figure 4.2.3.4A), analysis of the peptides obtained showed that Eco1 was successfully immunoprecipitated from the cell lysate, but no cohesin subunits could be detected (Figure 4.2.3.4C). PCNA and Replication Factor C complex subunits were identified in the eluate, suggesting that Eco1 that was localised to the replication fork had been purified (Bylund and Burgers, 2005; Lengronne *et al.*, 2006; Moldovan, Pfander and Jentsch, 2006).

An alternative approach was required to determine if Smc3 was acetylated in meiosis, therefore an antibody was generated using a synthetic acetylated peptide corresponding to the region of Smc3-108-122, which had K112 and K113 acetylated (Figure 4.2.3.5A). The antibody was then purified against the unacetylated peptide (Figure 4.2.3.5B). By western blotting, the antibody specifically recognised a band corresponding to the predicted molecular weight of acetylated Smc3 in an asynchronous mitotic yeast protein extract, but only weakly recognised a band of the same molecular weight in *eco1Δ rad61Δ* yeast protein extract (Figure 4.2.3.5C). The western blot for the expression of Eco1-6HIS-3FLAG in the *pCUP1-IME1*/*IME4* block/release time course (Figure 4.2.3.3A) was probed with the

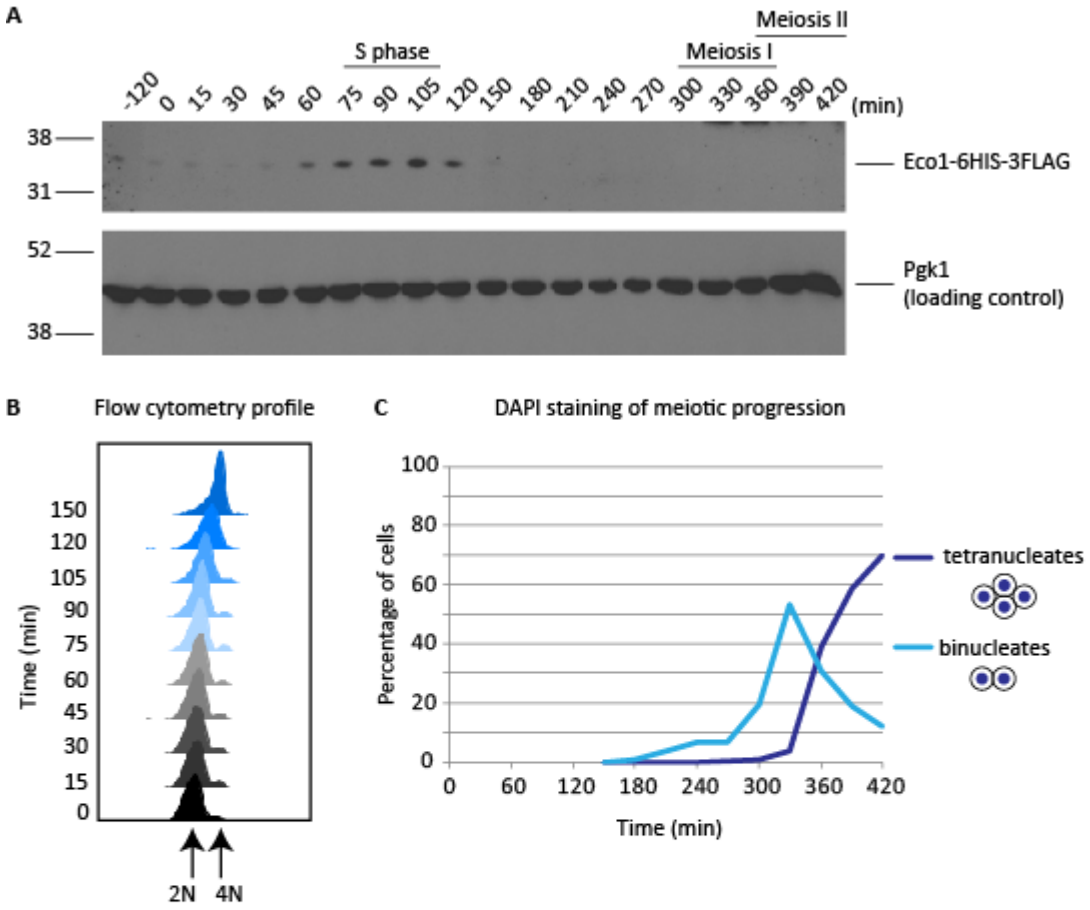

Figure 4.2.3.3: Eco1 is expressed during S phase of meiosis, followed by degradation as cells progress through prophase

A diploid strain containing Eco1-6HIS-3FLAG and the *pCUP1-IME1/IME4* block/release genetic background (strain 21574) was placed in sporulation media. After 2 h, 25 µM $CuSO_4$ was added to the culture to induce *IME1* and *IME4* expression, and allow progression through meiotic S phase and into meiosis I and II. Samples were removed at the timepoints indicated for protein extracts, flow cytometry and DAPI staining. A) Protein extracts were run on an 10 % SDS-PAGE gel and western blotting carried out. The western blot was developed by ECL using M2 FLAG antibody to probe against Eco1-6HIS-3FLAG and homemade rabbit anti-PGK1 for the loading control. B) Flow cytometry samples were taken between timepoints 0-150 min to monitor progression through S phase. Cells were fixed in ethanol before treatment with RNase and Proteinase K, then stained with Propridium Iodide and flow cytometry carried out (21574, n=20000 cells/timepoint). C) Graph showing DAPI scoring of the Eco1-6HIS-3FLAG timecourse in the *pCUP1-IME1/IME4* block/release genetic background (21574, n=200) as cells progress through meiosis I and meiosis II.

A

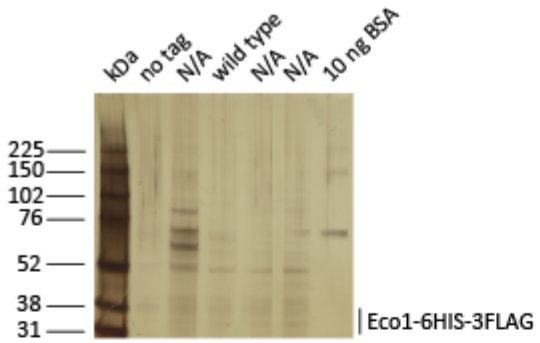

B

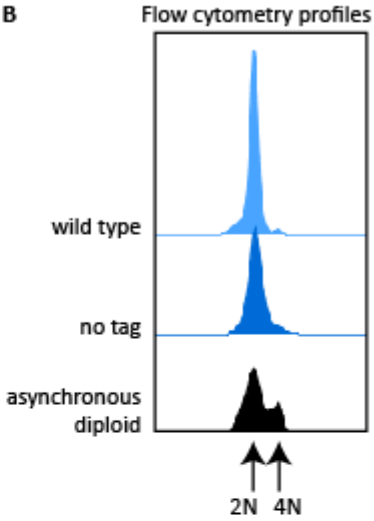

C

Interactors of Eco1 in S phase

		Number of peptides		% coverage
Protein group	**Protein**	**no tag**	**wild type**	**wild type**
Eco1	Eco1	0	21	66.9
Kinases	Cdc28	0	4	15.1
DNA Replication	Pol30	1	4	18.6
	Rfc3	0	2	6.2
	Rfc2	0	2	5.9
	Rfc4	0	1	3.4

Figure 4.2.3.4: Mass spectrometry of Eco1 in S phase of meiosis

Eco1-6HIS-3FLAG was immunoprecipitated from S phase meiotic cells. The meiotic S phase samples for no tag (12145) and wild type (21574) were obtained from inducing *pCUP1-IME1/IME4* arrested cells with 25 µM $CuSO_4$ followed by harvesting 45 min after induction. Cells were lysed, followed by Eco1-6HIS-3FLAG purificaton by M2-FLAG immunoprecipitation. A) A silver stained 4-12 % Bis-Tris protein gel of the eluate from the purification was used to visualise the immunoprecipitate (10 % total eluate). B) Flow cytometry samples for the S phase no tag (12145) and wild type (21574), and for an asynchronous diploid mitotic culture (1835) were taken. Cells were fixed in ethanol before treatment with RNase and Proteinase K, then stained with Propridium Iodide and flow cytometry carried out (n=20000 cells/sample. C) Results of mass spectrometry after trypsin digestion of Eco1-6HIS-3FLAG immunoprecipitate from cells in S phase of meiosis. Results were analysed using MAXQUANT. Shown is the number of peptides for each protein identified in either no tag (12145) or wild type (21574), and the percentage of sequence coverage for each protein identified in wild type (21574).

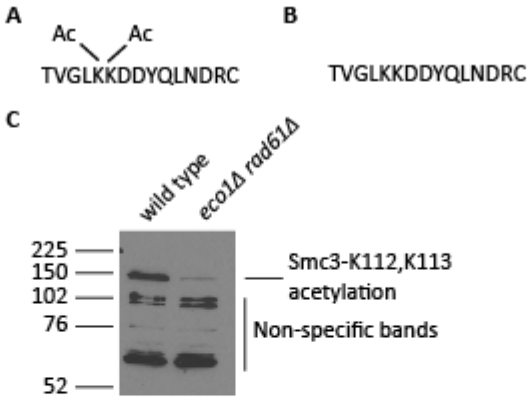

Figure 4.2.3.5: An antibody to specifically recognise Smc3-K112,K113 acetylation
A) Sequence of the peptide used as an immunogen for Smc3-K112,K113 acetylation antibody generation, with the acetylation sites indicated. B) The purification of the anti-Smc3-K112,K113 acetylation antibody included a cross-absorption step against the unacetylated peptide. C) Asynchronous cultures of w303 haploid wild type (1176) and *eco1Δ rad61Δ* (5432) strains were grown into logarithmic phase, and then TCA extraction carried out. Cell pellets were lysed and boiled in LDS sample buffer. Samples were run on an 10 % SDS-PAGE gel, and western blotting carried out using the homemade rabbit anti-Smc3-K112,K113 acetylation antibody.

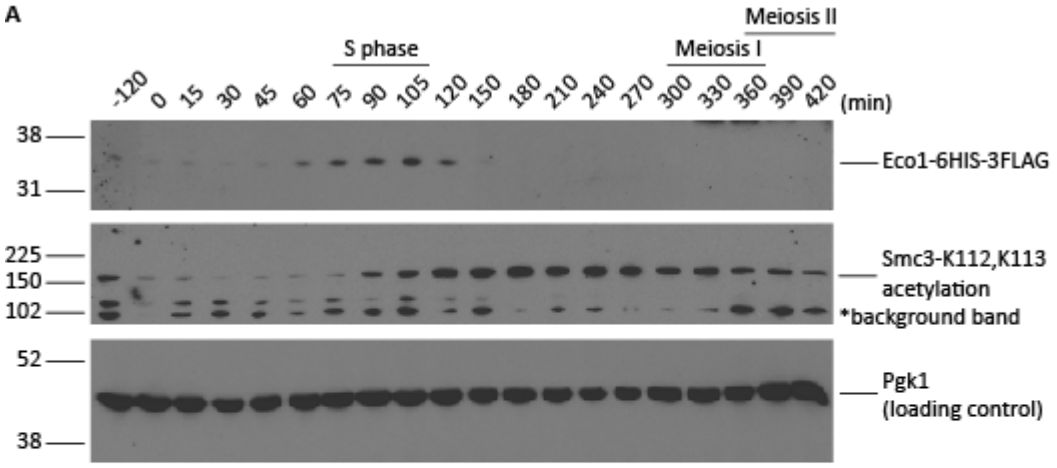

Figure 4.2.3.6: Smc3-K112,K113 acetylation coincides with Eco1 expression in meiosis
A diploid strain containing Eco1-6HIS-3FLAG and the *pCUP1-IME1/IME4* block/release genetic background (strain 21574) was placed in sporulation media. After 2 h, 25 µM $CuSO_4$ was added to the culture to induce *IME1* and *IME4* expression, and allow progression through meiotic S phase and into meiosis I and meiosis II. A) Protein extracts were run on an 10 % SDS-PAGE gel and western blotting carried out. The western blot was developed by ECL using M2 FLAG antibody to probe against Eco1-6HIS-3FLAG, homemade rabbit anti-Smc3-K112,K113 acetylation antibody to probe for cohesin acetylation, and homemade rabbit anti-PGK1 for the loading control.

antibody raised against Smc3-K112,K113 acetylation. This showed that Smc3 was acetylated in S phase of meiosis, as Eco1 expression occurred, and the acetylation was maintained until the later stages of meiosis (Figure 4.2.3.6A). Therefore Smc3 is acetylated on K112 and/or K113 in budding yeast meiosis.

4.2.4 The cohesin deacetylase, Hos1, is not required for faithful meiotic chromosome segregation

In anaphase of mitosis, separase cleaves the Scc1 kleisin subunit of cohesin, promoting Smc3 deacetylation by Hos1, and thus the timely release of cohesin from the chromosomes to allow sister chromatid segregation (Beckouet *et al.*, 2010; Borges *et al.*, 2010; Xiong, Lu and Gerton, 2010; Li, Yue and Tanaka, 2017). Smc3 deacetylation by Hos1 allows recycling of Smc3 back into the unacetylated form, which allows the Smc3 protein to form a cohesive cohesin ring in the next cell cycle (Beckouet *et al.*, 2010; Borges *et al.*, 2010; Xiong, Lu and Gerton, 2010; Li, Yue and Tanaka, 2017). *HOS1* mutants have a delay in anaphase due to delayed cohesin release, and weakened sister chromatid cohesion as the recycling of cohesin is impaired without deacetylation (Beckouet *et al.*, 2010; Borges *et al.*, 2010; Li, Yue and Tanaka, 2017). Whether deacetylation of cohesin is important for meiotic chromosome segregation is unknown, therefore an investigation was undertaken in the Marston lab by J. Drake as to the role of Hos1 in meiosis.

In mitosis, Hos1 protein levels stay constant throughout the cell cycle (Borges *et al.*, 2010). To analyse Hos1 expression in meiosis, a diploid strain containing *HOS1-6HA* under the endogenous promoter, and the *pGAL-NDT80* block/release construct, was arrested in prophase, before release with β-estradiol. At the indicated time points, samples were removed for analysis of Hos1-6HA expression by western immunoblot, which revealed that Hos1 was present from prophase throughout the meiosis I and II nuclear divisions (Figure 4.2.4.1A, B performed by J. Drake (Marston lab)).

Hos1 was expressed throughout anaphase I and anaphase II of meiosis, at the time points when Smc3 deacetylation may occur, as Rec8 is cleaved and released from the chromatin. The timing of Rec8-6HIS-3FLAG cleavage was compared to Smc3-K112,K113 acetylation in wild type and *hos1Δ* diploid strains during meiosis. Diploid strains containing *REC8-6HIS-3FLAG* and the *pGAL-NDT80* block/release construct, with or without *HOS1*,

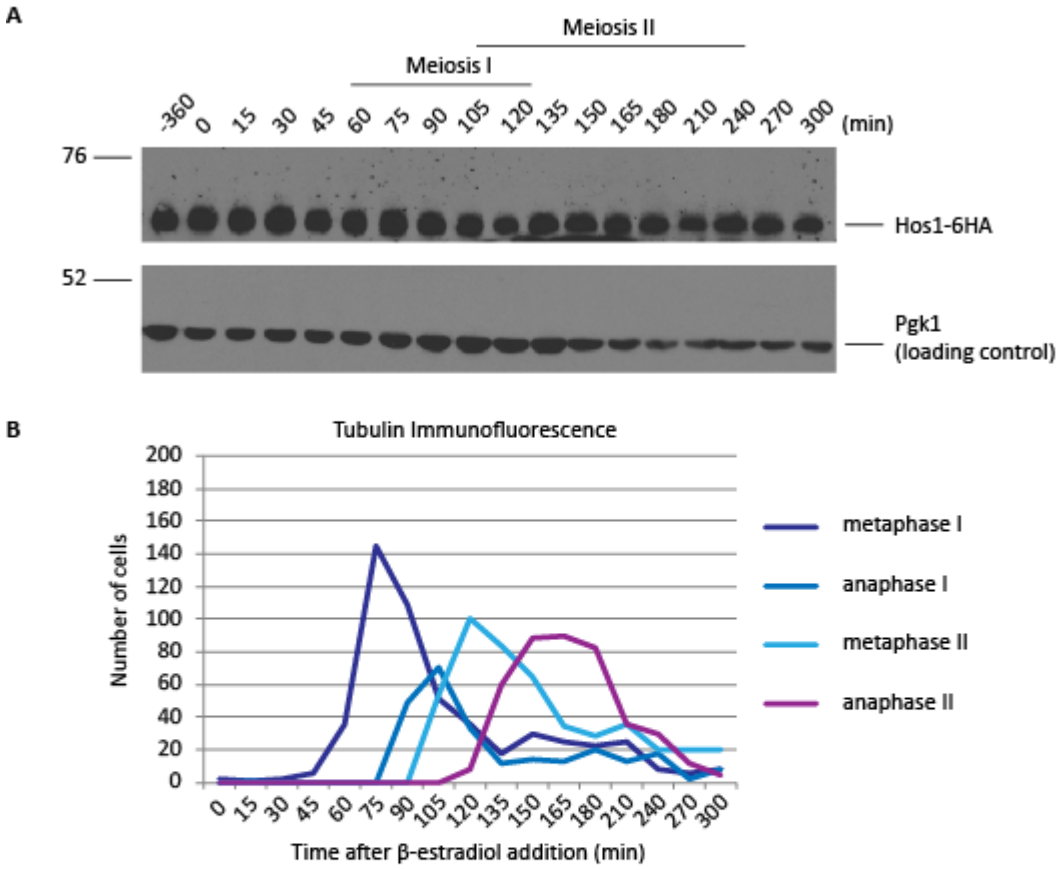

Figure 4.2.4.1: Hos1 is expressed throughout meiosis

A diploid strain containing *HOS1-6HA* and the *pGAL-NDT80* block/release genetic background (strain 23196) was placed in sporulation media. After 6 h, 1 µM β-estradiol was added to the culture to induce *NDT80* expression, and allow progression through late prophase and into meiosis I and meiosis II. Samples were removed at the timepoints indicated for protein extracts and tubulin immunofluorescence. A) Protein extracts were run on an 10 % SDS-PAGE gel and western blotting carried out. The western blot was developed by ECL using HA11 to probe against Hos1-6HA and homemade rabbit anti-PGK1 for the loading control. B) After release from the *NDT80* arrest cells were collected at each timepoint for tubulin immunofluoresence to assess cell cycle stage (23196, n=200 cells/timepoint). Experiment performed by J. Drake (Marston lab).

were arrested in late prophase, before releasing through meiosis I and II. Western blotting for Rec8-6HIS-3FLAG in wild type showed that much of Rec8 was cleaved at around 75 min, corresponding to metaphase I, and to a decrease in the intensity of the Smc3-K112,K113 acetylation signal (Figure 4.2.4.2A, B). However, in *hos1Δ*, the signal for Smc3-K112,K113 acetylation remained strong throughout the time course, suggesting Hos1 may deacetylate cohesin in meiosis (Figure 4.2.4.2C). In the *hos1Δ* time course there was an increase in slower migrating species of Rec8, suggestive of increased phosphorylation, and Rec8 cleavage was slightly delayed in meiosis I (Figure 4.2.4.2C, D). By tubulin morphology, the subsequent meiosis II was then delayed by around 15 min (Figure 4.2.4.2C, D).

The delay in Rec8 cleavage and in meiosis II progression suggested that *hos1Δ* may have problems in chromosome segregation in meiosis I, which may activate the spindle assembly checkpoint and thus cause the delay in meiotic progression. Chromosome segregation defects can result in decreased spore viability, therefore a diploid strain homozygous for *hos1Δ* was sporulated and dissected for spore viability. Analysis of spore growth showed that *hos1Δ* had spore viability of over 94 %, and therefore was comparable to wild type (Figure 4.2.4.3A, B, performed by J. Drake (Marston lab)). As an additional assay for chromosome segregation, homozygous *CEN5 tetO*/TetR-GFP dot segregation in *hos1Δ* mutants was analysed. Diploid strains homozygous for *CEN5 tetO*/TetR-GFP dots were placed in sporulation media for 9 h to allow meiosis to occur. Fluorescence microscopy of DAPI stained cells showed that *hos1Δ* formed tetranucleates with the similar efficiency to wild type (Figure 4.2.4.4A, performed by J. Drake (Marston lab)). Analysis of the *CEN5 tetO*/TetR-GFP dot segregation in *hos1Δ* by fluorescence microscopy showed that chromosome segregation was correct in over 94 % of tetranucleates (Figure 4.2.4.4B, performed by J. Drake (Marston lab)). Therefore, *HOS1* is not essential for faithful chromosome segregation in budding yeast meiosis.

4.3 Discussion

4.3.1 Smc3 is acetylated in budding yeast meiosis, and functional Eco1 is essential for viability

Eco1 peaks in expression during S phase of budding yeast mitosis, and interacts with the replication fork (Toth *et al.*, 1999; Lengronne *et al.*, 2006; Moldovan, Pfander and Jentsch, 2006; Lyons and Morgan, 2011). As the replication fork encounters cohesin, a so-far

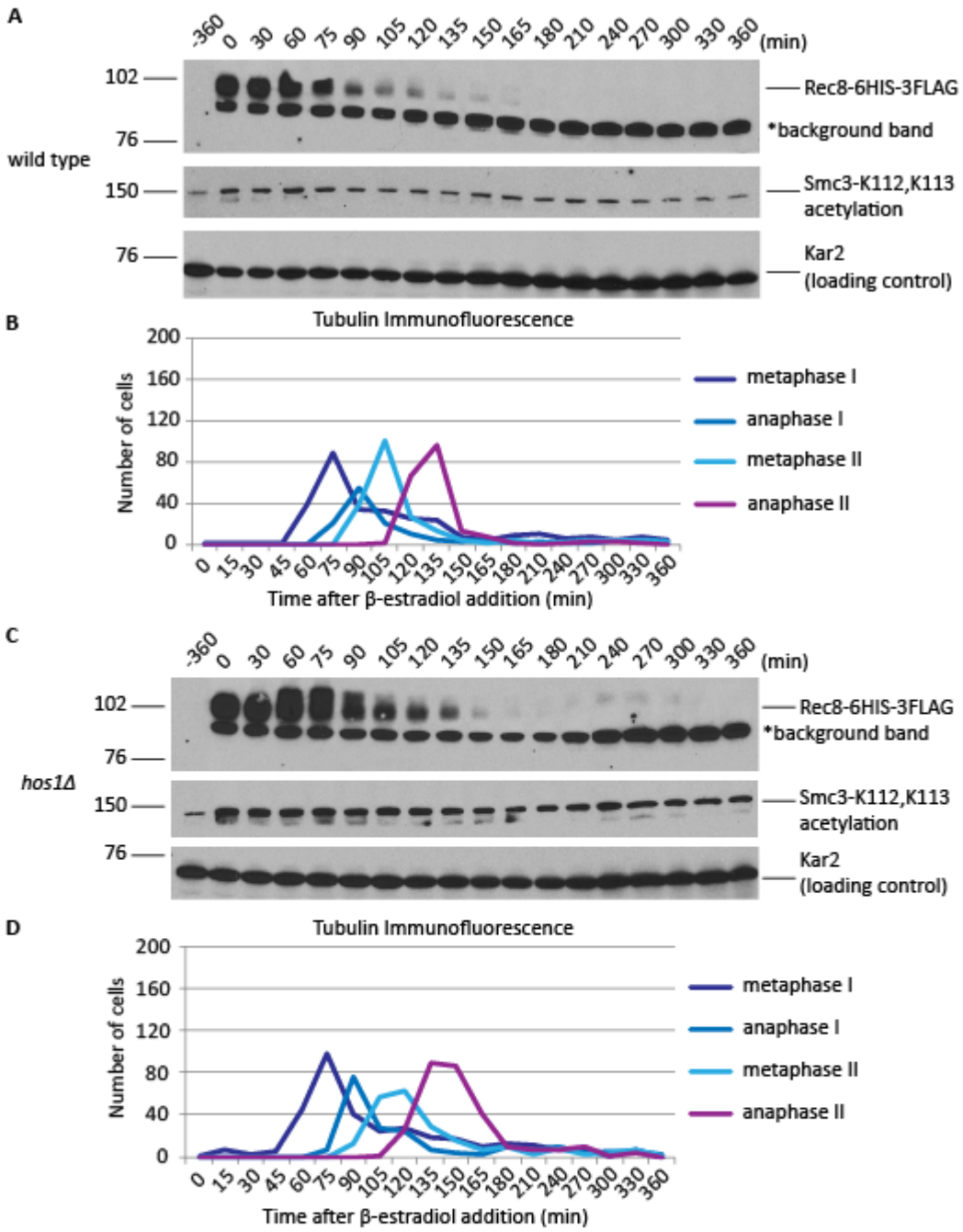

Figure 4.2.4.2: Smc3 acetylation remains after cohesin cleavage in *hos1Δ*

Wild type or *hos1Δ* diploid strains containing Rec8-6HIS-3FLAG and the *pGAL-NDT80* block/release genetic background were placed in sporulation media. After 6 h, 1 µM β-estradiol was added to induce *NDT80* expression, and allow progression into meiosis I and II. Samples were removed at the timepoints indicated for protein extracts and tubulin immunofluorescence. Western blotting was carried out by ECL using M2 FLAG antibody to probe against Rec8-6HIS-3FLAG, homemade rabbit anti-Smc3-K112,K113 acetylation antibody to probe for cohesin acetylation, and homemade rabbit anti-KAR2 for the loading control. A) Protein extracts for wild type (16180) were run on an 8 % SDS-PAGE gel and western blotting carried out. B) After release from the *NDT80* arrest, cells were collected at each timepoint for tubulin immunofluorescence for wild type (16180, n=200 cells/time-point). C) Protein extracts for *hos1Δ* (22997) were run on an 8 % SDS-PAGE gel and western blotting carried out. D) After release from the *NDT80* arrest, cells were collected at each timepoint for tubulin immunofluorescence for *hos1Δ* (22997, n=200 cells/timepoint).

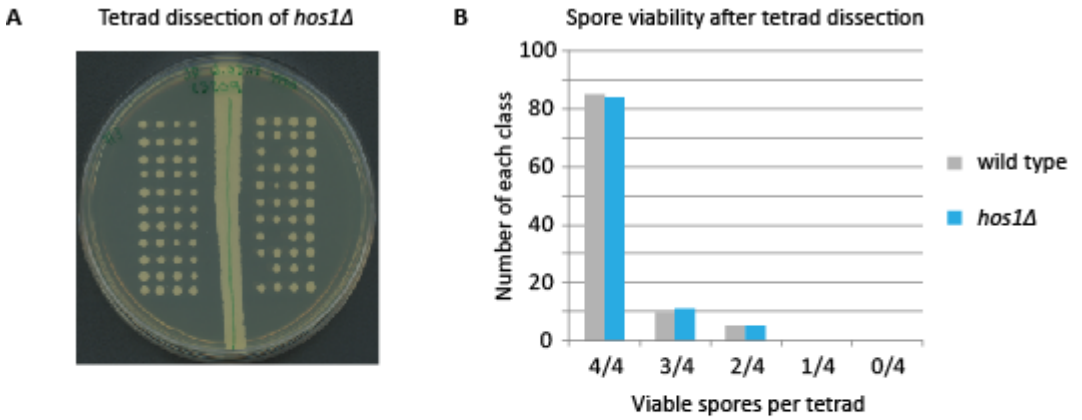

Figure 4.2.4.3: Deletion of *HOS1* does not affect spore viability
Dissection of wild type and *hos1Δ* tetrads to assess spore viability. Diploid wild type (1835) and *hos1Δ* (23209) were patched onto sporulation media and placed at 30 °C for 48 h to sporulate, before digestion with zymolyase and dissection of tetrads onto YPD. A) Example YPD plate containing *hos1Δ* (23209) tetrad dissection. B) Graph showing viable spores per tetrad after dissection of 100 tetrads for wild type (1835) and *hos1Δ* (23209), resulting in 95 % and 94.75 % viability respectively. Experiment performed by J. Drake (Marston lab).

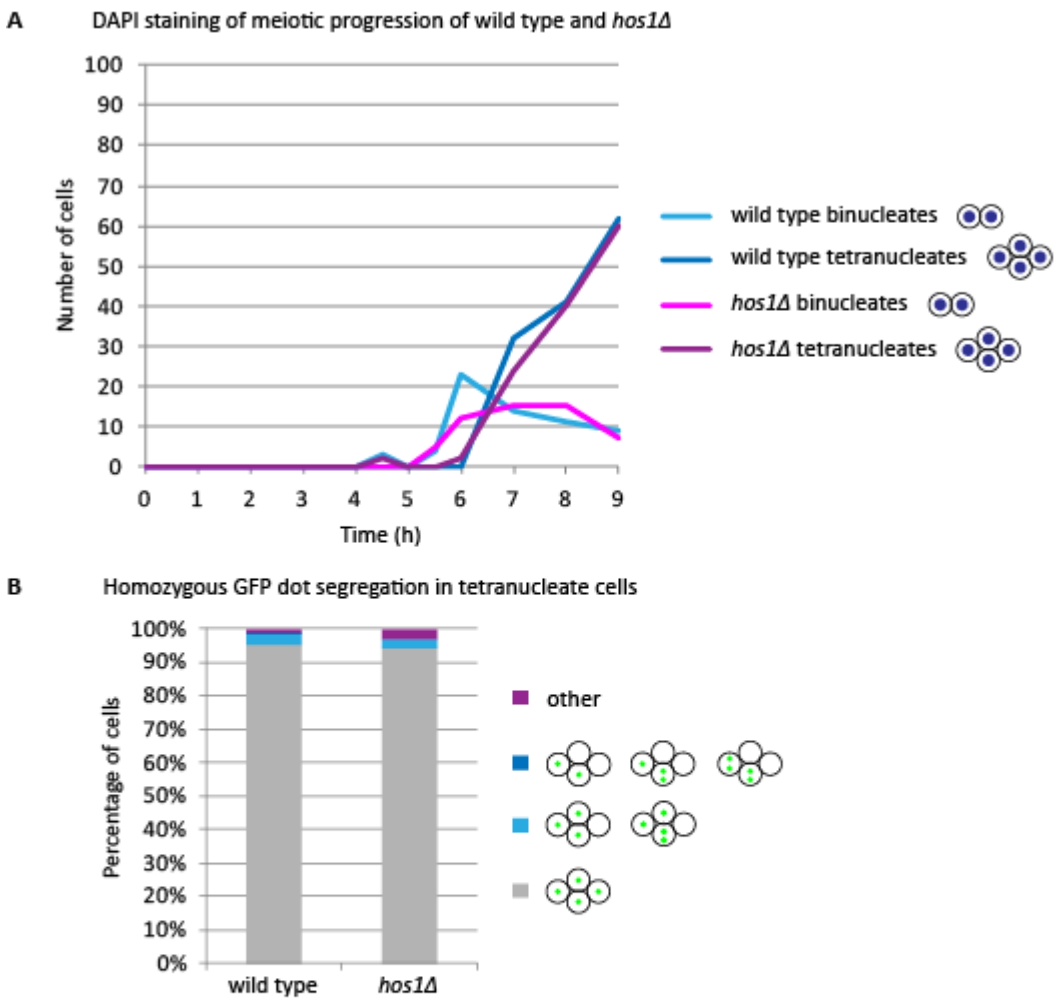

Figure 4.2.4.4: *HOS1* mutants do not have chromosome missegregation during meiosis
A) Wild type (9968, n=100) and *hos1Δ* (23212, n=100) were placed in sporulation media and meiotic progression assessed by DAPI staining for binucleate and tetranucleate cells through an asynchronous meiotic time course. B) Homozygous *CEN5 tetO*/TetR-GFP dot segregation in tetranucleate cells. Diploid strains were placed in sporulation media to induce meiosis, and after 9 h GFP dot segregation was counted in tetranucleates by fluorescence microscopy. Graph shown is the percentage of each phenotype. Average from 3 repeats for wild type (9968, n=300) and *hos1Δ* (23212, n=299) with cells grown at 30 ℃. Experiment performed by J. Drake (Marston lab).

undefined event occurs that promotes cohesin to embrace the newly replicated sister chromatids and become acetylated on Smc3-K112,K113, which converts cohesin into a "locked" cohesive state (Rolef Ben-Shahar *et al.*, 2008; Unal *et al.*, 2008; Zhang *et al.*, 2008b; Rowland *et al.*, 2009; Sutani *et al.*, 2009). This holds the sister chromatids together until anaphase, when all of the cohesin on the chromosomes is cleaved by separase to allow segregation. Analysis of Eco1 expression and Smc3 acetylation in meiosis revealed that Eco1 is similarly expressed in S phase of meiosis, concomitant with the appearance of acetylated cohesin. Although cohesin did not co-purify with Eco1, as shown by mass spectrometry analysis of purified Eco1-6HIS-3FLAG, Eco1 did co-elute with proteins involved in DNA replication, suggesting that Eco1 is localised to replication forks in meiosis, as in mitosis (Bylund and Burgers, 2005; Lengronne *et al.*, 2006; Moldovan, Pfander and Jentsch, 2006). This suggests that Eco1 may acetylate cohesin in meiosis, although whether Eco1 is the acetyltransferase for Smc3 in meiosis remains to be confirmed.

In mitosis, Eco1 acetylates cohesin on Smc3-K112,K113 to establish cohesive cohesin only in S phase (Skibbens *et al.*, 1999; Rolef Ben-Shahar *et al.*, 2008; Unal *et al.*, 2008; Zhang *et al.*, 2008b; Rowland *et al.*, 2009; Sutani *et al.*, 2009). However, Eco1 activity is important in G2 of mitosis for DNA repair and acetylates cohesin on Scc1 to promote cohesin establishment at the site of DNA damage (Strom *et al.*, 2007; Unal, Heidinger-Pauli and Koshland, 2007; Heidinger-Pauli, Unal and Koshland, 2009). During prophase of meiosis, programmed double strand breaks occur due to the activity of Spo11 (Keeney, Giroux and Kleckner, 1997). This is important in the formation of crossovers between homologous chromosomes, to ultimately form chiasmata to hold the homologues together in meiosis I and promote their segregation. As a result, there is a substantial level of DNA damage and repair during prophase of meiosis. By western blotting Eco1 appears to be absent in prophase of meiosis, as it is degraded as cells exit S phase. However, this may be due to the limited sensitivity of the western blotting, and it remains to be determined if Eco1 has an additional role in acetylating cohesin in prophase of meiosis.

Whilst undertaking the western blot time course experiments to determine the timing of Eco1 protein expression during meiosis, it became apparent that diploid strains containing *ECO1-6HA* accumulated at the binucleate stage and had a reduced level of tetranucleates. This was confirmed through comparison with a wild type diploid, and a diploid containing

ECO1-6HIS-3FLAG, which revealed that *ECO1-6HA* strains had extremely low cell viability of 7 %, and after 24 h in sporulation media had over 50 % cells with aberrant DNA segregation. As strains containing *ECO1-6HA* are viable in mitosis, and have extremely low viability in meiosis, this suggests that *ECO1-6HA* may specifically disrupt a meiosis-specific function of Eco1 that is essential for viability. Whether Smc3 acetylation of cohesin is equally important for chromosome segregation in meiosis remains to be determined.

4.3.2 Rad61 is regulated in meiosis, and deletion of *RAD61* results in increased cohesin levels on the DNA and decreased cell viability

The role of Wapl in destabilising cohesin from chromosomes in mitosis has been thoroughly documented throughout evolution, however the role of Wapl in meiosis is less clear. In prophase in *C. elegans*, *A. thaliana*, and budding yeast, Wapl has a role in promoting correct homologous recombination and has been implicated in accurate double strand break formation and repair, as well as in synaptonemal complex formation (De *et al.*, 2014; Challa *et al.*, 2016; Crawley *et al.*, 2016). I aimed to characterise the expression of Rad61 during the early stages of budding yeast meiosis. Synchronous meiotic time course experiments revealed that Rad61 is expressed throughout the early stages of budding yeast meiosis and becomes post-translationally modified during S phase. Mass spectrometry analysis of purified Rad61 failed to detect any phosphorylated or acetylated peptides of Rad61, thus the nature and role of the post-translational modification remains unclear.

However, in a recent study post-translational modification of Rad61 was partly dependent on DDK and Cdc5, and mutation of seven putative DDK sites in the N-terminus of Rad61 reduced the intensity of slower-migrating bands on Rad61 immunoblots (Challa *et al.*, 2019). Cohesin destabilisation in prophase was diminished in the phospho-null *rad61-7A* mutant, suggesting that meiosis-specific phosphorylation of Rad61 was activatory, and stimulates Rad61-dependent destabilisation of phosphorylated Rec8-containing cohesin (Challa *et al.*, 2019). In mouse, NEK1 kinase phosphorylates and activates PP1γ, which subsequently maintains Wapl in an unphosphorylated state and retains Wapl on the chromatin (Brieno-Enriquez *et al.*, 2016). Therefore, in mouse, phosphorylation inhibits Wapl function, whereas in budding yeast phosphorylation activates the cohesin destabilisation activity of Rad61 (Brieno-Enriquez *et al.*, 2016; Challa *et al.*, 2019).

After prophase, Rad61 is degraded in a separase-independent manner, prior to metaphase I. Analysis of Rad61 amino acid sequence revealed two KEN box motifs and a putative APC/C D-box motif, thus suggesting that Rad61 may a target of the APC/C (Glotzer, Murray and Kirschner, 1991; Pfleger and Kirschner, 2000). In mitosis, the main activatory subunits of the APC/C are Cdc20 and Cdh1, however in meiosis there is an additional regulatory subunit, Ama1, which is crucial for regulating the prophase to metaphase I transition (Cooper *et al.*, 2000; Okaz *et al.*, 2012). Therefore, this activity coincides with the timing of Rad61 degradation. It is interesting that Rad61 degradation coincides with the destabilisation of cohesin from the chromatin in late prophase, therefore degradation of Rad61 may be a mechanism to regulate the proportion of cohesin which is removed (Challa *et al.*, 2019). Mutational analysis of the destruction box of Rad61 will reveal if the timely degradation of Rad61 plays a crucial role in meiosis.

Between prophase and metaphase I of budding yeast meiosis, a pool of phosphorylated cohesin is destabilised from the chromosomes in a condensin and Rad61-dependent manner, without separase cleavage (Yu and Koshland, 2005; Challa *et al.*, 2019). *WAPL1* and *WAPL2* in *A. thaliana* destabilise Rec8-containing cohesin from the chromosomes from diplotene of prophase, although in *C. elegans*, WAPL-1 is only important for removal of COH3/4-containing cohesin (De *et al.*, 2014; Crawley *et al.*, 2016). In this study, *RAD61* mutants were shown to have increased levels of cohesin on the chromosomes in metaphase I, contradictory to previous reports of Rad61 having no effect on cohesin levels in prophase (Challa *et al.*, 2016), but consistent with the finding that *RAD61* mutants have delayed disappearance of Rec8 from the chromatin at the end of meiotic prophase (Challa *et al.*, 2019). This increase in cohesin supports the hypothesis that cohesin is removed in a Rad61-dependent manner after prophase, but prior to Rad61 degradation.

The increase in cohesin on the DNA in metaphase I of meiosis in *RAD61* mutants did not cause a defect in sister chromatid mono-orientation in meiosis I, and sister chromatids co-segregated faithfully. However, previously published analysis of chromosome segregation in (Challa *et al.*, 2016) showed a 30 % loss of homologue pairing and sister chromatid cohesion previously documented in *rad61Δ*. Reduced spore viability can be indicative of chromosome missegregation during meiosis, but spore viability was only decreased slightly in *RAD61* mutants compared to wild type, similar to the previously reported 83.8 % viability (Challa *et al.*, 2016). However, spore formation of *RAD61* mutants was decreased to under

25 %, compared to 67 % in wild type, therefore only a subpopulation of the cells were correctly undergoing meiosis and sporulation, therefore inadvertently masking the defects of the population of cells which failed to undergo meiosis I and II. Fluorescence microscopy analysis of *CEN5 tetO*/TetR-GFP dot segregation in *rad61Δ* revealed 14 % of tetranucleates had chromosome missegregation. This is likely to be an over-estimate due to weak GFP dots, as 5 % of wild type tetranucleates had improper segregation the GFP dots, and if all 16 chromosomes missegregated at a 14 % error rate this would result in much higher aneuploidy and cell death. Although it may be that defects caused by *RAD61* deletion cause cells to arrest, and so only the healthiest cells are again counted in this assay. In mitosis, *RAD61* mutants have cohesion and DNA repair defects, thus it may be that these defects also occur in meiosis, but only have a modest effect on chromosome segregation (Rowland *et al.*, 2009; Sutani *et al.*, 2009; Guacci and Koshland, 2012; Lopez-Serra *et al.*, 2013; Bloom, Koshland and Guacci, 2018).

4.3.3 Deletion of *HOS1* delays meiotic progression without effecting chromosome segregation

In mitosis, Hos1 is expressed, and has deacetylase activity, throughout the whole cell cycle (Borges *et al.*, 2010). However, cohesin deacetylation is restricted to anaphase, when, after separase cleaves Scc1, Hos1 deacetylates Smc3 to promote cohesin release (Beckouet *et al.*, 2010; Borges *et al.*, 2010; Xiong, Lu and Gerton, 2010). How cohesin is protected from the deacetylation activity of Hos1 prior to anaphase is unknown but has been hypothesised to be due to the protective activity of Pds5 (Beckouet *et al.*, 2010; Chan *et al.*, 2013). Western blot for Hos1 expression in meiosis showed that Hos1 was also expressed throughout the entire meiotic cell cycle, and as in mitosis, did not undergo any visible post-translational modifications or degradation (Borges *et al.*, 2010). Analysis of Rec8 cleavage and Smc3 acetylation in wild type meiosis shows that levels Smc3 acetylation decrease slightly after anaphase I of meiosis. This decrease is not apparent in *HOS1* mutants, suggesting that Hos1 is active in meiosis, but only deacetylates a proportion of cohesin.

Depletion of Hos1 during one cell cycle revealed that this caused a delay in anaphase of mitosis due to cohesin being stabilised on the DNA after separase cleavage of Scc1 (Li, Yue and Tanaka, 2017). Although the mechanism is not fully understood, deacetylation may promote a conformational change in the Smc3 ATPase head domain, allowing

disengagement from Smc1, and thus dissociation from the DNA (Li, Yue and Tanaka, 2017). In *hos1Δ* diploids in meiosis, time course analysis of meiotic progression revealed a delay in Rec8 cleavage and in meiosis II progression, suggesting there was a delay in anaphase I. This may be due to a failure to release acetylated cleaved cohesin from the arms of the chromosomes, and this could in the future be tested by ChIP time courses and live cell imaging.

HOS1 mutants in mitosis are viable, however, they do have cohesion defects similar to *smc3-K112N,K113N* acetyl-mimic mutant (Beckouet *et al.*, 2010; Borges *et al.*, 2010; Li, Yue and Tanaka, 2017). This is due to no deacetylation of Smc3 occurring, thus this pool of Smc3 is unable to be recycled into the unacetylated state, and can't be converted back into cohesive cohesin during DNA replication of the next cell cycle (Beckouet *et al.*, 2010; Borges *et al.*, 2010; Li, Yue and Tanaka, 2017). Therefore only a minor pool of newly synthesised Smc3 in G1 can be loaded on DNA and freshly acetylated by Eco1 to form cohesive cohesin, and as a result of the diminished pool of cohesin, *HOS1* mutants are sick and have cohesion defects (Beckouet *et al.*, 2010; Borges *et al.*, 2010; Li, Yue and Tanaka, 2017). However, analysis of *HOS1* mutants in meiosis showed that homozygous diploids had cell viability comparable to wild type strains, and no defects in sporulation efficiency or in chromosome segregation from analysis of homozygous *CEN5 tetO*/TetR-GFP dots by fluorescence microscopy. This suggests that Smc3 deacetylation after meiotic divisions may not be as crucial as in mitosis.

Overall, there is increasing evidence for a cohesin destabilisation pathway in budding yeast meiosis (Yu and Koshland, 2005; Challa *et al.*, 2019). Eco1 is expressed during S phase of meiosis, corresponding to the timing of the appearance of acetylated Smc3-K112,K113. The proportion of cohesin acetylated in meiosis is not known, but may only represent a minor pool. In late prophase phosphorylated Rad61 is hypothesised to destabilise a pool of phosphorylated Rec8-containing cohesin, which may aid DNA damage repair and correct chromosome condensation (Yu and Koshland, 2005; Challa *et al.*, 2016; Challa *et al.*, 2019). Chromatin fractionation experiments suggest that some acetylated cohesin may be destabilised in prophase, but whether this acetylated cohesin is important for chromosome cohesion remains to be determined. The prophase removal may decrease levels of cohesin on the chromosomes prior to the meiosis I division, and thus the delay in release of cohesin

which causes lagging chromosomes in *HOS1* mutants in mitosis may not have as higher detrimental effect in meiosis as there is less cohesin to withstand the pulling forces of the spindle. However, this hypothesis remains to be tested, however analysis of telomere GFP dot segregation in *HOS1* mutants with and without condensin may reveal if co-depletion enhances the telomere pairing in anaphase I in condensin mutants (Yu and Koshland, 2005; Li, Yue and Tanaka, 2017).

Chapter 5. Acetylated cohesin is important for faithful chromosome segregation in budding yeast meiosis

5.1 Introduction

Faithful chromosome segregation during the meiotic nuclear divisions is essential for cell viability in budding yeast, and it has long been established that this depends on the timely and accurate loading and removal of Rec8-cohesin from DNA. Prior to the first meiotic division the Rec8 subunit of cohesin is extensively phosphorylated by DDK, Hrr25 and Cdc5, which promotes Rec8 cleavage by separase in anaphase I (Lee and Amon, 2003; Brar *et al.*, 2006; Ishiguro *et al.*, 2010; Katis *et al.*, 2010; Attner *et al.*, 2013). There is now increasing evidence for an episode of cohesin removal in budding yeast meiosis prior to the first meiotic division, due to the activity of the conserved prophase pathway components (Yu and Koshland, 2005; Challa *et al.*, 2019).

The Eco1 acetyltransferase is expressed during S phase of meiosis, concomitant with the appearance of acetylated Smc3-K112,K113. In the mitotic cell cycle, Eco1 directly acetylates Smc3-K112,K113 during S phase to generate cohesive cohesin that is essential for faithful sister chromatid segregation (Rolef Ben-Shahar *et al.*, 2008; Unal *et al.*, 2008; Zhang *et al.*, 2008b; Rowland *et al.*, 2009; Sutani *et al.*, 2009; Beckouet *et al.*, 2010; Lyons and Morgan, 2011; Lopez-Serra *et al.*, 2013; Guacci *et al.*, 2015). If Eco1 is the acetyltransferase for Smc3 in budding yeast meiosis, and whether this modification is essential for generation of cohesion, remains to be determined. The loss of spore viability upon tagging Eco1 with 6HA however, strongly suggests that Eco1 has an essential function in meiotic chromosome segregation.

In budding yeast, a proportion of cohesin is acetylated during S phase of meiosis, and this is maintained throughout prophase and into the meiotic nuclear divisions. However, in late prophase, around 50-60 % of cohesin is released from the chromatin by a mechanism that does not depend on Rec8 cleavage by separase, and which is reminiscent of the destabilisation of cohesin that occurs in mammalian mitotic prophase (Yu and Koshland, 2005; Challa *et al.*, 2019). Phosphorylation of Rec8 by DDK and Cdc5 is crucial for cohesin destabilisation, and *rec8-17A* and *rec8-29A* phosphomutants have severely delayed cohesin release from the chromatin prior to metaphase I (Challa *et al.*, 2019). This correlates with the finding that the condensin complex promotes cohesin release in late prophase through

facilitating Cdc5 association with cohesin (Yu and Koshland, 2005). Cohesin release is dependent upon activation of Rad61 through phosphorylation by DDK and Cdc5 (Challa *et al.*, 2019), and consequently increased cohesin levels are observed both in *RAD61* phosphomutants (Challa *et al.*, 2019) and in *rad61Δ* by ChIP-qPCR (Figure 4.2.2.1). Rad61 is subsequently degraded between prophase and metaphase I which may act as a mechanism to limit the amount of cohesin that is destabilised. The remaining chromatin bound cohesin is cleaved by separase prior to the meiosis I and II nuclear divisions (Buonomo *et al.*, 2000).

An outstanding question remains as to why there is a cohesin destabilisation pathway prior to chromosome segregation in budding yeast meiosis, but not prior to mitotic DNA segregation? In the mitotic cell cycle in budding yeast, G2 is very short, therefore the time during which cohesin destabilisation may occur is limited. One major difference in meiosis is the extended prophase, during which homologous recombination occurs that involves Spo11-mediated double strand break formation and repair of these breaks via the homologous recombination cross-over pathway, to form chiasmata. Cohesin complexes make up part of the chromosome axes and are important for formation of the synaptonemal complex between homologous chromosomes (reviewed in (Marston, 2014)). Rad61 in budding yeast meiosis is important for DSB repair and for efficient processing of recombination intermediates, similar to as in *C. elegans* (Challa *et al.*, 2016; Crawley *et al.*, 2016), and one hypothesis is that removal of cohesin may aid chiasmata formation and resolution, and promote chromosome condensation in late prophase (Challa *et al.*, 2019). In condensin mutants, a subset of cohesin remains on chromosome arms in anaphase I, and results in tangling of telomeric regions, therefore removal of cohesin in meiosis aids chromosome segregation (Yu and Koshland, 2005).

It may be that only arm cohesin is susceptible to the destabilisation pathway in budding yeast meiosis, as this is the region in which chiasmata occur. By super resolution microscopy (structural illumination microscopy (SIM)), Rec8 on the chromosome arms was seen to have a "beads on a string" morphology along the two parallel axis of the synapsed homologous chromosomes (Challa *et al.*, 2019). Co-staining of the kinetochore component, Ctf19, revealed that the two axes of Rec8 staining were fused around the Ctf19 signal, suggesting that the pericentromeric cohesin is structured differently to the bulk of cohesin (Challa *et al.*, 2019). Is this pericentromeric cohesin protected from the destabilisation

pathway, and if so, does the acetylation state of this pool of cohesin promote this protection?

One candidate for a protector of pericentromeric cohesin from the destabilisation pathway in meiosis is Sgo1. Although Sgo1 is important for faithful mitotic chromosome segregation through roles in biorientation and tension sensing, *sgo1Δ* mutants do not lose sister chromatid cohesion prematurely, and Sgo1 does not protect cohesin from separase (Katis *et al.*, 2004a; Indjeian, Stern and Murray, 2005; Kiburz *et al.*, 2005; Verzijlbergen *et al.*, 2014). However, in budding yeast meiosis, Sgo1-PP2A has the additional function of dephosphorylating, and thus protecting, Rec8-cohesin from cleavage in anaphase I (Katis *et al.*, 2004a; Kitajima, Kawashima and Watanabe, 2004; Marston *et al.*, 2004; Kiburz *et al.*, 2005; Brar *et al.*, 2006; Riedel *et al.*, 2006; Katis *et al.*, 2010). The centromeric cohesin protection activity of meiotic Sgo1-PP2A by dephosphorylation in budding yeast is analogous to that found in mammalian mitosis, during which Sgo1-PP2A dephosphorylates both sororin and SA2 to protect cohesin from destabilisation by the prophase pathway (Salic, Waters and Mitchison, 2004; Tang *et al.*, 2004; Hauf *et al.*, 2005; Kitajima *et al.*, 2005; McGuinness *et al.*, 2005; Kitajima *et al.*, 2006; Tang *et al.*, 2006; Dreier, Bekier and Taylor, 2011; Liu, Jia and Yu, 2013; Nishiyama *et al.*, 2013; Hara *et al.*, 2014). Therefore, it is possible that Sgo1-PP2A in budding yeast may additionally protect centromeric cohesin from the destabilisation pathway through dephosphorylation.

In budding yeast there is an additional meiosis-specific cohesin protector known as Spo13 (Wang *et al.*, 1987). *SPO13* was initially discovered as mutants in meiosis only underwent one division, with mixed reductional and equational chromosome segregation, to form dyads (Klapholz and Esposito, 1980; Wang *et al.*, 1987; Hugerat and Simchen, 1993; Shonn, McCarroll and Murray, 2002). Although entry into meiosis, meiotic DNA replication, synaptonemal complex formation and recombination occur normally in *spo13Δ*, once cells exit prophase numerous defects occur (Hugerat and Simchen, 1993; Shonn, McCarroll and Murray, 2002; Mehta *et al.*, 2018). Spo13 interacts with Cdc5 kinase, and both are essential for the maintenance of the monopolin complex at kinetochores, and as a consequence, for mono-orientation of sister chromatid kinetochores (Shonn, McCarroll and Murray, 2002; Lee and Amon, 2003; Lee, Kiburz and Amon, 2004; Katis *et al.*, 2004b; Monje-Casas *et al.*, 2007; Matos *et al.*, 2008). The failure of *spo13Δ* to maintain monopolin causes a proportion

of sister chromatid kinetochores to biorient in meiosis I (Shonn, McCarroll and Murray, 2002; Lee, Kiburz and Amon, 2004; Katis *et al.*, 2004b). Additionally, *spo13Δ* mutants fail to protect centromeric Rec8 during the first meiotic division and all cohesin is cleaved in anaphase I (Shonn, McCarroll and Murray, 2002; Lee, Kiburz and Amon, 2004; Katis *et al.*, 2004b). This in turn allows both mono-oriented and bioriented chromosomes to segregate, thus resulting in the mixed reductional and equational chromosome segregation (Hugerat and Simchen, 1993; Shonn, McCarroll and Murray, 2002; Lee, Kiburz and Amon, 2004; Katis *et al.*, 2004b).

How exactly Spo13 protects centromeric cohesin is not fully understood. Over-expression of Spo13 in mitosis causes a metaphase delay, which is due to protection of Scc1 (or mitotically expressed Rec8) from cleavage by separase (McCarroll and Esposito, 1994; Shonn, McCarroll and Murray, 2002; Lee, Amon and Prinz, 2002; Katis *et al.*, 2004b). Although *SPO13* mutants do cleave all cohesin during the first meiotic division, the arm cohesin is still cleaved first, with residual centromeric Rec8 (and cohesion) persisting into anaphase I (Katis *et al.*, 2004b; Lee, Kiburz and Amon, 2004). Spo13 is an inhibitor of APC/C activity, therefore one hypothesis is that *SPO13* mutants can't restrict APC/C activity after anaphase I due to a failure to re-accumulate Pds1, and that this unregulated APC/C activity allows all cohesin to be cleaved by separase (Katis *et al.*, 2004b; Sullivan and Morgan, 2007).

In wild type, Spo13 protein is expressed in early meiosis and is maintained until anaphase I, when Spo13 is degraded by APC-Cdc20 (Wang *et al.*, 1987; Katis *et al.*, 2004b; Sullivan and Morgan, 2007). Therefore it was hypothesised that Spo13 may regulate Sgo1 activity to specifically turn Sgo1 into a "cohesin protector" in meiosis I. Although Sgo1 levels and post-translational modifications were unaffected by deletion of *SPO13*, the Sgo1 foci at kinetochores were smaller and levels of pericentromeric Sgo1 reduced by ChIP, suggesting a decrease in protective centromeric Sgo1 (Lee, Kiburz and Amon, 2004; Kiburz *et al.*, 2005). However, in separate studies, Spo13 was found to have no discernible impact on Sgo1 localisation to kinetochores ((Katis *et al.*, 2004b). Through both live cell imaging of Sgo1-GFP and deep sequencing of Sgo1 ChIP (ChIP-seq), Sgo1 localisation was found to be unaffected in *spo13Δ* mutants (S. Galander, unpublished data). Therefore, the exact relationship between Spo13 and Sgo1 has still not been fully resolved.

In summary, I aimed to first establish the importance of Eco1 function in meiosis, and the effect that disruption of Eco1 function has on meiotic cohesin acetylation, levels of chromatin bound cohesin, and on cell viability. I also aimed to establish if there was a relationship between the cohesin protectors, Spo13 and Sgo1, and the activity of the destabilisation pathway.

5.2 Results

5.2.1 Disruption of Eco1 function in meiosis

Eco1 is expressed during S phase of budding yeast meiosis (Figure 4.2.3.3), and the timing of expression coincides with the appearance of Smc3-K112,K113 acetylation (Figure 4.2.3.6). Although expression of *ECO1-6HIS-3FLAG* allowed cells to progress through meiosis and form viable spores (Figures 4.2.3.2 and 4.2.3.3), strains expressing *ECO1-6HA* had low sporulation efficiency, and dissection of the tetrads formed resulted in low spore viability (Figure 4.2.3.2). This suggested that tagging Eco1 disrupted the protein function and had a detrimental effect on meiotic progression and DNA segregation, therefore I aimed to further investigate the role of Eco1 in meiosis. Deletion of *ECO1* is lethal in vegetatively growing budding yeast, but this can be rescued by deletion of *RAD61* (Rolef Ben-Shahar *et al.*, 2008; Unal *et al.*, 2008; Rowland *et al.*, 2009; Sutani *et al.*, 2009; Guacci and Koshland, 2012; Chan *et al.*, 2012; Lopez-Serra *et al.*, 2013; Bloom, Koshland and Guacci, 2018). However, attempts to dissect sporulated diploid SK1 strains containing *eco1Δ rad61Δ* were unsuccessful due to low sporulation efficiency and poor spore viability. Temperature sensitive alleles of *ECO1* have been generated, however many require temperatures exceeding 30 ^{o}C, which can result in restricting meiotic progression of even healthy wild type cells.

An alternative approach, known as the anchor-away system, was adopted to disrupt Eco1 function in meiosis (Figure 5.2.1.1A) (Haruki, Nishikawa and Laemmli, 2008). The anchor-away system utilises the dimerisation of human proteins FKBP12 and the FRB domain of mTOR in response to the presence of rapamycin (Haruki, Nishikawa and Laemmli, 2008). In the system that I employed, the Rpl13a subunit of the ribosome was tagged with FKBP12, and Eco1 was tagged with FRB-GFP. Theoretically, in cells without rapamycin, Eco1-FRB-GFP will remain in the nucleus and acetylate cohesin, as in wild type (Figure 5.2.1.1A).

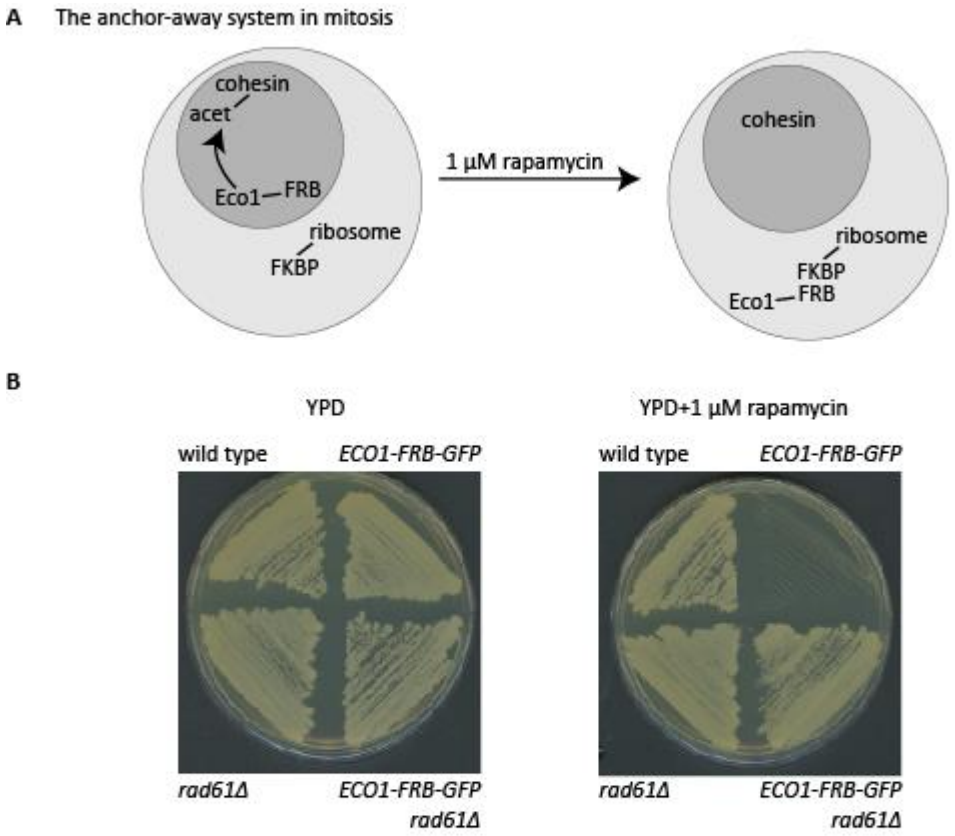

Figure 5.2.1.1: Anchoring Eco1-FRB-GFP out of the nucleus is lethal in mitosis
A) Schematic of the anchor-away system. In vegetative cells, Eco1-FRB-GFP is present in the nucleus and can acetylate cohesin. Upon addition of 1 µM rapamycin, Eco1-FRB-GFP is shuttled out of the nucleus, and is anchored to the ribosome through binding to Rpl13a-FKBP12. Through anchoring Eco1 out of the nucleus cohesin acetylation by Eco1 is prevented. B) *ECO1-FRB-GFP* is lethal to cells exposed to rapamycin, and this lethality is rescued by deletion of *RAD61*. Haploid wild type (13762), *ECO1-FRB-GFP* (22004), *rad61Δ* (22440), and *ECO1-FRB-GFP rad61Δ* (22981) were patched onto either YPD or YPD+1 µM rapamycin agar plates and placed at 30 °C for 48 h to allow growth.

Rpl13a-FKBP12 readily shuttles in and out of the nucleus, and upon addition of rapamycin, Rpl13a-FKBP12 binds to rapamycin forming the interaction site for FRB on Eco1-FRB-GFP. This binding of FKBP12-rapamycin to FRB causes Eco1-FRB-GFP to be shuttled out of the nucleus with Rpl13a (Figure 5.2.1.1A). In addition to the introduction of FKBP12 and FRB-GFP tags, the yeast also require two extra mutations: the *tor1-1* mutation to allow rapamycin resistance, and *fpr1Δ* to eliminate competition for binding of rapamycin to FRB (Haruki, Nishikawa and Laemmli, 2008). Budding yeast containing *tor1-1*, *fpr1Δ*, and *RPL13A-FKBP12* will be referred to as the anchor-away system for simplicity.

Haploid strains containing the anchor-away system and *ECO1-FRB-GFP* were patched onto rich media, and were found to be viable, and grew with similar efficiency to wild type (Figure 5.2.1.1B). The wild type anchor-away strain was viable on rich media containing rapamycin, however strains containing *ECO1-FRB-GFP* were inviable, and this lethality was rescued by deletion of *RAD61* (Figure 5.2.1.1B). The lethality of anchoring away *ECO1-FRB-GFP*, and the rescue by *rad61Δ*, suggests that the anchor-away system is fully disrupting Eco1 function in vegetative cells and behaves as *eco1Δ* (Skibbens *et al.*, 1999; Toth *et al.*, 1999; Brands and Skibbens, 2005; Rolef Ben-Shahar *et al.*, 2008; Unal *et al.*, 2008; Rowland *et al.*, 2009; Sutani *et al.*, 2009; Chan *et al.*, 2012; Guacci and Koshland, 2012; Lopez-Serra *et al.*, 2013).

The impact of disruption of *ECO1* function on meiotic progression and DNA segregation could now be assessed through utilising the anchor-away system. Diploid anchor-away strains were placed into sporulation media either containing rapamycin or DMSO (the solvent in which rapamycin is dissolved) and incubated at 30 ^{o}C for 24 h to allow meiosis to occur, before fixation and DAPI staining to assess nuclear morphology by fluorescence microscopy. Wild type strains underwent meiosis in both DMSO and rapamycin media, and over 60 % of cells formed tetranucleates (Figure 5.2.1.2A). This was considerably higher than the tetranucleate formation of *ECO1-FRB-GFP* cells in rapamycin, and surprisingly, in DMSO media, when Eco1 should not be anchored out of the nucleus (5.2.1.2A). This suggests that tagging Eco1 with FRB-GFP disrupted Eco1 function, as with Eco1-6HA (Figure 4.2.3.2). The low level of tetranucleate formation in *ECO1-FRB-GFP* was not rescued by deletion of *RAD61*, although *rad61Δ* mutants alone had over 50% sporulation efficiency (Figure 5.2.1.2A). In all strains containing *ECO1-FRB-GFP*, there was a high proportion of

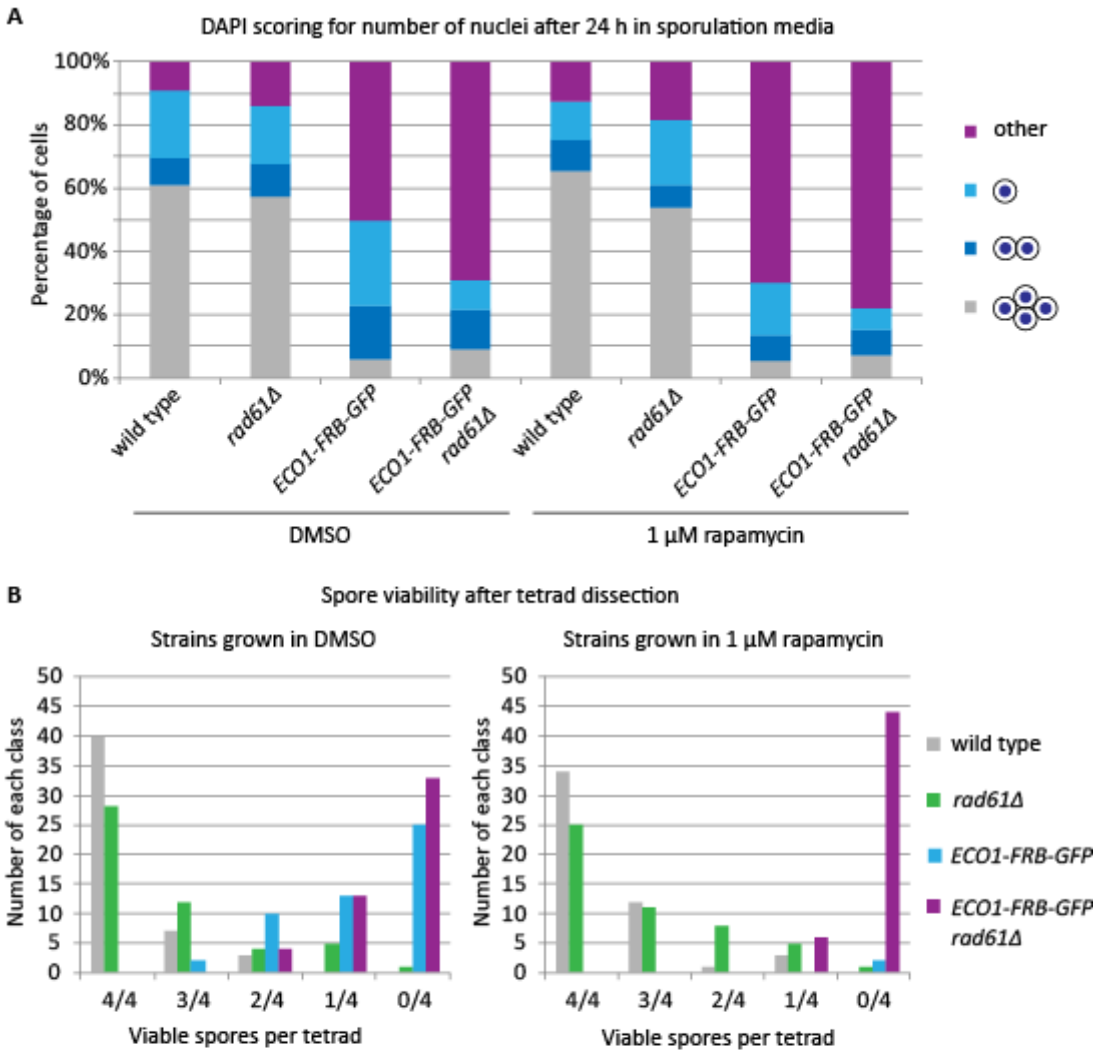

Figure 5.2.1.2: *ECO1-FRB-GFP* strains have decreased viability
Diploid wild type (24170), *rad61Δ* (24265), *ECO1-FRB-GFP* (24171), and *ECO1-FRB-GFP rad61Δ* (24289), were placed in sporulation media, with addition of either DMSO or 1 µM rapamycin, and grown at 30 °C to allow meiosis to occur. A) After 24 h in sporulation media cells were fixed in 80 % EtOH, and DAPI staining carried out. Graph shows number of nuclei as scored by fluorescence microscopy (n=200 cells/strain). The "other" category represents cells with fragmented DAPI staining, 3 DAPI masses or diffuse DAPI staining. B) Dissection of wild type (24170), *rad61Δ* (24265), *ECO1-FRB-GFP* (24171), and *ECO1-FRB-GFP rad61Δ* (24289) diploid strains for viability after incubation in sporulation media at 30 °C. Graphs showing viable spores per tetrad after dissection of 50 tetrads for each strain, apart from *ECO1-FRB-GFP* in 1 µM rapamycin for which only 2 spores were dissected. The resulting viability in DMSO was: wild type 93.5 %; *rad61Δ* 80.5 %; *ECO1-FRB-GFP* 19.5 %; and *ECO1-FRB-GFP rad61Δ* 10.5 %. The resulting viability in 1 µM rapamycin was: wild type 88.5 %; *rad61Δ* 77 %; *ECO1-FRB-GFP* 0 %; and *ECO1-FRB-GFP rad61Δ* 3 %.

cells which had diffuse or fragmented DNA morphology by DAPI staining (classified as "other"), therefore suggesting that gross DNA missegregation had occurred in these strains.

After incubation of the anchor-away strains in sporulation media containing either DMSO or rapamycin, the resulting tetrads were dissected to assess spore viability (Figure 5.2.1.2B). Wild type anchor-away spores were 93.5 % and 88.5 % viable after sporulation in DMSO and rapamycin media respectively, and a slightly reduced viability of 80.5 % in DMSO and 77 % in rapamycin was observed for *rad61Δ* (Figure 5.2.1.2B). Viability of *ECO1-FRB-GFP* in DMSO was reduced to 19.5 %, and this further decreased to 10.5 % by deletion of *RAD61*. Sporulation of *ECO1-FRB-GFP rad61Δ* strains in rapamycin media further reduced viability to 3 %. Only two tetrads could be successfully dissected after *ECO1-FRB-GFP* diploids were sporulated in rapamycin media, both of which had 0 % viability (Figure 5.2.1.2B). Therefore, tagging Eco1 with FRB-GFP disrupts Eco1 function in meiosis, but addition of rapamycin further abrogates Eco1 activity and severely compromises meiotic DNA segregation.

Smc3-K112,K113 acetylation levels during meiosis could now be compared in wild type and *ECO1-FRB-GFP*, to determine if Eco1 is the acetyltransferase for Smc3 in meiosis. Diploid wild type and *ECO1-FRB-GFP* anchor-away strains were placed into sporulation media for 9 h at 30 ^{o}C to induce meiosis, and at regular time intervals samples for protein extracts and DAPI staining were removed. Western immunoblot analysis showed that in the wild type strain, Smc3-K112,K113 acetylation was present at the start of the time course, increased slightly between 2-6 h, before modestly decreasing at the time of Rec8 cleavage (Figure 5.2.1.3A), corresponding to the time of binucleate formation from visualisation of the number of DAPI stained nuclei by fluorescence microscopy (Figure 5.2.1.3B). In contrast, Smc3-K112,K113 acetylation was not detectable throughout the *ECO1-FRB-GFP* meiotic time course, although Rec8 was first detected at the same time as in wild type, showing meiotic entry was not affected (Figure 5.2.1.3A). Unlike in the wild type western blot, Rec8 levels did not decrease during the *ECO1-FRB-GFP* meiotic time course, and by scoring of nuclear morphology after DAPI staining, very few binucleate and tetranucleate cells developed throughout the time course, suggesting meiotic progression was compromised (Figure 5.2.1.3B).

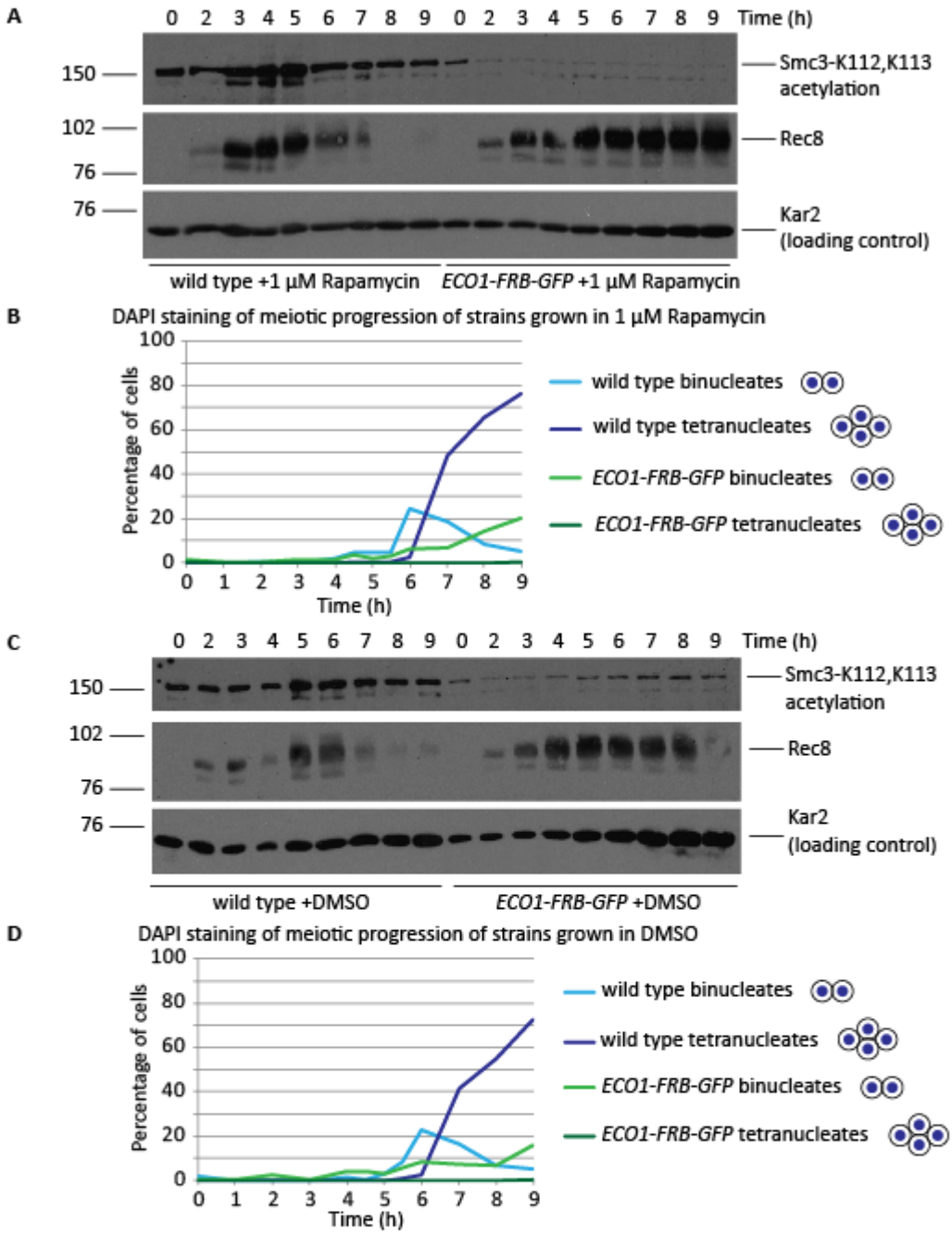

Figure 5.2.1.3: Smc3 acetylation is absent in meiosis in strains containing *ECO1-FRB-GFP*, and meiotic progression is disrupted

Wild type and *ECO1-FRB-GFP* diploid strains were placed in sporulation media to induce meiosis, with either DMSO or 1 µM Rapamycin. Samples were removed at the timepoints indicated for TCA protein extracts and for DAPI staining. Western blotting was carried out by ECL using homemade rabbit anti-Smc3-K112,K113 acetylation antibody to probe for Smc3 acetylation, homemade rabbit anti-Rec8 antibody against Rec8, and homemade rabbit anti-KAR2 for the loading control. A) Protein extracts for wild type (25532) and *ECO1-FRB-GFP* (22034) grown in 1 µM Rapamycin were run on an 8 % SDS-PAGE gel and western blotting carried out. B) Graph of DAPI stain scoring through the asynchronous meiotic time course in 1 µM Rapamycin for wild type (25532) and *ECO1-FRB-GFP* (22034) (n=200 cells/timepoint). C) Protein extracts for wild type (25532) and *ECO1-FRB-GFP* (22034) grown in DMSO were run on an 8 % SDS-PAGE gel and western blotting carried out. D) Graph of DAPI stain scoring through the asynchronous meiotic time course in DMSO for wild type (25532) and *ECO1-FRB-GFP* (22034) (n=200 cells/timepoint).

The asynchronous meiotic time course protocol was repeated for wild type and *ECO1-FRB-GFP* diploid strains in media containing DMSO rather than rapamycin. Analysis of Smc3-K112,K113 acetylation by western immunoblot again showed that there was a reduction in Smc3 acetylation levels in *ECO1-FRB-GFP* anchor-away strains, and that these strains did not progress through meiosis efficiently due to low levels of binucleate and tetranucleate formation, and a stabilisation of Rec8 protein levels (Figure 5.2.1.3C, D). Therefore, Eco1 is important for Smc3 acetylation in meiosis, and for efficient meiotic progression.

5.2.2 Rad61 destabilises cohesin from the chromatin during meiosis

Disruption of cohesin function in meiosis through deletion of *REC8* results in 85-90% of cells arresting in late prophase due to defects in recombination (Klein *et al.*, 1999). The failure of Rec8 cleavage and binucleate formation upon anchoring-away Eco1 during meiosis (Figure 5.2.1.2) may therefore be due to a lack of cohesin on the DNA causing a prophase arrest.

I carried out ChIP for the Rec8 subunit of cohesin in a *pGAL-NDT80* prophase I arrest in the anchor-away strains. Enrichment of Rec8-6HIS-3FLAG at three loci on chromosome IV was analysed by qPCR and revealed that Rec8 was significantly decreased at the arm, pericentromeric and centromeric sites analysed in a diploid strain containing *ECO1-FRB-GFP* that had been induced to undergo meiosis in the presence of rapamycin (Figure 5.2.2.1A). Rec8 levels were also significantly decreased at the arm and pericentromeric, but not the centromeric loci, in *ECO1-FRB-GFP rad61Δ* (Figure 5.2.2.1A). Western blotting of protein extracts taken from the cell cultures used for ChIP-qPCR showed that Smc3-K112,K113 acetylation was reduced in the anchor-away strains containing *ECO1-FRB-GFP* both in the presence of DMSO and rapamycin, and also that Rec8 protein levels were comparable in all strains (Figure 5.2.2.1B). Additionally, flow cytometry analysis confirmed that *ECO1-FRB-GFP* strains progressed through meiotic S phase (Figure 5.2.2.1C). In conclusion, chromosomal-bound cohesin levels are reduced, but not abolished, in *ECO1-FRB-GFP* anchor-away strains in prophase I, therefore showing that non-acetylated cohesin is susceptible to destabilisation by Rad61 in meiosis.

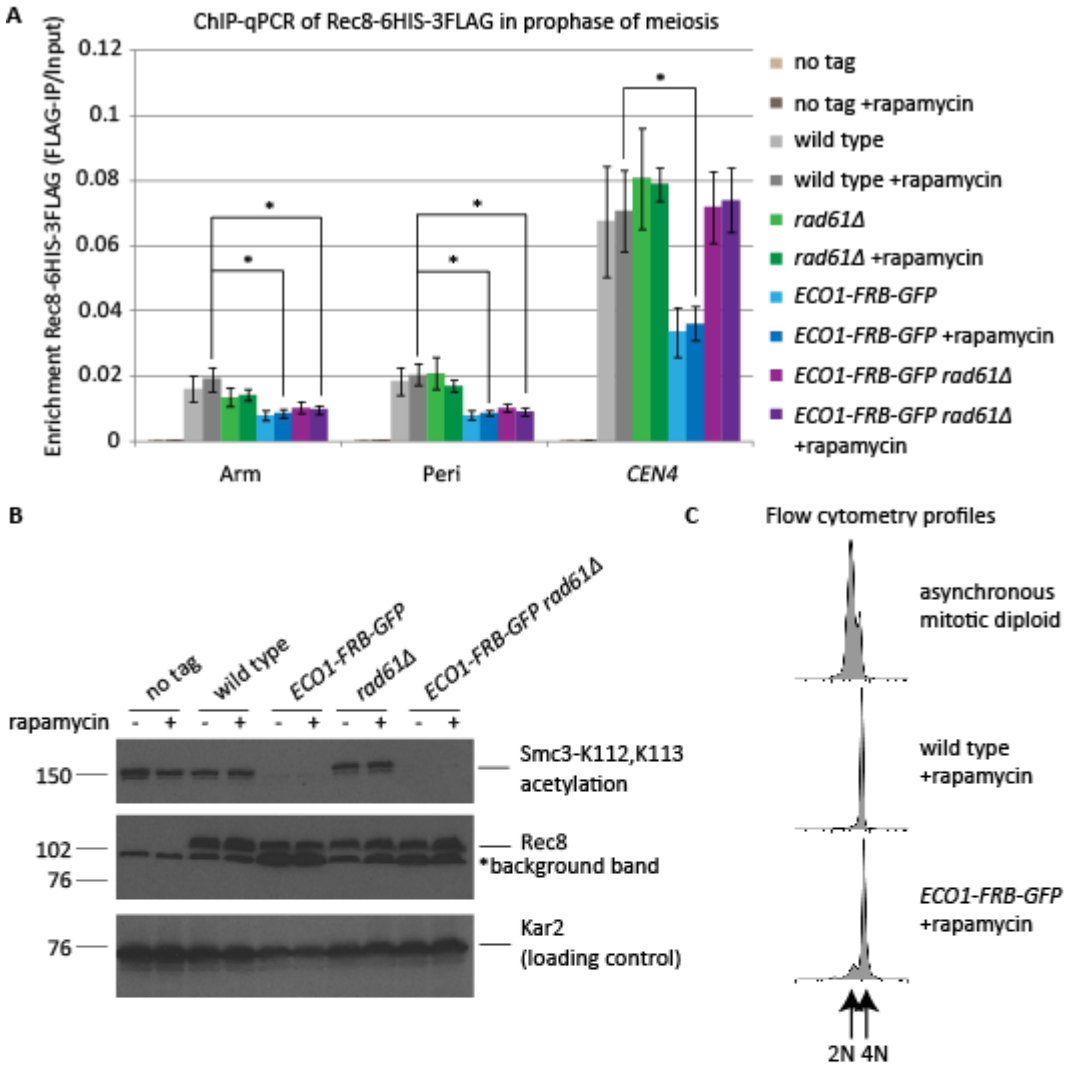

Figure 5.2.2.1: Anchoring away Eco1 causes a significant decrease in cohesin levels on the DNA in prophase of meiosis

ChIP-qPCR of Rec8-6HIS-3FLAG in prophase of meiosis, shows Rec8 localisation to chromatin is reduced when Eco1 is anchored-away A) Strains containing *REC8-6HIS-3FLAG* were arrested in prophase of meiosis using *pGAL-NDT80,* in the presence of DMSO or 1 µM rapamycin, before harvesting for ChIP-qPCR. ChIP for Rec8-6HIS-3FLAG was carried out in wild type (23130), *rad61Δ* (23414), *ECO1-FRB-GFP* (22998) and *ECO1-FRB-GFP rad61Δ* (23415), as well as in a no tag background (23416), using M2 FLAG antibody against 3FLAG. Average of 5 repeats for Arm, Peri and *CEN4*. Error bars show standard error. Paired student T test gave a p values of Arm=0.0183, Peri=0.0162, *CEN4*=0.0158 for *ECO1-FRB-GFP* in rapamycin, and p values of Arm=0.0273 and Peri=0.0120 for *ECO1-FRB-GFP rad61Δ* in rapamycin. No other site or mutant was significantly increased or decreased in Rec8-6HIS-3FLAG enrichment compared to wild type. B) Western blotting for Rec8-6HIS-3FLAG, Smc3-K112,K113 acetylation and a loading control (Kar2) in the strains used for ChIP-qPCR. Western blot developed by ECL, using M2 FLAG antibody to probe against Rec8-6HIS-3FLAG, homemade rabbit antibody against anti-Smc3-K112,K113 acetylation, and homemade rabbit anti-Kar2 for the loading control. No tag (23416), wild type (23130), *rad61Δ* (23414), *ECO1-FRB-GFP* (22998) and *ECO1-FRB-GFP rad61Δ* (23415) samples shown. C) Flow cytometry samples were taken to ensure progression through S phase. Cells were fixed in ethanol before treatment with RNase and Proteinase K, then stained with Propridium Iodide and flow cytometry carried out. Samples for asynchronous mitotic diploid (1835), wild type (23130), and *ECO1-FRB-GFP* (22998) (n=20000 cells/timepoint).

Cohesin acetylation is substantially reduced in *ECO1-FRB-GFP* anchor-away strains, indicating that the remaining chromatin-associated cohesin in prophase is unacetylated. Rad61 in vegetatively growing cells can destabilise unacetylated cohesin from the DNA, therefore the remaining chromatin-associated cohesin in *ECO1-FRB-GFP* anchor-away strains may be susceptible to this destabilisation activity. The *RAD61* promoter was swapped to the inducible *CUP1* promoter to allow over-expression of *RAD61* by addition of 25 µM $CuSO_4$, and a 6HA tag was introduced at the C-terminus of Rad61 to monitor protein levels. ChIP of Rec8 was carried out in *pGAL-NDT80* prophase I arrest in the *ECO1-FRB-GFP* anchor-away strains, both with and without *pCUP1-RAD61-6HA*. Analysis of chromatin bound Rec8-6HIS-3FLAG by qPCR showed that unlike in Figure 5.2.2.1A, cohesin enrichment was not significantly decreased in *ECO1-FRB-GFP*, but was significantly decreased in *ECO1-FRB-GFP pCUP1-RAD61-6HA* strains (Figure 5.2.2.2A). This discrepancy in cohesin enrichment in *ECO1-FRB-GFP* strains between Figures 5.2.2.1A and 5.2.2.2A, may be due to the presence of *RAD61-6HA* in the strain background in the latter experiment disrupting Rad61 protein function, and therefore reducing cohesin destabilisation. Western blotting of protein extracts taken from the cultures used for ChIP, revealed a decrease in Rec8 protein levels in *ECO1-FRB-GFP pCUP1-RAD61-6HA* extracts, and flow cytometry analysis further revealed that a proportion of *ECO1-FRB-GFP pCUP1-RAD61-6HA* cells had 2N DNA content, and thus had not entered meiosis and progressed through S phase (Figure 5.2.2.2B, C). Therefore, the effect of Rad61 over-expression on cohesin association is difficult to assess due to the defective meiotic progression (Figure 5.2.2.2B, C).

Cohesin destabilisation by a prophase-pathway-like mechanism has been proposed to occur after at the end of prophase I, but prior to metaphase I (Yu and Koshland, 2005; Challa *et al.*, 2019). Previously, deletion of *RAD61* resulted in a significant increase in chromatin-bound Rec8 in metaphase I of meiosis by ChIP-qPCR (Figure 4.2.2.1). ChIP of Rec8-3HA was carried out in the anchor-away strains in a metaphase I arrest, to determine if a further loss of chromatin-bound cohesin was observed in *ECO1-FRB-GFP* strains, and if this could be rescued by *rad61Δ*. Rec8 enrichment on the chromatin was assayed by qPCR, and only pericentromeric cohesin enrichment was found to be significantly decreased in *ECO1-FRB-GFP* strains in metaphase I (Figure 5.2.2.3A). However, analysis of the overall pattern of Rec8 enrichment showed that *rad61Δ* mutants did show an increase in cohesin at all of the sites tested, and deletion of *RAD61* in *ECO1-FRB-GFP* increased cohesin levels in

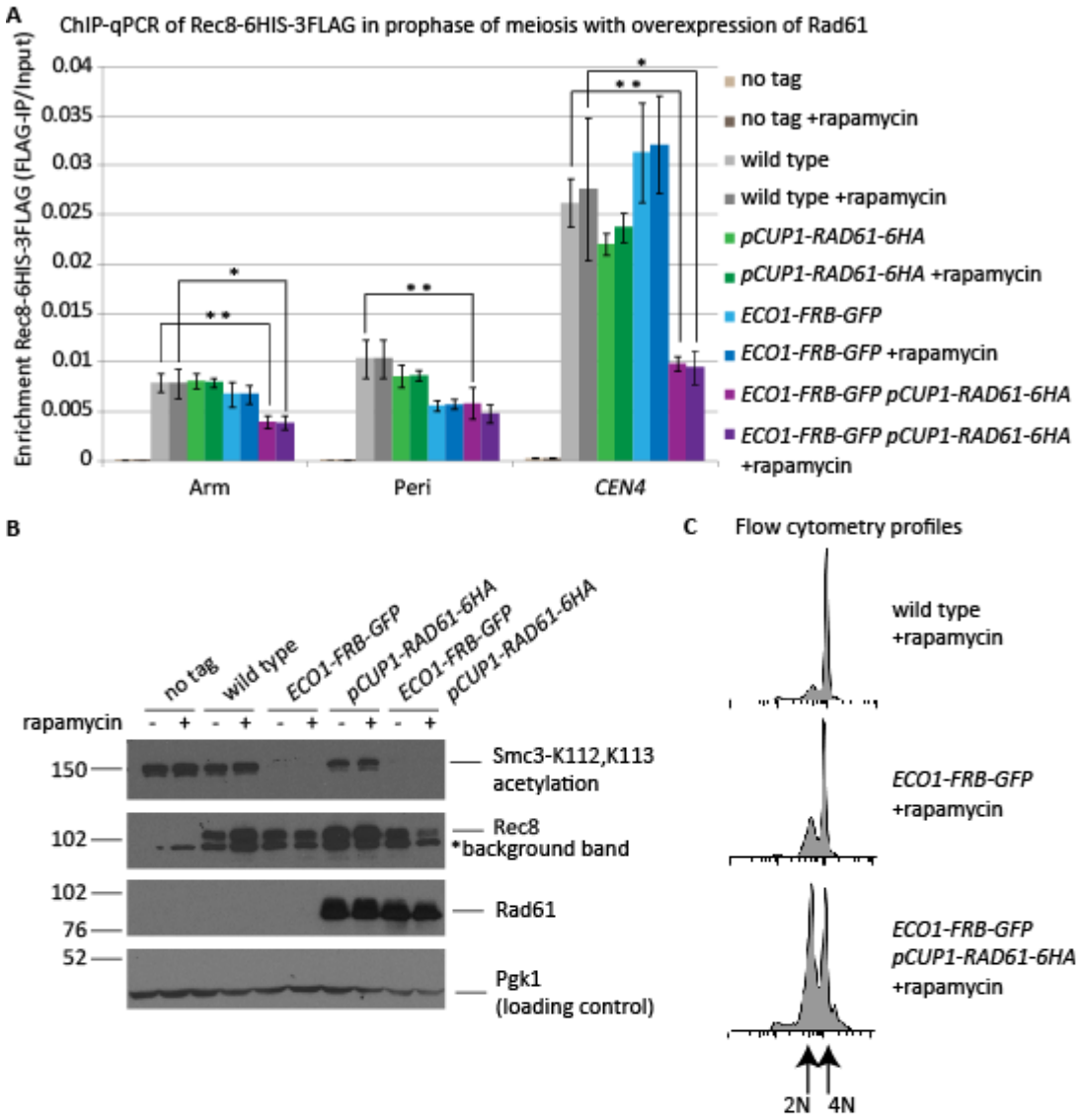

Figure 5.2.2.2: Anchoring away Eco1 under conditions when *RAD61* is over-expressed, causes a significant decrease in cohesin levels on the DNA in prophase of meiosis

ChIP-qPCR of Rec8-6HIS-3FLAG in prophase of meiosis, shows Rec8 localisation to chromatin is reduced in conditions when *RAD61* is over-expressed and Eco1 is anchored away A) Strains containing Rec8-6HIS-3FLAG were arrested in prophase of meiosis using *pGAL-NDT80,* in the presence of DMSO or 1 µM rapamycin, and 25 µM $CuSO_4$ before harvesting for ChIP-qPCR. ChIP for Rec8-6HIS-3FLAG was carried out in wild type (23445), *pCUP1-RAD61-6HA* (23446), *ECO1-FRB-GFP* (23161) and *ECO1-FRB-GFP pCUP1-RAD61-6HA* (23447), and in a no tag background (24088), using M2 FLAG antibody against 3FLAG. All strains used contained *RAD61-6HA*. Average of 4 repeats for Arm, Peri and *CEN4*. Error bars show standard error. Paired student T test gave p values of Arm=0.0348 and *CEN4*=0.0458 for *ECO1-FRB-GFP pCUP1-RAD61-6HA* in 1 µM rapamycin, and p values of Arm=0.0022, Peri=0.0020, and *CEN4*=0.0076 for *ECO1-FRB-GFP pCUP1-RAD61-6HA* in DMSO. B) Western blotting for Rec8-6HIS-3FLAG, Smc3-K112,K113 acetylation, Rad61-6HA and a loading control (Pgk1) in the strains used for ChIP-qPCR. Western blot developed by ECL, using M2 FLAG to probe against Rec8-6HIS-3FLAG, HA11 to probe against Rad61-6HA, homemade rabbit antibody against anti-Smc3-K112,K113 acetylation, and homemade rabbit anti-Pgk1 for the loading control. C) Flow cytometry samples were taken to ensure progression through S phase. Cells were fixed in ethanol before processing, before staining with Propridium Iodide and flow cytometry carried out. Samples for wild type (23445), *ECO1-FRB-GFP* (23161), and *ECO1-FRB-GFP pCUP1-RAD61-6HA* (23447) (n=20000 cells/timepoint).

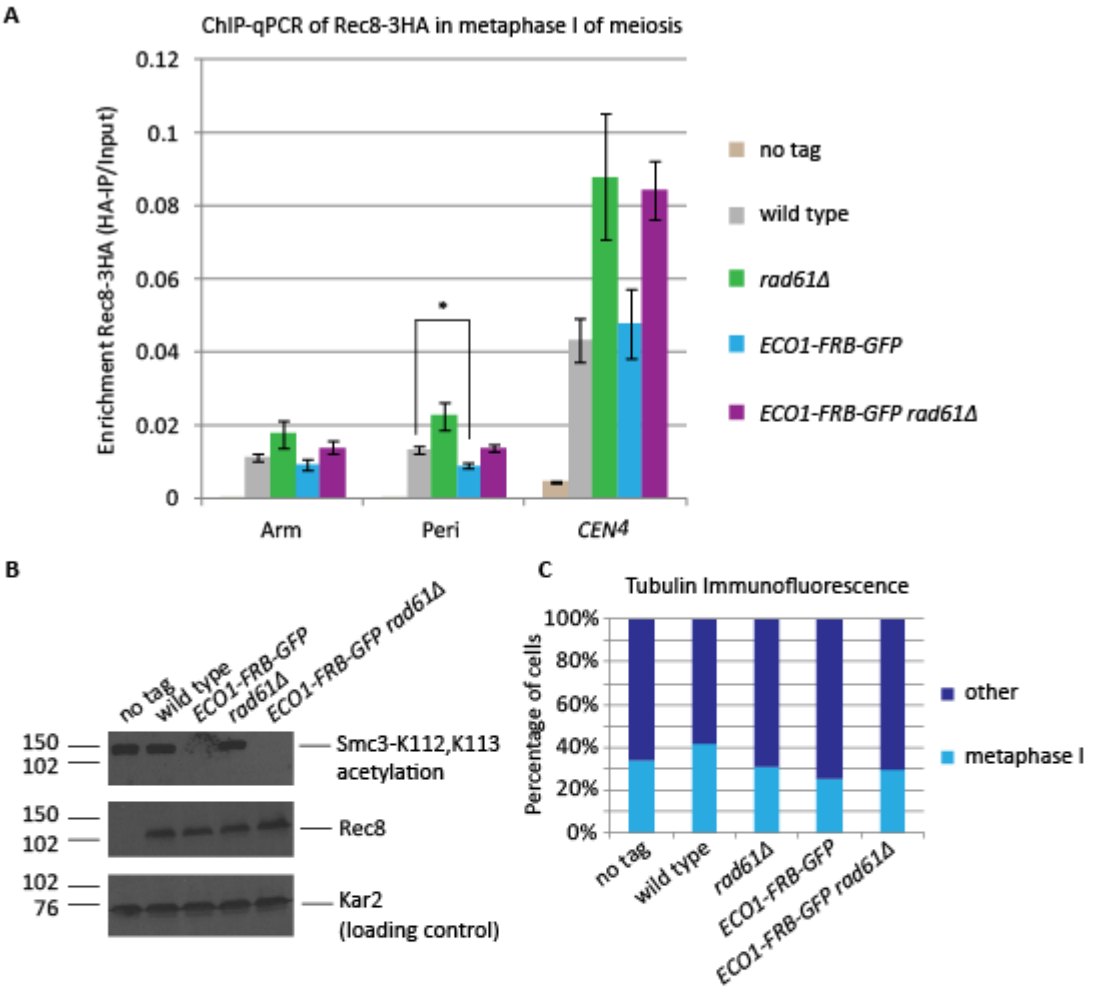

Figure 5.2.2.3: Anchoring away Eco1 does not cause an overall decrease in cohesin levels on the DNA in metaphase I

ChIP-qPCR of Rec8-3HA in metaphase I of meiosis, shows Rec8 localisation to chromatin does not depend significantly on Eco1 A) Strains containing Rec8-3HA were arrested in metaphase I of meiosis for 6 h using the *pCLB2-CDC20* arrest, in the presence of 1 µM rapamycin, before harvesting for ChIP-qPCR. ChIP for Rec8-3HA was carried out in wild type (24236), *rad61Δ* (24263), *ECO1-FRB-GFP* (24262) and *ECO1-FRB-GFP rad61Δ* (24261), as well as in a no tag background (24235), using 12CA5 antibody against 3HA. All strains used contained *SPO13-3FLAG* and *pCLB2-CDC20* in the genetic background. Average of 4 repeats for Arm, Peri and *CEN4*. Error bars show standard error. Paired student T test gave a p value=0.0106 for *ECO1-FRB-GFP* at the pericentromere. No other site or mutant was significantly increased or decreased in Rec8-3HA enrichment compared to wild type. B) Western blotting for Rec8-3HA, Smc3-K112,K113 acetylation and a loading control (Kar2) in the strains used for ChIP-qPCR. Western blot developed by ECL, using 12CA5 to probe against Rec8-3HA, homemade rabbit antibody against anti-Smc3-K112,K113 acetylation, and homemade rabbit anti-Kar2 for the loading control. No tag (24235), wild type (24236), *rad61Δ* (24263), *ECO1-FRB-GFP* (24262) and *ECO1-FRB-GFP rad61Δ* (24261) samples shown. C) Tubulin immunofluorescence for the metaphase I arrest of no tag (24235), wild type (24236), *rad61Δ* (24263), *ECO1-FRB-GFP* (24262) and *ECO1-FRB-GFP rad61Δ* (24261). Average of 4 repeats, n=200.

comparison to both wild type and *ECO1-FRB-GFP*. This overall increase in cohesin was not due to differences in Rec8 protein levels between strains, as by western immunoblot Rec8 levels were comparable between strains (Figure 5.2.2.3B), and a similar percentage of cells were arrested in metaphase I, as judged by spindle morphology (Figure 5.2.2.3C).

Overall, the ChIP-qPCR experiments in the *ECO1-FRB-GFP* anchor-away strains show a decrease, but not complete loss, of Rec8 from the chromatin. This reveals that in the absence of Eco1 acetyltransferase function, Rad61 can destabilise a greater proportion of cohesin from the DNA and that acetylated cohesin must be stably bound.

5.2.3 Eco1 function is important for sister chromatid cohesion in meiosis

The severe decrease in spore viability after tetrad dissection of *ECO1-FRB-GFP* and *ECO1-FRB-GFP rad61Δ* strains suggests that there may be gross chromosome missegregation in meiosis when the spores are generated. In the absence of cohesin acetylation the sister chromatids may prematurely separate, which would result in aneuploidy and cell death, and explain the loss of spore viability. I decided to analyse sister chromatid cohesion in the anchor-away strains through employing the heterozygous *CEN5 tetO*/TetR-GFP dot assay.

Diploid strains containing heterozygous *CEN5 tetO*/TetR-GFP dots and heterozygous Spc42-tdTomato, to mark spindle pole bodies (SPBs), were placed in sporulation media containing rapamycin, and live cell imaging carried out (Figure 5.2.3.1). The morphologies of the cells were then analysed throughout the 12 h live cell imaging experiment, with four categories for the mononucleate cells being observed (Figure 5.2.3.1A). In a wild type meiosis, one SPB and one GFP dot should be visualised in mononucleate cells until meiosis I, when the two SPBs segregate to opposite sides of the cell, with one GFP dot remaining closely associated to one of these poles (Figure 5.2.3.1A, C). In mononucleate cells, the observation of one SPB and one GFP dot occurred in over 90 % of wild type and *rad61Δ* strains, whereas under 80 % of cells containing *ECO1-FRB-GFP* had this pattern (Figure 5.2.3.1B). In over 30 % of *ECO1-FRB-GFP* anchor-away strains, two GFP dots were frequently visualised in strains with one SPB, showing that sister chromatids had prematurely separated in these cells (Figure 5.2.3.1A, B). Fewer cells containing *ECO1-FRB-GFP rad61Δ* had this morphology, although 11 % of cells arrested with two SPBs

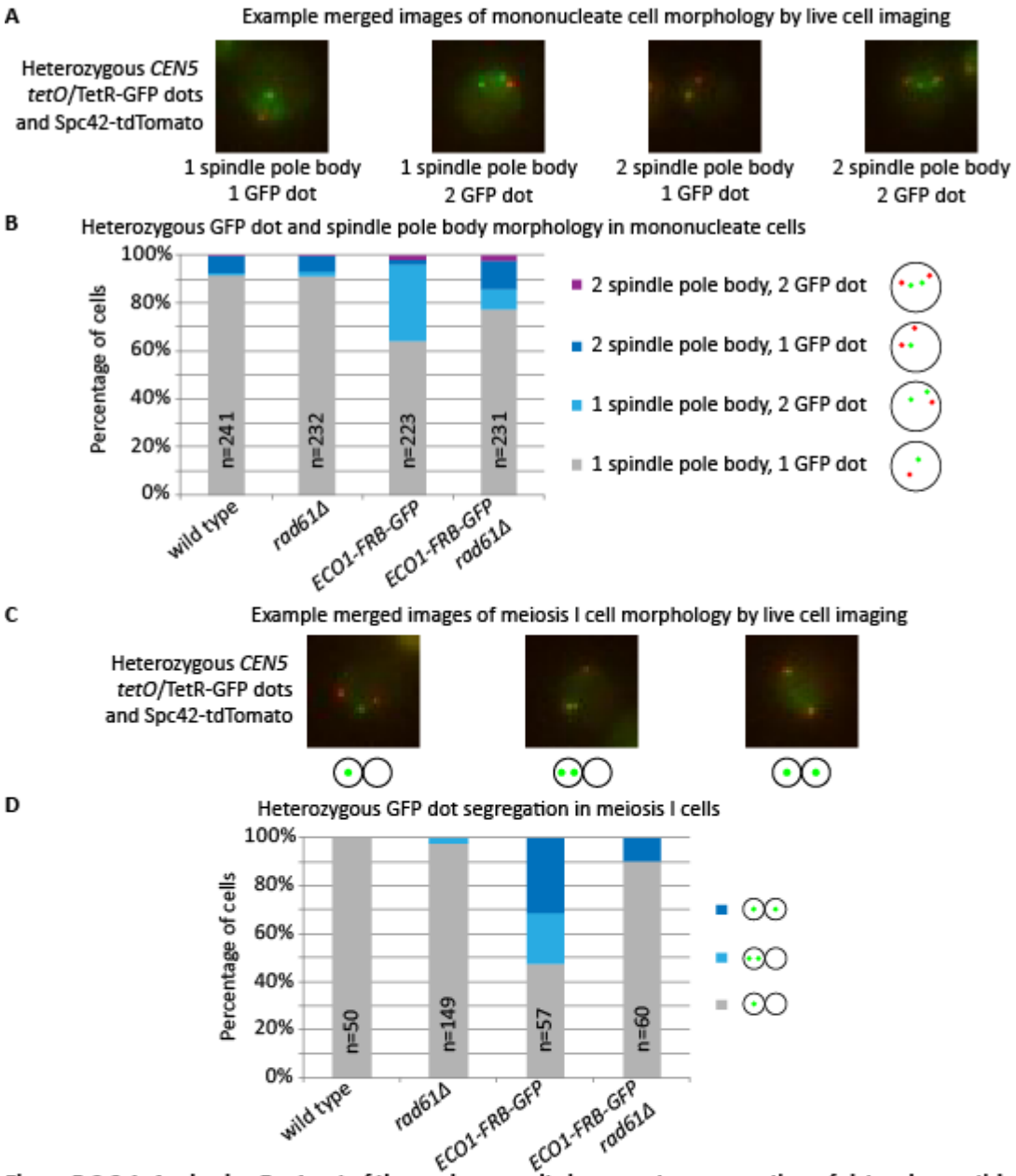

Figure 5.2.3.1: Anchoring Eco1 out of the nucleus results in premature separation of sister chromatids and a mono-orientation defect in meiosis I

A) Live cell imaging of cells containing heterozygous *CEN5 tetO*/TetR-GFP dots, and the fluorescently labelled spindle pole body component Spc42-tdTomato, allows sister chromatid cohesion and segregation in meiosis I to be visualised. Diploid strains were placed in sporulation media with 1µM rapamycin to induce meiosis, and live cell imaging carried out for 12 h, with Z-stack images taken every 15 min. Example images of the different morphologies of mononucleate cells from *ECO1-FRB-GFP* (24184), and *ECO1-FRB-GFP rad61Δ* (24169). In wild type, the sister chromatids remain cohesed when there is only one spindle pole body. However, in some circumstances other cell morphologies are visualised. B) Morphology of mononucleate cells as visualised by live cell imaging in wild type (24167), *rad61Δ* (24168), *ECO1-FRB-GFP* (24184), and *ECO1-FRB-GFP rad61Δ* (24169). Graph shown is the percentage of each phenotype, with number of cells analysed indicated on the graph. C) Example images of heterozygous *CEN5 tetO*/TetR-GFP dot segregation in cells which have two separated spindle pole bodies, indicating that cells have undergone meiosis I. D) Morphology of cells which have separated spindle pole bodies, and have undergone meiosis I, as visualised by live cell imaging in wild type (24167), *rad61Δ* (24168), *ECO1-FRB-GFP* (24184), and *ECO1-FRB-GFP rad61Δ* (24169). Graph shown is the percentage of each phenotype, with number of cells analysed indicated on the graph.

only slightly separated and one GFP dot (Figure 5.2.3.1A, B). The high incidence of two GFP dots prior to separation of SPBs shows that sister chromatids had prematurely come apart prior to metaphase I, and therefore that Eco1 activity is essential for sister chromatid cohesion in early meiosis.

As cells progress into anaphase I, the SPBs separate to opposite poles of the cell. Disappearance of the cell cycle stage marker Pds1-tdTomato is also an indicator of anaphase I progression, therefore in future this experiment will be repeated with this marker to ensure correct identification of anaphase I cells. However, in the wild type and *rad61Δ* strains, after separation of the two SPBs, one GFP dot segregated to one pole in over 97 % cells, compared to in less than 50 % of *ECO1-FRB-GFP* anchor-away strains (Figure 5.2.3.1C, D). Separation of the two GFP dots to opposite poles of the cell occurred in 31 % *ECO1-FRB-GFP* and 10 % *ECO1-FRB-GFP rad61Δ* strains, which is indicative of both a loss of cohesion and defective mono-orientation (Figures 4.2.2.4 and 5.2.3.1C, D). Therefore, Eco1 is important in meiosis for sister chromatid cohesion prior to meiosis I, and may have a role in promoting mono-orientation of sister chromatid kinetochores.

5.2.4 Chromosome missegregation in *spo13Δ* mutants is not due to loss of protection from the prophase pathway

At the end of prophase I, around 50-60 % of cohesin is destabilised from the chromatin, and depends on the phosphorylation of Rec8 (Challa *et al.*, 2019). Super resolution microscopy has revealed that the pericentromeric cohesin has a distinct structure to arm cohesin at the end of prophase (Challa *et al.*, 2019). It is crucial that at least some of this pericentromeric cohesin is protected from the end of prophase until anaphase II, to ensure that the sister chromatids do not prematurely separate, as this would result in aneuploidy. Spo13 has been identified as a cohesin-protector in meiosis I, due to complete loss of all cohesin during the first meiotic division in *spo13Δ* cells (Shonn, McCarroll and Murray, 2002; Lee, Kiburz and Amon, 2004; Katis *et al.*, 2004b). I wanted to determine if Spo13 could play a role in protecting cohesin from the destabilisation pathway.

I first aimed to compare the timing of cohesin cleavage and deacetylation in meiosis I between wild type and *spo13Δ* diploid strains. The *pGAL-NDT80* block/release time course protocol was utilised, in which cells are grown for 6 h into a late prophase arrest, before

synchronously releasing through the meiotic nuclear divisions by addition of β-estradiol. Samples were collected at the indicated times, protein extracts prepared, and both Rec8 and Smc3-K112,K113 acetylation levels analysed by western immunoblot for both wild type and *spo13Δ* (Figure 5.2.4.1A, C). In wild type, both the Rec8 and the Smc3-K112,K113 acetylation signals decreased as anaphase I occurred, as deduced from the tubulin morphology at this time point (Figure 5.2.4.1A, B). In the *spo13Δ* cells, metaphase I and anaphase I were delayed from comparison to the spindle morphology to wild type, as previously reported (Figure 5.2.4.1B, D) (Shonn, McCarroll and Murray, 2002; Katis *et al.*, 2004b). However, it was clear that there was acetylated Smc3 maintained between prophase and metaphase I, and therefore *spo13Δ* mutants did not prematurely lose cohesin acetylation before Rec8 cleavage (Figure 5.2.4.1C). Overall, the decrease in Smc3-K112,K113 acetylation in meiosis I is not obviously perturbed by western blotting in *spo13Δ*.

Spo13 binding sites on the chromatin have been shown to correspond to the sites of cohesin binding (Katis *et al.*, 2004b). I hypothesised that mislocalisation of Spo13 in *ECO1* mutants could contribute to the loss of sister chromatid cohesion. Spo13 is also essential for mono-orientation of sister chromatid kinetochores in meiosis I, and I reasoned that mislocalisation of Spo13 in *ECO1-FRB-GFP* anchor-away strains may be the cause of the mono-orientation defects visualised by live cell imaging of heterozygous *CEN5 tetO*/TetR-GFP dots (Figure 5.2.3.1). To test these ideas, I carried out ChIP of Spo13-3FLAG in the anchor-away strains, followed by qPCR for Spo13 enrichment at three chromosomal loci (Figure 5.2.4.2A). The cultures used for the ChIP were the same cultures used to ChIP Rec8-3HA in Figure 5.2.2.3, therefore direct comparisons can be made between Spo13 enrichment and Rec8 enrichment. Spo13 binding to all three loci was increased in both *rad61Δ* and *ECO1-FRB-GFP rad61Δ* double mutants, and although these increases were not significant (other than for *rad61Δ* at the pericentromere), the pattern reflected the slight increase in Rec8 binding to these loci (Figure 5.2.2.3A and 5.2.4.2A). In *ECO1-FRB-GFP* anchor-away strains, Spo13-FLAG was only significantly decreased at the pericentromere (Figure 5.2.4.2A). Western immunoblotting carried out on protein extracts from the Spo13-3FLAG ChIP cultures showed that Spo13 protein levels were comparable between strains, and analysis of spindle morphology by tubulin immunofluorescence showed all the strains were arrested in metaphase I to similar levels (Figure 5.2.4.2B, C). Therefore, Spo13 localisation is slightly decreased in *ECO1-FRB-GFP* anchor-away strains, but this is probably

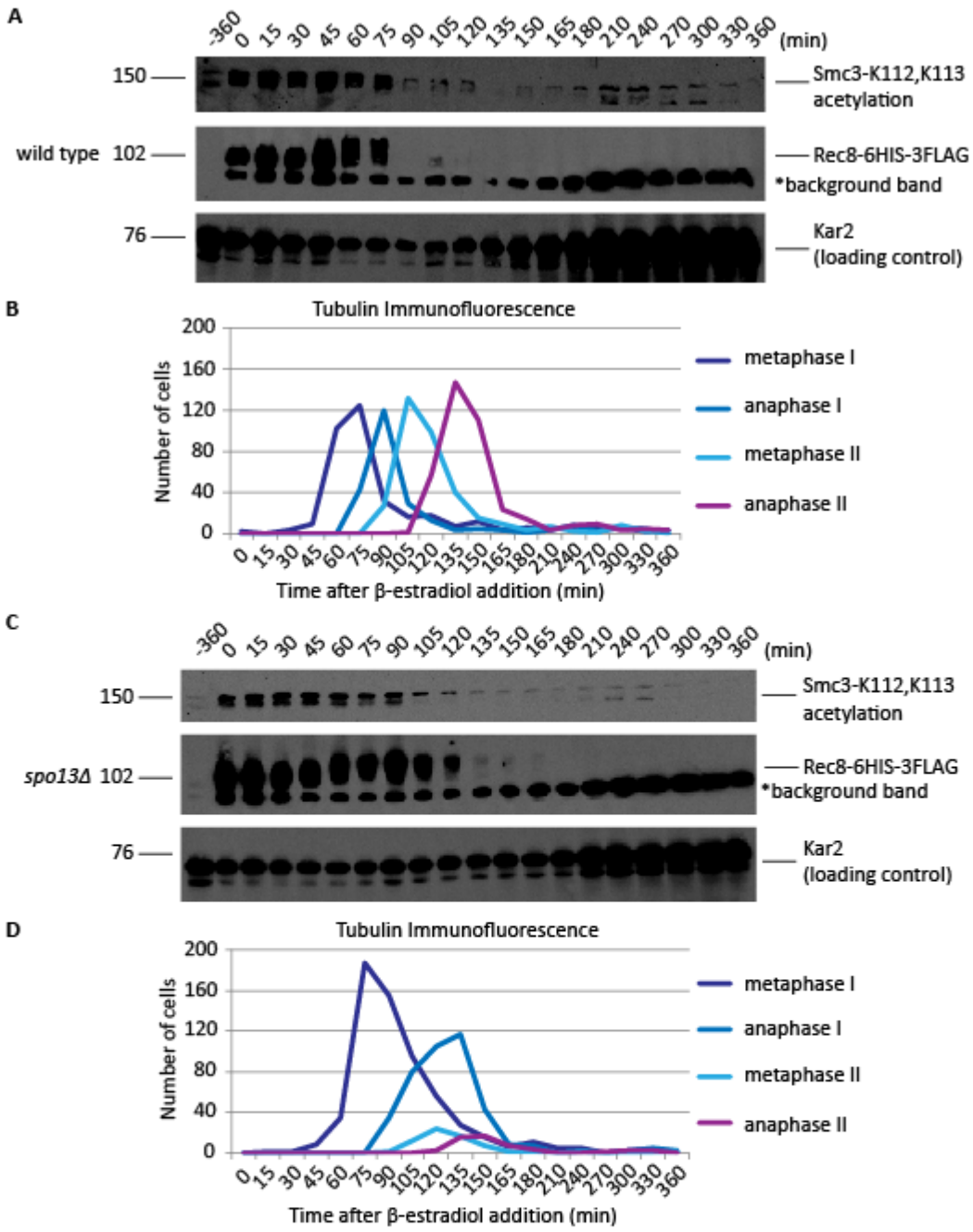

Figure 5.2.4.1: Smc3 acetylation decreases as cohesin is cleaved during meiosis I in *SPO13* mutants as in wild type

Wild type or *spo13Δ* diploid strains containing Rec8-6HIS-3FLAG and the *pGAL-NDT80* block/release genetic background were placed in sporulation media. After 6 h, 1 µM β-estradiol was added to induce *NDT80* expression, and allow progression into meiosis I and II. Samples were removed at the timepoints indicated for protein extracts and tubulin immunofluorescence. Western blotting was carried out by ECL using M2 FLAG antibody to probe against Rec8-6HIS-3FLAG, homemade rabbit anti-Smc3-K112,K113 acetylation antibody to probe for Smc3 acetylation, and homemade rabbit anti-KAR2 for the loading control. A) Protein extracts for wild type (16180) were run on an 8 % SDS-PAGE gel and western blotting carried out. B) After release from the *NDT80* arrest, cells were collected at each timepoint for tubulin immunofluorescence for wild type (16180, n=200 cells/time-point). C) Protein extracts for *spo13Δ* (19553) were run on an 8 % SDS-PAGE gel and western blotting carried out. D) After release from the *NDT80* arrest, cells were collected at each timepoint for tubulin immunofluorescence for *spo13Δ* (19553, n=200 cells/timepoint).

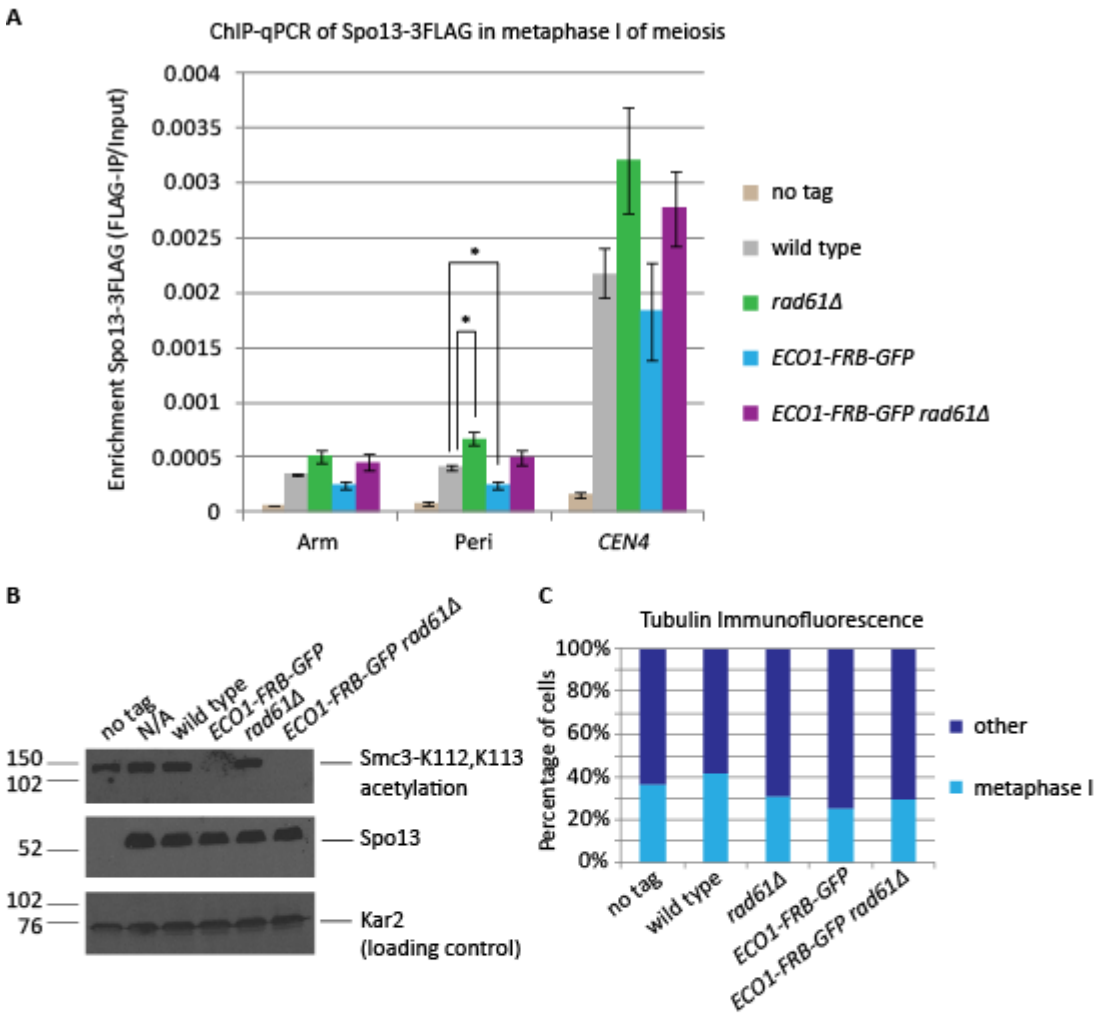

Figure 5.2.4.2: Anchoring away Eco1 has a slight effect on Spo13 localisation to the chromatin
ChIP-qPCR of Spo13-3FLAG in metaphase I of meiosis, shows Spo13 localisation to chromatin does not depend on Eco1 or Rad61 A) Strains containing Spo13-3FLAG were arrested in metaphase I of meiosis for 6 h using the *pCLB2-CDC20* arrest, in the presence of 1 µM rapamycin, before harvesting for ChIP-qPCR. ChIP for Spo13-3FLAG was carried out in wild type (24236), *rad61Δ* (24263), *ECO1-FRB-GFP* (24262) and *ECO1-FRB-GFP rad61Δ* (24261), as well as in a no tag background (24234), using M2 anti-FLAG antibody against 3FLAG. All strains used contained *REC8-3HA* and *pCLB2-CDC20* in the genetic background, and ChIP-qPCR of Rec8 is shown in Figure 5.2.2.3. Average of 4 repeats for Arm, Peri and *CEN4*. Error bars show standard error. Paired student T test gave a p value=0.0377 for *rad61Δ* and p value=0.0432 for *ECO1-FRB-GFP* at the pericentromere. No other site or mutant was significantly increased or decreased in Spo13-3FLAG enrichment compared to wild type. B) Western blotting for Spo13-3FLAG, Smc3-K112,K113 acetylation and a loading control (Kar2) in the strains used for ChIP-qPCR. Western blot developed by ECL, using M2 FLAG to probe against Spo13-3FLAG, homemade rabbit antibody against anti-Smc3-K112,K113 acetylation, and homemade rabbit anti-Kar2 for the loading control. No tag (24234), wild type (24236), *rad61Δ* (24263), *ECO1-FRB-GFP* (24262) and *ECO1-FRB-GFP rad61Δ* (24261) samples shown. C) Tubulin immunofluorescence for the metaphase I arrest of no tag (24234), wild type (24236), *rad61Δ* (24263), *ECO1-FRB-GFP* (24262) and *ECO1-FRB-GFP rad61Δ* (24261). Average of 4 repeats, n=200.

due to a decrease in cohesin levels at these loci (Figure 5.2.2.3A). I conclude that Spo13 localisation is not dependent on acetylated cohesin, but enrichment of Spo13 on the chromatin reflects levels of total cohesin binding.

In chromatin fractionation experiments of metaphase I cell extracts, some acetylated cohesin is observed in the supernatant (Challa *et al.*, 2019). In metaphase I, Rad61 may destabilise a pool of the cohesive cohesin from the DNA, and if this activity were to be unregulated, complete sister chromatid cohesion may be lost. To determine whether such a mechanism could account for complete loss of cohesion in *spo13Δ*, I performed ChIP of Rec8 in cells arrested in prophase I of meiosis using the *ndt80Δ* genetic background. However, Rec8 levels were not altered at two centromeres and one arm loci in *spo13Δ* compared to wild type (Figure 5.2.4.3A). There was a significant increase in cohesin enrichment at the centromeres in *spo13Δ rad61Δ* mutants at both *CEN* loci and in *rad61Δ* at *CEN4*, therefore confirming that Rad61 may contribute to destabilisation of cohesin at centromeres (Figure 5.2.4.3A). Western immunoblotting of protein extracts taken from the cultures used for ChIP-qPCR confirmed that this increase in cohesin was not due to obvious differences in cohesin levels in the cell extracts (Figure 5.2.4.3B).

Deletion of *SPO13* did not cause an obvious decrease in chromatin-bound cohesin at the loci analysed in prophase I. However, the destabilisation pathway activity is stimulated by Cdc5-dependent phosphorylation of both Rec8 and Rad61 in late prophase (Yu and Koshland, 2005; Challa *et al.*, 2019). Spo13 may only protect against the destabilisation pathway after this activation has occurred, so levels of cohesin may only decrease after prophase I. ChIP of Rec8-3HA was carried out on cells in a *pCLB2-3HA-CDC20* arrest, followed by qPCR to determine cohesin enrichment at two centromeres and one arm loci (Figure 5.2.4.4A). Cohesin levels were not reduced in *spo13Δ* in comparison to wild type but were significantly increased at all loci tested in *rad61Δ* (Figure 5.2.4.4A). Cohesin levels were only significantly increased at *CEN4* in *spo13Δ rad61Δ* mutants, however by western blotting whole cell levels of Rec8-3HA were decreased in *spo13Δ rad61Δ* cell extracts, though this wasn't due to failure to enter meiosis as scoring of tubulin morphology revealed these mutants had a comparable metaphase I arrest when compared to the other strains (Figure 5.2.4.4B, C). The increased levels of cohesin in *RAD61* mutants again confirms that Rad61 can destabilise cohesin prior to metaphase I. Conversely, Spo13 does not have a role

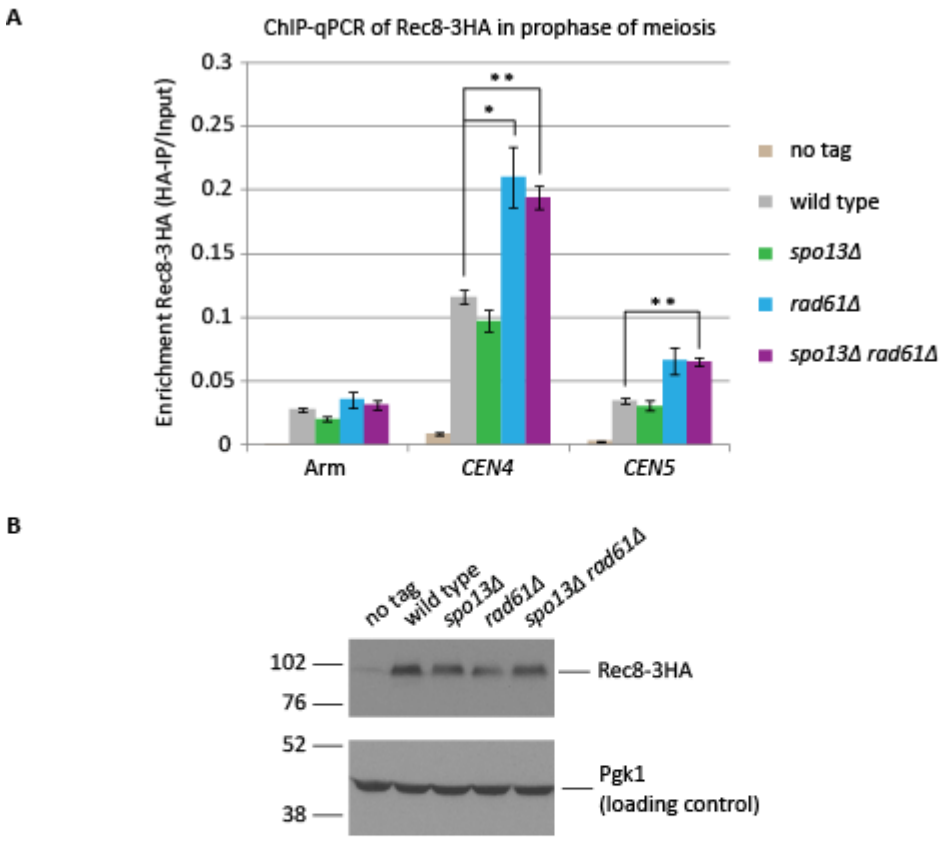

Figure 5.2.4.3: Cohesin levels in *spo13Δ* mutants are increased by deletion of *RAD61* in prophase
ChIP-qPCR of Rec8-3HA in prophase of meiosis shows cohesin levels in *spo13Δ* mutants are increased at centromeres by deletion of *RAD61* A) Diploid strains containing Rec8-3HA were placed sporulation media and grown for 6 h into a *ndt80Δ* prophase arrest, before harvesting for ChIP-qPCR. ChIP for Rec8-3HA was carried out in wild type (4015), *spo13Δ* (21261), *rad61Δ* (21147), and *spo13Δ rad61Δ* (21146), as well as in a no tag background (11633), using 12CA5 antibody against 3HA. Average of 4 repeats for Arm, *CEN4*, and *CEN5*. Error bars show standard error. Paired Student T-test gave p values of *CEN4*=0.0288 for *rad61Δ*, and p values of *CEN4*=0.0021 and *CEN5*=0.0036 for *spo13Δ rad61Δ*. B) Western blotting for Rec8-3HA and a loading control (Pgk1) in the strains used for ChIP-qPCR. Western blot developed by ECL using HA11 to probe against Rec8-3HA, and homemade rabbit anti-PGK1 for the loading control. No tag (11633), wild type (4015), *spo13Δ* (21261), *rad61Δ* (21147), and *spo13Δ rad61Δ* (21146) samples shown.

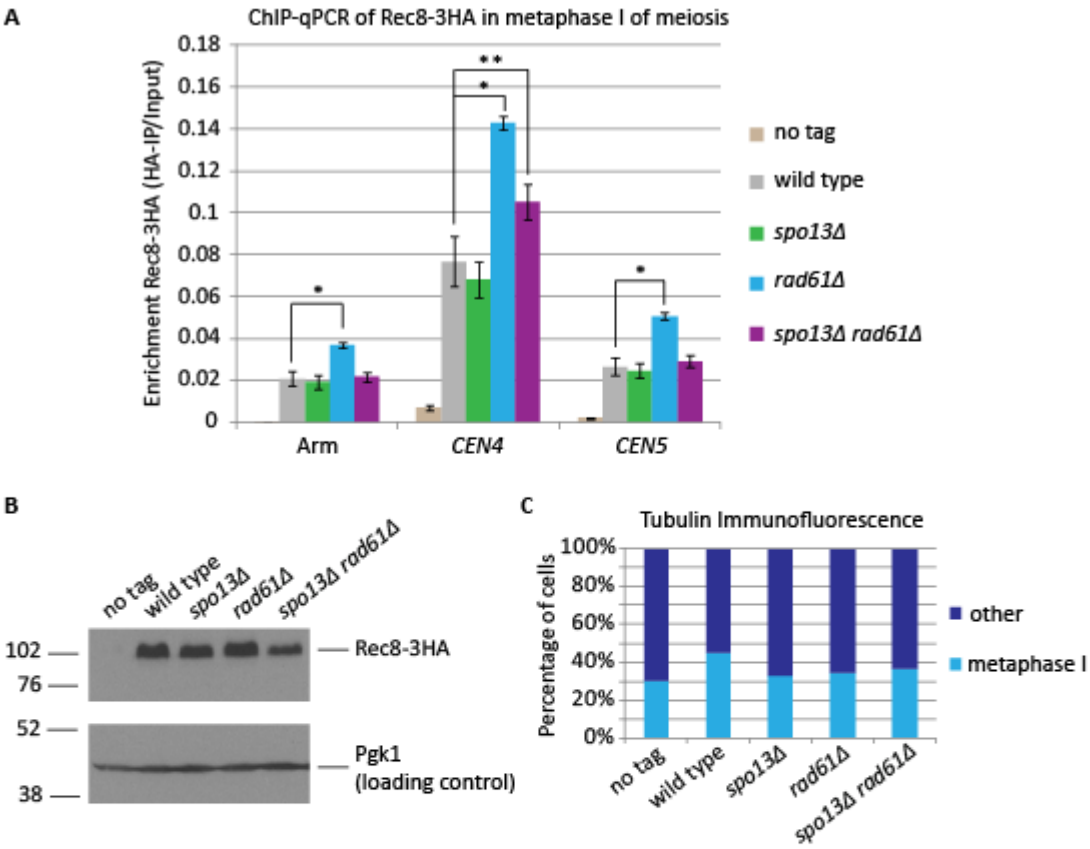

Figure 5.2.4.4: Cohesin levels in *spo13Δ* mutants are unaffected by deletion of *RAD61* in metaphase I of meiosis

ChIP-qPCR of Rec8-3HA in metaphase I of meiosis shows cohesin levels in *spo13Δ* mutants are unaffected by deletion of *RAD61* A) Diploid strains containing Rec8-3HA were placed sporulation media and grown for 6 h into a *pCLB2-3HA-CDC20* metaphase I arrest, before harvesting for ChIP-qPCR. ChIP for Rec8-3HA was carried out in wild type (3375), *spo13Δ* (21148), *rad61Δ* (21260), and *spo13Δ rad61Δ* (21232), as well as in a no tag background (3560), using 12CA5 antibody against 3HA. Average of 4 repeats for Arm, *CEN4*, and *CEN5*. Error bars show standard error. Paired Student T-test gave p values of Arm= 0.0272, *CEN4*=0.0114, and *CEN5*=0.0109 for *rad61Δ*, and *CEN4*=0.0047 for *spo13Δ rad61Δ*. B) Western blotting for Rec8-3HA and a loading control (Pgk1) in the strains used for ChIP-qPCR. Western blot developed by ECL using HA11 to probe against Rec8-3HA, and home-made rabbit anti-PGK1 for the loading control. No tag (3560), wild type (3375), *spo13Δ* (21148), *rad61Δ* (21260) and *spo13Δ rad61Δ* (21232) samples shown. C) Tubulin immunofluorescence for the metaphase I arrest of no tag (3560), wild type (3375), *spo13Δ* (21148), *rad61Δ* (21260) and *spo13Δ rad61Δ* (21232). Average of 4 repeats, n=200.

in cohesin maintenance on the DNA prior to anaphase I, and does not protect cohesin from destabilisation by Rad61.

ChIP-qPCR of cohesin in both prophase and metaphase I showed a significant increase in Rec8 at centromeric loci in *spo13Δ rad61Δ* mutants compared to wild type (Figures 5.2.4.3 and 5.2.4.4). I decided to test whether this increase in cohesin levels could rescue the cohesion defects of *SPO13* mutants in anaphase I. *SPO13* mutants have defects in both mono-orientation and sister chromatid cohesion in meiosis I, therefore to assay for loss of cohesion in anaphase I, live cell imaging of heterozygous *CEN5 tetO*/TetR-GFP dots was carried out as previously described in Figure 4.2.2.4. The timing of anaphase I can be deduced by the disappearance of nuclear Pds1-tdTomato signal and segregation of two Spc42-tdTomato SPB foci to opposite poles of the cell. In wild type and *rad61Δ* mutants, the majority of anaphase I cells have one GFP foci at this time in meiosis (Figure 5.2.4.5A). In contrast, nearly 50 % of *spo13Δ* cells displayed split GFP foci of which 35 % were separated more than 2 µM, indicative of both a loss of sister chromatid cohesion and mono-orientation defects (S. Galander, unpublished data) (Figure 5.2.4.5A). If this was caused by Rad61-dependent cohesin destabilisation, deletion of *RAD61* would be expected to decrease the proportion of cells with GFP dots separated to a distance of greater than 2 µM, however this was not the case. I observed that 64 % of *spo13Δ rad61Δ* mutants cells had two GFP dots separated to a distance of over 2 µM (Figure 5.2.4.5A). Therefore, loss of sister chromatid cohesion in meiosis I in *SPO13* mutants is not due to the precocious centromeric cohesin destabilisation activity by Rad61.

5.2.5 The Sgo1-cohesin interaction is maintained in *spo13Δ*

Sgo1-PP2A protects the pericentromeric region of cohesin from cleavage by separase in anaphase I of meiosis, and loss of Sgo1 causes complete loss of sister chromatid cohesion during meiosis I (Katis *et al.*, 2004a; Kitajima, Kawashima and Watanabe, 2004; Marston *et al.*, 2004; Kiburz *et al.*, 2005; Brar *et al.*, 2006; Riedel *et al.*, 2006; Xu *et al.*, 2009; Katis *et al.*, 2010). Similarly, mutants of *SPO13* also have complete loss of sister chromatid cohesion in meiosis I (Shonn, McCarroll and Murray, 2002; Lee, Kiburz and Amon, 2004; Katis *et al.*, 2004b). Recent unpublished data has shown that Sgo1 localisation to the pericentromeric region is not perturbed in *spo13Δ*, both by live cell imaging of Sgo1-GFP and ChIP-seq of Sgo1 enrichment on the DNA (S. Galander, unpublished data). Therefore the loss of sister

A

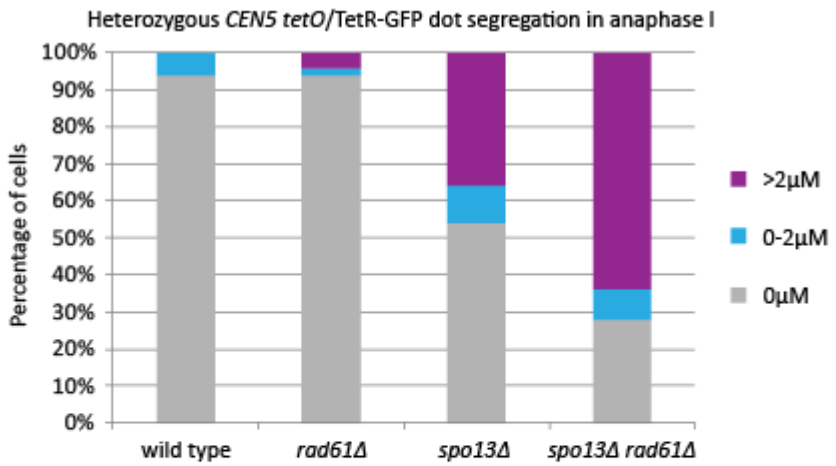

Figure 5.2.4.5: Sister chromatid cohesion defects of *spo13Δ* mutants are not rescued by deletion of *RAD61*

A) Measuring heterozygous *CEN5 tetO*/TetR-GFP dot separation by live cell imaging in anaphase I of meiosis, as shown previously in Figure 4.2.2.4. Diploid strains were placed in sporulation media to induce meiosis, and live cell imaging carried out for 12 h, with Z-stack images taken every 15 min. Separation of *CEN5 tetO*/TetR-GFP dots was then measured using ImageJ. Percentage of each category shown for wild type (15190, n=50), *rad61Δ* (21068, n=50), *spo13Δ* (20146, n=50) and *spo13Δ rad61Δ* (21358, n=50).

chromatid cohesion in *SPO13* mutants is unlikely to be due to a loss of centromeric localisation of Sgo1.

In a previous investigation, I purified Sgo1-6HIS-3FLAG from cells arrested in metaphase I of meiosis, and trypsin digestion of the eluate from Sgo1-6HIS-3FLAG immunoprecipitation was carried followed by mass spectrometry analysis of the resulting peptides (Figure 2.2.3.2). In this experiment, many subunits of the cohesin complex were identified as co-immunoprecipitating with Sgo1, including Smc1, Smc3, Rec8, Pds5 and Scc3 (Figure 2.2.3.2C). This suggested that Sgo1 may directly bind to the cohesin complex, as in mammalian mitosis (Liu, Rankin and Yu, 2013). In *SPO13* mutants, it may be that the Sgo1-cohesin interaction is perturbed and prevents Sgo1-PP2A dephosphorylation of Rec8, but doesn't fully result in Sgo1 delocalisation from the centromeric region. I aimed to test this prediction by both co-immunoprecipitation and mass spectrometry experiments.

To carry out the co-immunoprecipitation of Sgo1 and Rec8, diploid wild type and *spo13Δ* strains containing *SGO1-6HIS-3FLAG* and *REC8-3HA* were grown for 6 h into a *pGAL-NDT80* prophase arrest and released into metaphase I before harvesting of the cells. Benzonase treatment of the cell lysate was carried out to release chromatin bound Sgo1, before purification of Sgo1-6HIS-3FLAG. The resulting eluate of the pull-down was run on an SDS-PAGE gel and western blotting carried out. This revealed that Sgo1 had been successfully pulled-down, and that Rec8 co-immunoprecipitated with Sgo1 from cell lysate both in wild type and *spo13Δ* meiotic cells (Figure 5.2.5.1A, B). Therefore this suggested that Spo13 was not important for the interaction between Sgo1 and cohesin.

However, the signal of the co-immunoprecipitated Rec8 on the western blot was only slightly stronger than the background band detected in the no tag control, and so this result may be due to non-specific binding (Figure 5.2.5.1A). To try to increase the yield and sensitivity of the Sgo1/Rec8 co-immunoprecipitation, the experiment was repeated with increased amount of cells grown, and analysis of the resulting immunoprecipitate by mass spectrometry. Wild type and *spo13Δ* diploid cells containing *SGO1-6HIS-3FLAG* were grown according to the same protocol as for the co-immunoprecipitation experiment and a scaled up purification of Sgo1-6HIS-3FLAG was carried out. A fraction of the eluate was run on an SDS-PAGE gel and silver-staining carried out (Figure 5.2.5.2A). However, Sgo1 was not

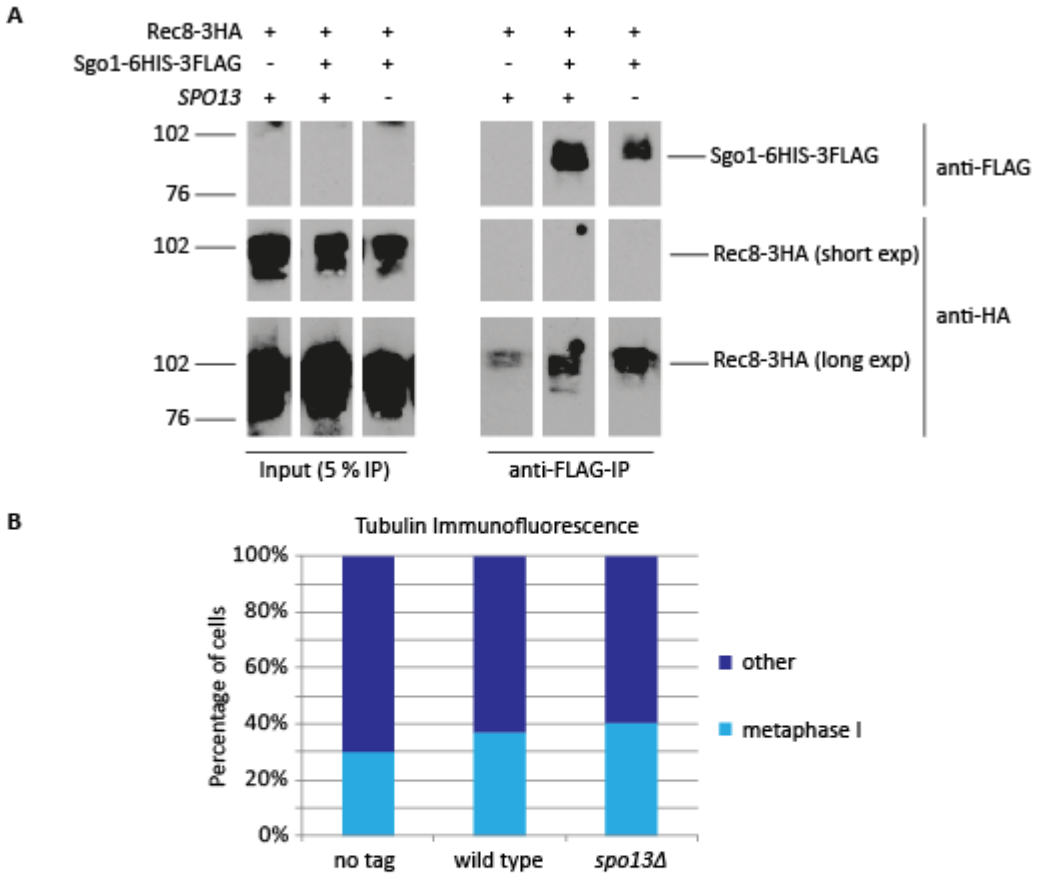

Figure 5.2.5.1: The interaction between Sgo1 and cohesin is maintained in *SPO13* mutants
A) Diploid strains were placed into sporulation media for 6 h into a *pGAL-NDT80* prophase arrest, before 1 µM β-estradiol was added to induce *NDT80* expression, and allow progression into meiosis I. Cells were harvested 1 h after addtion of β-estradiol; the time at which metaphase I occurs. Sgo1-6HIS-3FLAG was immunoprecipitated from 3 mg benzonase-treated cell lysate from no tag (18715), wild type (18716), and *spo13Δ* (18717) strains containing Rec8-3HA, using M2 FLAG antibody coupled to Protein G dynabeads. Sgo1-6HIS-3FLAG was eluted from the beads with 0.5 mg/ml FLAG peptide. After boiling, all eluate and 5 % INPUT was loaded onto an 10 % SDS-PAGE gel. Western blotting using M2 Flag and HA11 antibody showed that Rec8-3HA co-immunoprecipitated with Sgo1-6HIS-3FLAG in both wild type and *spo13Δ*. B) Tubulin immunofluorescence analysis of the metaphase I arrest of no tag (18715), wild type (18716), and *spo13Δ* (18717) (n=100 cells/strain).

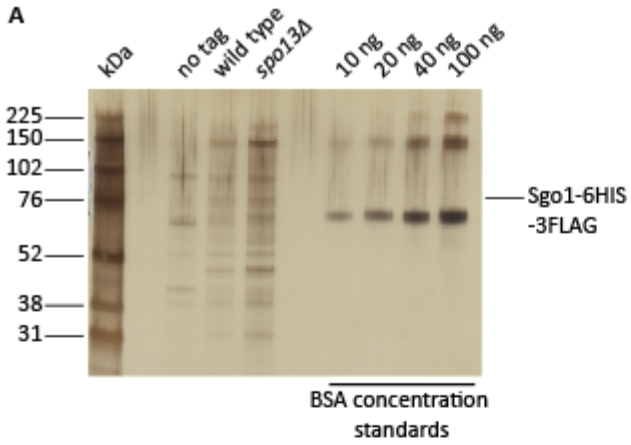

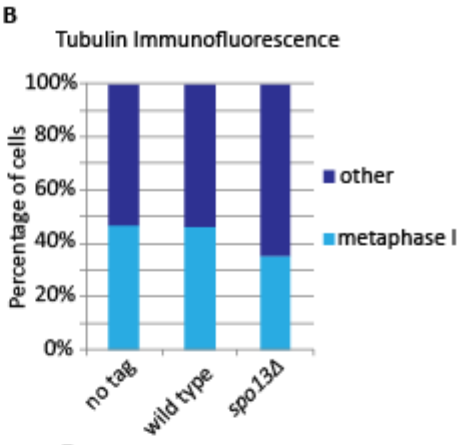

C

		Number of peptides			% coverage	
Protein group	**Protein**	**no tag**	**wild type**	***spo13Δ***	**wild type**	***spo13Δ***
Sgo1	Sgo1	0	40	46	53.1	59.2
PP2A	Rts1	0	21	21	33.0	28.3
	Tpd3	0	17	21	29.3	35.3
	Pph22	0	16	21	67.6	74.0
	Pph21	0	11	15	47.4	61.8
Cohesin	Pds5	1	64	86	46.7	56.0
	Smc1	0	55	68	50.7	59.6
	Scc3	0	43	55	40.7	47.3
	Smc3	0	42	54	38.5	53.2
	Rec8	0	17	28	27.2	43.2
Condensin	Ycs4	1	21	27	17.8	22.9
	Smc2	0	14	33	15.8	38.5
	Smc4	0	14	24	13.2	21.4
	Ycg1	0	14	16	18.3	22.6
	Brn1	0	7	12	10.1	17.6
Other	Spt16	0	47	44	49.2	46.7
	Isw1	0	45	59	43.3	54.3
	Pob3	0	18	19	35.7	48.2
	Cdc5	0	14	19	25.7	31.1

D

	Phosphorylation site	
Protein	**wild type**	***spo13Δ***
Cdc28	/	T169
Hho1	S173, S174	S174
Isw1	/	S175
Pds5	/	S13
Pph22	S56	T43, S57
Rec8	S314	S136, S314, S421
Rts1	T272	T257
Scc3	/	T27, S28, S34
Sgo1	S423, S518	S421, S487, S518

E

	Acetylation site	
Protein	**wild type**	***spo13Δ***
Pds5	/	10, 725, 965, 1129
Rts1	/	721
Scc3	/	340, 513
Sgo1	85, 124, 420, 485	71, 124, 420, 485
Smc3	112, 113	112, 113, 1023
Tpd3	60	60

Figure 5.2.5.2: Shugoshin and cohesin interact in metaphase I of meiosis in *spo13Δ* mutants
A) Diploid strains were placed into sporulation media for 6 h into a *pGAL-NDT80* prophase arrest, before 1 µM β-estradiol was added to induce *NDT80* expression, and allow progression into meiosis I. Cells were harvested 1 h after addition of β-estradiol; the time at which metaphase I occurs. Sgo1-6HIS-3FLAG was immunoprecipitated from benzonase-treated cell lysate of no tag (11189), wild type (17070) and *spo13Δ* (17071) using M2-FLAG coupled dynabeads. A silver stained 4-12 % Bis-Tris protein gel of the eluate from the purification of no tag (11189), wild type (17070) and *spo13Δ* (17071) was used to visualise the immunoprecipitate (10 % total eluate). BSA concentration standards of 10 ng, 20 ng, 40 ng and 100 ng were used. B) Tubulin immunofluorescence for the metaphase I arrest of no tag (11189), wild type (17070) and *spo13Δ* (17071) (n=200 cells/strain). C) Results of mass spectrometry after trypsin digestion of Sgo1-6HIS-3FLAG immunoprecipitate. Results were analysed using MAXQUANT. Shown is the number of peptides for each protein identified in no tag (11189), wild type (17070) and *spo13Δ* (17071), and the percentage of sequence coverage for each protein identified in wild type (17070) and *spo13Δ* (17071). D) Examples of phosphorylated Serine (S) and Threonine (T) residues identified by mass spectrometry of Sgo1-6HIS-3FLAG immunoprecipitation from wild type (17070) and *spo13Δ* (17071). E) Examples of acetylated residues identified by mass spectrometry of Sgo1-6HIS-3FLAG immunoprecipitation from wild type (17070) and *spo13Δ* (17071).

obvious by silver-staining, but the cells were arrested in metaphase I through analysis of spindle morphology by tubulin immunofluorescence scoring (Figure 5.2.5.2A, B). The remaining eluate was digested with trypsin and the resulting peptides analysed by mass spectrometry, confirming that Sgo1 and its known binding partner, PP2A, had been successfully purified (Figure 5.2.5.2C).

Additionally, the cohesin subunits Smc1, Smc3, Rec8, Pds5 and Scc3 were all identified by mass spectrometry in both the wild type and *spo13Δ* samples, showing that Sgo1 and cohesin do co-immunoprecipitate in *spo13Δ* mutants (Figure 5.2.5.2C). As only one repeat of the pull-down was carried out, the experiment was not quantitative, however, the interaction between Sgo1 and cohesin was at least partially maintained in the absence of Spo13. As previously seen, Sgo1 phosphorylation and acetylation sites were identified, however additional modified residues were also identified on several cohesin and PP2A subunits (Figure 2.2.3.2D, E and Figure 5.2.5.2D, E). Interestingly, Smc3-K112 and Smc3-K113 were identified in both the wild type and *spo13Δ* samples (Figure 5.2.5.2E). The presence of acetylated cohesin in the mass spectrometry shows that acetylated cohesin is present at the centromeric region in metaphase I of meiosis, and may be important for cohesion of the sister chromatids.

5.2.6 A possible relationship between Sgo1 and acetylated cohesin

The identification of peptides containing acetylated Smc3-K112,K113 by mass spectrometry of Sgo1 immunoprecipitate suggests that Sgo1 may bind to acetylated cohesin at the centromere in meiosis to ensure sister chromatid cohesion. This raised the possibility that Sgo1 selectively associates with acetylated cohesin and protects it from Rad61-mediated destabilisation. If this were the case, premature loss of acetylated cohesin may be expected to occur prior to anaphase I upon depletion of Sgo1. To test this idea I monitored Rec8 levels and Smc3-K112,K113 acetylation as wild type and *pCLB2-3HA-SGO1* cells progressed through meiosis. Diploid wild type and *pCLB2-3HA-SGO1* strains containing the *pGAL-NDT80* block/release construct were arrested in prophase after 6 h in sporulation media, before release through synchronous nuclear divisions. Samples of cell culture were collected at regular intervals for protein extracts, and western immunoblot carried out to analyse the timing of Rec8 cleavage in comparison to Smc3-K112,K113 acetylation. In both wild type and *pCLB2-3HA-SGO1*, Rec8 signal decreased at the time of anaphase I, as

deduced from spindle morphology, and this corresponded to a decrease in Smc3-K112,K113 acetylation levels (Figure 5.2.6.1). Smc3-K112,K113 acetylation was present in the prophase arrest in the *pCLB2-3HA-SGO1* time course, and levels did not visibly decrease until the time of Rec8 cleavage, suggesting that premature deprotection of acetylated cohesin had not occurred (Figure 5.2.6.1C).

To determine if Sgo1 could specifically bind to acetylated (i.e. cohesive) cohesin, which is presumably the most critical to protect, a co-immunoprecipitation of Sgo1 and Rec8 was carried out using the *ECO1-FRB-GFP* anchor-away strains. Co-immunoprecipitation of Sgo1-SZZ-TAP and Rec8-6HIS-3FLAG was carried out in metaphase-I arrested anchor-away strains containing *ECO1-FRB-GFP* both in the presence and absence of *RAD61* (Figure 5.2.6.2). The strains were grown for 7 h into a metaphase I arrest before harvesting and grinding of the cells. The cell lysate was treated with benzonase to release chromatin bound Sgo1, before incubation with IgG coupled to dynabeads to purify Sgo1-SZZ-TAP and interacting partners. The eluate was run on an SDS-PAGE gel and western blotting carried out (Figure 5.2.6.2A). The interaction between Sgo1 and Rec8 was not detected in the wild type strain, however Rec8 co-immunoprecipitated with Sgo1 in *rad61Δ* (Figure 5.2.6.2A). This may be due to the metaphase I arrest being very variable between all of the strains, as the percentage of cells arrested in metaphase I was much higher in *rad61Δ* than wild type, and *ECO1-FRB-GFP* strains arrested particularly poorly (Figure 5.2.6.2B). A weak band for Rec8-6HIS-3FLAG can be visualised in the *ECO1-FRB-GFP rad61Δ* double mutant pull-down lane, suggesting Sgo1 and cohesin may interact in the absence of Smc3 acetylation. Further experiments such as mass spectrometry of Sgo1 immunoprecipitate or live cell imaging of Sgo1-GFP will clarify this result.

Co-immunoprecipitation of Sgo1 and Rec8 in the *ECO1-FRB-GFP rad61Δ* double mutant showed that Sgo1 may weakly bind to cohesin in the absence of acetylation, however the result from this experiment was not very clear. To address if Sgo1 localisation to the centromeric region in metaphase I of meiosis depends on acetylation of cohesin, I decided to carry out ChIP of Sgo1 in the *ECO1-FRB-GFP* anchor-away strains. Sgo1 enrichment was analysed by qPCR at three different loci on chromosome IV in wild type and *ECO1-FRB-GFP* anchor-away strains (Figure 5.2.6.3A). All of the strains contained *REC8-6HIS-3FLAG* in the genetic background, therefore a wild type strain lacking *REC8-6HIS-3FLAG* was included

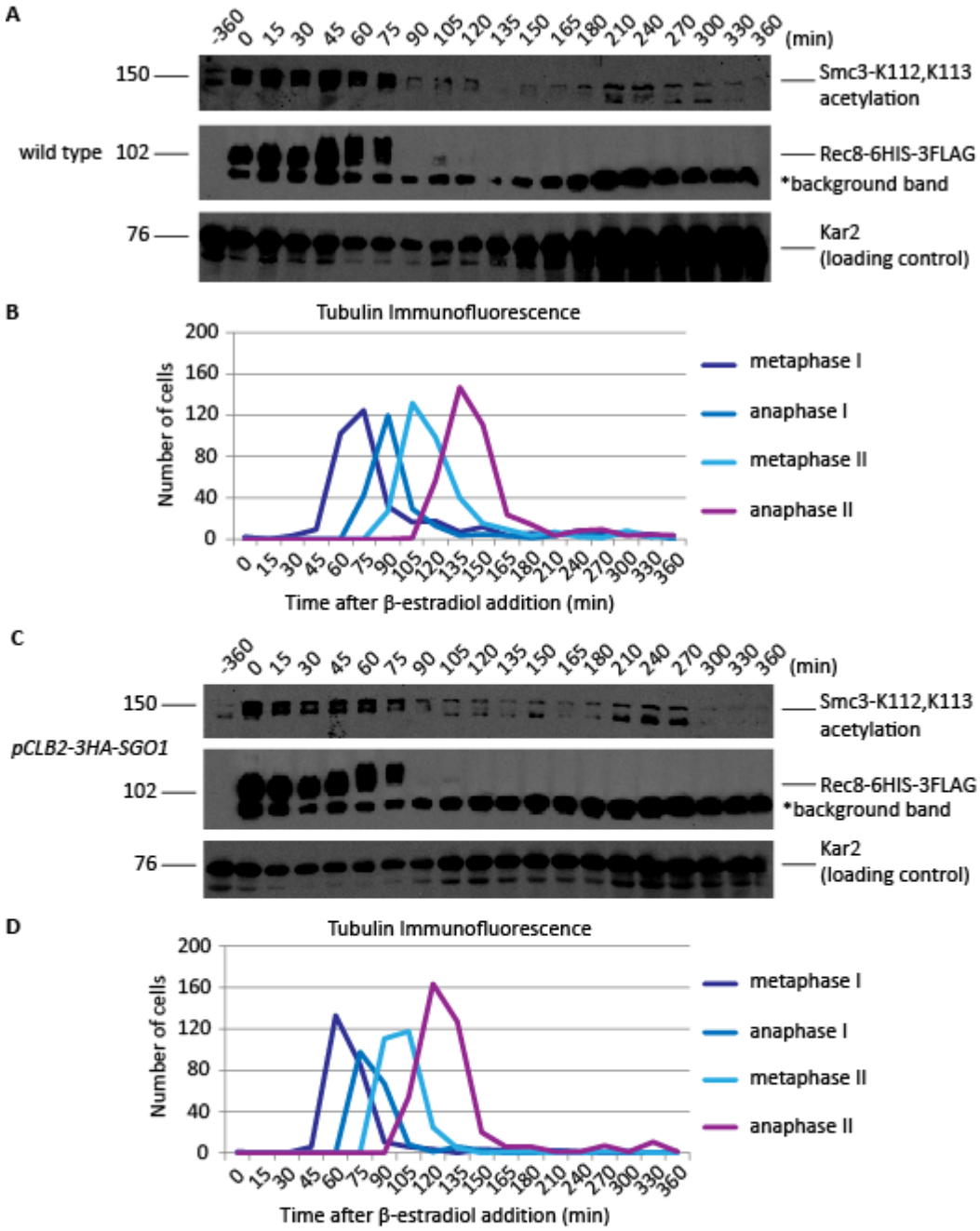

Figure 5.2.6.1: Smc3 acetylation decreases as cohesin is cleaved during meiosis I in *SGO1* mutants
Wild type or *pCLB2-3HA-SGO1* diploid strains containing Rec8-6HIS-3FLAG and the *pGAL-NDT80* block/release genetic background were placed in sporulation media. After 6 h, 1 μM β-estradiol was added to induce *NDT80* expression, and allow progression into meiosis I and II. Samples were removed at the timepoints indicated for protein extracts and tubulin immunofluorescence. Western blotting was carried out by ECL using M2 FLAG antibody to probe against Rec8-6HIS-3FLAG, home-made rabbit anti-Smc3-K112,K113 acetylation antibody to probe for cohesin acetylation, and home-made rabbit anti-KAR2 for the loading control. A) Protein extracts for wild type (16180) were run on an 8 % SDS-PAGE gel and western blotting carried out. B) After release from the *NDT80* arrest, cells were collected at each timepoint for tubulin immunofluorescence for wild type (16180, n=200 cells/-timepoint). C) Protein extracts for *pCLB2-3HA-SGO1* (23079) were run on an 8 % SDS-PAGE gel and western blotting carried out. D) After release from the *NDT80* arrest, cells were collected at each timepoint for tubulin immunofluorescence for *pCLB2-3HA-SGO1* (23079, n=200 cells/timepoint).

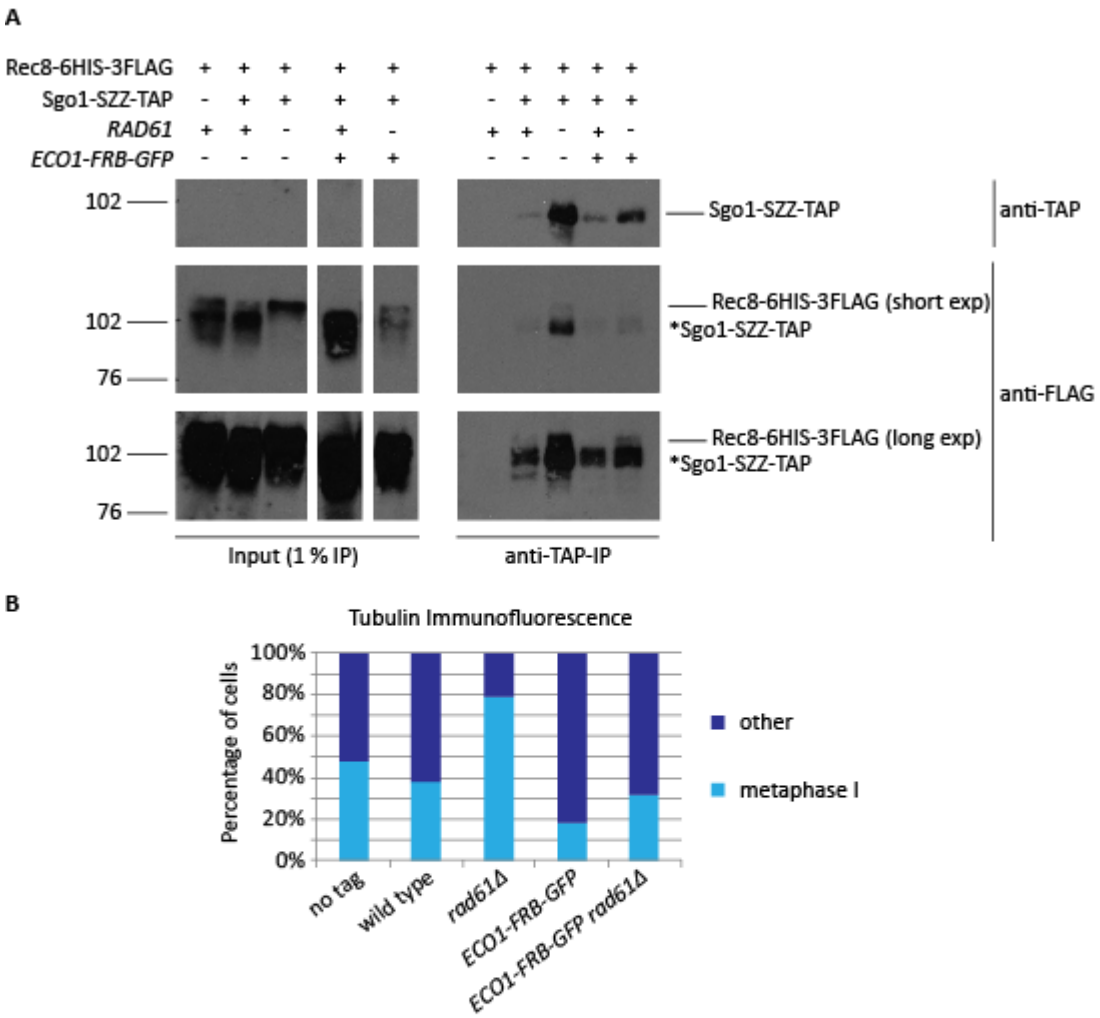

Figure 5.2.6.2: The interaction between Sgo1 and cohesin may be maintained in *ECO1-FRB-GFP rad61Δ* double mutants

A) Co-immunoprecipitation of Rec8-6HIS-3FLAG and Sgo1-SZZ-TAP from cells arrested in metaphase I of meiosis for 7 h in strains containing *ECO1-FRB-GFP* and *rad61Δ* in the presence of 1 µM rapamycin. Sgo1-SZZ-TAP was immunoprecipitated from 40 mg cell lysate of no tag (23701), wild type (25533), *rad61Δ* (25737), *ECO1-FRB-GFP* (25736) and *ECO1-FRB-GFP rad61Δ* (25684) containing Rec8-6HIS-3FLAG, using rabbit IgG coupled to epoxy-activated dynabeads. After boiling, all eluate and 1 % INPUT were loaded onto an 8 % SDS-PAGE gel. Western blotting using M2 Flag and TAP antibody showed that Rec8-6HIS-3FLAG co-immunoprecipitated with Sgo1-SZZ-TAP in metaphase I of meiosis, and the interaction was maintained in *ECO1-FRB-GFP rad61Δ*. B) Tubulin immunofluorescence for the metaphase I arrest of no tag (23701), wild type (25533), *rad61Δ* (25737), *ECO1-FRB-GFP* (25736) and *ECO1-FRB-GFP rad61Δ* (25684) (n=200 cells/strain).

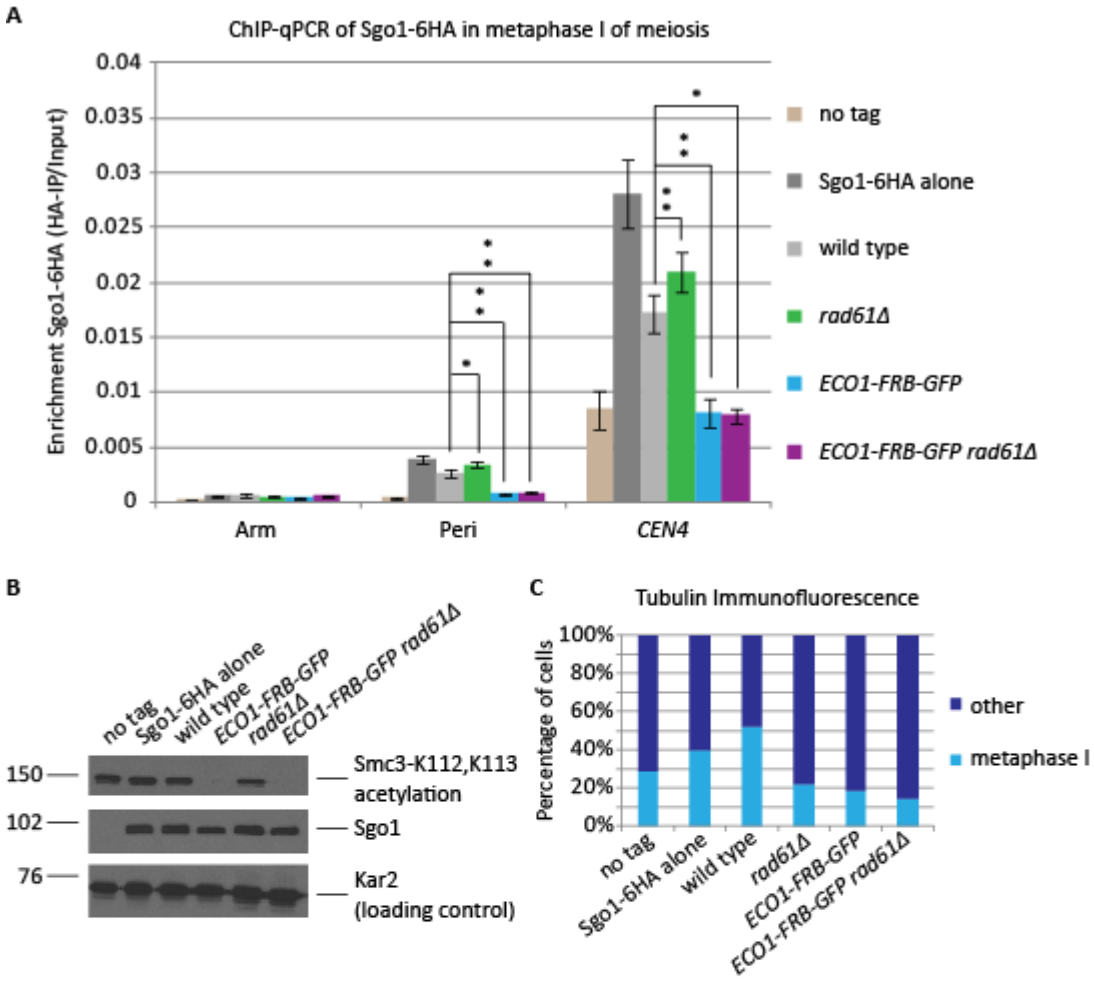

Figure 5.2.6.3: Anchoring away Eco1 causes delocalisation of Sgo1 from the centromere and pericentromere

ChIP-qPCR of Sgo1-6HA in metaphase I of meiosis, shows Sgo1 is delocalised from the centromere and pericentromere when Eco1 is anchored out of the nucleus A) Strains containing Sgo1-6HA were arrested in metaphase I of meiosis for 6 h using the *pCLB2-CDC20* arrest, in the presence of 1 μM rapamycin, before harvesting for ChIP-qPCR. ChIP for Sgo1-6HA was carried out in wild type (24055), *rad61Δ* (24057), *ECO1-FRB-GFP* (24264) and *ECO1-FRB-GFP rad61Δ* (24056), as well as in a no tag background (23701), using 12CA5 anti-HA antibody. All strains used contained *REC8-6HIS-3FLAG* in the genetic background, therefore the strains labelled "Sgo1-6HA alone" was used as a wild type which did not contain *REC8-6HIS-3FLAG* (24054). Average of 5 repeats for Arm, Peri and *CEN4*. Error bars show standard error. Paired student T test gave p values of Peri=0.0069 and *CEN4*=0.0037 for *ECO1-FRB-GFP,* Peri=0.0033 and *CEN4*=0.0102 for *rad61Δ*, and Peri=0.0471 and *CEN4*=0.0063 for *ECO1-FRB-GFP rad61Δ*. B) Western blotting for Sgo1-6HA, Smc3-K112,K113 acetylation and a loading control (Kar2) in the strains used for ChIP-qPCR. Western blot developed by ECL, using 12CA5 to probe against Sgo1-6HA, homemade rabbit antibody against anti-Smc3-K112,K113 acetylation, and homemade rabbit anti-Kar2 for the loading control. No tag (23701), Sgo1-6HA alone (24054), wild type (24055), *rad61Δ* (24057), *ECO1-FRB-GFP* (24264) and *ECO1-FRB-GFP rad61Δ* (24056) samples shown. C) Tubulin immunofluorescence for the metaphase I arrest of no tag (23701), Sgo1-6HA alone (24054), wild type (24055), *rad61Δ* (24057), *ECO1-FRB-GFP* (24264) and *ECO1-FRB-GFP rad61Δ* (24056). Average of 5 repeats, n=200.

"Sgo1-6HA alone". Sgo1 enrichment in the "Sgo1-6HA alone" strain was higher at both the pericentromere and *CEN4* compared to in the wild type anchor-away strain, suggesting that the presence of Rec8-6HIS-3FLAG disrupted Sgo1 localisation to the chromatin. By western blotting Sgo1 levels were comparable between the two strains, and the metaphase I arrest was actually poorer in the "Sgo1-6HA alone" strain (Figure 5.2.6.3B, C). Comparison of the strains containing *ECO1-FRB-GFP* and *ECO1-FRB-GFP rad61Δ* to the wild type anchor-away strain, showed a significant reduction of Sgo1 enrichment at the pericentromere and *CEN4* down to no tag levels (Figure 5.2.6.3A). This suggests that Sgo1 localisation to the pericentromeric and centromeric regions may depend upon Eco1 activity, and therefore potentially on acetylated cohesin.

However, the diploid strains used to carry out the ChIP of Sgo1-6HA in the *ECO1-FRB-GFP* anchor-away strains also contained tagged *REC8-6HIS-3FLAG* in the strain background. I was concerned that the tags on Rec8 and Sgo1 may both slightly impair protein function, which when in the *ECO1-FRB-GFP rad61Δ* mutant background, may lead to an additive effect that could disrupt Sgo1 localisation. I repeated the ChIP of Sgo1-6HA in the *ECO1-FRB-GFP* anchor-away strains that were arrested in metaphase I using *pCLB2-CDC20*. Analysis of Sgo1-6HA enrichment at three different centromeric loci by qPCR revealed that Sgo1 was significantly enriched in *rad61Δ* mutants at all centromeric loci tested (Figure 5.2.6.4A). In the *ECO1-FRB-GFP* anchor-away strain, Sgo1 enrichment was decreased at all centromeric loci, although this was only significant at *CEN4*. Interestingly, Sgo1 enrichment at the centromeric loci was rescued by *RAD61* deletion in the *ECO1-FRB-GFP* mutant to above wild type levels, in contrast to in the ChIP of Sgo1-6HA in the *REC8-6HIS-3FLAG* strains in which Sgo1 enrichment was significantly decreased to near no tag levels (Figures 5.2.6.3A and 5.2.6.4A). By western blotting Sgo1 levels were comparable between the all of the strains, apart from in the *ECO1-FRB-GFP* anchor-away strain that showed slightly reduced Sgo1 levels (Figure 5.2.6.4B). By immunofluorescence for tubulin, the efficiency of metaphase I arrest was found to similar in all strains, apart from in the *ECO1-FRB-GFP* anchor-away strain in which the arrest was less efficient (Figure 5.2.6.4C). Overall, Sgo1 localisation is impaired in the *ECO1-FRB-GFP* anchor-away strain, but not in the *ECO1-FRB-GFP rad61Δ* mutant, suggesting that Sgo1 localisation does not rely on cohesin acetylation, but instead corresponds to cohesin enrichment in these mutants (Figure 5.2.2.3A).

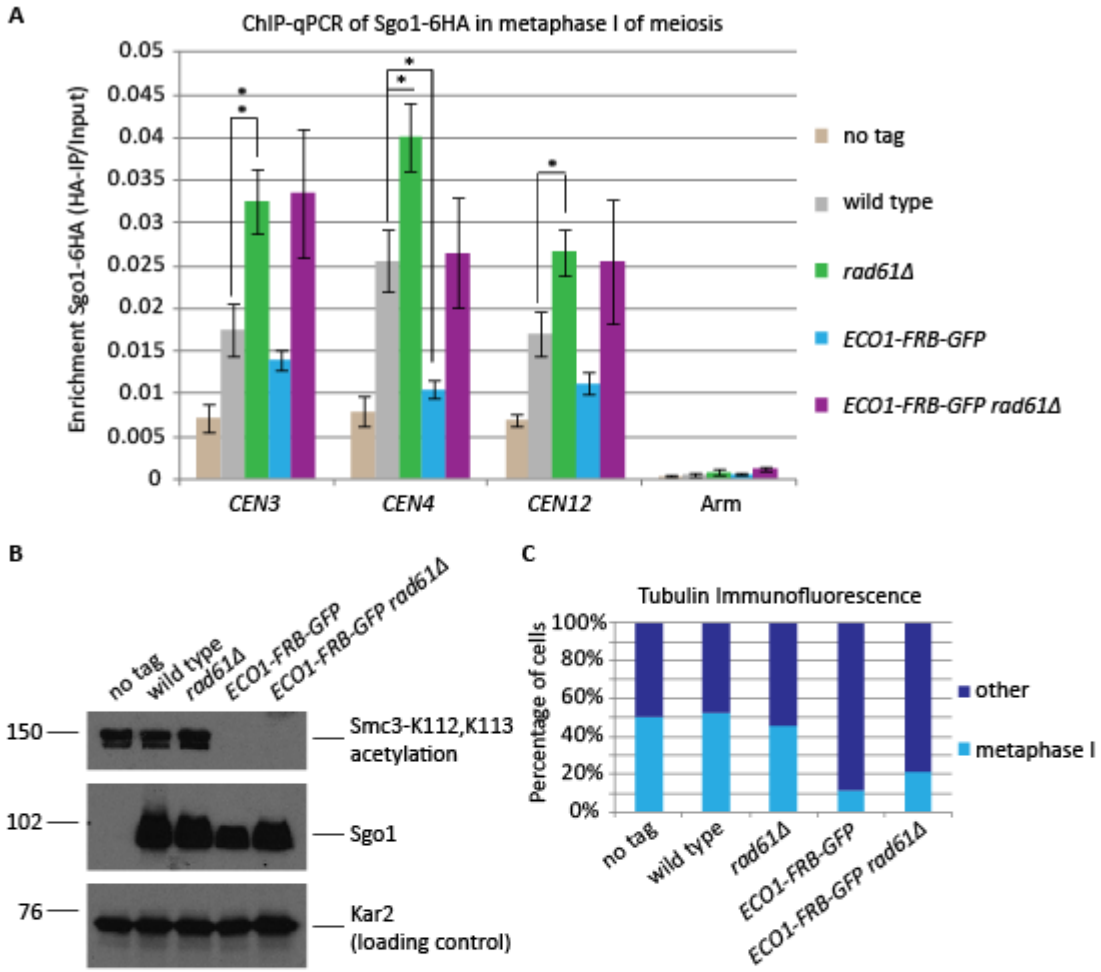

Figure 5.2.6.4: Anchoring away Eco1 causes delocalisation of Sgo1 from the centromere and pericentromere, but only in the presence of Rad61

ChIP-qPCR of Sgo1-6HA in metaphase I of meiosis, shows Sgo1 is partially delocalised from the centromere when Eco1 is anchored out of the nucleus A) Strains containing Sgo1-6HA were arrested in metaphase I of meiosis for 6 h using the *pCLB2-CDC20* arrest, in the presence of 1 µM rapamycin, before harvesting for ChIP-qPCR. ChIP for Sgo1-6HA was carried out in wild type (24054), *rad61Δ* (25103), *ECO1-FRB-GFP* (25104) and *ECO1-FRB-GFP rad61Δ* (25102), as well as in a no tag background (23700), using 12CA5 anti-HA antibody, and the following qPCR carried out using LUNA. Average of 4 repeats for *CEN3, CEN4, CEN12*, and Arm. Error bars show standard error. Paired student T test gave p values of *CEN4*=0.0427 for *ECO1-FRB-GFP,* and *CEN3*=0.0060, *CEN4*=0.0160 and *CEN12*=0.0403 for *rad61Δ*. B) Western blotting for Sgo1-6HA, Smc3-K112,K113 acetylation and a loading control (Kar2) in the strains used for ChIP-qPCR. Western blot developed by ECL, using 12CA5 to probe against Sgo1-6HA, homemade rabbit antibody against anti-Smc3-K112,K113 acetylation, and homemade rabbit anti-Kar2 for the loading control. No tag (23700), wild type (24054), *rad61Δ* (25103), *ECO1-FRB-GFP* (25104) and *ECO1-FRB-GFP rad61Δ* (25102) samples shown. C) Tubulin immunofluorescence for the metaphase I arrest of no tag (23700), wild type (24054), *rad61Δ* (25103), *ECO1-FRB-GFP* (25104) and *ECO1-FRB-GFP rad61Δ* (25102). Average of 4 repeats, n=200.

5.3 Discussion

5.3.1 Acetylation of cohesin by Eco1 is essential for sister chromatin cohesion in meiosis

In the budding yeast mitotic cell cycle, Eco1 acetylates Smc3-K112,K113 during S phase to establish the cohesion between the sister chromatids that is essential for faithful chromosome segregation (Rolef Ben-Shahar *et al.*, 2008; Unal *et al.*, 2008; Zhang *et al.*, 2008b; Rowland *et al.*, 2009; Sutani *et al.*, 2009; Beckouet *et al.*, 2010; Lopez-Serra *et al.*, 2013; Guacci *et al.*, 2015). In this investigation I employed the anchor-away technique to study Eco1 function in budding yeast meiosis (Haruki, Nishikawa and Laemmli, 2008). Eco1 was found to acetylate Smc3-K112,K113 during meiotic S phase, the majority of which was maintained until the first meiotic division, suggesting that acetylated Smc3 may form part of the pool of cohesive cohesin in meiosis I that is released only upon cohesin cleavage. The evidence presented in this study however, suggests that this acetylated cohesin may also be important for centromeric cohesion, and that Eco1 may play an additional role in mono-orientation. It is likely that cohesin acetylation is also important for cohesion of chromosome arms, which in future will be assayed using GFP dots located on the sister chromatid arms.

Disruption of Eco1 function resulted in considerable loss of spore viability and gross DNA missegregation, indicative of severe chromosome missegregation during the meiotic divisions. Analysis of sister chromatid cohesion in *ECO1-FRB-GFP* strains by live cell imaging of heterozygous GFP dots revealed that there was premature loss of sister chromatid cohesion prior to the first meiotic division in 30 % of cells analysed. Therefore, loss of Eco1 function resulted in a failure to maintain, if not also to establish, cohesion after meiotic S phase. Live cell imaging of heterozygous GFP dots in *smc3-K112R,K113R* mutants will reveal if this is due to a failure to acetylate cohesin. In a previous study, *SMC3* mutants separated sister chromatids in around 50 % of mononucleate cells during meiosis, and very few cells underwent the meiosis I nuclear division (and none meiosis II). Additionally, *rec8Δ* cells also exhibited a similar morphology of premature GFP dot segregation, although a higher percentage of cells underwent meiosis (Klein *et al.*, 1999). The similarity between these cohesin mutants and the *ECO1-FRB-GFP* anchor-away strains strongly suggests that the phenotype of *ECO1-FRB-GFP* anchor-away strains is due to a failure to acetylate Smc3 that results in loss of cohesin function. Overall, Smc3 is a substrate of Eco1 in meiosis, as in

mitosis, but there may be additional targets of Eco1 that also promote faithful chromosome segregation.

ChIP-qPCR of Rec8 in *ECO1-FRB-GFP* anchor-away strains revealed that, although there was a significant decrease in levels of chromatin-bound Rec8, this was variable, and overall there was at least half of the cohesin bound to the DNA as in wild type. Direct comparison between *ECO1-FRB-GFP* anchor-away strains and *SMC3* mutants has not been carried out in this study, but comparison to the results presented in (Klein *et al.*, 1999) suggests that the *ECO1-FRB-GFP* anchor-away phenotype may not be as severe as the *smc3-42* temperature sensitive mutant (Klein *et al.*, 1999). This suggests that non-acetylated cohesin may play important functions during meiosis, such as in recombination and condensation. Therefore, the different pools of cohesin on the DNA may have distinct roles, and dissection of these functions will be a key point of study in the future.

In vegetative cells, deletion of the Wapl homologue, *RAD61*, rescues the inviability of *ECO1* mutants but does not rescue the cohesion defects (Rolef Ben-Shahar *et al.*, 2008; Unal *et al.*, 2008; Rowland *et al.*, 2009; Sutani *et al.*, 2009; Guacci and Koshland, 2012; Chan *et al.*, 2012; Lopez-Serra *et al.*, 2013; Guacci *et al.*, 2015; Bloom, Koshland and Guacci, 2018). Deletion of *RAD61* failed to rescue the inviability of *ECO1-FRB-GFP* spores, although the live cell imaging of heterozygous GFP dots showed that fewer cells separated sister chromatids prior to meiosis I in *ECO1-FRB-GFP rad61Δ* than in *ECO1-FRB-GFP* cells. The rescue of some sister chromatid cohesion may suggest that unacetylated cohesin can maintain a minor amount of cohesion, at least prior to microtubule attachment and application of spindle force. Additionally, *rad61Δ* rescues chromatin-bound cohesin levels in *ECO1-FRB-GFP* strains to wild type levels in both prophase and metaphase I arrested cells, suggesting that Rad61 can promote destabilisation of cohesin from the chromatin prior to prophase, as well as during the documented pathway between prophase and metaphase I (Yu and Koshland, 2005; Challa *et al.*, 2019).

Live cell imaging of heterozygous GFP dots in binucleate cells revealed over 30 % sister chromatid segregation in *ECO1-FRB-GFP* and 10 % in *ECO1-FRB-GFP rad61Δ* mutants, which is indicative of a mono-orientation defect as well as a sister chromatid cohesion defect in these strains. The Eco1 homologue in *S. pombe* has previously been implicated in

mono-orientation, due to an acetyltransferase function independent of cohesin acetylation (Kagami *et al.*, 2011). Further investigation is required to determine if this is a true mono-orientation defect, or just a consequence of defective sister chromatid cohesion during S phase. Decreased centromeric cohesin levels are also known to result in an increase in centromere-proximal cross-over events in meiosis (Vincenten *et al.*, 2015). Therefore, the increased occurrence of binucleate cells with one GFP dot in each nuclei in *ECO1* mutants may be due to decreased centromeric cohesin in these cells resulting in an increase in crossovers near the centromere.

Overall, this study has shed additional light on a growing body of evidence for the importance of the Eco1 acetyltransferase family for faithful chromosome segregation during meiosis throughout evolution (Kagami *et al.*, 2011; Bolanos-Villegas *et al.*, 2013; De *et al.*, 2014; Lu *et al.*, 2017; Lu *et al.*, 2018; Reichmann *et al.*, 2017).

5.3.2 Is there a mechanism for protection of acetylated cohesin at the centromere?

Increasing evidence is accumulating for the presence of a cohesin-destabilisation pathway in budding yeast meiosis that is comparable to the prophase pathway of cohesin removal in mammalian mitosis (Yu and Koshland, 2005; Challa *et al.*, 2019). The meiosis-specific nature of this pathway has been attributed to both the presence of the meiosis-specific cohesin subunit, Rec8, and the meiosis-specific activation of Rad61 by phosphorylation (Yu and Koshland, 2005; Challa *et al.*, 2019). Chromatin fractionation experiments in prophase and metaphase I showed that around half of cohesin is destabilised from the chromatin at the end of prophase I (Challa *et al.*, 2019).

In the mitotic cell cycle, acetylated cohesin is resistant to destabilisation by Rad61, however, in the meiotic chromatin fractionation experiments the majority of acetylated Smc3 was present in the soluble (non-chromatin bound) fraction by metaphase I (Lopez-Serra *et al.*, 2013; Challa *et al.*, 2019). A major caveat is that chromatin fractionation experiments are difficult to accurately carry out in budding yeast, but if true, the destabilisation of acetylated cohesin is intriguing for several reasons. One, is how acetylated cohesin is destabilised in meiosis but not in mitosis, and although this has simply been attributed to the increased "activation" of Rad61 through phosphorylation by DDK and Cdc5 it would be interesting to determine how phosphorylation causes this (Challa *et*

al., 2019). Two, is that removal of acetylated cohesin from the chromatin usually results in deacetylation by Hos1, and therefore this would be predicted to result in a decrease in acetylated cohesin levels, however in the synchronous meiotic time course experiments carried out in this study no decrease in acetylated cohesin was detected by western blotting (Beckouet *et al.*, 2010; Borges *et al.*, 2010; Xiong, Lu and Gerton, 2010; Li, Yue and Tanaka, 2017). Three, loss of acetylation of cohesin through anchoring Eco1 out of the nucleus results in a decrease of sister chromatid cohesion, therefore if acetylated cohesive cohesin was destabilised then this could be predicted to result in premature loss of cohesion before anaphase I. Analysis of GFP dots on the arms of the sister chromatids may reveal if these also separate prematurely upon anchoring-away Eco1.

A minor centromeric pool of cohesin is essential for maintenance of sister chromatid cohesion until meiosis II. Therefore the small pool of acetylated cohesin remaining on the chromatin in the metaphase I chromatin fractionation experiments may represent the centromeric cohesive cohesin (Challa *et al.*, 2019). This suggests that this pool of cohesin may be protected by one of the meiosis-specific cohesin protectors: Sgo1 or Spo13.

Spo13 localises to various regions along the chromosomes corresponding to sites of cohesin binding, as well as at the centromeric region (Katis *et al.*, 2004b). Deletion of *SPO13* results in deprotection of centromeric cohesin during meiosis I, therefore all of the cohesin is cleaved during the first meiotic division resulting in a mixed reductional and equational segregation of chromosome into binucleate cells (Klapholz and Esposito, 1980; Wang *et al.*, 1987; Hugerat and Simchen, 1993; Shonn, McCarroll and Murray, 2002; Lee, Kiburz and Amon, 2004; Katis *et al.*, 2004b). The mechanism by which Spo13 protects centromeric cohesin is not fully understood, however in this study deletion of *RAD61* failed to rescue the cohesion loss phenotype of *spo13Δ*, therefore Spo13 does not only protect centromeric cohesin from destabilisation by Rad61.

The shugoshin family of proteins are conserved throughout evolution and have a well-documented role in cohesin protection (Kerrebrock *et al.*, 1995; Katis *et al.*, 2004a; Kitajima, Kawashima and Watanabe, 2004; Marston *et al.*, 2004; Rabitsch *et al.*, 2004; Salic, Waters and Mitchison, 2004; McGuinness *et al.*, 2005). In mammalian mitosis, Sgo1-PP2A directly binds to centromeric cohesin and dephosphorylates both sororin and the SA2 subunit of

cohesin to protect centromeric cohesin from destabilisation by Wapl (Salic, Waters and Mitchison, 2004; Tang *et al.*, 2004; Hauf *et al.*, 2005; Kitajima *et al.*, 2005; McGuinness *et al.*, 2005; Kitajima *et al.*, 2006; Tang *et al.*, 2006; Dreier, Bekier and Taylor, 2011; Liu, Jia and Yu, 2013; Nishiyama *et al.*, 2013; Hara *et al.*, 2014). In budding yeast meiosis, Sgo1-PP2A also protects centromeric cohesin through dephosphorylation, however this has previously been thought to only be important for protection from cleavage by separase in anaphase I (Katis *et al.*, 2004a; Kitajima, Kawashima and Watanabe, 2004; Marston *et al.*, 2004; Kiburz *et al.*, 2005; Brar *et al.*, 2006; Riedel *et al.*, 2006; Xu *et al.*, 2009; Katis *et al.*, 2010). Recent evidence suggests that phosphorylation of Rec8 is not only essential for cleavage by separase but also for promoting destabilisation of cohesin by Rad61 prior to metaphase I (Yu and Koshland, 2005; Challa *et al.*, 2019). Therefore, Sgo1 may have a role in protecting the centromeric pool of cohesin from destabilisation, and as acetylated cohesin is essential for cohesion, Sgo1 may selectively protect acetylated cohesin.

Mass spectrometry analysis of Sgo1 immunoprecipitate revealed that acetylated Smc3 co-purifies with Sgo1 from metaphase I arrested cells. This provides evidence that not all acetylated cohesin is destabilised in prophase I, and that there is at least a pool remaining at the centromeres. Co-immunoprecipitation experiments did not reveal clear results as to if Sgo1 specifically interacts with acetylated cohesin. However, the localisation of Sgo1 to the pericentromeric region was significantly decreased in *ECO1-FRB-GFP* anchor-away strains, and as with cohesin, this decrease was rescued by deletion of *RAD61*. This suggests that Sgo1 localisation to the centromeric region may not depend on acetylated cohesin, but this still does not rule out that it is the protection of acetylated cohesin by Sgo1 that maintains cohesion between the sister chromatids until metaphase II. In the future, the full relationship between Sgo1 and acetylated centromeric cohesin will be fully dissected to determine if Sgo1 additionally protects cohesin from the destabilisation pathway in budding yeast meiosis.

Chapter 6. Discussion

6.1 Final discussion

Meiosis is a specialised form of cell division which results in the production of haploid progeny from a diploid progenitor cell. In humans, meiotic cell division allows the production of sperm and egg, which are crucial for sexual reproduction. However, faithful chromosome segregation is crucial during meiotic cell division for the production of healthy gametes, and the resulting aneuploidy from chromosome missegregation can have severe consequences. Ongoing research has shown that aneuploidy in gametes is the leading cause of infertility, miscarriage and of birth defects, such as Down Syndrome (Hassold and Hunt, 2001; Nagaoka, Hassold and Hunt, 2012).

Cohesin is a multi-subunit ring-shaped protein complex essential for holding the chromosomes together from the time of DNA replication until the chromosome segregation events of meiosis I and meiosis II. In human women, the early stages of meiosis occur in the ovaries of the three month old foetus, during which time the diploid progenitor cells undergo DNA replication and homologous recombination to form bivalents, which then arrest in dictyate of meiotic prophase. Cohesin is crucial in stabilisation of the chiasmata, and in maintaining cohesion between the sister chromatids. The bivalent state has to be stably maintained throughout the reproductive lifetime of the woman, until ovulation, when the bivalent undergoes meiosis I, extruding a polar-body, and arresting in metaphase II. Only upon fertilisation does meiosis resume, and the second polar body is extruded, to form a zygote. Therefore, cohesin has to maintain cohesion between sister chromatids for decades, and it is premature dissociation of this cohesin from the DNA that can cause aneuploidy (Hassold and Hunt, 2001; Nagaoka, Hassold and Hunt, 2012).

Understanding the mechanisms by which cohesion is established between the meiotic chromosomes, and how this is maintained, and then faithfully removed after long periods of arrest, is crucial in understanding the causes of infertility and miscarriages. This research carried out in *S. cerevisiae* has shed further light onto the mechanisms of cohesin establishment, protection, and removal throughout meiosis.

During S phase of budding yeast meiosis, cohesin is acetylated by Eco1 acetyltransferase as DNA replication occurs, presumably by an analogous mechanism to in mitosis (Skibbens *et*

al., 1999; Toth *et al.*, 1999; Rolef Ben-Shahar *et al.*, 2008; Unal *et al.*, 2008; Zhang *et al.*, 2008b; Rowland *et al.*, 2009; Sutani *et al.*, 2009; Beckouet *et al.*, 2010; Lopez-Serra *et al.*, 2013). The Eco1 homologue in *S. pombe* also acetylates Smc3 during meiosis but has an additional role in sister chromatid kinetochore mono-orientation in meiosis I through acetylation of so-far-undefined targets (Kagami *et al.*, 2011). Eco1 in budding yeast may also have a role in mono-orientation in meiosis I, as *ECO1* mutants separate a proportion of sister chromatids in meiosis I, but this requires further investigation.

Acetylated cohesin in mouse oocytes has been shown to localise to the chromosome axes in prometaphase I, and loss of Tex19.1 results in a decrease in chromatin-bound acetylated cohesin that is hypothesised to cause aneuploidy in *Tex19.1*$^{-/-}$ oocytes (Reichmann *et al.*, 2017). Therefore the evidence suggests that cohesin acetylation in meiosis may be essential for cohesion of sister chromatids in oocytes, and it may be this pool of established cohesin which stabilises the bivalent for long periods of time (Lu *et al.*, 2017; Reichmann *et al.*, 2017; Lu *et al.*, 2018). The presence of sororin at centromeres in spermatocytes again suggests that this may be the case, and sororin may protect the acetylated centromeric DNA (Gomez *et al.*, 2016; Huang *et al.*, 2017).

Acetylated cohesin is maintained from S phase of meiosis through until the meiosis I division in budding yeast. However, prior to metaphase I there is a step of cohesin removal due to the destabilisation activity of Rad61, in what appears to be a prophase-pathway-like mechanism (Challa *et al.*, 2019). Previously, it has been thought that the cohesin destabilisation pathway is solely confined to higher eukaryotes, therefore limiting comparisons which can be made between cohesin regulation in yeast and in humans. However, the findings of (Challa *et al.*, 2019) reveal that cohesin regulation may be more conserved than previously thought, and opens up new avenues of research to be carried out in the more genetically tractable yeasts.

In this study, I corroborated previous reports that *RAD61* mutants have slightly decreased spore viability due to slight chromosome missegregation defects, which may either be due to defects in homologous recombination in these strains, or failure to remove a proportion of cohesin prior to metaphase I (Challa *et al.*, 2016; Challa *et al.*, 2019). Rad61 is activated by phosphorylation between S phase and prophase of meiosis, before degradation prior to

metaphase I (Challa *et al.*, 2019). The mechanism by which Rad61 is signalled for degradation is unknown, and whether this is a mechanism to limit the amount of cohesin destabilised from the chromatin remains to be tested. Wapl is also important for cohesin destabilisation in mouse meiosis, during which dephosphorylation maintains Wapl in an active chromatin-bound state and allows removal of a subset of cohesin (Brieno-Enriquez *et al.*, 2016), and in plants the destabilisation activity of Wapl is important for faithful chromosome segregation (De *et al.*, 2014).

The literature strongly suggests that there is a broadly conserved pathway of cohesin removal in meiosis throughout evolution. However, cohesin needs to be maintained on the bivalents for long periods of time, with centromeric cohesin being of particular importance for holding the sister chromatids together (Chiang *et al.*, 2010; Lister *et al.*, 2010; Tachibana-Konwalski *et al.*, 2010). In meiosis, it has so far only been thought that shugoshin-PP2A is important for dephosphorylation of centromeric cohesin to allow protection from cleavage by separase in anaphase I by a conserved mechanism, from budding yeast to mice (Kerrebrock *et al.*, 1995; Katis *et al.*, 2004a; Kitajima, Kawashima and Watanabe, 2004; Marston *et al.*, 2004; Rabitsch *et al.*, 2004; Clarke *et al.*, 2005; Kiburz *et al.*, 2005; Brar *et al.*, 2006; Riedel *et al.*, 2006; Llano *et al.*, 2008; Lee *et al.*, 2008; Xu *et al.*, 2009; Ishiguro *et al.*, 2010; Katis *et al.*, 2010). The remaining pool of centromeric cohesin is important in maintaining cohesion between sister chromatids until meiosis II, when this remaining pool of cohesin is removed. However, phosphorylation of Rec8-cohesin in budding yeast meiosis is important for the destabilisation of cohesin, as well as the cleavage (Yu and Koshland, 2005; Challa *et al.*, 2019). Shugoshin is known to localise to the pericentromeric region of chromosomes from prophase in budding yeast, and is present at centromeres in mammalian oocytes (Kitajima, Kawashima and Watanabe, 2004; Marston *et al.*, 2004; Kiburz *et al.*, 2005; Yu and Koshland, 2007; Lee *et al.*, 2008; Rattani *et al.*, 2017).

In metaphase I of budding yeast meiosis, Sgo1 interacts with acetylated cohesin, and depletion of acetylated cohesin resulted in loss of Sgo1 localisation in the presence of Rad61. In higher eukaryotes, Sgo1-Thr346 phosphorylation allows direct binding of Sgo1 to cohesin (Liu, Rankin and Yu, 2013), but whether Sgo1 binds specifically to the pool of acetylated cohesin is unknown. Although a screen of identified Sgo1 phosphorylation sites did not reveal any sites important in the protective activity of Sgo1, identification of

additional phosphorylation and acetylation sites leaves an avenue of research open that could lead to identification of post-translational modifications on Sgo1 important in centromere, or specifically cohesin, binding.

Additionally in this study, Sgo1 was shown to co-immunoprecipitate with condensin in metaphase I of meiosis, and condensin localisation to the centromeric region depended on Sgo1, as in mitosis of budding yeast (Peplowska, Wallek and Storchova, 2014; Verzijlbergen *et al.*, 2014). Abrogation of condensin function through use of a temperature sensitive allele revealed that condensin is important for meiotic chromosome segregation in a role separate to the function of condensin in homologous recombination. This is likely through condensin playing a role in regulating the elasticity of the pericentromeric chromatin, and thus promoting mono-orientation and biorientation in meiosis I and II respectively. Sgo1 recruitment of Ipl1 to the centromeric region is also important in mono-orientation of sister chromatid kinetochores and for maintenance of PP2A-Rts1 at the centromere to protect cohesin in meiosis I (Yu and Koshland, 2007; Meyer *et al.*, 2015; Mehta *et al.*, 2018). Therefore, Sgo1 has important roles in ensuring correct kinetochore orientation in meiosis, as well as in cohesin protection.

Overall, Sgo1 appears to act like a pericentromeric hub in meiosis, as in mitosis. This pericentromeric hub is important for recruitment of adaptor proteins such as condensin, to structure the pericentromere, and Ipl1, to promote mono-orientation. The most well-defined role of Sgo1 in meiosis is to recruit PP2A to this centromeric region and protect cohesin from cleavage by separase. This dephosphorylation activity may now also be expanded to protect cohesin from the activity of the destabilisation pathway. Whether or not this latter point is a function of Sgo1 remains to be fully discerned. However, if this were to be true it would open up a potentially exciting avenue of research in mammalian oocytes, to determine if the failure of Sgo1-PP2A to protect centromeric cohesin from destabilisation is the true cause of cohesin fatigue.

Chapter 7. Materials and Methods

7.1 General information

7.1.1 Supplier information

The chemicals used to carry out this study were obtained from the following suppliers, unless otherwise stated: Acros Organics, BDH Laboratory Supplies, Biorad, Calbiochem, Fisher, Gibco BRL, Invitrogen, Melford, New England Biolabs, Novex, Oxoid, Qiagen, Roche, Sigma, Scientific Laboratory Supplies, Thermoscientific. The reagents used to make the growth media for both bacteria and yeast were supplied by: Formedium, Difco and Sigma.

7.1.2 Sterilisation

Chemical solutions were sterilised by filtration using Nalgene 0.2 µM PES membrane rapid-flow bottle top filters, and stored in sterile glass bottles according to manufacturers specifications. The growth media for both bacteria and yeast was autoclaved for 15 min, at 120 ^{o}C and 15 pounds/inch^{2}. All glassware was sterilised by baking for 16 h at 250 ^{o}C.

7.2 Bacterial methods

7.2.1 Bacterial strains

The *E. coli* strains used in this thesis are shown in Table 7.2.1.

Table 7.2.1: *E. coli* strains

Strain	Genotype	Application
DH5α	F^{-} *endA1 glnV44 thi-1 recA1 relA1 gyrA96 deoR nupG purB20* ϕ80d*lacZ*ΔM15 Δ(*lacZYA-argF*)U169, hsdR17($r_K^{-}m_K^{+}$), λ^{-}	Propagation and cloning of plasmids
BL21 (DE3)	B F^{-} *ompT gal dcm lon hsdS$_B$*($r_B^{-}m_B^{-}$) λ(DE3 [*lacI lacUV5-T7p07 ind1 sam7 nin5*]) [*malB*$^{+}$]$_{K-12}$(λ^{S})	Expression of GST-Sgo1
XL10-Gold	endA1 glnV44 recA1 thi-1 gyrA96 relA1 lac Hte Δ(mcrA)183 Δ(mcrCB-hsdSMR-mrr)173 tet^{R} F'[proAB lacI^{q}ZΔM15 Tn10(Tet^{R} Amy Cm^{R})]	Site directed mutagenesis

7.2.2 Bacterial media and drugs

The following media shown in Table 7.2.2 was used to grow *E. coli* strains in this study.

Table 7.2.2: Bacterial media

Media	Composition
LB (Luria-Bertani) media	1 % w/v Bacto-tryptone 0.5 % w/v Bacto-yeast extract 0.5 % w/v NaCl Adjusted to pH 7.2 with NaOH
LB (Luria-Bertani) agarose plate	1 % w/v Bacto-tryptone 0.5 % w/v Bacto-yeast extract 0.5 % w/v NaCl Adjusted to pH 7.2 with NaOH 2 % w/v agarose
SOC (Super Optimal Broth with Catabolite Repression) media	2 % w/v Bacto-tryptone 0.5 % w/v Bacto-yeast extract 20 mM NaCl 20 mM Glucose 10 mM $MgCl_2$ 10 mM $MgSO_4$ 10 mM KCl

All *E. coli* used in this study were grown in either LB or SOC media. All plasmids used in this study contained Ampicillin-resistance markers. To select for and maintain the plasmids in the *E. coli*, all media/agarose plates contained 100 µg/ml Ampicillin (stock 100 mg/ml in water). To induce expression of recombinant protein in BL21 *E. coli*, the LB media with 100 µg/ml Ampicillin was additionally supplemented with 1 mM IPTG (stock 1 M in water).

7.2.3 Bacterial growth

The *E. coli* strains were either grown on LB agarose containing 100 µg/ml Ampicillin (LB+Amp) at 37 ^{o}C, or inoculated into LB media containing 100 µg/ml Ampicillin (LB+Amp) and grown at 37 ^{o}C at 200 rpm shaking, for up to 16 h. Recombinant protein expression in BL21 *E. coli* was carried out in LB+Amp media with 1 mM IPTG at 25 ^{o}C.

7.2.4 Bacterial storage

For long term storage, 500 µl of the *E. coli* culture, which was grown in LB media containing 100 µg/ml ampicillin for 15 h at 37 ^{o}C, was placed in 500 µl 40 % glycerol, mixed, and frozen at -80 ^{o}C in a cryovial. For short term storage, the colonies/patches of *E. coli* on LB+Amp agarose plates were stored at 4 ^{o}C.

7.2.5 *E. coli* transformation with plasmid DNA

7.2.5.1 Transformation of DH5α *E. coli* by electroporation

A 50 µl aliquot of frozen *E. coli* was gently thawed on ice until liquid. Approximately 40 µl *E. coli* and 1-5 µl of plasmid DNA were mixed together and transferred into a pre-chilled

electroporation cuvette (Thistle Scientific, Cell Project, 2 mM gap). The cuvette was stored on ice until just before use, before which it was immediately dried. Electroporation was carried out using a Biorad Gene Pulser II at 2.5 V, 200 Ω and 2.5 µF. Immediately after electroporation, 1 ml of pre-warmed (37 ^{o}C) LB was added to the electroporation cuvette, and the *E. coli* transferred to a 1.5 ml eppendorf. The *E. coli* were then incubated at 37 ^{o}C shaking at 200 rpm for 1 hr. The *E. coli* were centrifuged for 3 min at 3000 rpm, the supernatant removed, and the cells resuspended gently in 200 µl LB followed by plating with glass beads onto a pre-warmed LB+Amp agarose plates (37 ^{o}C), and incubated at 37 ^{o}C overnight (approximately 15 h).

7.2.5.2 Transformation of chemically competent DH5α and BL21 *E. coli* by heat shock

A 50 µl aliquot of frozen *E. coli* was gently thawed on ice until liquid. Approximately 50 µl *E. coli* and 0.5-5 µl of plasmid DNA were combined together in a 1.5 ml eppendorf and mixed gently by flicking the tube, the *E. coli* were then incubated for 30 min on ice. The *E. coli* were then heat-shocked in a water-bath pre-heated to 42 ^{o}C for 45 sec, then placed on ice for 2 min. To the eppendorf containing the *E. coli*, 500 µl of pre-heated LB or SOC was added. The eppendorf was then incubated at 37 ^{o}C shaking at 200 rpm for 1 h to allow recovery of the *E. coli*. The *E. coli* were centrifuged for 3 min at 3000 rpm, the supernatant removed, and the cells gently resuspended in 200 µl LB or SOC and plated with glass beads onto pre-warmed LB+Amp agarose plates (37 ^{o}C), and incubated at 37 ^{o}C overnight (approximately 15 h).

7.2.5.3 Transformation of XL10-Gold *E. coli*

Transformation of XL10-Gold *E. coli* was only carried out during the site directed mutagenesis protocol, according to standard manufacturers protocol, as cited in QuikChange XLII Site-directed Mutagenesis Kit (Agilent Technologies). The XL10-Gold *E. coli* were gently thawed on ice until liquid, then 45 µl of cells were transferred into a pre-chilled 14 ml BD Falcon Polypropylene round-bottomed tube. To the *E. coli*, 2 µl of the β-mercaptoethanol mix (supplied with the QuikChange XLII Site-directed Mutagenesis Kit) was added to the cells, and the mixture swirled and placed on ice. The mixture was briefly swirled every 2 min for 10 min in total, with incubations on ice in-between, before 2 µl of plasmid DNA was added and the reaction swirled once more, before incubation on ice for 30 min. The *E. coli* were then heat-shocked in a water-bath pre-heated to 42 ^{o}C for 30 sec, then placed on ice for 2 min, before 500 µl pre-heated LB or SOC was added. The *E. coli* were then incubated at 37 ^{o}C shaking at 200 rpm for 1 h to allow recovery. The cells were

plated with glass beads onto two pre-warmed LB+Amp agarose plates (37 ^{o}C), with one containing 100 µl *E. coli* and one containing 400 µl *E. coli*. These were then incubated at 37 ^{o}C overnight (approximately 15 h).

7.3 Budding yeast methods

7.3.1 Budding yeast strains

The budding yeast strains used in this thesis are shown in Table 7.2.1. The majority of the yeast strains used in this study were either w303 or SK1, which were generally used for mitotic or meiotic studies respectively.

Table 7.3.1: *S. cerevisiae* strains

Strain	Genotype
359	*MATa,* *MATalpha, promURA3::TetR::GFP::LEU2, tetOx224-HIS3 (Tomo's centromeric)* *SK1*
877	*MATa, leu2::pURA3-TetR-GFP::LEU2, ura3::TETOx224::URA3, sgo1Δ::KanMX6* *MATalpha, leu2::pURA3-TetR-GFP::LEU2, ura3::TETOx224::URA3, sgo1Δ::KanMX6* *SK1*
1176	*MATa, ade2-1, leu2-3, ura3, trp1-1, his3-11,15, can1-100, GAL, psi+* *W303* wild type
1282	*MATalpha, his1* (mating type tester strain)
1827	*MATa, ho::LYS2, lys2, ura3, leu2::hisG, his3::hisG, trp1::hisG* *SK1* wild type
1828	*MATalpha, ho::LYS2, lys2, ura3, leu2::hisG, his3::hisG, trp1::hisG* *SK1* wild type
1835	*MATa, MATalpha,* *SK1* wild type
2584	*MATa, ura3-52, leu2-3, his3, trp1, gal4del, gal80del, GAL2-ADE2, LYS2::GAL1-HIS3, met2::GAL7-lacZ* (Yeast-two-Hybrid Strain)
2594	*MATa, his1* (mating type tester strain)
3375	*MATa, REC8-3HA::URA3, cdc20::pCLB2-3HA-CDC20::KanMX6* *MATalpha, REC8-3HA::URA3, cdc20::pCLB2-3HA-CDC20::KanMX6* *SK1*
3560	*MATa, cdc20::pCLB2-3HA-CDC20::KanMX6* *MATalpha, cdc20::pCLB2-3HA-CDC20::KanMX6* *SK1*

Table 7.3.1: *S. cerevisiae* strains continued

Strain	Genotype
4015	*MATalpha, REC8-3HA::URA3, ndt80Δ::LEU2* *MATa, REC8-3HA::URA3, ndt80Δ::LEU2* *SK1*
5432	*MATalpha, rad61Δ::KanMX6, eco1Δ::hphMX w303*
5572	*MATalpha, promURA3::TetR::GFP::LEU2, tetOx224-HIS3 (Tomo's centromeric), rad61Δ::KanMX6* *MATa, promURA3::TetR::GFP::LEU2, tetOx224-HIS3 (Tomo's centromeric), rad61Δ::KanMX6* *SK1*
5708	*MATa, BRN1-6HA::TRP w303*
7509	*MATa, SGO1-SZZ(TAP)::KanMX6 w303*
8067	*MATa, cdc20::pCLB2-CDC20::KanMX6* *MATalpha, cdc20::pCLB2-CDC20::KanMX6* *SK1*
8834	*MATa, BRN1-6HA::TRP, sgo1Δ::KanMX6 w303*
8892	*MATa, HST1-SZZ(TAP)::KanMX6 w303*
9218	*MATa, rts1Δ::KanMX6, BRN1-6HA::TRP w303*
9266	*MATa, SGO1-SZZ(TAP)::KanMX6, BRN1-6HA::TRP w303*
9276	*MATa, BRN1-6HA::TRP, sgo1(Y47A;Q50A;S52A)::hphMX4 w303*
9968	*MATa, promURA3::TetR::GFP::LEU2, tetOx224-HIS3 (Tomo's centromeric)* *MATalpha, promURA3::TetR::GFP::LEU2, tetOx224-HIS3 (Tomo's centromeric)* *SK1*
11189	*MATa, GAL-NDT80::TRP1, ura3::pGPD1-GAL4(848).ER::URA3* *MATalpha, GAL-NDT80::TRP1, ura3::pGPD1-GAL4(848).ER::URA3* *SK1*
11358	*MATa, GAL-NDT80::TRP1, ura3::pGPD1-GAL4(848).ER::URA3, promURA3::TetR::GFP::LEU2, tetOx224-HIS3 (Tomo's centromeric)* *MATalpha, GAL-NDT80::TRP1, ura3::pGPD1-GAL4(848).ER::URA3, promURA3::TetR::GFP::LEU2, tetOx224-HIS3 (Tomo's centromeric)* *SK1*
11624	*MATalpha, cdc20::pCLB2-CDC20::KanMX6, sgo1::KanMX6::pCLB2-3HA-SGO1, brn1::BRN1-6HA-TRP* *MATa, cdc20::pCLB2-CDC20::KanMX6, sgo1::KanMX6::pCLB2-3HA-SGO1, brn1::BRN1-6HA-TRP* *SK1*
11625	*MATalpha, cdc20::pCLB2-CDC20::KanMX6, brn1::BRN1-6HA-TRP* *MATa, cdc20::pCLB2-CDC20::KanMX6, brn1::BRN1-6HA-TRP* *SK1*

Table 7.3.1: *S. cerevisiae* strains continued

Strain	Genotype
11668	*MATa, promURA3::TetR::GFP::LEU2, tetOx224-HIS3 (Tomo's centromeric), sgo1::KanMX6::PCLB2-3HA-SGO1* *MATalpha, promURA3::TetR::GFP::LEU2, tetOx224-HIS3 (Tomo's centromeric), sgo1::KanMX6::PCLB2-3HA-SGO1* *SK1*
12145	*MATa, irt1::NAT::pCUP-IME1, pIME4::NAT::pCUP-IME4* *MATalpha, irt1::NAT::pCUP-IME1, pIME4::NAT::pCUP-IME4* *SK1*
12953	*MATa, promURA3::TetR::GFP::LEU2, tetOx224-HIS3 (Tomo's centromeric), sgo1::sgo1-S151A::LEU2* *MATalpha, promURA3::TetR::GFP::LEU2, tetOx224-HIS3 (Tomo's centromeric), sgo1::sgo1-S151A::LEU2* *SK1*
13762	*MATalpha, RPL13A-2xFKBP12::TRP1, fpr1::KANMX4, tor1-1::HIS3* *SK1*
14218	*MATa, sgo1::sgo1-S482D/S487D::LEU2, promURA3::TetR::GFP::LEU2, tetOx224-HIS3 (Tomo's centromeric)* *MATalpha, sgo1::sgo1-S482D/S487D::LEU2, promURA3::TetR::GFP::LEU2, tetOx224-HIS3 (Tomo's centromeric)* *SK1*
14222	*MATa, sgo1::sgo1-S173A::LEU2, promURA3::TetR::GFP::LEU2, tetOx224-HIS3 (Tomo's centromeric)* *MATalpha, sgo1::sgo1-S173A::LEU2, promURA3::TetR::GFP::LEU2, tetOx224-HIS3 (Tomo's centromeric)* *SK1*
14223	*MATa, sgo1::sgo1-S482D::LEU2, promURA3::TetR::GFP::LEU2, tetOx224-HIS3 (Tomo's centromeric)* *MATalpha, sgo1::sgo1-S482D::LEU2, promURA3::TetR::GFP::LEU2, tetOx224-HIS3 (Tomo's centromeric)* *SK1*
14245	*MATa, sgo1::sgo1-S421D::LEU2, promURA3::TetR::GFP::LEU2, tetOx224-HIS3 (Tomo's centromeric)* *MATalpha, sgo1::sgo1-S421D::LEU2, promURA3::TetR::GFP::LEU2, tetOx224-HIS3 (Tomo's centromeric)* *SK1*
14414	*MATa, sgo1::sgo1-T478A/S479A/S482A::LEU2, promURA3::TetR::GFP::LEU2, tetOx224-HIS3 (Tomo's centromeric)* *MATalpha, sgo1::sgo1-T478A/S479A/S482A::LEU2, promURA3::TetR::GFP::LEU2, tetOx224-HIS3 (Tomo's centromeric)* *SK1*
14440	*MATa, sgo1::sgo1-T478D/S479D/S482D/S487D::LEU2, promURA3::TetR::GFP::LEU2, tetOx224-HIS3 (Tomo's centromeric)* *MATalpha, sgo1::sgo1-T478D/S479D/S482D/S487D::LEU2, promURA3::TetR::GFP::LEU2, tetOx224-HIS3 (Tomo's centromeric)* *SK1*

Table 7.3.1: *S. cerevisiae* strains continued

Strain	Genotype
14441	*MATa, sgo1::SGO1::LEU2, promURA3::TetR::GFP::LEU2, tetOx224-HIS3 (Tomo's centromeric)* *MATalpha, sgo1::SGO1::LEU2, promURA3::TetR::GFP::LEU2, tetOx224-HIS3 (Tomo's centromeric)* *SK1*
14451	*MATa, sgo1::sgo1-S151D::LEU2, promURA3::TetR::GFP::LEU2, tetOx224-HIS3 (Tomo's centromeric)* *MATalpha, sgo1::sgo1-S151D::LEU2, promURA3::TetR::GFP::LEU2, tetOx224-HIS3 (Tomo's centromeric)* *SK1*
14479	*MATa, sgo1::sgo1-S487A::LEU2, promURA3::TetR::GFP::LEU2, tetOx224-HIS3 (Tomo's centromeric)* *MATalpha, sgo1::sgo1-S487A::LEU2, promURA3::TetR::GFP::LEU2, tetOx224-HIS3 (Tomo's centromeric)* *SK1*
14480	*MATa, sgo1::sgo1-S482A/S487A::LEU2, promURA3::TetR::GFP::LEU2, tetOx224-HIS3 (Tomo's centromeric)* *MATalpha, sgo1::sgo1-S482A/S487A::LEU2, promURA3::TetR::GFP::LEU2, tetOx224-HIS3 (Tomo's centromeric)* *SK1*
14541	*MATa, sgo1::sgo1-S482A::LEU2, promURA3::TetR::GFP::LEU2, tetOx224-HIS3 (Tomo's centromeric)* *MATalpha, sgo1::sgo1-S482A::LEU2, promURA3::TetR::GFP::LEU2, tetOx224-HIS3 (Tomo's centromeric)* *SK1*
14563	*MATa, sgo1::sgo1-S172A::LEU2, promURA3::TetR::GFP::LEU2, tetOx224-HIS3 (Tomo's centromeric)* *MATalpha, sgo1::sgo1-S172A::LEU2, promURA3::TetR::GFP::LEU2, tetOx224-HIS3 (Tomo's centromeric)* *SK1*
15190	*MATa, SPC42-tdTomato::NAT, PDS1-tdTomato-KITRP1* *MATalpha, SPC42-tdTomato::NAT, PDS1-tdTomato-KITRP1, promURA3::TetR::GFP::LEU2, tetOx224-HIS3 (Tomo's centromeric)* *SK1*
15406	*MATa, arg4-nsp, DED82-URA3-DED81, ycg1-2::KanMX6* *MATalpha, arg4-bgl, ycg1-2::KanMX6* *SK1*
15409	*MATa, arg4-nsp, DED82-URA3-DED81, ycs4S(YCS4-linkers-12Myc::HIS3MX6)* *MATalpha, arg4-bgl, ycs4S(YCS4-linkers-12Myc::HIS3MX6)* *SK1*

Table 7.3.1: *S. cerevisiae* strains continued

Strain	Genotype
16180	*MATa, GAL-NDT80::TRP1, ura3::pGPD1-GAL4(848).ER::URA3, REC8-6HIS-3FLAG:URA3* *MATalpha, GAL-NDT80::TRP1, ura3::pGPD1-GAL4(848).ER::URA3, REC8-6HIS-3FLAG:URA3* *SK1*
16640	*MATalpha, ycg1-2::KanMX6, promURA3::TetR::GFP::LEU2, tetOx224-HIS3 (Tomo's centromeric)* *MATa, ycg1-2::KanMX6, promURA3::TetR::GFP::LEU2, tetOx224-HIS3 (Tomo's centromeric)* *SK1*
16713	*MATa, sgo1::sgo1-S172A/S173A::LEU2, promURA3::TetR::GFP::LEU2, tetOx224-HIS3 (Tomo's centromeric)* *MATalpha, sgo1::sgo1-S172A/S173A::LEU2, promURA3::TetR::GFP::LEU2, tetOx224-HIS3 (Tomo's centromeric)* *SK1*
16967	*MATa, sgo1::sgo1-S172D/S173D::LEU2, promURA3::TetR::GFP::LEU2, tetOx224-HIS3 (Tomo's centromeric)* *MATalpha, sgo1::sgo1-S172D/S173D::LEU2, promURA3::TetR::GFP::LEU2, tetOx224-HIS3 (Tomo's centromeric)* *SK1*
16984	*MATa, sgo1::sgo1-S172D::LEU2, promURA3::TetR::GFP::LEU2, tetOx224-HIS3 (Tomo's centromeric)* *MATalpha, sgo1::sgo1-S172D::LEU2, promURA3::TetR::GFP::LEU2, tetOx224-HIS3 (Tomo's centromeric)* *SK1*
17070	*MATa, SGO1-6HIS-3FLAG::URA3, GAL-NDT80::TRP1, ura3::pGPD1-GAL4(848).ER::URA3* *MATalpha, GAL-NDT80::TRP1, ura3::pGPD1-GAL4(848).ER::URA3, SGO1-6HIS-3FLAG::URA3* *SK1*
17071	*MATa, GAL-NDT80::TRP1, ura3::pGPD1-GAL4(848).ER::URA3, SGO1-6HIS-3FLAG::URA3, spo13Δ::hphMX6* *MATalpha, GAL-NDT80::TRP1, ura3::pGPD1-GAL4(848).ER::URA3, SGO1-6HIS-3FLAG::URA3, spo13Δ::hphMX6* *SK1*
17113	*MATa, ycs4S(YCS4-linkers-12Myc::HIS3MX6), promURA3::TetR::GFP::LEU2, tetOx224-HIS3 (Tomo's centromeric)* *MATalpha, ycs4S(YCS4-linkers-12Myc::HIS3MX6), promURA3::TetR::GFP::LEU2, tetOx224-HIS3 (Tomo's centromeric)* *SK1*
17115	*MATa, sgo1::sgo1-T478A/S479A/S482A/S487A::LEU2, promURA3::TetR::GFP::LEU2, tetOx224-HIS3 (Tomo's centromeric)* *MATalpha, sgo1::sgo1-T478A/S479A/S482A/S487A::LEU2, promURA3::TetR::GFP::LEU2, tetOx224-HIS3 (Tomo's centromeric)* *SK1*

Table 7.3.1: *S. cerevisiae* strains continued

Strain	Genotype
17213	*MATa, Sgo1(1-308)-SZZ(TAP)::KanMX6, BRN1-6HA::TRP w303*
17214	*MATa, Sgo1(1-208)-SZZ(TAP)::KanMX6, BRN1-6HA::TRP w303*
17215	*MATa, SGO1-SZZ(TAP)::KanMX6, BRN1-6HA::TRP, bub1::KanMX6 w303*
17347	*MATa, sgo1::sgo1-T478D/S479D/S482D::LEU2, promURA3::TetR::GFP::LEU2, tetOx224-HIS3 (Tomo's centromeric) MATalpha, sgo1::sgo1-T478D/S479D/S482D::LEU2, promURA3::TetR::GFP::LEU2, tetOx224-HIS3 (Tomo's centromeric) SK1*
17439	*MATa, Sgo1(409-590)-SZZ(TAP)::KanMX6, BRN1-6HA::TRP w303*
17458	*MATa, sgo1::sgo1-S151D/S482D/S487D::LEU2, promURA3::TetR::GFP::LEU2, tetOx224-HIS3 (Tomo's centromeric) MATalpha, sgo1::sgo1-S151D/S482D/S487D::LEU2, promURA3::TetR::GFP::LEU2, tetOx224-HIS3 (Tomo's centromeric) SK1*
17528	*MATa, ycs4S(YCS4-linkers-12Myc::HIS3MX6) MATalpha, ycs4S(YCS4-linkers-12Myc::HIS3MX6), promURA3::TetR::GFP::LEU2, tetOx224-HIS3 (Tomo's centromeric) SK1*
17529	*MATa, ycg1-2::KanMX6 MATalpha, ycg1-2::KanMX6, promURA3::TetR::GFP::LEU2, tetOx224-HIS3 (Tomo's centromeric) SK1*
17558	*MATa, Sgo1(309-590)-SZZ(TAP)::KanMX6, BRN1-6HA::TRP w303*
17559	*MATa, Sgo1(1-508)-SZZ(TAP)::KanMX6, BRN1-6HA::TRP w303*
17714	*MATalpha, sgo1::sgo1-S487D::LEU2, promURA3::TetR::GFP::LEU2, tetOx224-HIS3 (Tomo's centromeric) MATa, sgo1::sgo1-S487D::LEU2, promURA3::TetR::GFP::LEU2, tetOx224-HIS3 (Tomo's centromeric) SK1*
17720	*MATa, Sgo1(209-590)-SZZ(TAP)::KanMX6, BRN1-6HA::TRP w303*
17840	*MATa, Sgo1(509-590)-SZZ(TAP)::KanMX6, BRN1-6HA::TRP w303*
17864	*MATa, sgo1::sgo1-S421A::LEU2, promURA3::TetR::GFP::LEU2, tetOx224-HIS3 (Tomo's centromeric) MATalpha, sgo1::sgo1-S421A::LEU2, promURA3::TetR::GFP::LEU2, tetOx224-HIS3 (Tomo's centromeric) SK1*
18039	*MATa, SGO1-6HIS-3FLAG::URA3, cdc20::pCLB2-CDC20::KanMX6 MATalpha, SGO1-6HIS-3FLAG::URA3, cdc20::pCLB2-CDC20::KanMX6 SK1*
18103	*MATa, cdc20::pCLB2-3HA-CDC20::KanMX6, SGO1-SZZ(TAP)::KanMX6, brn1::BRN1-6HA-TRP MATalpha, cdc20::pCLB2-3HA-CDC20::KanMX6, SGO1-SZZ(TAP)::KanMX6, brn1::BRN1-6HA-TRP SK1*
18106	*MATa, Sgo1(1-408)-SZZ(TAP)::KanMX6, BRN1-6HA::TRP w303*

Table 7.3.1: *S. cerevisiae* strains continued

Strain	Genotype
18217	*MATa, sgo1::sgo1-S151A/S482A/S487A::LEU2, promURA3::TetR::GFP::LEU2, tetOx224-HIS3 (Tomo's centromeric) MATalpha, sgo1::sgo1-S151A/S482A/S487A::LEU2, promURA3::TetR::GFP::LEU2, tetOx224-HIS3 (Tomo's centromeric) SK1*
18305	*MATa, SGO1-SZZ(TAP)::KanMX6, BRN1-6HA::TRP, rts1Δ::KanMX6 w303*
18403	*MATa, sgo1::sgo1-S173D::LEU2, promURA3::TetR::GFP::LEU2, tetOx224-HIS3 (Tomo's centromeric) MATalpha, sgo1::sgo1-S173D::LEU2, promURA3::TetR::GFP::LEU2, tetOx224-HIS3 (Tomo's centromeric) SK1*
18715	*MATa, GAL-NDT80::TRP1, ura3::pGPD1-GAL4(848).ER::URA3, REC8-3HA::URA3 MATalpha, GAL-NDT80::TRP1, ura3::pGPD1-GAL4(848).ER::URA3, REC8-3HA::URA3 SK1*
18716	*MATa, GAL-NDT80::TRP1, ura3::pGPD1-GAL4(848).ER::URA3, REC8-3HA::URA3, SGO1-6HIS-3FLAG::URA3 MATalpha, GAL-NDT80::TRP1, ura3::pGPD1-GAL4(848).ER::URA3, REC8-3HA::URA3, SGO1-6HIS-3FLAG::URA3 SK1*
18717	*MATa, GAL-NDT80::TRP1, ura3::pGPD1-GAL4(848).ER::URA3, REC8-3HA::URA3, SGO1-6HIS-3FLAG::URA3, spo13Δ::hphMX6 MATalpha, GAL-NDT80::TRP1, ura3::pGPD1-GAL4(848).ER::URA3, REC8-3HA::URA3, SGO1-6HIS-3FLAG::URA3, spo13Δ::hphMX6 SK1*
19055	*MATa, GAL-NDT80::TRP1, ura3::pGPD1-GAL4(848).ER::URA3, ycg1-2::KanMX6, promURA3::TetR::GFP::LEU2, tetOx224-HIS3 (Tomo's centromeric) MATalpha, GAL-NDT80::TRP1, ura3::pGPD1-GAL4(848).ER::URA3, ycg1-2::KanMX6, promURA3::TetR::GFP::LEU2, tetOx224-HIS3 (Tomo's centromeric) SK1*
19553	*MATa, GAL-NDT80::TRP1, ura3::pGPD1-GAL4(848).ER::URA3, REC8-6HIS-3FLAG:URA3, spo13Δ::hphMX6 MATalpha, GAL-NDT80::TRP1, ura3::pGPD1-GAL4(848).ER::URA3, REC8-6HIS-3FLAG:URA3, spo13Δ::hphMX6 SK1*
20146	*MATa, SPC42-tdTomato::NAT, PDS1-tdTomato-KITRP1, spo13Δ::hphMX6 MATalpha, SPC42-tdTomato::NAT, PDS1-tdTomato-KITRP1, promURA3::TetR::GFP::LEU2, tetOx224-HIS3 (Tomo's centromeric), spo13Δ::hphMX6 SK1*
20188	*MATa, BRN1-6HA::TRP, HST1-SZZ(TAP)::KanMX6 w303*
20255	*MATa, Sgo1(109-590)-SZZ(TAP)::KanMX6, BRN1-6HA::TRP w303*

Table 7.3.1: *S. cerevisiae* strains continued

Strain	Genotype
20912	*MATa, Eco1-6HA::TRP1, irt1::NAT::pCUP-IME1, pIME4::NAT::pCUP-IME4* *MATalpha, Eco1-6HA::TRP1, irt1::NAT::pCUP-IME1,* *pIME4::NAT::pCUP-IME4* *SK1*
20916	*MATa, Rad61-6HA::TRP1, irt1::NAT::pCUP-IME1, pIME4::NAT::pCUP-IME4* *MATalpha, Rad61-6HA::TRP1, irt1::NAT::pCUP-IME1,* *pIME4::NAT::pCUP-IME4* *SK1*
20953	*MATa, Rad61-6HA::TRP1, GAL-NDT80::TRP1,* *ura3::pGPD1-GAL4(848).ER::URA3* *MATalpha, Rad61-6HA::TRP1, GAL-NDT80::TRP1,* *ura3::pGPD1-GAL4(848).ER::URA3* *SK1*
21068	*MATa, SPC42-tdTomato::NAT, PDS1-tdTomato-KITRP1, rad61Δ::KanMX6* *MATalpha, SPC42-tdTomato::NAT, PDS1-tdTomato-KITRP1,* *promURA3::TetR::GFP::LEU2, tetOx224-HIS3 (Tomo's centromeric),* *rad61Δ::KanMX6* *SK1*
21146	*MATa, REC8-3HA::URA3,ndt80Δ::LEU2, spo13Δ::hphMX6, rad61Δ::KanMX6* *MATalpha, REC8-3HA::URA3, ndt80Δ::LEU2, spo13Δ::hphMX6,* *rad61Δ::KanMX6* *SK1*
21147	*MATa, REC8-3HA::URA3, ndt80Δ::LEU2, rad61Δ::KanMX6* *MATalpha, REC8-3HA::URA3, ndt80Δ::LEU2, rad61Δ::KanMX6* *SK1*
21148	*MATa, REC8-3HA::URA3, cdc20::pCLB2-3HA-CDC20::KanMX6,* *spo13Δ::hphMX6* *MATalpha, REC8-3HA::URA3, cdc20::pCLB2-3HA-CDC20::KanMX6,* *spo13Δ::hphMX6* *SK1*
21232	*MATa, REC8-3HA::URA3, cdc20::pCLB2-3HA-CDC20::KanMX6,* *spo13Δ::hphMX6, rad61Δ::KanMX6* *MATalpha, REC8-3HA::URA3, cdc20::pCLB2-3HA-CDC20::KanMX6,* *spo13Δ::hphMX6, rad61Δ::KanMX6* *SK1*
21260	*MATa, REC8-3HA::URA3, cdc20::pCLB2-3HA-CDC20::KanMX6,* *rad61Δ::KanMX6* *MATalpha, REC8-3HA::URA3, cdc20::pCLB2-3HA-CDC20::KanMX6,* *rad61Δ::KanMX6* *SK1*
21261	*MATa, REC8-3HA::URA3,ndt80Δ::LEU2, spo13Δ::hphMX6* *MATalpha, REC8-3HA::URA3, ndt80Δ::LEU2, spo13Δ::hphMX6* *SK1*

Table 7.3.1: *S. cerevisiae* strains continued

Strain	Genotype
21328	*MATalpha, RAD61-6HIS-3FLAG::URA3, GAL-NDT80::TRP1, ura3::pGPD1-GAL4(848).ER::URA3* *MATa, RAD61-6HIS-3FLAG::URA3, GAL-NDT80::TRP1, ura3::pGPD1-GAL4(848).ER::URA3* *SK1*
21358	*MATalpha, SPC42-tdTomato::NAT, PDS1-tdTomato-KITRP1, promURA3::TetR::GFP::LEU2 , tetOx224-HIS3 (Tomo's centromeric), rad61Δ::KanMX6, spo13Δ::hphMX6* *MATa, SPC42-tdTomato::NAT, PDS1-tdTomato-KITRP1, rad61Δ::KanMX6, spo13Δ::hphMX6* *SK1*
21574	*MATa, ECO1-6HIS-3FLAG::URA3, irt1::NAT::pCUP-IME1, pIME4::NAT::pCUP-IME4* *MATalpha, ECO1-6HIS-3FLAG::URA3, irt1::NAT::pCUP-IME1, pIME4::NAT::pCUP-IME4* *SK1*
21663	*MATa, RAD61-6HIS-3FLAG::URA3, irt1::NAT::pCUP-IME1, pIME4::NAT::pCUP-IME4* *MATalpha, RAD61-6HIS-3FLAG::URA3, irt1::NAT::pCUP-IME1, pIME4::NAT::pCUP-IME4* *SK1*
21903	*MATa, RAD61-6HA::TRP1, GAL-NDT80::TRP1, ura3::pGPD1-GAL4(848).ER::URA3,cdc20::pCLB2-3HA-CDC20::KanMX6* *MATalpha, RAD61-6HA::TRP1, GAL-NDT80::TRP1, ura3::pGPD1-GAL4(848).ER::URA3, cdc20::pCLB2-3HA-CDC20::KanMX6* *SK1*
21904	*MATa, RAD61-6HA::TRP1, GAL-NDT80::TRP1, ura3::pGPD1-GAL4(848).ER::URA3, esp1-2* *MATalpha, RAD61-6HA::TRP1,GAL-NDT80::TRP1, ura3::pGPD1-GAL4(848).ER::URA3, esp1-2* *SK1*
22004	*MATalpha, ECO1-FRB-GFP::KanMX6, RPL13A-2xFKBP12::TRP1, fpr1::KANMX4, tor1-1::HIS3* *SK1*
22034	*MATa, ECO1-FRB-GFP::KanMX6, RPL13A-2xFKBP12::TRP1, fpr1::KANMX4, tor1-1::HIS3* *MATalpha, ECO1-FRB-GFP::KanMX6, RPL13A-2xFKBP12::TRP1, fpr1::KANMX4, tor1-1::HIS3* *SK1*
22440	*MATalpha, RPL13A-2xFKBP12::TRP1, fpr1::KANMX4, tor1-1::HIS3, rad61Δ::KanMX6* *SK1*
22981	*MATalpha, RPL13A-2xFKBP12::TRP1, fpr1::KANMX4, tor1-1::HIS3, ECO1-FRB-GFP::KanMX6, rad61Δ::KanMX6* *SK1*

Table 7.3.1: *S. cerevisiae* strains continued

Strain	Genotype
22997	*MATalpha, GAL-NDT80::TRP1, ura3::pGPD1-GAL4(848).ER::URA3, REC8-6HIS-3FLAG:URA3, hos1::kanMX* *MATa, GAL-NDT80::TRP1, ura3::pGPD1-GAL4(848).ER::URA3, REC8-6HIS-3FLAG:URA3, hos1::kanMX* *SK1*
22998	*MATa, RPL13A-2xFKBP12::TRP1, fpr1::KANMX4, tor1-1::HIS3, GAL-NDT80::TRP1, ura3::pGPD1-GAL4(848).ER::URA3, REC8-6HIS-3FLAG:URA3, ECO1-FRB-GFP::KanMX6* *MATalpha, RPL13A-2xFKBP12::TRP1, fpr1::KANMX4, tor1-1::HIS3, GAL-NDT80::TRP1, ura3::pGPD1-GAL4(848).ER::URA3, REC8-6HIS-3FLAG:URA3, ECO1-FRB-GFP::KanMX6* *SK1*
23079	*MATa, GAL-NDT80::TRP1, ura3::pGPD1-GAL4(848).ER::URA3, REC8-6HIS-3FLAG:URA3, sgo1::KanMX6::PCLB2: 3HA-SGO1* *MATalpha, GAL-NDT80::TRP1, ura3::pGPD1-GAL4(848).ER::URA3, REC8-6HIS-3FLAG:URA3, sgo1::KanMX6::PCLB2: 3HA-SGO1* *SK1*
23130	*MATalpha, RPL13A-2xFKBP12::TRP1, fpr1::KANMX4, tor1-1::HIS3, GAL-NDT80::TRP1, ura3::pGPD1-GAL4(848).ER::URA3, REC8-6HIS-3FLAG:URA3* *MATa, RPL13A-2xFKBP12::TRP1, fpr1::KANMX4, tor1-1::HIS3, GAL-NDT80::TRP1, ura3::pGPD1-GAL4(848).ER::URA3, REC8-6HIS-3FLAG:URA3* *SK1*
23161	*MATa, RPL13A-2xFKBP12::TRP1, fpr1::KANMX4, tor1-1::HIS3, GAL-NDT80::TRP1, ura3::pGPD1-GAL4(848).ER::URA3, REC8-6HIS-3FLAG:URA3, ECO1-FRB-GFP::KanMX6, RAD61-6HA::TRP1* *MATalpha, RPL13A-2xFKBP12::TRP1, fpr1::KANMX4, tor1-1::HIS3, GAL-NDT80::TRP1, ura3::pGPD1-GAL4(848).ER::URA3, REC8-6HIS-3FLAG:URA3, ECO1-FRB-GFP::KanMX6, RAD61-6HA::TRP1* *SK1*
23196	*MATa, HOS1-6HA::TRP1, GAL-NDT80::TRP1, ura3::pGPD1-GAL4(848).ER::URA3* *MATalpha, HOS1-6HA::TRP1, GAL-NDT80::TRP1, ura3::pGPD1-GAL4(848).ER::URA3* *SK1*
23209	*MATa, hos1::kanMX* *MATalpha, hos1::kanMX* *SK1*
23212	*MATa, hos1::kanMX, promURA3::TetR::GFP::LEU2, tetOx224-HIS3 (Tomo's centromeric)* *MATalpha, hos1::kanMX, promURA3::TetR::GFP::LEU2, tetOx224-HIS3 (Tomo's centromeric)* *SK1*

Table 7.3.1: *S. cerevisiae* strains continued

Strain	Genotype
23414	*MATalpha, RPL13A-2xFKBP12::TRP1, fpr1::KANMX4, tor1-1::HIS3, GAL-NDT80::TRP1, ura3::pGPD1-GAL4(848).ER::URA3, REC8-6HIS-3FLAG:URA3, rad61Δ::KanMX6* *MATa, RPL13A-2xFKBP12::TRP1, fpr1::KANMX4, tor1-1::HIS3, GAL-NDT80::TRP1, ura3::pGPD1-GAL4(848).ER::URA3, REC8-6HIS-3FLAG:URA3, rad61Δ::KanMX6* *SK1*
23415	*MATa, RPL13A-2xFKBP12::TRP1, fpr1::KANMX4, tor1-1::HIS3, GAL-NDT80::TRP1, ura3::pGPD1-GAL4(848).ER::URA3, REC8-6HIS-3FLAG:URA3, ECO1-FRB-GFP::KanMX6, rad61Δ::KanMX6* *MATalpha, RPL13A-2xFKBP12::TRP1, fpr1::KANMX4, tor1-1::HIS3, GAL-NDT80::TRP1, ura3::pGPD1-GAL4(848).ER::URA3, REC8-6HIS-3FLAG:URA3, ECO1-FRB-GFP::KanMX6, rad61Δ::KanMX6* *SK1*
23416	*MATa, RPL13A-2xFKBP12::TRP1, fpr1::KANMX4, tor1-1::HIS3, GAL-NDT80::TRP1, ura3::pGPD1-GAL4(848).ER::URA3,* *MATalpha, RPL13A-2xFKBP12::TRP1, fpr1::KANMX4, tor1-1::HIS3, GAL-NDT80::TRP1, ura3::pGPD1-GAL4(848).ER::URA3,* *SK1*
23445	*MATa, RPL13A-2xFKBP12::TRP1,fpr1::KANMX4, tor1-1::HIS3, GAL-NDT80::TRP1, ura3::pGPD1-GAL4(848).ER::URA3, REC8-6HIS-3FLAG:URA3, RAD61-6HA::TRP1* *MATalpha, RPL13A-2xFKBP12::TRP1, fpr1::KANMX4, tor1-1::HIS3, GAL-NDT80::TRP1, ura3::pGPD1-GAL4(848).ER::URA3, REC8-6HIS-3FLAG:URA3, RAD61-6HA::TRP1* *SK1*
23446	*MATa, RPL13A-2xFKBP12::TRP1, fpr1::KANMX4, tor1-1::HIS3, GAL-NDT80::TRP1, ura3::pGPD1-GAL4(848).ER::URA3, REC8-6HIS-3FLAG:URA3, rad61::KanMX6::pCUP1-RAD61-6HA::TRP1* *MATalpha, RPL13A-2xFKBP12::TRP1, fpr1::KANMX4, tor1-1::HIS3, GAL-NDT80::TRP1, ura3::pGPD1-GAL4(848).ER::URA3, REC8-6HIS-3FLAG:URA3, rad61::KanMX6::pCUP1-RAD61-6HA::TRP1* *SK1*
23447	*MATa, RPL13A-2xFKBP12::TRP1, fpr1::KANMX4,tor1-1::HIS3, GAL-NDT80::TRP1, ura3::pGPD1-GAL4(848).ER::URA3, REC8-6HIS-3FLAG:URA3, ECO1-FRB-GFP::KanMX6, rad61::KanMX6::pCUP1-RAD61-6HA::TRP1* *MATalpha, RPL13A-2xFKBP12::TRP1, fpr1::KANMX4, tor1-1::HIS3,GAL-NDT80::TRP1, ura3::pGPD1-GAL4(848).ER::URA3, REC8-6HIS-3FLAG:URA3, ECO1-FRB-GFP::KanMX6, rad61::KanMX6::pCUP1-RAD61-6HA::TRP1* *SK1*
23700	*MATa, RPL13A-2xFKBP12::TRP1, tor1-1::HIS3, fpr1::KANMX4, cdc20::pCLB2-CDC20::KANMX6* *MATalpha, RPL13A-2xFKBP12::TRP1, tor1-1::HIS3, fpr1::KANMX4, cdc20::pCLB2-CDC20::KANMX6* *SK1*

Table 7.3.1: *S. cerevisiae* strains continued

Strain	Genotype
23701	*MATa, cdc20::pCLB2-CDC20::KANMX6, RPL13A-2xFKBP12::TRP1, tor1-1::HIS3, fpr1::KANMX4, REC8-6HIS-3FLAG:URA3* *MATalpha, cdc20::pCLB2-CDC20::KANMX6, RPL13A-2xFKBP12::TRP1, tor1-1::HIS3, fpr1::KANMX4,REC8-6HIS-3FLAG:URA3* *SK1*
24054	*MATa, RPL13A-2xFKBP12::TRP1, tor1-1::HIS3, fpr1::KANMX4, cdc20::pCLB2-CDC20::KANMX6, SGO1-6HA:TRP1* *MATalpha, RPL13A-2xFKBP12::TRP1, tor1-1::HIS3, fpr1::KANMX4, cdc20::pCLB2-CDC20::KANMX6, SGO1-6HA:TRP1* *SK1*
24055	*MATa, RPL13A-2xFKBP12::TRP1, fpr1::KANMX4, tor1-1::HIS3, cdc20::pCLB2-CDC20::KANMX6, SGO1-6HA:TRP1, REC8-6HIS-3FLAG:URA3* *MATalpha, RPL13A-2xFKBP12::TRP1, fpr1::KANMX4, tor1-1::HIS3, cdc20::pCLB2-CDC20::KANMX6, SGO1-6HA:TRP1, REC8-6HIS-3FLAG:URA3* *SK1*
24056	*MATa, RPL13A-2xFKBP12::TRP1, fpr1::KANMX4, tor1-1::HIS3, cdc20::pCLB2-CDC20::KANMX6, SGO1-6HA:TRP1, REC8-6HIS-3FLAG:URA3, ECO1-FRB-GFP::KanMX6, rad61Δ::KanMX6* *MATalpha, RPL13A-2xFKBP12::TRP1, fpr1::KANMX4, tor1-1::HIS3, cdc20::pCLB2-CDC20::KANMX6, SGO1-6HA:TRP1, REC8-6HIS-3FLAG:URA3, ECO1-FRB-GFP::KanMX6, rad61Δ::KanMX6* *SK1*
24057	*MATa, RPL13A-2xFKBP12::TRP1, fpr1::KANMX4, tor1-1::HIS3, cdc20::pCLB2-CDC20::KANMX6, SGO1-6HA:TRP1, REC8-6HIS-3FLAG:URA3, rad61Δ::KanMX6* *MATalpha, RPL13A-2xFKBP12::TRP1, fpr1::KANMX4, tor1-1::HIS3, cdc20::pCLB2-CDC20::KANMX6, SGO1-6HA:TRP1, REC8-6HIS-3FLAG:URA3, rad61Δ::KanMX6* *SK1*
24088	*MATa, RPL13A-2xFKBP12::TRP1, fpr1::KANMX4, tor1-1::HIS3, GAL-NDT80::TRP1, ura3::pGPD1-GAL4(848).ER::URA3, RAD61-6HA::TRP1* *MATalpha, RPL13A-2xFKBP12::TRP1, fpr1::KANMX4, tor1-1::HIS3, GAL-NDT80::TRP1, ura3::pGPD1-GAL4(848).ER::URA3, RAD61-6HA::TRP1* *SK1*
24167	*MATa, RPL13A-2xFKBP12::TRP1, fpr1::KANMX4, tor1-1::HIS3, SPC42-tdTomato::NAT, promURA3::TetR::GFP::LEU2, tetOx224-HIS3 (Tomo's centromeric)* *MATalpha, RPL13A-2xFKBP12::TRP1, fpr1::KANMX4, tor1-1::HIS3* *SK1*
24168	*MATa, RPL13A-2xFKBP12::TRP1, fpr1::KANMX4, tor1-1::HIS3, SPC42-tdTomato::NAT, promURA3::TetR::GFP::LEU2, tetOx224-HIS3 (Tomo's centromeric), rad61Δ::KanMX6* *MATalpha, RPL13A-2xFKBP12::TRP1, fpr1::KANMX4, tor1-1::HIS3, rad61Δ::KanMX6* *SK1*

Table 7.3.1: *S. cerevisiae* strains continued

Strain	Genotype
24169	*MATa, RPL13A-2xFKBP12::TRP1, fpr1::KANMX4, tor1-1::HIS3, SPC42-tdTomato::NAT, promURA3::TetR::GFP::LEU2 , tetOx224-HIS3 (Tomo's centromeric), ECO1-FRB-GFP::KanMX6, rad61Δ::KanMX6* *MATalpha, RPL13A-2xFKBP12::TRP1, fpr1::KANMX4, tor1-1::HIS3, ECO1-FRB-GFP::KanMX6, rad61Δ::KanMX6* *SK1*
24170	*MATa, RPL13A-2xFKBP12::TRP1, tor1-1::HIS3, fpr1::KANMX4, promURA3::TetR::GFP::LEU2,tetOx224-HIS3 (Tomo's centromeric)* *MATalpha, RPL13A-2xFKBP12::TRP1, fpr1::KANMX4, tor1-1::HIS3* *SK1*
24171	*MATa, RPL13A-2xFKBP12::TRP1, fpr1::KANMX4, tor1-1::HIS3, promURA3::TetR::GFP::LEU2, tetOx224-HIS3 (Tomo's centromeric), ECO1-FRB-GFP::KanMX6* *MATalpha, RPL13A-2xFKBP12::TRP1, fpr1::KANMX4, tor1-1::HIS3, ECO1-FRB-GFP::KanMX6* *SK1*
24184	*MATa, RPL13A-2xFKBP12::TRP1, fpr1::KANMX4, tor1-1::HIS3, SPC42-tdTomato::NAT, promURA3::TetR::GFP::LEU2, tetOx224-HIS3 (Tomo's centromeric), ECO1-FRB-GFP::KanMX6* *MATalpha, RPL13A-2xFKBP12::TRP1, fpr1::KANMX4, tor1-1::HIS3, ECO1-FRB-GFP::KanMX6* *SK1*
24234	*MATa, RPL13A-2xFKBP12::TRP1, fpr1::KANMX4, tor1-1::HIS3, cdc20::pCLB2-CDC20::KanMX6, REC8-3HA::URA3* *MATalpha, RPL13A-2xFKBP12::TRP1, fpr1::KANMX4, tor1-1::HIS3, cdc20::pCLB2-CDC20::KanMX6, REC8-3HA::URA3* *SK1*
24235	*MATa, RPL13A-2xFKBP12::TRP1, fpr1::KANMX4, tor1-1::HIS3, cdc20::pCLB2-CDC20::KanMX6, SPO13-3FLAG::KanMX6* *MATalpha, RPL13A-2xFKBP12::TRP1, fpr1::KANMX4, tor1-1::HIS3, cdc20::pCLB2-CDC20::KanMX6, SPO13-3FLAG::KanMX6* *SK1*
24236	*MATa, RPL13A-2xFKBP12::TRP1, fpr1::KANMX4, tor1-1::HIS3, cdc20::pCLB2-CDC20::KanMX6, SPO13-3FLAG::KanMX6, REC8-3HA::URA3* *MATalpha, RPL13A-2xFKBP12::TRP1, fpr1::KANMX4, tor1-1::HIS3, cdc20::pCLB2-CDC20::KanMX6, SPO13-3FLAG::KanMX6, REC8-3HA::URA3* *SK1*
24261	*MATa, RPL13A-2xFKBP12::TRP1, fpr1::KANMX4, tor1-1::HIS3, cdc20::pCLB2-CDC20::KanMX6, SPO13-3FLAG::KanMX6, REC8-3HA::URA3, ECO1-FRB-GFP::KanMX6, rad61Δ::KanMX6* *MATalpha, RPL13A-2xFKBP12::TRP1, fpr1::KANMX4, tor1-1::HIS3,cdc20::pCLB2-CDC20::KanMX6, SPO13-3FLAG::KanMX6, REC8-3HA::URA3, ECO1-FRB-GFP::KanMX6, rad61Δ::KanMX6* *SK1*

Table 7.3.1: *S. cerevisiae* strains continued

Strain	Genotype
24262	*MATa, RPL13A-2xFKBP12::TRP1, fpr1::KANMX4, tor1-1::HIS3, cdc20::pCLB2-CDC20::KanMX6, SPO13-3FLAG::KanMX6, REC8-3HA::URA3, ECO1-FRB-GFP::KanMX6* *MATalpha, RPL13A-2xFKBP12::TRP1, fpr1::KANMX4, tor1-1::HIS3, cdc20::pCLB2-CDC20::KanMX6, SPO13-3FLAG::KanMX6, REC8-3HA::URA3, ECO1-FRB-GFP::KanMX6* *SK1*
24263	*MATa, RPL13A-2xFKBP12::TRP1, fpr1::KANMX4, tor1-1::HIS3, cdc20::pCLB2-CDC20::KanMX6, SPO13-3FLAG::KanMX6, REC8-3HA::URA3, rad61Δ::KanMX6* *MATalpha, RPL13A-2xFKBP12::TRP1, fpr1::KANMX4, tor1-1::HIS3, cdc20::pCLB2-CDC20::KanMX6, SPO13-3FLAG::KanMX6, REC8-3HA::URA3, rad61Δ::KanMX6* *SK1*
24264	*MATa, RPL13A-2xFKBP12::TRP1, fpr1::KANMX4, tor1-1::HIS3, cdc20::pCLB2-CDC20::KANMX6, SGO1-6HA:TRP1, REC8-6HIS-3FLAG:URA3, ECO1-FRB-GFP::KanMX6* *MATalpha, RPL13A-2xFKBP12::TRP1, fpr1::KANMX4, tor1-1::HIS3, cdc20::pCLB2-CDC20::KANMX6, SGO1-6HA:TRP1, REC8-6HIS-3FLAG:URA3, ECO1-FRB-GFP::KanMX6* *SK1*
24265	*MATa, RPL13A-2xFKBP12::TRP1, tor1-1::HIS3, fpr1::KANMX4, promURA3::TetR::GFP::LEU2, tetOx224-HIS3 (Tomo's centromeric), rad61Δ::KanMX6* *MATalpha, RPL13A-2xFKBP12::TRP1, fpr1::KANMX4, tor1-1::HIS3, rad61Δ::KanMX6* *SK1*
24289	*MATa, RPL13A-2xFKBP12::TRP1, tor1-1::HIS3, fpr1::KANMX4, promURA3::TetR::GFP::LEU2, tetOx224-HIS3 (Tomo's centromeric), ECO1-FRB-GFP::KanMX6, rad61Δ::KanMX6* *MATalpha, RPL13A-2xFKBP12::TRP1, fpr1::KANMX4, tor1-1::HIS3, ECO1-FRB-GFP::KanMX6, rad61Δ::KanMX6* *SK1*
25102	*MATa, RPL13A-2xFKBP12::TRP1, tor1-1::HIS3, fpr1::KANMX4, cdc20::pCLB2-CDC20::KANMX6, SGO1-6HA:TRP1, Eco1-FRB-GFP::KanMX6, rad61Δ::KanMX6* *MATalpha, RPL13A-2xFKBP12::TRP1, tor1-1::HIS3, fpr1::KANMX4, cdc20::pCLB2-CDC20::KANMX6, SGO1-6HA:TRP1, Eco1-FRB-GFP::KanMX6, rad61Δ::KanMX6* *SK1*
25103	*MATa, RPL13A-2xFKBP12::TRP1, tor1-1::HIS3, fpr1::KANMX4, cdc20::pCLB2-CDC20::KANMX6, SGO1-6HA:TRP1, rad61Δ::KanMX6* *MATalpha, RPL13A-2xFKBP12::TRP1, tor1-1::HIS3, fpr1::KANMX4, cdc20::pCLB2-CDC20::KANMX6, SGO1-6HA:TRP1, rad61Δ::KanMX6* *SK1*

Table 7.3.1: *S. cerevisiae* strains continued

Strain	Genotype
25104	*MATa, RPL13A-2xFKBP12::TRP1, tor1-1::HIS3, fpr1::KANMX4, cdc20::pCLB2-CDC20::KANMX6, SGO1-6HA:TRP1, Eco1-FRB-GFP::KanMX6* *MATalpha, RPL13A-2xFKBP12::TRP1, tor1-1::HIS3, fpr1::KANMX4, cdc20::pCLB2-CDC20::KANMX6, SGO1-6HA:TRP1, Eco1-FRB-GFP::KanMX6* *SK1*
25532	*MATa, RPL13A-2xFKBP12::TRP1, fpr1::KANMX4, tor1-1::HIS3* *MATalpha, RPL13A-2xFKBP12::TRP1, fpr1::KANMX4, tor1-1::HIS3* *SK1*
25533	*MATa, cdc20::pCLB2-CDC20::KANMX6, RPL13A-2xFKBP12::TRP1, tor1-1::HIS3,fpr1::KANMX4, REC8-6HIS-3FLAG:URA3, SGO1-SZZ(TAP)::KanMX6* *MATalpha, cdc20::pCLB2-CDC20::KANMX6, RPL13A-2xFKBP12::TRP1, tor1-1::HIS3,fpr1::KANMX4, REC8-6HIS-3FLAG:URA3, SGO1-SZZ(TAP)::KanMX6* *SK1*
25684	*MATa, cdc20::pCLB2-CDC20::KANMX6, RPL13A-2xFKBP12::TRP1, tor1-1::HIS3, fpr1::KANMX4, REC8-6HIS-3FLAG:URA3, SGO1-SZZ(TAP)::KanMX6, ECO1-FRB-GFP::KanMX6, rad61Δ::KanMX6* *MATalpha, cdc20::pCLB2-CDC20::KANMX6, RPL13A-2xFKBP12::TRP1, tor1-1::HIS3, fpr1::KANMX4, REC8-6HIS-3FLAG:URA3, SGO1-SZZ(TAP)::KanMX6, ECO1-FRB-GFP::KanMX6, rad61Δ::KanMX6* *SK1*
25736	*MATa, cdc20::pCLB2-CDC20::KANMX6, RPL13A-2xFKBP12::TRP1, tor1-1::HIS3, fpr1::KANMX4, REC8-6HIS-3FLAG:URA3, SGO1-SZZ(TAP)::KanMX6, ECO1-FRB-GFP::KanMX6* *MATalpha, cdc20::pCLB2-CDC20::KANMX6, RPL13A-2xFKBP12::TRP1, tor1-1::HIS3, fpr1::KANMX4, REC8-6HIS-3FLAG:URA3, SGO1-SZZ(TAP)::KanMX6, ECO1-FRB-GFP::KanMX6* *SK1*
25737	*MATa, cdc20::pCLB2-CDC20::KANMX6, RPL13A-2xFKBP12::TRP1, tor1-1::HIS3, fpr1::KANMX4, REC8-6HIS-3FLAG:URA3, SGO1-SZZ(TAP)::KanMX6, rad61Δ::KanMX6* *MATalpha, cdc20::pCLB2-CDC20::KANMX6, RPL13A-2xFKBP12::TRP1, tor1-1::HIS3, fpr1::KANMX4, REC8-6HIS-3FLAG:URA3, SGO1-SZZ(TAP)::KanMX6, rad61Δ::KanMX6* *SK1*
25844	*MATa, ECO1-6HIS-3FLAG::URA3* *MATalpha, ECO1-6HIS-3FLAG::URA3* *SK1*
25926	*MATa, ECO1-6HA::TRP1* *MATalpha, ECO1-6HA::TRP1* *SK1*

7.3.2 Budding yeast strain origin

The origin of the alleles used in this study are shown in Table 7.3.2.

Table 7.3.2: Origin of alleles used in this study

Genotype	Origin
BRN1-6HA::TRP SK1	Lab strain generated by K. Verzijlbergen
BRN1-6HA::TRP w303	(Verzijlbergen *et al.*, 2014)
bub1::KanMX6 w303	Lab strain generated by B. Lee
cdc20::pCLB2-3HA-CDC20::KanMX6	(Lee and Amon, 2003)
cdc20::pCLB2-CDC20::KanMX6	(Brar *et al.*, 2006)
CEN5 tetOx224::HIS3 (Tomo's centromeric)	(Tanaka *et al.*, 2000)
eco1Δ::hphMX	Lab strain generated by O. Nerusheva
ECO1-6HA::TRP1	PCR-based tagging with 6HA using AMp470 (Knop *et al.*, 1999)
ECO1-6HIS-3FLAG::URA3	PCR-based tagging with 6HIS-3FLAG using AMp770
ECO1-FRB-GFP::KanMX6	PCR-based tagging with FRB-GFP using AMp885 (Longtine *et al.*, 1998)
esp1-2	(Buonomo *et al.*, 2000)
GAL-NDT80::TRP1, ura3::pGPD1-GAL4(848).ER::URA3	(Benjamin *et al.*, 2003)
hos1::kanMX	PCR-based gene deletion using AMp195 (Longtine *et al.*, 1998)
HOS1-6HA::TRP1	PCR-based tagging with 6HA using AMp470 (Knop *et al.*, 1999)
HST1-SZZ(TAP)::KanMX6	Lab strain generated by A. Marston
irt1::NAT::pCUP-IME1, pIME4::NAT::pCUP-IME4	(Berchowitz *et al.*, 2013)
leu2::promURA3::TetR-GFP::LEU2	(Michaelis, Ciosk and Nasmyth, 1997)
ndt80Δ::LEU2	(Xu *et al.*, 1995)
PDS1-tdTomato-KITRP1	(Matos *et al.*, 2008)
rad61::KanMX6::pCUP1-RAD61-6HA::TRP1	PCR-based tagging with 6HA using AMp470 (Knop *et al.*, 1999), followed by PCR-based promoter swap using AMp408 (Longtine *et al.*, 1998)
rad61Δ::KanMX6	Lab strain generated by A. Marston
RAD61-6HA::TRP1	PCR-based tagging with 6HA using AMp470 (Knop *et al.*, 1999)
RAD61-6HIS-3FLAG::URA3	PCR-based tagging with 6HIS-3FLAG using AMp770
REC8-3HA::URA3	(Klein *et al.*, 1999)
REC8-6HIS-3FLAG:URA3	Lab strain generated by S. Galander
RPL13A-2xFKBP12::TRP1, fpr1::KANMX4, tor1-1::HIS3	(Haruki, Nishikawa and Laemmli, 2008)
rts1Δ::KanMX6	(Clift, Bizzari and Marston, 2009)

Table 7.3.2: Origin of alleles used in this study continued

Genotype	Origin
Sgo1(109-590)-SZZ(TAP)::KanMX6	*Sgo1(109-590)* truncation made by C. Schaffner. PCR-based tagging with TAP using AMp636 (Longtine *et al.*, 1998)
Sgo1(1-208)-SZZ(TAP)::KanMX6	PCR-based tagging with TAP using AMp636 (Longtine *et al.*, 1998)
Sgo1(1-308)-SZZ(TAP)::KanMX6	PCR-based tagging with TAP using AMp636 (Longtine *et al.*, 1998)
Sgo1(1-408)-SZZ(TAP)::KanMX6	PCR-based tagging with TAP using AMp636 (Longtine *et al.*, 1998)
Sgo1(1-508)-SZZ(TAP)::KanMX6	PCR-based tagging with TAP using AMp636 (Longtine *et al.*, 1998)
Sgo1(209-590)-SZZ(TAP)::KanMX6	*Sgo1(209-590)* truncation made by C. Schaffner. PCR-based tagging with TAP using AMp636 (Longtine *et al.*, 1998)
Sgo1(309-590)-SZZ(TAP)::KanMX6	*Sgo1(309-590)* truncation made by C. Schaffner. PCR-based tagging with TAP using AMp636 (Longtine *et al.*, 1998)
Sgo1(409-590)-SZZ(TAP)::KanMX6	*Sgo1(409-590)* truncation made by C. Schaffner. PCR-based tagging with TAP using AMp636 (Longtine *et al*., 1998)
Sgo1(509-590)-SZZ(TAP)::KanMX6	*Sgo1(509-590)* truncation made by C. Schaffner. PCR-based tagging with TAP using AMp636 (Longtine *et al*., 1998)
sgo1(Y47A;Q50A;S52A)::hphMX4	(Xu *et al*., 2009)
sgo1::KanMX6::pCLB2-3HA-SGO1	(Lee, Kiburz and Amon, 2004)
sgo1::SGO1::LEU2	Lab strain generated by C. Barnard
sgo1::sgo1-S151A/S482A/S487A::LEU2	Lab strain generated by C. Barnard
sgo1::sgo1-S151A::LEU2	Lab strain generated by C. Barnard
sgo1::sgo1-S151D/S482D/S487D::LEU2	Lab strain generated by C. Barnard
sgo1::sgo1-S151D::LEU2	Lab strain generated by C. Barnard
sgo1::sgo1-S172A/S173A::LEU2	Lab strain generated by C. Barnard
sgo1::sgo1-S172A::LEU2	Lab strain generated by C. Barnard
sgo1::sgo1-S172D/S173D::LEU2	Lab strain generated by C. Barnard
sgo1::sgo1-S172D::LEU2	Lab strain generated by C. Barnard
sgo1::sgo1-S173A::LEU2	Lab strain generated by C. Barnard
sgo1::sgo1-S173D::LEU2	Lab strain generated by C. Barnard

Table 7.3.2: Origin of alleles used in this study continued

Genotype	Origin
sgo1::sgo1-S421A::LEU2	Lab strain generated by S. Galander
sgo1::sgo1-S421D::LEU2	Lab strain generated by S. Galander
sgo1::sgo1-S482A/S487A::LEU2	Lab strain generated by C. Barnard
sgo1::sgo1-S482A::LEU2	Lab strain generated by C. Barnard
sgo1::sgo1-S482D/S487D::LEU2	Lab strain generated by C. Barnard
sgo1::sgo1-S482D::LEU2	Lab strain generated by C. Barnard
sgo1::sgo1-S487A::LEU2	Lab strain generated by S. Galander
sgo1::sgo1-S487D::LEU2	Lab strain generated by S. Galander
sgo1::sgo1-T478A/S479A/S482A/S487A::LEU2	Lab strain generated by C. Barnard
sgo1::sgo1-T478A/S479A/S482A::LEU2	Lab strain generated by C. Barnard
sgo1::sgo1-T478D/S479D/S482D/S487D::LEU2	Lab strain generated by C. Barnard
sgo1::sgo1-T478D/S479D/S482D::LEU2	Lab strain generated by C. Barnard
SGO1-6HA:TRP1	(Marston *et al.*, 2004)
SGO1-6HIS-3FLAG::URA3	Lab strain generated by S. Galander
SGO1-SZZ(TAP)::KanMX6 SK1	Lab strain generated by A. Marston
SGO1-SZZ(TAP)::KanMX6 w303	(Verzijlbergen *et al.*, 2014)
sgo1Δ::KanMX6 SK1	(Lee, Kiburz and Amon, 2004)
sgo1Δ::KanMX6 w303	(Clift, Bizzari and Marston, 2009)
SPC42-tdTomato::NAT	(Fernius and Hardwick, 2007)
SPO13-3FLAG::KanMX6	Lab strain generated by E. Duro
spo13Δ::hphMX6	Lab strain generated by S. Galander
ycg1-2::KanMX6	(Lavoie, Hogan and Koshland, 2002)
ycs4S(YCS4-linkers-12Myc::HIS3MX6)	(Yu and Koshland, 2003)

7.3.3 Budding yeast media and drugs

The following media shown in Table 7.3.3 was used to grow budding yeast strains in this study.

Table 7.3.3: Budding yeast media

Media	Composition
YEPDA agar plate	1 % w/v Bacto-yeast extract 2 % w/v Bacto-peptone 2 % w/v Glucose 0.3 mM Adenine 2 % w/v agar

Table 7.3.3: Budding yeast media continued

Media	Composition
4 % YEPDA agar plate	1 % w/v Bacto-yeast extract 2 % w/v Bacto-peptone 4 % w/v Glucose 0.3 mM Adenine 2 % w/v agar
YPG agar plate	1 % w/v Bacto-yeast extract 2 % w/v Bacto-peptone 2.5 % w/v Glycerol 0.3 mM Adenine 2 % w/v agar
Amino-acid dropout agar plates	To make dropout media, yeast nitrogen base without amino acids was mixed with synthetic complete mixture without a specific amino acid (SC/-AAs): 1 % w/v yeast nitrogen base w/o AA 1 x Formedium SC/-AAs 2 % w/v glucose 0.3 mM Adenine 2 % w/v agar
SPO (sporulation) agar plates	1 % w/v $C_2H_3KO_2$ (potassium acetate) 1 x synthetic complete amino acids 2 % w/v agar
YEPDA media	1 % w/v Bacto-yeast extract 2 % w/v Bacto-peptone 2 % w/v Glucose 0.3 mM Adenine
Amino-acid dropout media	To make dropout media, yeast nitrogen base without amino acids was mixed with synthetic complete mixture without a specific amino acid (SC/-AAs): 1 % w/v yeast nitrogen base w/o AA 1 x Formedium SC/-AAs 2 % w/v glucose 0.3 mM Adenine
BYTA media	1 % w/v Bacto-yeast extract 2 % w/v Bacto-tryptone 1 % w/v $C_2H_3KO_2$ (potassium acetate) 50 mM $C_8H_5KO_4$ (potassium phthalate)
YPA media	1 % w/v Bacto-yeast extract 2 % w/v Bacto-peptone 1 % w/v $C_2H_3KO_2$ (potassium acetate)
SPO (sporulation) media	0.3 % $C_2H_3KO_2$ (potassium acetate) Adjusted to pH 7 with glacial acetic acid

To select for the KanMX6 marker in budding yeast strains, G418 was used at a concentration of 400 µg/ml (made by dissolving the powder in water) in YEPDA agar plates. To select for the hphMX6 marker in budding yeast strains, hygromycin (HPH) was used at a

concentration of 400 µg/ml (stock HPH 50 mg/ml) in YEPDA agar plates. To select for the NatMX6 marker in budding yeast strains, Clonat was used at a concentration of 100 µg/ml (200 mg/ml Clonat stock in water) in YEPDA agar plates. To make diploid strains, α-factor was spread onto YEPDA plates to a final concentration of 10 µg/ml (5 mg/ml stock α-factor in DMSO, synthesised by Peptide Protein Research). To arrest mitotic cells in metaphase without microtubules, 15 µg/ml nocodazole (1.5 mg/ml nocodazole stock dissolved in DMSO) was added to YEPDA cell culture, and then 7.5 µg/ml nocodazole re-added every hour. In the anchor-away experiments, 1 µM rapamycin (5 mM rapamycin stock in DMSO (Dimethyl sulphoxide)) was added to the cultures, and for the control cultures the same volume of DMSO was added as rapamycin added. In strains that contained the inducible *pCUP1* promoter, 25 µM $CuSO_4$ (100 mM $CuSO_4$ stock in water) was added to induce protein expression. In meiotic strains containing the *pGAL-NDT80* block/release construct, 1 µM β-estradiol (5 mM β-estradiol stock in ethanol) was added to the cultures to induce *NDT80* expression.

7.3.4 Budding yeast vegetative growth

7.3.4.1 w303, mating testers and yeast-two-hybrid strains

Budding yeast were placed from -80 ^{o}C onto YEPDA agar plates, and incubated at 30 ^{o}C. Selective drop-out or YEPDA+drug agar plates were used to select for the presence of specific markers, and all plates were incubated at 30 ^{o}C. Budding yeast cultures were grown by placing a small amount of yeast into YEPDA or selective media to a maximum of 20 % total volume of the flask. All budding yeast liquid media cultures were grown at 30 ^{o}C shaking at 250 rpm.

7.3.4.2 SK1 strains

Haploid SK1 budding yeast were placed from -80 ^{o}C onto YPG agar plates, and incubated at 30 ^{o}C overnight, and then transferred to YEPDA the next morning and incubated at 30 ^{o}C. Haploid SK1 strains are then treated in the same manner as w303 strains, as described in 7.3.4.1. All temperature sensitive strains were grown at 25 ^{o}C for the permissive temperature and 34 ^{o}C for the restrictive temperature.

Diploid SK1 budding yeast were placed from -80 ^{o}C onto YPG agar plates, and incubated at 30 ^{o}C overnight, and then transferred to 4 % YEPDA the next morning and incubated at 30 ^{o}C to grow up. To maintain the diploid state, and prevent sporulation, diploid SK1

budding yeast were transferred onto a fresh 4 % YEPDA agar plate every 24 h. To vegetatively grow diploid SK1 budding yeast, cultures were grown by placing a small amount of yeast into YEPDA or selective media to a maximum of 10 % total volume of the flask. All budding yeast liquid media cultures were grown at 30 ^{o}C shaking at 250 rpm. All temperature sensitive strains were grown at 25 ^{o}C for the permissive temperature and 34 ^{o}C for the restrictive temperature.

7.3.5 Growing w303 haploid cells into a mitotic nocodazole arrest

For mitotic experiments, such as ChIP and co-immunoprecipitation experiments, haploid budding yeast were inoculated into 10 ml YEPDA and grown at 30 ^{o}C shaking at 250 rpm for 15 h. In the morning, cells were diluted to OD_{600}=0.2 in 200 ml YEPDA, and grown at room temperature for 3 h. The OD (optical density) was measured, and the cells again diluted to OD_{600}=0.2 in 200 ml YEPDA with 15 µg/ml nocodazole added, grown for 1 h, then 7.5 µg/ml nocodazole added. After 1 h further growth the cells were harvested for the experiment.

7.3.6 Growing cells in meiosis

In the evening of Day 1, the diploid yeast strains were placed from -80 ^{o}C onto a YPG plate (to ensure maintenance of mitochondria in the cells), and incubated at 30 ^{o}C overnight for around 15 h. In the morning of Day 2, a small amount of the budding yeast from the YPG plate was transferred onto a 4 % YEPDA plate using a toothpick and incubated at 30 ^{o}C for 9 h. In the evening of Day 2, 10-25 ml YEPDA was inoculated with a small amount of budding yeast, to a maximum of 10 % total volume of the flask, and placed at 30 ^{o}C shaking at 250 rpm for 24 h. In the evening of Day 3, the OD_{600} of the YEPDA culture was calculated and BYTA inoculated to a final OD_{600}=0.2, and the culture then placed at 30 ^{o}C shaking at 250 rpm for 14-16 h. The volume of BYTA used was equal to that of SPO culture required the following day, and the volume was always to a maximum of 10 % total volume of the flask. For mass spectrometry experiments, YPA was used rather than BYTA. In the morning of Day 4, the OD_{600} of the BYTA/YPA cultures was calculated (usually between OD_{600}=2.5-4), and enough cells for OD_{600}=1.8 placed in a 50 ml falcon tube. The cells were pelleted by centrifugation at 3000 rpm for 3 min, and the supernatant removed. The cells were then washed twice by fully resuspending the pellet in dH_2O centrifuging at 3000 rpm for 3 min and removing the supernatant. The cells were then resuspended in SPO (with drugs if required), and incubated at 30 ^{o}C shaking at 250 rpm, for the duration of the experiment.

All temperature sensitive strains were grown at 25 ^{o}C for the permissive temperature whilst on YPG agar, 4 % YEPDA agar, YEPDA media, and in BYTA media. On placing cells in SPO media, the cells were grown in a 25 ^{o}C incubator at 250 rpm until protein inactivation was required, upon which the SPO cultures were shifted to the restrictive temperature of 34 ^{o}C in a water-bath.

7.3.6.1 Asynchronous meiosis

For asynchronous meiotic experiments, the cells were induced to undergo meiosis as described above. The SPO cultures were typically incubated for 9-10 h to allow the meiotic nuclear divisions to take place and formation of tetranucleates to occur. Cultures were typically left for a total of 24-48 h to allow sporulation to occur. Ethanol fixation and DAPI (4',6-diamidino-2-phenylindole) staining was typically used to monitor meiotic progression by taking samples approximately every hour.

7.3.6.2 Prophase I arrest using *ndt80Δ* construct

Diploid strains containing the *ndt80Δ* construct were induced to undergo meiosis, as described above. The SPO cultures were incubated at 30 ^{o}C shaking at 250 rpm for 6 h to allow the prophase I arrest to occur. For sick strains, where there was a concern that some of the cells may not progress through S phase, samples for flow cytometry were taken at 6 h.

7.3.6.3 Metaphase I arrest using the *pCLB2-CDC20* construct

Diploid strains containing the *pCLB2-CDC20* construct were induced to undergo meiosis, as described above. The SPO cultures were incubated at 30 ^{o}C shaking at 250 rpm for 6 h to allow the metaphase I arrest to occur. The arrest was monitored by tubulin immunofluorescence, as metaphase I arrested cells have a distinct short, rectangular spindle by immunofluorescence.

7.3.6.4 *pCUP1-IME1/IME4* block/release synchronous time course protocol

Diploid strains containing the *pCUP1-IME1/IME4* constructs were induced to undergo meiosis, as described above, and incubated at 30 ^{o}C shaking at 250 rpm for 2 h into the early meiotic arrest. The diploid strains were induced to undergo meiosis by addition of 25 μM $CuSO_4$, the culture swirled and then incubated at 30 ^{o}C shaking at 250 rpm for the duration of the experiment (up to 8 h). To monitor progression through meiosis, samples for flow cytometry and for ethanol fixation with DAPI staining were collected. After addition

of 25 µM $CuSO_4$, samples were typically collected every 15 min for 2 h, then every 30 min for 6 h.

7.3.6.5 *pGAL-NDT80* block/release synchronous time course protocol

Diploid strains containing the *pGAL-NDT80* construct were induced to undergo meiosis, as described above, and incubated at 30 ^{o}C shaking at 250 rpm for 6 h into the prophase I arrest. The diploid strains were induced to exit from the prophase I arrest and undergo meiosis I and II nuclear divisions by addition of 1 µM β-estradiol, the culture swirled and then incubated at 30 ^{o}C shaking at 250 rpm for the duration of the experiment (up to 6 h). To monitor progression through meiosis, samples for tubulin immunofluorescence were collected, as metaphase I, anaphase I, metaphase II, and anaphase II cells have distinct spindle morphologies (Figure 2.2.2.4). After addition of 1 µM β-estradiol, samples were typically collected every 15 min for 3 h, then every 30 min for 3 h.

7.3.7 Budding yeast storage

7.3.7.1 Storage of w303, mating testers and yeast-two-hybrid strains

For long term storage, the strains were grown on YEPDA agar plates for 16-24 h at 30 ^{o}C, before all of the cells were transferred into a cryovial containing 1 ml of 20 % glycerol, vortexed briefly, and frozen at -80 ^{o}C. For short term storage, the colonies/patches of budding yeast were stored on YEPDA agar plates at 4 ^{o}C for several weeks.

7.3.7.2 Storage of SK1 strains

For long term storage, the strains were grown on YPG agar plates for 16 h at 30 ^{o}C, before all of the cells were transferred into a cryovial containing 1 ml of 20 % glycerol, vortexed briefly, and frozen at -80 ^{o}C. For short term storage, the colonies/patches of haploid budding yeast were stored on YEPDA agar plates at 4 ^{o}C for several weeks. Diploid budding yeast were maintained for short periods of time by transferring onto a new 4 % YEPDA plate every 24 h and incubating at 30 ^{o}C.

7.3.8 High efficiency transformation for budding yeast

The following solutions shown in Table 7.3.8 were used to carry out the high efficiency transformation for budding yeast.

Table 7.3.8: High efficiency yeast transformation solutions

Solution	Composition
LiTE	100 mM LiAc pH 7.5 10 mM Tris-HCl pH 7.5 1 mM EDTA pH 7.5
40 % PEG solution	40 % PEG4000 100 mM LiAc pH 7.5, 10 mM Tris-HCl pH 7.5 1 mM EDTA pH 7.5
TE	10 mM Tris-HCl pH 7.5 1 mM EDTA pH 7.5

The budding yeast strain was inoculated into 10 ml YEPDA pre-culture, and incubated overnight at 30 ^{o}C shaking at 250 rpm. In the morning, the OD_{600} of the culture was measured, and the cells diluted to OD_{600}=0.2 in 50 ml YEPDA, and incubated at 30 ^{o}C shaking at 250 rpm for 4-5 h, or until the OD_{600}=0.6-1. The cells were harvested by centrifugation in a 50 ml falcon tube at 3000 rpm for 3 min. The cells were washed in 10 ml dH_2O, centrifuged at 3000 rpm for 3 min, and the supernatant removed. The cells were transferred into a 1.5 ml eppendorf with 1 ml dH_2O, and centrifuged at 3000 rpm for 2 min, and the supernatant removed. The cells were then washed in 1 ml LiTE, the cells pelleted then resuspended in 300 µl LiTE. In a fresh eppendorf either 10 µl DNA (400 µl ExTaq PCR DNA, ethanol precipitated and resuspended in 10 µl dH_2O) or 1 µl plasmid DNA was mixed with 50 µl yeast in LiTE, 100 µg carrier DNA (10 µl 10 mg/ml sonicated salmon sperm DNA), and 40 % PEG solution. The yeast were incubated at 30 ^{o}C shaking at 250 rpm for 30 min, then heat-shocked at 42 ^{o}C for 15 min. The yeast were centrifuged 3000 rpm for 2 min, the supernatant removed, and the cells resuspended in 200 µl TE, and the cells plated with glass beads onto a YEPDA agar plate and incubated at 30 ^{o}C. To select for auxotrophic markers the cells were plated immediately onto the amino-acid dropout plates. For drug-selection markers, transformed cells were grown on YEPDA for 16 h at 30 ^{o}C, then replica plated onto the YEPDA agar drug plate.

Single colonies that grew on the transformation plates were then streaked to single colonies on selective media, and correct transformation strains checked by yeast colony PCR.

7.3.9 Budding yeast strain generation

7.3.9.1 Crossing yeast strains for sporulation or diploid generation

Haploid budding yeast of opposite mating types were thawed from -80 ^{o}C onto YPG (SK1) or YEPDA (w303), and incubated at 30 ^{o}C for 24 h. On a YEPDA agar plate, a small amount of the strain with a unique selective marker was mixed with a large amount of the strain with the opposite mating type that did not contain the selective marker. The cross was incubated at 30 ^{o}C for 8 h to allow mating, then the cells were streaked to single colonies on the selective media plate to select for diploid cells containing the selective marker. After 48 h at 30 ^{o}C, single colonies from the selection plate were patched onto YEPDA and incubated at 30 ^{o}C overnight. To induce sporulation for dissection, the diploids were then patched onto SPO agar plates and incubated at 30 ^{o}C for 48 h.

To generate diploid SK1 for an experiment, a large amount of *MATα* cells were mixed with a little *MATα* on YEPDA, and incubated at 30^{o}C for 8 h, before streaking to single colonies on YEPDA containing 10 µg/ml alpha-factor (to arrest excess *MATα* haploid cells) and the plate incubated at 30 ^{o}C for 48 h. Single colonies were patched onto YEPDA and incubated at 30 ^{o}C for 24 h. The diploid patches were replica plated onto minimal plates containing mating tester strains to ensure the strains were diploid, as well as on 4 % YEPDA. After 24 h growth at 30 ^{o}C, the mating testers were scored for growth, and correct diploid strains patched onto YPG for freezing.

7.3.9.2 Tetrad dissection

Diploid strains were incubated for 48 h on a sporulation plate to induce sporulation. Alternatively, diploids were sporulated in liquid SPO media for 48 h, and 200 µl cells centrifuged at 3000 rpm for 3 min and the supernatant removed. A small amount of cells were then digested by incubation in 20 µl 1 mg/ml zymolyase (AMS Biotechnology) in 2 M sorbitol for 8 min, before 1 ml dH_2O added to stop the digestion. A streak of 20 µl of cells was placed down the centre of a dry YEPDA agar plate, and the tetrads dissected into individual spores using a micromanipulator on a Nikon Eclipse 50i light microscope. The YEPDA plate was then incubated at 30 ^{o}C for 48 h to allow spore germination and colony formation. Single colonies were patched onto fresh YEPDA plates and incubated at 30 ^{o}C for 24 h, before the genotype being verified by replica plating on selective media and by yeast colony PCR.

7.3.10 Budding yeast viability

To assess viability of spores, diploid budding yeast were sporulated and dissected, as described in section 7.3.9. After incubation of the dissection plate for 48 h at 30 ^{o}C, the number of spores that had grown in each tetrad was counted, and a picture of the dissection plate taken using the Epson Perfection V550 Photo scanner.

7.3.11 Yeast-two-hybrid assay

The parental yeast-two-hybrid strain was transformed with plasmids that allowed selective growth on -LEU or -TRP selective agar plates. The yeast-two-hybrid assay was carried out according to standard protocol (James et al., 1996). The yeast were streaked to single colonies on either -HIS (to detect weak protein-protein interactions) or -ADE (to detect stronger protein-protein interactions) agar plates, and incubated at 30 ^{o}C. Pictures of the yeast-two-hybrid plates were taken using the Epson Perfection V550 Photo scanner.

7.4 DNA methods

7.4.1 Plasmid list

The following plasmids shown in Table 7.4.1 were used in this study.

Table 7.4.1: Plasmid list

Plasmid	Description	Source
AMp195	pFA6a-kanMX6	(Longtine *et al.*, 1998)
AMp348	pFA6a-kanMX6-pCLB2-3HA	Angelika Amon lab (Longtine *et al.*, 1998)
AMp408	pFA6a-kanMX6-pCUP1A	Angelika Amon lab (Longtine *et al.*, 1998)
AMp470	pYM3	(Knop *et al.*, 1999)
AMp636	TAP plasmid	Kevin Hardwick lab (Longtine *et al.*, 1998)
AMp646	YIplac128	Jean Beggs lab
AMp770	pSB1590	Sue Biggins lab
AMp815	pGAD-C1	(James, Halladay and Craig, 1996)
AMp818	pGBD-C1	(James, Halladay and Craig, 1996)
AMp885	pFA6a-FRB-GFP-KanMX6	EUROSCARF (P30580) (Longtine *et al.*, 1998)
AMp1050	pDEST-GST-SGO1	Lab plasmid - made by S. Galander
AMp1148	pGEX6P expressing GST	Kevin Hardwick lab
AMp1167	SGO1 in AMp815	SGO1 cloned into AMp815 using restriction enzymes

Table 7.4.1: Plasmid list continued

Plasmid	Description	Source
AMp1168	RTS1 in AMp815	RTS1 cloned into AMp815 using restriction enzymes
AMp1170	SGO1 in AMp818	SGO1 cloned into AMp818 using restriction enzymes
AMp1171	RTS1 in AMp818	RTS1 cloned into AMp818 using restriction enzymes
AMp1172	YCS5 (YCG1) in AMp818	YCS5 (YCG1) cloned into AMp818 using restriction enzymes
AMp1177	BRN1 in AMp818	BRN1 cloned into AMp818 using restriction enzymes
AMp1178	YCS4 in AMp815	YCS4 cloned into AMp815 using restriction enzymes
AMp1179	YCS4 in AMp818	YCS4 cloned into AMp818 using restriction enzymes

7.4.2 Mini-prep from *E. coli*

The following solutions shown in Table 7.4.2 were used to carry out minipreps.

Table 7.4.2: Mini-prep solutions

Solution	Composition
GTE	50 mM Glucose 10 mM EDTA pH 7.5 25 mM Tris-HCl pH 7.5
Alkaline SDS (make fresh)	1 % v/v SDS 200 mM NaOH
High Salt Buffer	2.5 M $C_2H_3KO_2$ (potassium acetate) Adjusted to pH 4.8 using glacial acetic acid
TE	10 mM Tris-HCl pH 7.5, 1 mM EDTA pH 7.5

To carry out a mini-prep, a 2 ml LB+Amp *E. coli* culture was grown overnight at 37 ^{o}C, to allow plasmid propagation. Approximately 1.3 ml of the *E. coli* culture was transferred to a 1.5 ml eppendorf, and the cells pelleted at 13000 rpm for 10 min at 4 ^{o}C and the supernatant discarded. The *E. coli* pellet was resuspended in 100 µl GTE and vortexed briefly, before 150 µl Alkaline SDS solution and 150 µl High Salt Buffer was added, and the solutions mixed by inversion. The mixture was then incubated on ice for 15 min. To pellet the cell debris, the solution was centrifuged at 13000 rpm for 5 min at 4 ^{o}C, and all of the supernatant transferred to a new 1.5 ml eppendorf containing 900 µl 100 % ice cold EtOH

(making sure not to transfer any cell debris). The eppendorf was mixed by inversion, and centrifuged 13000 rpm for 5 min at 4 ^{o}C, and all of the supernatant removed, and the DNA pellet resuspended in 200 µl of 70 % ice cold EtOH, and the centrifugation step repeated. After removal of all the EtOH, the DNA pellet was air-dried, then resuspended in 50 µl TE, and stored at -20 ^{o}C.

7.4.3 Midi-prep from *E. coli*

To carry out a midi-prep, a 50 ml LB+Amp *E. coli* culture was grown overnight at 37 ^{o}C, to allow plasmid propagation. The *E. coli* culture was transferred to a 50 ml falcon tube, and the cells pelleted at 3600 rpm for 10 min at 4 ^{o}C and the supernatant discarded. The *E. coli* pellet was resuspended in 2.5 ml GTE and vortexed briefly, before 5 ml of Alkaline SDS solution was slowly added, followed by 2.5 ml High Salt Buffer and the mixture vortexed briefly. To pellet the cell debris, the solution was centrifuged at 3600 rpm for 5 min at 4 ^{o}C, and all of the supernatant transferred into a new 50 ml falcon tube by pouring through a sterile kimwipe. To the supernatant 10 ml of 100 % isopropanol was added, and the solution again centrifuged at 3600 rpm for 5 min at 4 ^{o}C and the supernatant removed. The pellet was resuspended in 750 µl TE and 1 ml LiCl, and placed on ice for 20 min to precipitate the RNA, before again centrifuging at 3600 rpm for 5 min at 4 ^{o}C. The supernatant was transferred into a new falcon tube containing 3.5 ml ice cold 100 % EtOH, and the solution placed at -20 ^{o}C for 10 min, before centrifuging at 3600 rpm for 5 min at 4 ^{o}C. The pellet was then dissolved in 200 µl of TE and transferred to a 1.5 ml eppendorf, and 500 µl of 0.3 M NaAc in EtOH added, then the solution placed at -20 ^{o}C for 10 min, before centrifuging at 13000 rpm for 5 min at 4 ^{o}C. The pellet was washed in 200 µl of 70 % ice cold EtOH, and the centrifugation step repeated. After removal of all the EtOH, the DNA pellet was air-dried, then resuspended in 200 µl TE, and stored at -20 ^{o}C.

7.4.4 Genomic DNA extraction from budding yeast

The following solutions shown in Table 7.4.4 were used to carry out genomic DNA extraction from budding yeast.

Table 7.4.4: Genomic DNA extraction solutions

Solution	Composition
DNA breakage buffer	2 % v/v Triton X-100 1 % v/v SDS 100 mM NaCl 10 mM Tris-HCl pH 8.0 1 mM EDTA pH 8.0
TE	10 mM Tris-HCl pH 7.5, 1 mM EDTA pH 7.5

Haploid or diploid budding yeast for genomic DNA extraction were grown for 24 h at 30 ^{o}C on a YEPDA agar plate. A toothpick was used to resuspend a patch of budding yeast in 200 µl of DNA breakage buffer in a 1.5 ml eppendorf. Once resuspended, a scoop of glass beads (0.5mM zirconia/silica glass beads, Biospec Products) and 200 µl phenol:chloroform was added (careful to add the lower layer of liquid of the phenol:chloroform) to the yeast, and the mixture then vortexed on a multi-vortexer for 2-4 min. The lysed yeast were then pelleted by centrifugation at 13000 rpm for 5 min and the upper aqueous layer transferred into 1 ml ice-cold 100 % EtOH in a fresh 1.5 ml eppendorf, then mixed by inversion. The DNA was then pelleted by centrifugation at 13000 rpm for 5 min and the supernatant discarded. The DNA pellet was air-dried and resuspended in 50 µl TE and stored at -20 ^{o}C.

7.4.5 Polymerase Chain Reaction (PCR) protocols

7.4.5.1 PCR using TaKaRa ExTaq DNA polymerase

To amplify DNA with high accuracy, such as for yeast transformation or sequencing, PCR was carried out using TaKaRa ExTaq (order number: RR001) according to standard manufacturers protocol. Primers were designed to have an annealing temperature of 55 ^{o}C. The following PCR reaction composition and programme was used to carry out DNA amplification, as shown in Tables 7.4.5.1.A and B.

Table 7.4.5.1A: Composition for ExTaq PCR

Solution	Volume (µl)
dH_2O	71.25
10x ExTaq PCR Buffer	10
ExTaq dNTPs	8
20 µM forward primer	2
20 µM reverse primer	2
ExTaq	0.5
DNA (plasmid 200-500 ng/µl)	0.25

Table 7.4.5.1B: Programme for ExTaq PCR

Step	Temperature (°C)	Time (min)
1	95	5:00
2	95	0:30
3	55	0:30
4	72	1 min/kb
Repeat steps 2-4 for 29 cycles		
5	72	3:00
6	10	Forever

7.4.5.2 PCR using Q5 polymerase

To amplify DNA for cloning, Q5 polymerase (NEB, order number: M0491) was used according to standard manufacturers protocol. Primers were designed to have an annealing temperature of 55 °C. The following PCR reaction composition and programme was used to carry out DNA amplification, as shown in Tables 7.4.5.2.A and B.

Table 7.4.5.2A: Composition for Q5 PCR

Solution	Volume (µl)
dH_2O	64
5x Q5 Reaction Buffer	20
2.5 mM dNTPs (Promega)	8
20 µM forward primer	2.5
20 µM reverse primer	2.5
Q5	1
DNA (plasmid 200-500 ng/µl)	2

Table 7.4.5.2B: Programme for Q5 PCR

Step	Temperature (°C)	Time (min)
1	98	0:30
2	98	0:10
3	55	0:30
4	72	1 min/kb
Repeat steps 2-4 for 29 cycles		
5	72	3:00
6	10	Forever

7.4.5.3 Yeast colony PCR

To carry out yeast colony PCR, Taq Polymerase purified in the Marston lab was utilised. This was used with 2.5 mM dNTPs and 10x PCR Buffer (100 mM Tris-HCl pH 8.3, 500 mM KCl, 20 mM $MgCl_2$, 0.1 % gelatin). Primers were designed to have an annealing temperature of

55-60 ^{o}C. The PCR reaction was set up on ice, and a small amount of yeast added directly to the PCR tube (0.2 mm thin wall PCR tube Axygen), gently mixed, and the PCR tube placed directly into a pre-heated PCR machine. The following PCR reaction composition and programme was used to carry out DNA amplification, as shown in Tables 7.4.5.3.A and B.

Table 7.4.5.3A: Composition for yeast colony PCR

Solution	Volume (µl)
dH_2O	14
10x PCR Buffer	2
2.5 mM dNTPs (Promega)	1.6
20 µM forward primer	1
20 µM reverse primer	1
LabTaq	0.4

Table 7.4.5.3B: Programme for yeast colony PCR

Step	Temperature (^{o}C)	Time (min)
1	95	10:00
2	95	0:30
3	55-60	0:30
4	72	3:00
Repeat steps 2-4 for 29 cycles		
5	72	5:00
6	10	Forever

7.4.5.4 Quantitative PCR (qPCR) with SYBR GreenER and NEB Luna Universal qPCR mix

DNA samples acquired from the ChIP protocol in section 7.5.11 were used to carry out qPCR. For qPCR with SYBR GreenER the Input DNA was diluted 1:500 and for qPCR with NEB Luna the Input DNA was diluted 1:300 in Hyclone Water (Hypure Molecular Biology Grade Water, GE Lifesciences). For qPCR with SYBR GreenER the ChIP DNA was diluted 1:10 and for qPCR with NEB Luna the ChIP DNA was diluted 1:6 in Hyclone Water. The following PCR reactions for either SYBR GreenER and NEB Luna were set up as in Tables 7.4.5.4A and 7.4.5.4C in a 96-well plate (Roche) with 3 repeats for each reaction, and the qPCR reaction run on a Lightcycler 480 Roche machine on the PCR programme shown in Table 7.4.5.4B for SYBR GreenER and Table 7.4.5.4D for NEB Luna.

Table 7.4.5.4A: Composition for qPCR with SYBR GreenER

Solution	Volume (µl)
SYBR GreenER master mix (Life Technologies)	5
Hyclone water	8.2
10 x qPCR Buffer	1
20 µM forward primer	0.4
20 µM reverse primer	0.4
DNA	5

Table 7.4.5.4B: Programme for qPCR with SYBR GreenER

Step	Temperature (^{o}C)	Time (min)	Acquisition
Pre-incubation	95	2:00	No
Amplification	95	0:05	No
	52	0:20	No
	72	0:12	Single
Repeat Amplification steps 2-4 for 40 cycles			
Melting curve	90	0:05	No
	65	0:40	No
	97	0.3 ^{o}C/sec increase in temperature from 65-97	Two per 1 ^{o}C increase
Hold	55	Forever	No

Table 7.4.5.4C: Composition for qPCR with NEB Luna Universal qPCR mix

Solution	Volume (µl)
NEB Luna Universal qPCR mix	5
Hyclone water	1.75
20 µM forward primer	0.125
20 µM reverse primer	0.125
DNA	3

Table 7.4.5.4D: Programme for qPCR with NEB Luna Universal qPCR mix

Step	Temperature (^{o}C)	Time (min)	Acquisition
Pre-incubation	95	5:00	No
Amplification	95	0:15	No
	60	0:30	Single
Repeat Amplification steps 2-4 for 45 cycles			
Melting curve	90	0:05	No
	65	0:40	No
	97	0.3 ^{o}C/sec increase in temperature from 65-97	Two per 1 ^{o}C increase
Hold	55	Forever	No

Using the Roche Lightcycler 480 software, the threshold cycle (Ct) values of the individual qPCR reactions was calculated using the 2nd derivative maximum algorithm. The enrichment of the ChIP (ChIP/Input) could then be calculated using Microsoft Excel. Using the Ct values obtained from the Lightcycler, the following formula was used: $\Delta Ct = Ct_{(ChIP)} - (Ct_{(Input)} - \log_{(primer\ efficiency)}(\text{Input dilution factor}))$. The ChIP enrichment could then be calculated by ChIP/Input = $(\text{primer efficiency})^{\wedge(-\Delta Ct)}$. The following primers shown in Table 7.4.5.4E were used for qPCR with SYBR GreenER and in Table 7.4.5.4F for qPCR with NEB Luna Universal qPCR mix.

Table 7.4.5.4E: qPCR primers for SYBR GreenER

Primer	Sequence	Primer efficiency	Distance from centromere	Amplicon size (bp)
782	AGATGAAACTCAGGCTACCA	2.013	95 kb to the left of *CEN4*	93
783	TGCAACATCGTTAGTTCTTG			
794	CCGAGGCTTTCATAGCTTA	2.061	150 bp to the right of *CEN4*	80
795	ACCGGAAGGAAGAATAAGAA			
945	TGAAGGTGAGCTTAAGACAG	1.891	125 bp to the right of *CEN5*	114
946	CAACCATGTTCGTAGCTAAA			
1319	ATGATTCAATGGATTTAGCC	1.919	9.5 kb to the left of *CEN4*	103
1320	GTCAGTCTTATGCTGTTCCC			

Table 7.4.5.4F: qPCR primers for NEB Luna Universal qPCR mix

Primer	Sequence	Primer efficiency	Distance from centromere	Amplicon size (bp)
8172	GCCGAGGCTTTCATAGCTTA	2.098	51 bp to the right of *CEN4*	90
8173	GACGATAAAACCGGAAGGAAG			
8175	GCTACCACCAATAACACAGTTGAG	1.881	95 kb to the left of *CEN4*	173
8176	GTACCTTCCCTGATAATCCGTCT			
8196	ATAAACCAAACCCTTCCCCTTC	2.050	42 bp to the right of *CEN3*	87
8197	CCATATTGTTTGGCGCTGAT			
8206	GGTTTGTAGACAACCAAACTGGTG	1.890	45 bp to the right of *CEN12*	97
8207	ACTCTTTACGCGGGTGTGTACT			

7.4.6 PCR purification

Purification of PCR products was carried out using the Qiagen QIAquick PCR purification kit (order number: 28104), according to standard manufacturers protocol. The resulting DNA was stored at -20 ^{o}C.

7.4.7 Agarose gel electrophoresis

To visualise DNA products from PCR or cloning, the DNA was analysed by agarose gel electrophoresis stained with ethidium bromide. To make the agarose gel, 1 % w/v agarose was dissolved in TAE buffer (40 mM Tris, 1 mM EDTA, 0.11 % v/v acetic acid) by heating using a microwave, until gently boiling and the agarose was dissolved. The agarose was allowed to cool, before 0.5 µg/ml ethidium bromide added and the mixture poured into a gel cast (Thermo Scientific) and the comb added. Between 5-20 µl of DNA product was mixed with Orange G (0.1 % w/v Orange G, 10 % glycerol, 1 mM EDTA pH 8.0). The agarose gel was submerged in TAE solution and the DNA loaded into the wells. To determine the size of the DNA product, 7.5 µl of 1 kb ladder (NEB 1 kb DNA ladder, order number: N3232L) was also run on the gel. The DNA ladder and the PCR products were loaded into the agarose gel, and between a constant voltage of 90-120 V applied for 30-45 min. A UV trans-illuminator was used to visualise the DNA products.

7.4.8 DNA extraction from an agarose gel

DNA extraction from an agarose gel was carried out using the Qiagen QIAquick Gel extraction kit (order number: 28704), according to standard manufacturers protocol. The resulting DNA was stored at -20 ^{o}C.

7.4.9 Ethanol precipitation

To ethanol precipitate DNA, 10 % the total volume of DNA of 3 M NaAc was added, followed by 2.5x volume of ice cold 100 % EtOH. The solution was mixed and placed at -20 ^{o}C for at least 30 min to precipitate the DNA, before centrifuging at 13000 rpm for 10 min at 4 ^{o}C. The supernatant was removed and the DNA washed in 400 µl of ice cold 70 % EtOH, and the centrifugation step repeated. The supernatant was removed, the DNA air-dried, and resuspended in 5-10 µl dH_2O, and frozen at -20 ^{o}C.

7.4.10 Cloning

7.4.10.1 Restriction enzyme based cloning

To carry out restriction enzyme based cloning, the following protocol was followed. A mini-prep of the vector was carried out and resuspended in 30 µl TE (10 mM Tris-HCl pH 7.5, 1 mM EDTA pH 7.5). The vector was then digested with NEB restriction enzymes according to manufacturers protocol, in a total volume of 50 µl and incubated at 37 ^{o}C for 2 h. After restriction enzyme digestion, 1 µl NEB CIP (calf intestinal alkaline phosphatase) was added

to the vector digestion reaction, and the reaction incubated at 37 ^{o}C for 1 h. The vector backbone was then purified using the Qiagen QIAquick PCR purification kit.

The insert was either prepared by PCR reaction or by plasmid digestion. To prepare the insert by PCR reaction, a 50 µl Q5 PCR reaction was carried out using yeast genomic DNA, and the following PCR reaction purified using the Qiagen QIAquick PCR purification kit, followed by restriction enzyme digestion in a total volume of 50 µl and incubated at 37 ^{o}C for 3 h. The insert was then purified using the Qiagen QIAquick PCR purification kit. Alternatively, the insert was prepared by plasmid digestion of a mini-prep of the vector (carrying the insert) with NEB restriction enzymes according to manufacturers protocol, in a total volume of 50 µl and incubated at 37 ^{o}C for 3 h. The restriction enzyme digestion was then run on an agarose gel, and the fragment of the correct size purified using the Qiagen QIAquick Gel extraction kit.

The ligation was then carried out with NEB Quick Ligase (order number: M2200) according to standard manufacturer protocol. The DNA was then transformed into DH5α *E. coli* by electroporation.

7.4.10.2 Cloning by Gibson Assembly

To amplify insert and backbone DNA, PCR was carried out using Q5 polymerase. To digest the plasmid DNA in the PCR reaction for the backbone DNA, 8 µl of the PCR reaction was added to 1 µl of Cutsmart Buffer (NEB) and 1 µl DpnI (NEB), and the reaction incubated at 37 ^{o}C for 30 min to digest the plasmid template, and then incubated at 80 ^{o}C for 20 min to inactivate DpnI. Cloning by Gibson Assembly was carried out using the Gibson Assembly Cloning Kit (NEB, order number: E5510), according to manufacturers protocol using a 5:1 Insert:Vector ratio.

7.4.10.3 Site directed mutagenesis

Site directed mutagenesis on plasmids was carried out using QuikChange II XL Site Directed Mutagen Kit (Agilent Technologies, order number: 200522), according to manufacturers protocol. XL10-Gold *E. coli* were then transformed with the plasmid as in section 7.2.5.3.

7.4.11 DNA sequencing

7.4.11.1 Sequencing a plasmid

To sequence a plasmid, the Big Dye Terminator Kit version 3.1 (Applied Biosystems) was used. Primers annealing to approximately every 500 bp along the region to be sequenced, and across the cloning junctions, were used to sequence the plasmid. The composition of the sequencing reaction is shown in Table 7.4.11.1A

Table 7.4.11.1A: Composition of the plasmid sequencing reaction

Solution	Volume (µl)
Plasmid DNA (200-500 ng/µl)	1
5 µM sequencing primer	0.5
BigDye v3.1	2
BigDye Sequencing Buffer (5x)	2
dH_2O	4.5

The sequencing reaction was placed in a pre-cooled PCR tube (0.2 mm thin wall PCR tube Axygen) on ice. After mixing, the reaction was placed in a pre-heated PCR machine and incubated on the following programme (Table 7.4.11.1B). The sequencing was analysed by Edinburgh Genomics on a ABI 3730 DNA Analyser (Applied Biosystems), and the sequencing results analysed on Lasergene.

Table 7.4.11.1B: PCR machine programme for the plasmid sequencing reaction

Step	Temperature (^{o}C)	Time (min)
1	95	5:00
2	95	0:30
3	55	0:15
4	60	4:00
Repeat steps 2-4 for 25 cycles		
5	10	Forever

7.4.11.2 Sequencing yeast

To sequence a genomic region of budding yeast, the DNA region for sequenced needs to be amplified. This can be done by two methods. The first method is by carrying out budding yeast genomic DNA extraction, and using 3 µl of the PCR product and amplifying the region of interest with a standard ExTaq PCR composition and protocol. The second method is to carry out a yeast colony PCR programme using ExTaq rather than homemade Taq polymerase to amplify the region.

To sequence the yeast PCR product, the Big Dye Terminator Kit version 3.1 (Applied Biosystems) was used. Primers annealing to approximately every 500 bp along the region to be sequenced were used to sequence the DNA. The reaction first needs to undergo a deactivation reaction, the composition of which is shown in Table 7.4.11.2A. The deactivation reaction was placed in a pre-cooled PCR tube (0.2 mm thin wall PCR tube Axygen) on ice, and incubated on the following PCR machine programme shown in Table 7.4.11.2B.

Table 7.4.11.2A: Composition of the yeast sequencing deactivation reaction

Solution	Volume (µl)
PCR product	3
Exonuclease I (NEB, Order: M0293S)	0.5
Thermosensitive Alkaline Phosphatase (Promega, Order: M991A)	0.5

Table 7.4.11.2B: PCR machine programme for the deactivation reaction

Step	Temperature (^{o}C)	Time (min)
1	37	15:00
2	80	15:00
3	10	Forever

The deactivation reaction was then spun down briefly, then the sequencing reagents added to this, as shown in Table 7.4.11.2C. After mixing, the reaction was placed in a pre-heated PCR machine and incubated on the following programme (Table 7.4.11.2D). The sequencing was analysed by Edinburgh Genomics on a ABI 3730 DNA Analyser (Applied Biosystems), and the sequencing results analysed on Lasergene.

Table 7.4.11.2C: Composition of the yeast sequencing reaction

Solution	Volume (µl)
Deactivation Reaction	4
8 µM sequencing primer	2
BigDye v3.1	4

Table 7.4.11.2D: PCR machine programme for the yeast sequencing reaction

Step	Temperature (°C)	Time (min)
1	96	0:30
2	50	0:15
3	60	4:00
Repeat steps 1-3 for 25 cycles		
5	10	Forever

7.4.12 Flow cytometry

7.4.12.1 Preparation of cell samples for flow cytometry

To fix cells for analysis of DNA content by flow cytometry, 150 µl of meiotic SPO cell culture was placed directly into a 1.5 ml eppendorf containing 350 µl of 100 % EtOH, and this was placed at 4 °C.

To prepare the cells for flow cytometry, the cells were pelleted by centrifugation at 13000 rpm for 1 min, the supernatant removed, and the cells resuspended in 1 ml 50 mM Tris pH 7.5. The cells were sonicated using a tip sonicator (Sonics Vibracell V505) at 20 % 1 sec ON, 5 sec OFF for 2 sec total sonication. The cells were then pelleted by centrifugation at 13000 rpm for 1 min, the supernatant removed, and the cells resuspended in 475 µl of 50 mM Tris-HCl pH 7.5 with 25 µl 20 mg/ml RNase A (Amresco) and placed in a 37 °C heat block overnight for 15 h. The next morning, the cells are pelleted at 13000 rpm for 1 min, washed in 1 ml 50 mM Tris pH 7.5, then resuspended in 500 µl 50 mM Tris pH 7.5 with 10 µl 20 mg/ml Proteinase K (Amresco) and placed in a 50 °C heat block for 2 h. The cells were pelleted at 13000 rpm for 1 min, washed in 1 ml 50 mM NaCitrate, then placed in 500 µl 50 mM NaCitrate with 9.17 µl 1 mg/ml propridium iodide (Sigma Aldrich). The samples were then placed in a Bioruptor Twin sonicating device (Diagenode) and sonicated on LOW 30 sec ON, 30 sec OFF for 10 min total sonication. The samples were then stored for up to one week at 4 °C.

7.4.12.2 Using the flow cytometer and data analysis

The cell sample was transferred into a 5 ml BD falcon polystyrene round-bottomed tube (12x75 mm) in preparation for flow cytometry. The flow cytometry machine (Becton Dickinson FACSCalibur) was used with CellQuest Pro programme. The settings used were: number of cells = 20000, Forward Scatter FSC=3.61 and Side Scatter SSC=4.26, FL2-H to

detect propridium iodide staining, and the flow of cells was controlled for each individual sample to a maximum flow of 1000 cells/sec (either 30 µl/min or 60 µl/min flow rate).

The results were then analysed using FlowJo V10. The graphs were converted to FLH-2 (x-axis) and SSC-H (y-axis), and the cells gated to omit debris and clumped cells, before converting into a histogram with FLH-2 on the x-axis. Graphs from individual time points were grouped within FlowJo to create the flow cytometry profiles.

7.5 Protein methods

7.5.1 Protein extracts

To obtain protein extracts from budding yeast, TCA (trichloroacetic acid) extraction was carried out. For mitotic protein extracts 10 ml of YEPDA cell culture OD_{600}=0.6-1 was collected, and for meiotic protein extracts 5 ml of SPO cell culture OD_{600}=1.8 was collected, and transferred into a 15 ml falcon tube. The cells were pelleted by centrifugation at 3000 rpm for 3 min at 4 ^{o}C, the supernatant removed, and the cells resuspended in 5 ml 5 % w/v TCA solution. The samples were incubated on ice (in the dark) for at least 10 min, and the cells then pelleted by centrifugation at 3000 rpm for 3 min at 4 ^{o}C. Approximately 4.5 ml supernatant was removed, and the cells resuspended in the remaining TCA solution and transferred into a 2 ml fast-prep tube (MP Biomedicals). The fast-prep tube was centrifuged at 13000 rpm for 1 min at 4 ^{o}C, all of the supernatant aspirated off, and the tube snap-frozen in liquid nitrogen then stored at -80 ^{o}C.

The buffers required for TCA protein extract preparation are shown in Table 7.5.1.

Table 7.5.1: Solutions required for TCA extract preparation

Solution	Composition
TE	10 mM Tris-HCl pH 7.5, 1 mM EDTA pH 7.5
Protein breakage buffer	1 ml TE 2.75 µl 1 M DTT (Dithioreitol) 20 µl 50 x Roche EDTA-free protease inhibitors (one Roche EDTA-free protease inhibitor tablet in 1 ml dH_2O)
3xSDS sample buffer	187 mM Tris-HCl pH 6.8 6 % v/v β-mercaptoethanol 30 % v/v glycerol 9 % v/v SDS 0.05 % w/v bromophenol blue

The TCA extracts were thawed at room temperature until just liquid, then 1 ml acetone added and the sample vortexed. The cells were pelleted by centrifugation at 13000 rpm for 7 min and the acetone removed. The samples were air-dried for 4 h in a fume hood until the pellet was dry and no acetone remained. The pellet was then resuspended in 100 µl of protein breakage buffer and one volume (half a scoop) of glass beads (0.5mM zirconia/silica glass beads, Biospec Products) added. The cells were broken by shaking in a Fastprep Bio-Pulveriser FP120 at 6.5 speed for 3 cycles of 45 sec. To the lysate, 50 µl of 3xSDS sample buffer was added, the sample mixed, and then boiled at 95 ^{o}C for 5 min. The samples were centrifuged at 13000 rpm for 5 min, and the supernatant transferred to a fresh 1.5 ml eppendorf and frozen at -20 ^{o}C. Before loading onto a SDS-PAGE (sodium dodecyl sulphate-polyacrylamide gel electrophoresis) gel, the samples were thawed and the final boiling and centrifugation steps repeated.

7.5.2 SDS-PAGE protein gels

The standard compositions for SDS-PAGE gels are shown in Table 7.5.2. For small Biorad SDS-PAGE gels, 5 ml of resolving gel and 2 ml of stacking gel was required. For large Biometra SDS-PAGE gels, 30 ml of resolving gel and 7.5 ml of stacking gel was required.

Table 7.5.2: Composition of SDS-PAGE resolving and stacking gels

Solution	Composition
8 % resolving gel	8 ml 30 % acrylamide:0.8 % bis-acrylamide (National Diagnostics) 7.5 ml 4x separation buffer (1.5 M Tris, 0.4 % w/v SDS, pH adjusted to pH 8.8 with glacial acetic acid) 14.5 ml dH_2O 450 µl 10 % ammonium persulphate (APS) 30 µl tetramethylethylenediamine (TEMED)
10 % resolving gel	10 ml 30 % acrylamide:0.8 % bis-acrylamide (National Diagnostics) 7.5 ml 4x separation buffer (1.5 M Tris, 0.4 % w/v SDS, pH adjusted to pH 8.8 with glacial acetic acid) 12.5 ml dH_2O 450 µl 10 % ammonium persulphate (APS) 30 µl tetramethylethylenediamine (TEMED)
4 % stacking gel	2 ml 30 % acrylamide:0.8 % bis-acrylamide (National Diagnostics) 7.5 ml 2x stacking buffer (250 mM Tris, 0.2 % w/v SDS, pH adjusted to pH 6.8 with glacial acetic acid) 5.3 ml dH_2O 150 µl 10 % ammonium persulphate (APS) 15 µl tetramethylethylenediamine (TEMED)

7.5.2.1 Biorad Mini Trans-Blot System

Two small glass plates were cleaned with ethanol, put into the gel pouring apparatus (assembled according to manufacturers instruction (Biorad)), and 5 ml resolving gel poured and topped with a thin layer of isopropanol. Once set, the isopropanol was removed and around 2 ml of stacking gel poured and a 10 or 15 well comb inserted. Once set, the gel was placed in a Mini Trans-Blot apparatus (Biorad) in SDS running buffer (25 mM Tris, 190 mM glycine, 0.01 % w/v SDS), and 7.5-15 µl of TCA protein extract loaded, with 7.5 µl Rainbow Ladder (Merck, order number: RPN800E) to allow molecular weight to be estimated. The SDS-PAGE gel was run at 100 V for 10 min, then 200 V until the loading dye had run off the bottom of the gel (around 45 min).

7.5.2.2 Biometra V17.15 system

Two large glass plates were assembled with 1.5 mm plastic spacers between them, which were held in placed using clips, then were sealed with 2 % agarose dissolved in H_2O. Once sealed, 30 ml resolving gel was poured in-between the glass plates and topped with isopropanol. Once set, the isopropanol was removed and 7.5 ml stacking gel added and a 20 or 21 well comb inserted. The gel was then sealed with 2 % agarose into a Biometra V17.15 electrophoresis apparatus. SDS running buffer (25 mM Tris, 190 mM glycine, 0.01 % w/v SDS) added to the top and bottom wells, and 7.5-15 µl of TCA protein extract loaded, with 7.5 µl Rainbow Ladder to allow molecular weight to be estimated. The SDS-PAGE gel was run at 50 mA for 30 min, then at 11 mA overnight.

7.5.3 Transfer and western blotting

7.5.3.1 Transfer of small Biorad gels by wet transfer

The small Biorad SDS-PAGE gel was transferred in a Biorad transfer unit according to manufacturers instruction in Transfer Buffer (25 mM Tris, 1.5 % w/v glycine, 0.02 % w/v SDS, 10 % v/v MeOH). The gel was transferred onto a nitrocellulose membrane (0.45 µM nitrocellulose blotting membrane, GE Healthcare, Amersham) between 4 sheets of blotting paper (GE Healthcare TE70) at 90 V for 90 min, with an ice-pack to prevent over-heating.

7.5.3.2 Transfer of large Biometra V17.15 system gels by semi-dry transfer

The large Biometra V17.15 SDS-PAGE gel was transferred by semi-dry transfer using a Amersham TE70 transfer unit according to manufacturers instruction. The gel was transferred onto a nitrocellulose membrane (0.45 µM nitrocellulose blotting membrane, GE Healthcare, Amersham) between 6 sheets of blotting paper (GE Healthcare TE70) that had

been pre-soaked in Transfer Buffer (25 mM Tris, 1.5 % w/v glycine, 0.02 % w/v SDS, 10 % v/v MeOH), at 1 mA/cm^2 for 150 min.

7.3.3.3 Western blotting

Once the transfer was complete, the nitrocellulose membrane was briefly washed in water, then stained for 2 min in Ponceau S (0.47 % w/v Ponceau S, 3 % w/v TCA, 1 % v/v acetic acid) to visualise the protein and ensure that the transfer was successful. The nitrocellulose membrane was then washed in water, then blocked in 5 % milk in PBS (13.7 mM NaCl, 270 µM KCl, 1 mM Na_2PO_4, 176 µM KH_2PO_4) with 0.05 % v/v Tween20 (PBST), for at least 1 h at room temperature. The primary antibody (see Table 7.3.3.3) was added to 2 % milk dissolved in PBST, and the nitrocellulose membrane incubated in the primary antibody overnight at 4 ^{o}C for 15 h. The nitrocellulose membrane was rinsed in PBS to remove excess milk, then washed in PBST three times for 15 min at room temperature. The secondary antibody for either ECL (Enhanced chemiluminescence) or Licor (see Table 7.3.3.3) was added to 2 % milk dissolved in PBST, and incubated with the nitrocellulose membrane for 1 h at room temperature. The nitrocellulose membrane was rinsed in PBS to remove excess milk, then washed in PBST two times for 15 min at room temperature, and then once in PBS for 15 min at room temperature.

For membranes incubated with Licor secondary antibodies, the proteins were visualised on the nitrocellulose membrane using the Odyssey Imaging System (Licor Biosciences) and analysed using Image Studio Software (Licor Biosciences).

For membranes incubated in Horseradish Peroxidase (HRP)-coupled secondary antibodies, the proteins were visualised by ECL. SuperSignal West Pico chemiluminescence kit (Thermo Scientific, order number: 34580) was used according to manufacturers instruction, and this was supplemented with SuperSignal West Femto chemiluminescence kit (Thermo Scientific, order number: 34094) for weaker protein signals. In a dark room, the nitrocellulose membrane was exposed to X-ray film (Agfa Healthcare CP-BU, blue), and the film developed using a Konica-Minolta SRX-101A developer.

The following antibodies in Table 7.3.3.3 were used to carry out western-blotting

Table 7.3.3.3: Antibodies for western blotting

Antibody	Species	Concentration	Primary/Secondary	Source/company
HA (12CA5)	Mouse	1/1000	Primary	Roche (11666606001)
HA (HA11)	Mouse	1/1000	Primary	Biolegend (MMS-101R)
FLAG (M2)	Mouse	1/1000	Primary	Sigma (F1804)
GFP	Mouse	1/1000	Primary	Sigma Aldrich (Roche 11814460001)
Sgo1	Rabbit	1/1000	Primary	Homemade (C. Schaffner)
Pgk1	Rabbit	1/10000	Primary	Homemade (C. Fox)
Kar2	Rabbit	1/10000	Primary	Homemade (C. Fox)
Rec8	Rabbit	1/15000	Primary	Homemade (K. Lesniewska and W. Borek) Rabbit 70060
Smc3-K112,K113 acetylation	Rabbit	1/1000	Primary	Homemade (R. Barton) Rabbit 6371
PAP (Peroxidase anti-peroxidase soluble complex)	Rabbit	1/1000	Primary antibody conjugated to HRP	Sigma (P1291)
Anti-mouse	Sheep	1/5000	Secondary ECL	VWR GE healthcare (NXA931)
Anti-rabbit	Donkey	1/5000	Secondary ECL	VWR GE healthcare (NA934)
Anti-mouse	Donkey	1/10000	Secondary Licor	LI-COR biosciences, IRDye 800CW (926-32212)
Anti-rabbit	Donkey	1/10000	Secondary Licor	LI-COR biosciences IRDYE 680RD (926-68073)

7.5.4 Large scale protein purification

7.5.4.1 Drop freezing cells in liquid nitrogen

To ensure that the appropriate yield of protein was obtained for mass spectrometry, 3 litres of SPO culture OD_{600}=2.5 was grown for each strain, as previously described in section 7.3.6. The cultures were then pelleted by centrifugation in a large Beckman Avanti J25 centrifuge at 4000 rpm for 5 min at 4 ^{o}C. The cells were washed in 400 ml of cold dH_2O, pelleted by centrifugation, then transferred into a 50 ml falcon tube. The cells were pelleted once more

by centrifugation at 3000 rpm for 5 min at 4 ^{o}C, and the supernatant removed. The cells were resuspended in 20 % w/v dH_2O supplemented with 0.2 mM PMSF. The yeast were then drop frozen in liquid nitrogen, and the yeast noodles stored at -80 ^{o}C.

7.5.4.2 Grinding budding yeast using Retsch Twin Biopulveriser

The yeast noodles were then ground using a Retsch MM400 Twin Biopulveriser. The capsules and ball bearings were cooled in liquid nitrogen, and up to 13 g of yeast noodles added to each capsule and a 25 mm ball-bearing added. The cells were broken by grinding at 30 Hz for 3 min for 5 cycles, with 5 min breaks in liquid nitrogen between cycles to prevent the yeast from thawing. The ground yeast were transferred into a 50 ml falcon tube pre-cooled in liquid nitrogen, then stored at -80 ^{o}C.

7.5.4.3 Antibody coupling to Protein G Dynabeads

The solutions for coupling antibodies to Protein G Dynabeads are shown in Table 7.5.4.3.

Table 7.5.4.3: Solutions for coupling antibodies to Protein G Dynabeads

Solution	Composition
0.1 M Na-Phosphate buffer pH 7.0	58 ml 0.5 M Na_2HPO_4 21 ml 1 M NaH_2PO_4 421 ml dH_2O

To carry out purification of FLAG-tagged proteins, 500 µl of Protein G Dynabeads (Invitrogen 20 mg/ml) were coupled to 1 mg/ml M2 FLAG antibody (Sigma, order number: F1804) according to the following protocol. The 500 µl of Protein G Dynabeads were placed in a 1.5 ml eppendorf and concentrated on a magnet. The supernatant was removed, and the beads washed twice in 1ml of 0.1 M Na-Phosphate buffer pH 7.0 for 5 min/wash on a rotating wheel. The supernatant was removed from the beads, and 50 µl M2 FLAG antibody and 50 µl 0.1 M Na-Phosphate buffer pH 7.0 added to the beads. The beads were then incubated shaking at room temperature in a multi-vortexer set at 500 rpm for 25 min. The beads were concentrated on a magnet and the supernatant removed. The beads were then washed twice in 1 ml of 0.1 M Na-Phosphate buffer pH 7.0 supplemented with 0.01 % v/v Tween20 for 5 min/wash on a rotating wheel. The supernatant was removed and the beads washed twice in 1 ml of 200 mM triethanolamine pH 8.2 for 5 min/wash, and the supernatant removed. To crosslink the antibody to the beads, 1ml of 20 mM DMP (dimethyl pimelimidate) (Thermo Scientific, order number: 21667) dissolved in 200 mM triethanolamine pH 8.2 was added to the beads, followed by incubation with rotational

mixing at room temperature for 30 min. The beads were concentrated, and the supernatant removed, then the beads incubated in 1 ml of 50 mM Tris-HCl pH 7.5 at room temperature for 15 min. The beads were then washed three times in 1 ml of PBST, and then stored in PBST at 4 ^{o}C for up to 48 h.

7.5.4.4 Large scale immunoprecipitation for mass spectrometry

The solutions for the immunoprecipitation are shown in Table 7.5.4.4.

Table 7.5.4.4: Solutions for immunoprecipitation

Solution	Composition
2000 x CLAAPE	10 mg/ml Chymostatin (Melford, C1104) 10 mg/ml Aprotinin (Melford, A2301) 10 mg/ml Leupeptin (Melford, L1001) 10 mg/ml E-64 (Melford, E1101) 10 mg/ml Pepstatin A (Melford, P2203) 10 mg/ml Antipain, dihydrochloride (Melford, A0105)
20 x Phosphatase Inhibitors	20 mM Na pyrophosphate 40 mM Na-β-glycerophosphate 100 mM NaF
Buffer H 0.15	25 mM Hepes-KOH pH 8.0 2 mM $MgCl_2$ 0.1 mM EDTA pH 8.0 0.5 mM EGTA-KOH pH 8.0 150 mM KCl 15 % v/v glycerol 0.1 % w/v NP-40
Buffer H 0.15 supplemented with inhibitors	60.5 ml Buffer H 0.15 70 µl 2000 x CLAAPE 350 µl 400 mM pefablock (Acros Organics, 32811010) 560 µl 100 mM Na orthovanadate 14 µl 100 µM microcystin (LKT Laboratories, M3406) 1.4 ml 50 x Roche EDTA-free protease inhibitor (Roche, 11873580001) 3.5 ml 40 mM NEM (Acros Organics, 156100050) 3.5 ml 20 x phosphatase inhibitors

The yeast grindate had been stored at -80 ^{o}C. This was gently thawed on ice, and an equal volume of Buffer H 0.15 supplemented with inhibitors was added (e.g 17 ml Buffer H 0.15 supplemented with inhibitors to 17 g grindate), and the lysate mixed until all lumps dissolved. If multiple samples were being processed at once, then equal volumes of lysate were used from this point forward e.g 30 ml/sample. The lysate was supplemented with 40 U/ml Benzonase (Merck Benzonase Nuclease 250 U/µl, order number: 71206), and

incubated for 1 h on ice with occasional mixing. The cell debris was pelleted by centrifugation at 3500 rpm for 10 min at 4 ^{o}C, and the supernatant was transferred to a new 50 ml falcon tube on ice. Protein G Dynabeads pre-coupled to M2 FLAG antibody were washed three times in 1 ml Buffer H 0.15 supplemented with inhibitors, then equal volumes added to each falcon tube containing cell lysate (either 250 µl or 500 µl Protein G Dynabeads/sample resuspended in 500 µl Buffer H 0.15 supplemented with inhibitors). The immunoprecipitation reactions were then incubated with rotational mixing at 4 ^{o}C for 150 min. The Protein G Dynabeads were separated from the cell lysate using a magnet, the supernatant removed, and the beads transferred to a 1.5 ml eppendorf on ice. The beads were washed with rotational mixing at 14 rpm at 4 ^{o}C in 1 ml Buffer H 0.15 supplemented with inhibitors and 2 mM DTT for 10 min, and the supernatant removed. The beads were then washed a further three times, for 10 min/wash, in 1 ml Buffer H 0.15 supplemented with inhibitors. The supernatant was removed and 100 µl 0.5 mg/ml FLAG peptide in Buffer H 0.15 supplemented with inhibitors added to the beads, and incubated with rotational mixing for 30 min at 4 ^{o}C. The lysate was separated from the beads and transferred to a new 1.5 ml eppendorf. The lysate was snap frozen in liquid nitrogen and stored at -80 ^{o}C.

7.5.5 Silver stain

To visualise proteins NuPAGE protein gels were run followed by silver staining. Protein samples obtained from large-scale protein purification were stored at -80 ^{o}C. These were thawed on ice, and 2.5 µl 4xLDS sample buffer (NuPAGE Invitrogen, order number: NP0007) supplemented with 5 % β-mercaptoethanol was added, and the samples boiled at 95 ^{o}C for 5 min followed by centrifugation at 13000 rpm for 5 min. A protein standard molecular weight marker was used, with 1 µl Rainbow Ladder added to 9 µl 1xLDS sample buffer supplemented with 5 % β-mercaptoethanol, as well as 10 µl of 10 µg/ml, 4 µg/ml, 2 µg/ml, 1 µg/ml Bovine Serum Albumin (BSA) protein standards (made from 10 mg/ml NEB BSA) added to 2.5 µl 4xLDS sample buffer supplemented with 5 % β-mercaptoethanol, to allow estimation of protein concentration. The BSA protein standards were also boiled at 95 ^{o}C for 5 min followed by centrifugation at 13000 rpm for 5 min. All protein samples were loaded onto a NuPAGE 4-12 % Bis-Tris 1 mm 10-well gel (Novex Life Technologies Invitrogen) in 1xMES SDS running buffer (Novex Life Technologies, order number: NP0002) for 45 min at 200 V. After the dye front had run off the bottom of the gel, the gel was transferred into a glass dish and washed in dH_2O. Silver-staining of the gel was then carried

out according to manufacturers protocol using the Invitrogen SilverQuest Staining Kit (order number: LC6070).

7.5.6 Drying SDS-PAGE protein gels

To preserve SDS-PAGE or NuPAGE gels for long-term record-keeping, the gels were dried using the Invitrogen DryEase Gel Drying System. The gel was incubated in drying solution (10 % v/v glycerol, 40 % v/v EtOH) for 30 min. The gel was the placed between two DryEase Mini Cellophane membranes (Novex Life Technologies, order number: NC2380) that had been briefly pre-soaked in drying solution, and assembled into the Invitrogen DryEase Gel Drying System and left to air-dry for 24 h at room temperature.

7.5.7 Mass spectrometry

7.5.7.1 Colloidal Blue staining

The first step of preparation of samples for trypsin digestion and mass spectrometry is to denature the protein samples and carry out coomassie staining of the samples on a NuPAGE protein gel. Protein samples obtained from large-scale protein purification were stored at -80 ^{o}C. These were thawed on ice and 20 µl 4xLDS sample buffer supplemented with 5 % β-mercaptoethanol added to the sample (normally around 80 µl), and the samples boiled at 95 ^{o}C for 5 min followed by centrifugation at 13000 rpm for 5 min. A protein standard molecular weight marker was also used with 1 µl Rainbow Ladder added to 9 µl 1xLDS sample buffer supplemented with 5 % β-mercaptoethanol. All protein samples were loaded onto NuPAGE 4-12 % Bis-Tris 1 mm 10-well gels, in 1xMES SDS running buffer (Novex Life Technologies, order number: NP0002) for 5 min at 200 V. Gaps were left between different protein samples to prevent cross-contamination during In-Gel Trypsin Digestion (See section 7.5.7.2). After the protein samples had just entered the gel, the gel was transferred into a glass dish and washed in dH_2O. Colloidal Blue staining of the gel was then carried out according to manufacturers protocol using the Invitrogen Colloidal Blue Staining Kit (order number: LC6025). The gels were typically left to stain for 5-6 h, then de-stained for 18 h in dH_2O, with the water being changed regularly to aid de-staining.

7.5.7.2 In-gel trypsin digestion

The Colloidal Blue-stained NuPage protein gels containing samples for mass spectrometry had been destaining in dH_2O overnight. To carry out In-gel trypsin digestion, a sterile fume hood was utilised. The gel slices were cut out, and with a clean scalpel cut into 1 mm^3 pieces and transferred to a sterile 1.5 ml eppendorf containing 50 mM ammonium

bicarbonate (ABC) solution, and incubated for 5 min. The 50 mM ABC was removed by pipetting, and equal volume of acetonitrile (ACN) added for 5 min at room temperature to shrink the gel pieces. The alternate 5 min washes in 50 mM ABC and ACN were continued until all coomassie staining was removed from the gel pieces. After the final ACN wash, 50 µl of 10 mM DTT (1 M DTT diluted in 50 mM ABC) was added to the gel pieces, which were then incubated at 37 ^{o}C for 30 min. After removal of the DTT solution, ACN solution was added and the gel pieces incubated at room temperature for 5 min. The gel pieces were then placed into 55 mM iodoacetamide (dissolved in 50 mM ABC) and incubated in the dark for 20 min at room temperature. The excess 55 mM iodoacetamide was removed and the gel slices incubated in 50 mM ABC for 5 min, the ABC then removed, and the gel slices incubated in ACN for 5 min. The ACN was removed and the gel slices placed in 150 µl trypsin digestion mix (13 µg/ml trypsin (Thermo Scientific, Pierce Trypsin order number: 90057, 10 % ACN, 10 mM ABC) and incubated on ice for 15 min, then incubated at 37 ^{o}C for 16 h.

7.5.7.3 Stage-Tip

The gel pieces had been in trypsin digestion solution overnight at 37 ^{o}C. Equal volume of 0.1 v/v TFA (trifluoroacetic acid) was added, then the pH adjusted to pH 3 with 10 % TFA. The gel pieces were then incubated at room temperature for 15 min to allow the peptides sufficient time to diffuse out of the gel. The Stage Tip was made by placing two Empore C18 Disks (3M) in a 200 µl sterile pipette tip. The Stage Tip was washed by passing 20 µl MeOH through the Empore C18 Disks, followed by 40 µl of 0.1 % TFA. The peptide sample was passed through the Stage Tip, followed by a wash of 60 µl of 0.1 % TFA. The Stage Tip was then stored at -20 ^{o}C.

7.5.7.4 Mass spectrometry and analysis

The final steps of processing the Stage Tip and injection of the peptides into an Orbitrap Fusion Lumos Tribrid Mass spectrometre (Thermo Fisher Scientific) was carried out by C. Spanos, as described in (Blyth *et al.*, 2018). The results were analysed by C. Spanos using the MaxQuant software platform.

7.5.8 Co-immunoprecipitation

7.5.8.1 Growing and cross-linking cells with DSP

Cells were grown according to standard protocols in sections 7.3.5 and 7.3.6. For some co-immunoprecipitation experiments, cells were cross-linked with DSP (dithiobis

succinimidyl propionate) (DSP, Thermo Scientific, order number: 22585). Cells grown for co-immunoprecipitation, either with or without cross-linking, were drop frozen as in section 7.5.4.1.

For cross-linking, after completion of cell growth, the cells were pelleted by centrifugation at 4000 rpm for 5 min, and resuspended in 5 ml Reaction Buffer (20 mM Hepes-KOH pH 7.4, 100 mM potassium acetate) supplemented with 400 µl of 25 mM DSP (DSP dissolved in DMSO). The cells were fixed with rotation or shaking at 90 rpm for 30 min at room temperature. The cells were pelleted by centrifugation at 3000 rpm for 5 min, then resuspended in 5 ml 10 mM Tris-HCl pH 7.5 and incubated with rotation or shaking at 90 rpm for 5 min at room temperature. The cells were pelleted by centrifugation at 3000 rpm for 5 min at 4 ^{o}C, washed in 20 ml dH_2O, then resuspended in 20 % w/v dH_2O for drop freezing in liquid nitrogen.

7.5.8.2 Grinding of cells for co-immunoprecipitation

For large scale co-immunoprecipitation experiments (Figure 5.2.7.2) cells were ground using a Retsch Twin Biopulveriser (see section 7.5.4.2). For all other co-immunoprecipitation experiments cells were ground by hand for 10 min using a pestle and mortar chilled on dry ice, until in all yeast noodles were powdered. The yeast grindate was then snap frozen in liquid nitrogen and stored at -80 ^{o}C.

7.5.8.3 Coupling beads to antibodies for co-immunoprecipitation experiments

For co-immunoprecipitation experiments carried out by immunoprecipitation of a FLAG-tagged protein, Protein G Dynabeads (Invitrogen 20 mg/ml) were coupled to 1 mg/ml M2 FLAG antibody (Sigma, order number: F1804) according to the protocol described in section 7.5.4.3. For each co-immunoprecipitation experiment, 50 µl of 20 mg/ml were used.

For co-immunoprecipitation experiments carried out by immunoprecipitation of SZZ-TAP-tagged protein, Epoxy-activated M270 Dynabeads (Invitrogen order number: 14302D) were coupled to 1 mg/ml Rabbit IgG (Sigma Aldrich, order number: I5006). Enough Epoxy-activated Dynabeads were weighed into a 1.5 ml eppendorf so that each there was 2 mg beads/co-immunoprecipitation experiment. For example, 6 mg Epoxy-activated Dynabeads were resuspended in 600 µl of 0.1 M sodium phosphate buffer pH 7.4 (500 ml made by dissolving 1.31 g $NaH_2PO_4{\cdot}H_2O$ and 7.21 g $Na_2HPO_4{\cdot}2H_2O$ in dH_2O) and washed for 5 min on a rotating wheel at room temperature. The beads were separated, and the supernatant

removed, and the wash in 1 ml of 0.1 M sodium phosphate buffer pH 7.4 repeated twice more. The beads were then resuspended in 118.8 µl of 0.1 M sodium phosphate buffer pH 7.4, 118.8 µl 1 mg/ml Rabbit IgG, and 118.8µl 3 M ammonium sulphate, and incubated with rotation at 37 ^{o}C for 24 h. The beads were then washed four times for 5 min/wash in 1 ml PBS (13.7 mM NaCl, 270 µM KCl, 1 mM Na_2PO_4, 176 µM KH_2PO_4), then washed three times for 5 min/wash in 1 ml of the IP buffer. For the IP, the beads were resuspended in 250 µl of the IP buffer, and 75 µl beads used/IP (equivalent to 1.8 mg beads/IP).

7.5.8.4 Bradford assay

To carry out a Bradford assay 20 µl 50 mM Tris pH 7.5 with 300 mM NaCl was placed in a 1.5 ml eppendorf, with one eppendorf required for each immunoprecipitation sample, and one for the blank. Once the lysate for the immunoprecipitation is obtained, 10 µl is placed in the eppendorf containing 20 µl 50 mM Tris pH 7.5 with 300 mM NaCl and vortexed briefly. For the blank, 10 µl of the lysis buffer is added instead. The eppendorfs were then centrifuged at 13000 rpm for 3 min at 4 ^{o}C, and 3 µl of each sample placed in a clean 1.5 ml cuvette. To each cuvette, 1 ml of Biorad Bradford Reagent (diluted to 20 % v/v in water) was added, and the cuvette vortexed and the OD_{595} measured. The protein concentration was then calculated by: Protein concentration mg/ml = OD_{595}/0.043.

7.5.8.5 Small scale immunoprecipitation of SZZ-TAP-tagged proteins

The buffer for the immunoprecipitation is shown in Table 7.5.8.5. As for the large-scale purification of proteins in section 7.5.4.4, Buffer H 0.15 was used, but was supplemented with different concentrations of protease inhibitors.

Table 7.5.8.5: Solutions for immunoprecipitation

Solution	Composition
Buffer H 0.15 supplemented with inhibitors	4.6 ml Buffer H 0.15 5 µl 2000 x CLAAPE 200 µl 400 mM pefablock 200 µl 50 x Roche EDTA-free protease inhibitor

The ground cells were thawed gently on ice, and 500 µl of Buffer H 0.15 supplemented with inhibitors (as in Table 7.5.8.5) was added to each tube and the lysate mixed until there were no lumps. The cell lysates were sonicated using a tip sonicator (Sonics Vibracell V505) at 20 % 1 sec ON, 15 sec OFF for 5 sec total sonication, in a glass beaker on ice to keep the sample cool. To each sample, 0.2 µl of benzonase was added to a final concentration of

40 U/ml, the samples mixed by inversion, and incubated on ice for 1 h. The cell debris was pelleted by centrifugation at 13000 rpm for 5 min at 4 ^{o}C, and the supernatant transferred to a fresh 1.5 ml eppendorf. A Bradford assay was carried out to determine protein concentration (see section 7.5.8.4). 3 mg of cell lysate was then transferred into a fresh eppendorf containing 75 µl of pre-coupled epoxy-activated Dynabeads to rabbit IgG (see section 7.5.8.3), and the immunoprecipitation reaction incubated at 4 ^{o}C for 90 min with rotation at 14 rpm. Input samples were taken from the cell lysate, of 1-5 % total IP volume, 4xLDS sample buffer supplemented with 5 % β-mercaptoethanol added, and the samples boiled at 95 ^{o}C for 5 min, then centrifuged at 13000 rpm for 5 min. After the immunoprecipitation reactions had been incubated for 90 min, the beads were separated from the lysate, the supernatant removed, and the beads then washed 5 times in 1 ml Buffer H 0.15 for 5 min/wash on a rotating wheel at 14 rpm at 4 ^{o}C. The final wash was removed, and the beads resuspended in 30 µl 1xLDS sample buffer with 5 % β-mercaptoethanol added, then the samples boiled at 95 ^{o}C for 5 min. The beads were separated from the supernatant, and the protein samples were then loaded directly onto an SDS-PAGE gel for western blotting.

7.5.8.6 Small scale co-immunoprecipitation of Sgo1-6HIS-3FLAG and Rec8-3HA

The buffer for the immunoprecipitation is shown in Table 7.5.8.6. As for the large-scale purification of proteins in section 7.5.4.4, Buffer H 0.15 was used with the same protease and phosphatase inhibitors.

Table 7.5.8.6: Solutions for immunoprecipitation

Solution	Composition
Buffer H 0.15 supplemented with inhibitors	8.66 ml Buffer H 0.15 10 µl 2000 x CLAAPE 50 µl 400 mM pefablock 80 µl 100 mM Na orthovanadate 2 µl 100 µM microcystin 200 µl 50 x Roche EDTA-free protease inhibitor 500 µl 40 mM NEM 500 µl 20 x phosphatase inhibitors

For each immunoprecipitation experiment, 50 µl of Protein G Dynabeads were coupled to M2 FLAG antibody, as described in section 7.5.4.3. The beads were blocked in 5 % milk in PBS for 1 h at 4 ^{o}C with rotation at 14 rpm, then washed three times in 1 ml Buffer H 0.15

for 5 min/wash, then resuspended in Buffer H 0.15 supplemented with inhibitors so there was 100 µl volume beads/IP.

The ground cells were thawed gently on ice, and 700 µl of Buffer H 0.15 supplemented with inhibitors (as in Table 7.5.8.6) was added to each tube and the lysate mixed until there were no lumps. To each sample, 0.2 µl of benzonase was added to a final concentration of 40 U/ml, the samples mixed by inversion, and incubated on ice for 1 h. The cell debris was pelleted by centrifugation at 3000 rpm for 5 min at 4 ^{o}C, and the supernatant transferred to a fresh 1.5 ml eppendorf. A Bradford assay was carried out to determine protein concentration (see section 7.5.8.4). 3 mg of cell lysate was transferred into a fresh eppendorf containing 100 µl of Protein G Dynabeads coupled to M2 FLAG antibody, and the immunoprecipitation incubated at 4 ^{o}C for 150 min with rotation at 14 rpm. Input samples were taken from the cell lysate, of 1-5 % total IP volume, 4xLDS sample buffer supplemented with 5 % β-mercaptoethanol added, and the samples boiled at 95 ^{o}C for 5 min, the centrifuged at 13000 rpm for 5 min. After the immunoprecipitation reactions had been incubated for 150 min, the Protein G Dynabeads were separated from the cell lysate using a magnet, the supernatant removed, and the beads were washed with rotational mixing at 14 rpm at 4 ^{o}C in 1 ml Buffer H 0.15 supplemented with inhibitors and 2 mM DTT for 10 min, and the supernatant removed. The beads were then washed a further three times, for 10 min/wash, in 1 ml Buffer H 0.15 supplemented with inhibitors. The supernatant was removed and 20 µl 0.5 mg/ml FLAG peptide in Buffer H 0.15 supplemented with inhibitors added to the beads, and incubated with rotational mixing for 30 min at 4 ^{o}C. The lysate was separated from the beads and 10 µl 4xLDS sample buffer with 5 % β-mercaptoethanol added, then the samples boiled at 95 ^{o}C for 5 min. The beads were separated from the supernatant, and the protein samples were then loaded directly onto an SDS-PAGE gel for western blotting.

7.5.8.7 Small scale co-immunoprecipitation of Sgo1-SZZ-TAP and cohesin

To carry out the immunoprecipitation of Sgo1-SZZ-TAP in section 5.2.7 the protocol in section 7.5.8.6, using the buffer in Table 7.5.8.6, was followed with some alterations.

A total of 3 g of cell pellet was obtained for each strain, and ground in the Retsch Twin Biopulveriser (see section 7.5.4.2). As before, the ground cells were thawed on ice, the Buffer H 0.15 supplemented with inhibitors added, and then the sample supplemented with

40 U/ml benzonase and incubated for 1 h at 4 °C. After pelleting the cell debris at 3000 rpm for 5 min at 4 °C, a Bradford assay was carried out, and 40 mg of protein lysate was added to 2 mg of Epoxy-activated Dynabeads pre-coupled to rabbit IgG (see section 7.5.8.3). The beads were incubated with rotation at 4 °C for 90 min, then washed four times in 1 ml Buffer H 0.15 supplemented with inhibitors for 10 min/wash (the first wash was supplemented with 2 mM DTT). The beads were resuspended in 20 µl 4xLDS sample buffer with 5 % β-mercaptoethanol added, then the samples boiled at 95 °C for 5 min. The beads were separated from the supernatant, and the protein samples were then loaded directly onto an SDS-PAGE gel for western blotting.

7.5.9 Expression of recombinant GST-Sgo1 in *E. coli*

7.5.9.1 Induction of recombinant protein expression

E. coli that had been transformed with the plasmid encoding the recombinant protein, were inoculated into LB+Amp and grown at 37 °C shaking at 200 rpm overnight. The *E. coli* culture was diluted 1 in 100 in fresh LB+Amp media and was grown for several hours at 37 °C shaking at 200 rpm until the culture density was OD_{600}=0.5. The culture was then placed at 25 °C for 30 min. If induction of protein expression was required, then 1 mM IPTG (Isopropyl β-D-1-thiogalactopyranoside) was added to the culture, and the cultures grown at 25 °C shaking at 200 rpm for a further 4 h. If no protein induction was required, the IPTG was omitted, and the cultures also grown for a further 4 h. The cells were harvested by centrifugation at 3000 rpm for 10 min at 4 °C, the supernatant removed, and the cell pellets stored at -20 °C.

7.5.9.2 Small-scale pull-down of recombinant GST-tagged protein

The buffer for the small-scale pull-down of GST-tagged proteins is shown in Table 7.5.9.2.

Table 7.5.9.2: Solutions for pull-down of GST-tagged proteins

Solution	Composition
Buffer X	50 mM Tris-HCl pH 8 150 mM NaCl 10 % glycerol 5 mM DTT 0.3 mM PMSF

To prepare the glutathione agarose resin, (glutathione-agarose lyophilised powder, Sigma Aldrich, order number G4510) was prepared according to standard protocol, with 5 mg of

glutathione agarose resin/pull-down prepared. Prior to the pull-down being carried out the beads were washed seven times in 1 ml of PBS and three times in Buffer X for 5 min/wash, with the beads being pelleted at 2000 rpm for 1 min between washes. The *E. coli* pellets from 30 ml of cell culture were gently thawed on ice and 1 ml of Buffer X added, and the lysate mixed until smooth. The lysate was transferred into a 2 ml fast-prep tube and lysed by sonication using a tip sonicator (Sonics Vibracell V505) at 20 % 1 sec ON, 1 sec OFF for 90 sec total sonication. The cell debris was pelleted at 13000 rpm for 10 min at 4 ^{o}C. Samples of pellet and supernatant were taken, 3xSDS sample buffer added, and the samples boiled at 95 ^{o}C for 5 min. To the glutathione agarose resin (5 mg agarose/sample), 900 µl of cell lysate was added and the beads incubated at 4 ^{o}C for 3 h with rotation at 14 rpm. The beads were pelleted by centrifugation at 2000 rpm for 1 min, then washed five times in 1 ml Buffer X, with the beads being pelleted by centrifugation at 2000 rpm for 1 min between each wash. After the final wash was removed, the beads were resuspended in 10 µl 3xSDS sample buffer, and boiled for 5 min at 95 ^{o}C, then the supernatant transferred to a new eppendorf.

7.5.9.3 Binding yeast Brn1-6HA to recombinant GST-Sgo1

Budding yeast containing *BRN1-6HA* were grown in YEPDA according to standard protocol. An overnight pre-culture was diluted to OD_{600}=0.2 in fresh 100 ml YEPDA and grown for 6 h at 30 ^{o}C shaking at 250 rpm. The cells were then pelleted by centrifugation at 4000 rpm for 5 min at 4 ^{o}C, resuspended in 20 % w/v ice cold dH_2O, and drop frozen in liquid nitrogen. The cell pellets were ground by hand as described in section 7.5.8.2.

The yeast grindate was thawed gently on ice, and 500 µl Buffer Y added and the lysate mixed until smooth, then 0.1 % v/v Triton-X-100 added. The lysate was sonicated using a tip sonicator (Sonics Vibracell V505) at 20 % 1 sec ON, 15 sec OFF for 5 sec total sonication. The cell debris was pelleted at 13000 rpm for 10 min at 4 ^{o}C, and the supernatant transferred into a fresh 1.5 ml eppendorf. A Bradford assay was carried out on the cell lysate, and 3.5 mg protein lysate added to 0.005 g glutathione agarose resin that had been pre-incubated with GST-Sgo1 or GST alone. The yeast lysate was incubated with the glutathione resin for 3 h at 4 ^{o}C with rotation at 14 rpm. The glutathione agarose resin was separated from the lysate by centrifugation at 2000 rpm for 1 min, and the supernatant removed. The glutathione agarose resin was washed five times in Buffer Y, the final wash removed, 20 µl 3xSDS sample buffer added, and the resin boiled for 5 min at 95 ^{o}C.

The buffer for the pull-down of Brn1-6HA with GST-tagged proteins is shown in Table 7.5.9.3.

Table 7.5.9.3: Solutions for pull-down of GST-tagged proteins

Solution	Composition
Buffer Y	50 mM Tris-HCl pH 8 50 mM NaCl 10 % glycerol 1x CLAAPE 1x Roche EDTA-free protease inhibitor 2 mM pefabloc 1 mM benzamidine 4 mM NEM 0.8 mM Na orthovanadate 0.2 µM microcystin 1 x phosphatase inhibitors

7.5.10 Coomassie staining

Recombinant protein samples were run on an SDS-PAGE gel. To visualise the proteins, the SDS-PAGE gel was placed in a glass container and coomassie stain added (0.1 % Coomassie Blue R250, 10 % acetic acid, 50 % MeOH). The gel was briefly placed in the microwave (about 10 sec) then incubated on a rocking platform at 15 rpm for 10 min to allow protein staining to occur. The coomassie stain was removed and the gel rinsed several times in dH_2O, then placed in destain (16.7 % v/v acetic acid, 16.7 % v/v MeOH) for 2-3 h to remove excess coomassie. The gel was then placed in dH_2O and stored at 4 ^{o}C.

7.5.11 Chromatin Immunoprecipitation (ChIP)

The solutions for ChIP are shown in Table 7.5.11.

Table 7.5.11: Solutions for ChIP

Solution	Composition
Diluent	143 mM NaCl 1.43 mM EDTA 71.43 mM Hepes-KOH pH 7.5
Fixing solution	1.5 ml 37 % Formaldehyde 3.5 ml Diluent
TBS	20 mM Tris-HCl pH 7.5 150 mM NaCl

Table 7.5.11: Solutions for ChIP continued

Solution	Composition
2 x FA lysis buffer	100 mM Hepes-KOH pH 7.5 300 mM NaCl 2 mM EDTA 2 % v/v Triton X-100 0.2 % v/v Na Deoxycholate
ChIP wash buffer 1	1 x FA lysis buffer 0.1 % v/v SDS 275 mM NaCl
ChIP wash buffer 2	1 x FA lysis buffer 0.1 % v/v SDS 500 mM NaCl
ChIP wash buffer 3	10 mM Tris-HCl pH 8 250 mM LiCl 1 mM EDTA 0.5 % v/v NP-40 0.5 % v/v Na Deoxycholate
ChIP wash buffer 4	10 mM Tris-HCl pH 8 1 mM EDTA

7.5.11.1 Fixation of cell culture for ChIP

For ChIP of mitotic cells 90 ml of cell culture was used, and for ChIP of meiotic cells 45 ml of cell culture was used. In a 50 ml falcon tube, 45 ml of cell culture was mixed with 5 ml of fixing solution, and incubated rocking at 12 rpm for 2 h at room temperature. The cells were pelleted at 3000 rpm for 3 min at 4 ^{o}C, and washed twice in 10 ml of ice-cold TBS, then once in 10 ml ice-cold 1xFA lysis buffer with 0.1 % v/v SDS. The cells were pelleted at 3000 rpm for 3 min at 4 ^{o}C and the supernatant removed. The pellet was resuspended in 500 µl of 1xFA lysis buffer with 0.1 % v/v SDS and transferred into a 2 ml fast-prep tube (MP Biomedicals). For mitotic ChIP, the two falcon tubes for each strain were combined into one fast-prep tube. The cells were pelleted at 13000 rpm for 1 min at 4 ^{o}C, the supernatant aspirated off, and the tube snap-frozen in liquid nitrogen and stored at -80 ^{o}C.

7.5.11.2 ChIP

The cell pellets for ChIP were thawed gently on ice, and the pellet resuspended in 300 µl 1xFA lysis buffer with 0.5 % v/v SDS, 1x Roche EDTA-free protease inhibitors and 1 mM PMSF. To the tube, 1 scoop of glass beads (0.5mM zirconia/silica glass beads, Biospec Products) was added, and the cells lysed by shaking in a Fastprep Bio-Pulveriser FP120 at 6.5 speed for 2 cycles of 30 sec, with a 10 min waiting period on ice between cycles. A small 0.5 mM hot needle was used to make a hole in the bottom of the fast-prep tube, which was subsequently placed onto a new 2 ml fast-prep tube, and both placed inside a 15 ml flacon

tube. The falcon tube was centrifuged at 2500 rpm for 3 min at 4 ^{o}C to transfer the cells and supernatant into the fresh fast-prep tube, and to separate the beads. The cell debris and supernatant were transferred into a 1.5 ml eppendorf, and the chromatin and cell debris pelleted at 13000 rpm for 15 min at 4 ^{o}C. The pellet was gently resuspended in 1 ml 1xFA lysis buffer with 0.1 % v/v SDS, 1x Roche EDTA-free protease inhibitors and 1 mM PMSF, and the centrifugation step repeated. The chromatin should be visible as a glass-like transparent layer across the top of the pellet. The pellet was gently resuspended in 300 µl 1xFA lysis buffer with 0.1 % v/v SDS, 1x Roche EDTA-free protease inhibitors and 1 mM PMSF, then sonicated at 4 ^{o}C in a Bioruptor Twin sonicating device (Diagenode) on HIGH 30 sec ON, 30 sec OFF for 30 min total sonication. The cell debris was pelleted at 13000 rpm for 15 min at 4 ^{o}C, and the supernatant transferred into a new 1.5 ml eppendorf containing 1 ml of 1xFA lysis buffer with 0.1 % v/v SDS, 1x Roche EDTA-free protease inhibitors and 1 mM PMSF. The centrifugation step was repeated, and the supernatant transferred into a new 1.5 ml eppendorf. For the INPUT sample, 10 µl of the supernatant was placed in a new 1.5 ml eppendorf and frozen at -20 ^{o}C overnight. For the IP, 15 µl Protein G Dynabeads (Invitrogen 20 mg/ml)/sample were pre-washed four times in 1 ml 1xFA lysis buffer with 0.1 % v/v SDS, 1x Roche EDTA-free protease inhibitors and 1 mM PMSF, then resuspended in 1xFA lysis buffer with 0.1 % v/v SDS, 1x Roche EDTA-free protease inhibitors and 1 mM PMSF. To 1 ml of cell supernatant, 100 µl of Protein G Dynabeads was added, along with the appropriate antibody (see Table 7.5.11.2), and the IP incubated at 4 ^{o}C on a rotating wheel at 14 rpm for 15-18 h.

The IP samples were incubated at 4 ^{o}C overnight. These were placed on a small magnet for 30 sec to allow the beads to separate, and the supernatant removed. The beads were washed 5 min/wash consecutively in ChIP wash buffer 1, ChIP wash buffer 2, ChIP wash buffer 3 and ChIP wash buffer 4, with 30 sec on a small magnet in-between each wash. After the final wash, all of the supernatant was removed from the beads. Chelex-100 Resin (Biorad) was resuspended at 0.1 g/ml in Hyclone water (Hypure Molecular Biology Grade Water, GE Lifesciences), and 100 µl added to the thawed and vortexed INPUT samples, and the IP samples. The samples were boiled at 100 ^{o}C for 10 min in a heat block, cooled on ice, then briefly centrifuged at 2000 rpm for 1 min. To each tube 2.5 µl 10 mg/ml Proteinase K (Invitrogen) was added, the samples vortexed and then incubated at 55 ^{o}C for 30 min. The samples again boiled at 100 ^{o}C for 10 min in a heat block, cooled on ice, then briefly

centrifuged at 2000 rpm for 1 min. Approximately 120 µl of supernatant containing the DNA was transferred into a new 1.5 ml eppendorf, and frozen at -20 ^{o}C.

The following antibodies in Table 7.5.11.2 were used to carry out ChIP.

Table 7.5.11.2: ChIP antibodies

Antibody	Species	Concentration	Volume (µl)	Company
HA (12CA5)	Mouse	0.4 mg/ml	7.5	Roche (11666606001)
FLAG (M2)	Mouse	1 mg/ml	5	Sigma (F1804)

7.6 Microscopy methods

7.6.1 Ethanol fixation and DAPI staining

For mitotic cell samples, 200 µl of cell culture was placed into a 1.5ml eppendorf and cells pelleted by centrifugation at 3000 rpm for 2 min. The supernatant was then removed, and the cells resuspended in 500 µl of 80 % EtOH and placed at 4 ^{o}C. For meiotic cell samples, 100 µl cell culture was added directly to 400 µl of 100 % EtOH in a 1.5 ml eppendorf, and placed at 4 ^{o}C. For DAPI staining, the cells were pelleted at 13000 rpm for 1 min, then resuspended in 20 µl of 1 µg/ml DAPI in PBS (Stock 100 µg/ml DAPI in PBS) and stored at 4 ^{o}C until scoring by fluorescence microscopy could be carried out. To score, 3 µl of the sample was placed onto a 1 mm thick glass slide (Fisher Scientific) and a 18 x18 mm cover slip (VWR) placed on this.

7.6.2 Visualisation of GFP dots

To visualise GFP dots, 100 µl of meiotic cell culture was placed directly into a 1.5 ml eppendorf containing 10 µl of 37 % formaldehyde. The cells were incubated in formaldehyde solution for 8 min at room temperature before the cells were pelleted by centrifugation at 13000 rpm for 1 min. The supernatant was removed by aspiration and 1 ml of 80 % EtOH added and the eppendorf briefly vortexed. The cells were pelleted at 13000 rpm for 15 sec, the supernatant removed, and the centrifugation step repeated. The remaining ethanol was removed by pipetting, and the cell pellet resuspended in 20 µl of 1 µg/ml DAPI in PBS, and stored at 4 ^{o}C for a maximum of 48 h, until scoring by fluorescence microscopy could be carried out. To score, 3 µl of the sample was placed onto a 1 mm thick glass slide (Fisher Scientific) and a 18 x18 mm cover slip (VWR) placed on this.

7.6.3 Immunofluorescence

The following solutions shown in Table 7.6.3A were used to carry out immunofluorescence.

Table 7.6.3A: Immunofluorescence solutions

Solution	Composition
0.1 M potassium phosphate buffer pH 6.4	27.8 ml of 1 M K_2HPO_4 72.2 ml of 1 M KH_2PO_4 900 ml dH_2O
3.7 % formaldehyde solution	10 % v/v 37 % formaldehyde 90 % v/v 0.1 M potassium phosphate buffer pH 6.4
1.2 M sorbitol-citrate	1.2 M sorbitol 0.1 M K_2HPO_4 36 mM citric acid
Digestion Solution	200 µl 1.2 M sorbitol-citrate 20 µl glusulase (Perkin-Elmer) 6 µl 10 mg/ml zymolyase (AMS Biotechnology)
PBS/BSA	1 % w/v BSA 40 mM K_2HPO_4 10 mM KH_2PO_4 150 mM NaCl 0.1 % NaN_3
DAPI-Mount	1 mg/ml *p*-phenylenediamine 0.05 µg/ml DAPI 40 mM K_2HPO_4 10 mM KH_2PO_4 150 mM NaCl 0.1 % NaN_3 90 % glycerol

To carry out immunofluorescence, 300 µl of meiotic cell culture was placed in a 1.5 ml eppendorf, and the cells pelleted by centrifugation at 13000 rpm for 1 min. The supernatant was removed by aspiration, and the cell pellet resuspended in 500 µl of 3.7 % formaldehyde solution, and placed at 4 ^{o}C overnight. The next day (maximum of 3 days later), the cells were pelleted by centrifugation and washed 3 times in 1 ml of 0.1 M potassium phosphate buffer pH 6.4, then resuspended in 1.2 M sorbitol-citrate. The cell solution was then either stored indefinitely at -20 ^{o}C, or the immunofluorescence protocol immediately continued.

To prepare the multi-well slides (Thermo Scientific, 30 well, 2 mM slides), 5 µl of 0.1 % polylysine was placed in each well and let to sit for 5 min before removing by washing in dH_2O, followed by air-drying the slide. In the meantime the cells were pelleted by

centrifugation at 13000 rpm for 1 min, the supernatant removed, and the cells resuspended in 226 µl of Digestion Solution. Cells were digested at 30 ^{o}C for 2-3 h, and the digestion checked by light microscopy for the presence of phase-dark cells with jagged edges. The cells were pelleted at 3000 rpm for 2 min, gently washed in 1.2 M sorbitol-citrate, then the cells resuspended in approximately 30 µl 1.2 M sorbitol-citrate. The cells were fully resuspended in 1.2 M sorbitol-citrate, and 5 µl placed onto each well of the slide and allowed to sit for 10 min, followed by excess liquid being removed by aspiration. Cell density was verified by light microscopy, then the slide was incubated in 100 % MeOH for 3 min followed by 10 sec in 100 % acetone. To each well, 5 µl of primary antibody was added (diluted to 1 x in PBS/BSA), and the slide incubated in the dark in a wet chamber at room temperature for 2 h. Each well of the slide was washed five times in 5 µl PBS/BSA with removal of excess liquid by aspiration between each wash. To each well, 5 µl of secondary antibody was added (diluted to 1 x in PBS/BSA), and the slide incubated in the dark in a wet chamber at room temperature for 2 h. Each well of the slide was washed five times in 5 µl PBS/BSA with removal of excess liquid by aspiration between each wash. To each well, 3 µl of DAPI-Mount was added, and a cover-slip (24x60 mm coverslip) placed on top, and all air bubbles removed, before sealing with clear nail varnish. Slides were then stored at -20 ^{o}C.

The following antibodies in Table 7.6.3B were used to carry out immunofluorescence.

Table 7.6.3B: Immunofluorescence antibodies

Antibody	Species	Concentration	Dilution	Company
Mono α-tubulin	Rat	1 mg/ml	1:50	Bio-Rad AbD Serotec
Anti-rat-FITC	Donkey	1.25 mg/ml	1:100	Jackson immunoResearch

7.6.4 Fluorescence microscopy

Fluorescence microscopy analysis was carried out on a Zeiss Axioplan 2 fluorescence microscope with a 100 x Plan ApoChromat NA 1.45 oil lens. Prior to microscopy, lens oil was placed on the cover slip (Zeiss Immersol 518F).

7.6.5 Live cell imaging

7.6.5.1 Live cell imaging using microfluidics on the Deltavision Elite System

To carry out live cell imaging using the microfluidics system, diploid cells were induced to undergo meiosis by placing in SPO media according to standard protocol. All strains were

incubated at 30 ^{o}C shaking at 250 rpm for 90-120 min (*rad61Δ* strains incubated for 60-90 min longer) before placing onto the microfluidics plate (CellASIC ONIX microfluidics plate, order number: Y04D-02). The microfluidics plate was prepared by first purging the plates by attaching to the manifold of a ONIX microfluidics system (CellASIC) and following the standard manufacturers purging protocol. The wells of the microfluidics plate were then washed three times in 200 µl SPO media, and the wells then filled with 200 µl SPO media, and the plate placed at 30 ^{o}C to pre-heat for a minimum of 30 min. After the cells had been in SPO media for 90-120 min, 200 µl cell culture was placed in the appropriate wells of the microfluidics plate. The cells were loaded into the microfluidics chamber by attaching the microfluidics plate to the manifold of the ONIX microfluidics system, and the manufacturers cell loading protocol followed. The microfluidics experiment was run for 12 h, with each well supplying the microfluidics system for 150 min at a pressure of 2 psi.

The microfluidics live cell imaging experiment was carried out on a Deltavision Elite System (Applied Precision) on an inverted Olympus IX-71 microscope with a 100 x UplanSApo NA 1.4 oil lens. A photometrics Cascade II EMCCD camera was used to acquire images for the experiments. The software used was SoftWorx (Applied Precision) on a Linux computer. The live cell imaging experiment was carried out for 12 h, with images taken every 15 min. For each strain 8 points containing a high density of cells were imaged for FITC, Tomato and Brightfield, with 7 Z-stacks of 0.85 µM taken for the FITC and Tomato channels. For imaging of *CEN5 tetO*/TetR-GFP dots, the FITC channel the imaging conditions were: Camera gain 390, 5 % transmitted light and 0.1 sec exposure. For imaging of Spc42-tdTomato and Pds1-tdTomato, the red channel the imaging conditions were: Camera gain 390, 5 % transmitted light and 0.1 sec exposure. The images were analysed using the ImageJ software version 2.0.0-rc-43/1.51g (National Institutes of Health).

7.6.5.2 Live cell imaging using 8-well Ibidi dishes on the Zeiss microscope

To carry out live cell imaging using Ibidi dishes, diploid cells were induced to undergo meiosis by placing in SPO media according to standard protocol. All strains were incubated at 30 ^{o}C shaking at 250 rpm for 90-120 min (*rad61Δ* strains incubated for 60-90 min longer) before placing onto the Ibidi dish. The Ibidi glass-bottomed 15 µ-slide 8 well dish (Ibidi, order number: 80827) was prepared by spreading 45 µl 5 mg/ml concanavalin A (dissolved in 50 mM $CaCl_2$, 50 mM $MnCl_2$) evenly in the bottom of each well of the Ibidi dish and incubating at 30 ^{o}C for 15 min. The excess concanavalin A was removed by aspiration, and

the each well washed three times in 500 µl dH_2O. After the cells had been in SPO media for 90-120 min, 1.5 ml of cell culture was placed in a 1.5 ml eppendorf, and the cells pelleted by centrifugation at 3000 rpm for 3 min. The cells were resuspended in 300 µl of the SPO media in which the cells were grown in, and added to the wells of the Ibidi dish. The dish was incubated at 30 ^{o}C for 20 min. The excess SPO culture was aspirated from the wells of the dish, and the wells washed twice in 500 µl of SPO media in which the cells had been grown in, before 300 µl of the SPO media was added to each well.

The live cell imaging experiment was carried out on a Zeiss Axio Observer Z1 (Zeiss UK, Cambridge) with a Prior motorised stage. A Hamamatsu Flash 4 sCMOS camera was used to acquire images for the experiments. The acquisition software used was Zen 2.3 on a Linux computer. The live cell imaging experiment was carried out for 12 h, with images taken every 15 min. For each strain 8 points containing a high density of cells were imaged for FITC, Tomato and Brightfield, with 8 Z-stacks of 0.8 µM taken for the FITC and Tomato channels. For imaging of *CEN5 tetO*/TetR-GFP dots, the FITC channel the imaging conditions were: Binning 4x4, 5 % transmitted light and 0.15 sec exposure. For imaging of Spc42-tdTomato and Pds1-tdTomato, the red channel the imaging conditions were: Binning 4x4, 5 % transmitted light and 0.2 sec exposure. The images were analysed using the ImageJ software version 2.0.0-rc-43/1.51g (National Institutes of Health).

References

Akiyoshi, B., Nelson, C. R., Ranish, J. A. and Biggins, S. (2009) 'Analysis of Ipl1-mediated phosphorylation of the Ndc80 kinetochore protein in Saccharomyces cerevisiae', *Genetics,* 183(4), pp. 1591-5.

Alexandru, G., Uhlmann, F., Mechtler, K., Poupart, M. A. and Nasmyth, K. (2001) 'Phosphorylation of the cohesin subunit Scc1 by Polo/Cdc5 kinase regulates sister chromatid separation in yeast', *Cell,* 105(4), pp. 459-72.

Alomer, R. M., da Silva, E. M. L., Chen, J., Piekarz, K. M., McDonald, K., Sansam, C. G., Sansam, C. L. and Rankin, S. (2017) 'Esco1 and Esco2 regulate distinct cohesin functions during cell cycle progression', *Proc Natl Acad Sci U S A,* 114(37), pp. 9906-9911.

Arguello-Miranda, O., Zagoriy, I., Mengoli, V., Rojas, J., Jonak, K., Oz, T., Graf, P. and Zachariae, W. (2017) 'Casein Kinase 1 Coordinates Cohesin Cleavage, Gametogenesis, and Exit from M Phase in Meiosis II', *Dev Cell,* 40(1), pp. 37-52.

Arumugam, P., Gruber, S., Tanaka, K., Haering, C. H., Mechtler, K. and Nasmyth, K. (2003) 'ATP hydrolysis is required for cohesin's association with chromosomes', *Curr Biol,* 13(22), pp. 1941-53.

Attner, M. A., Miller, M. P., Ee, L. S., Elkin, S. K. and Amon, A. (2013) 'Polo kinase Cdc5 is a central regulator of meiosis I', *Proc Natl Acad Sci U S A,* 110(35), pp. 14278-83.

Bachellier-Bassi, S., Gadal, O., Bourout, G. and Nehrbass, U. (2008) 'Cell cycle-dependent kinetochore localization of condensin complex in Saccharomyces cerevisiae', *J Struct Biol,* 162(2), pp. 248-59.

Bahler, J. (2005) 'Cell-cycle control of gene expression in budding and fission yeast', *Annu Rev Genet,* 39, pp. 69-94.

Beckouet, F., Hu, B., Roig, M. B., Sutani, T., Komata, M., Uluocak, P., Katis, V. L., Shirahige, K. and Nasmyth, K. (2010) 'An Smc3 acetylation cycle is essential for establishment of sister chromatid cohesion', *Mol Cell,* 39(5), pp. 689-99.

Benjamin, K. R., Zhang, C., Shokat, K. M. and Herskowitz, I. (2003) 'Control of landmark events in meiosis by the CDK Cdc28 and the meiosis-specific kinase Ime2', *Genes Dev,* 17(12), pp. 1524-39.

Berchowitz, L. E., Gajadhar, A. S., van Werven, F. J., De Rosa, A. A., Samoylova, M. L., Brar, G. A., Xu, Y., Xiao, C., Futcher, B., Weissman, J. S., White, F. M. and Amon, A. (2013) 'A developmentally regulated translational control pathway establishes the meiotic chromosome segregation pattern', *Genes Dev,* 27(19), pp. 2147-63.

Bhalla, N., Biggins, S. and Murray, A. W. (2002) 'Mutation of YCS4, a budding yeast condensin subunit, affects mitotic and nonmitotic chromosome behavior', *Mol Biol Cell,* 13(2), pp. 632-45.

Bloom, M. S., Koshland, D. and Guacci, V. (2018) 'Cohesin Function in Cohesion, Condensation, and DNA Repair Is Regulated by Wpl1p via a Common Mechanism in Saccharomyces cerevisiae', *Genetics,* 208(1), pp. 111-124.

Blyth, J., Makrantoni, V., Barton, R. E., Spanos, C., Rappsilber, J. and Marston, A. L. (2018) 'Genes Important for Schizosaccharomyces pombe Meiosis Identified Through a Functional Genomics Screen', *Genetics,* 208(2), pp. 589-603.

Bolanos-Villegas, P., Yang, X., Wang, H. J., Juan, C. T., Chuang, M. H., Makaroff, C. A. and Jauh, G. Y. (2013) 'Arabidopsis CHROMOSOME TRANSMISSION FIDELITY 7 (AtCTF7/ECO1) is required for DNA repair, mitosis and meiosis', *Plant J,* 75(6), pp. 927-40.

Borges, V., Lehane, C., Lopez-Serra, L., Flynn, H., Skehel, M., Rolef Ben-Shahar, T. and Uhlmann, F. (2010) 'Hos1 deacetylates Smc3 to close the cohesin acetylation cycle', *Mol Cell,* 39(5), pp. 677-88.

Brands, A. and Skibbens, R. V. (2005) 'Ctf7p/Eco1p exhibits acetyltransferase activity--but does it matter?', *Curr Biol: Vol. 2*. England, pp. R50-1.

Brar, G. A., Hochwagen, A., Ee, L. S. and Amon, A. (2009) 'The multiple roles of cohesin in meiotic chromosome morphogenesis and pairing', *Mol Biol Cell,* 20(3), pp. 1030-47.

Brar, G. A., Kiburz, B. M., Zhang, Y., Kim, J. E., White, F. and Amon, A. (2006) 'Rec8 phosphorylation and recombination promote the step-wise loss of cohesins in meiosis', *Nature,* 441(7092), pp. 532-6.

Brieno-Enriquez, M. A., Moak, S. L., Toledo, M., Filter, J. J., Gray, S., Barbero, J. L., Cohen, P. E. and Holloway, J. K. (2016) 'Cohesin Removal along the Chromosome Arms during the First Meiotic Division Depends on a NEK1-PP1gamma-WAPL Axis in the Mouse', *Cell Rep,* 17(4), pp. 977-986.

Brito, I. L., Yu, H. G. and Amon, A. (2010) 'Condensins promote coorientation of sister chromatids during meiosis I in budding yeast', *Genetics,* 185(1), pp. 55-64.

Buheitel, J. and Stemmann, O. (2013) 'Prophase pathway-dependent removal of cohesin from human chromosomes requires opening of the Smc3-Scc1 gate', *Embo j,* 32(5), pp. 666-76.

Buonomo, S. B., Clyne, R. K., Fuchs, J., Loidl, J., Uhlmann, F. and Nasmyth, K. (2000) 'Disjunction of homologous chromosomes in meiosis I depends on proteolytic cleavage of the meiotic cohesin Rec8 by separin', *Cell,* 103(3), pp. 387-98.

Buonomo, S. B., Rabitsch, K. P., Fuchs, J., Gruber, S., Sullivan, M., Uhlmann, F., Petronczki, M., Toth, A. and Nasmyth, K. (2003) 'Division of the nucleolus and its release of CDC14 during anaphase of meiosis I depends on separase, SPO12, and SLK19', *Dev Cell,* 4(5), pp. 727-39.

Bylund, G. O. and Burgers, P. M. (2005) 'Replication protein A-directed unloading of PCNA by the Ctf18 cohesion establishment complex', *Mol Cell Biol,* 25(13), pp. 5445-55.

Carlile, T. M. and Amon, A. (2008) 'Meiosis I is established through division-specific translational control of a cyclin', *Cell,* 133(2), pp. 280-91.

Challa, K., Fajish, V. G., Shinohara, M., Klein, F., Gasser, S. M. and Shinohara, A. (2019) 'Meiosis-specific prophase-like pathway controls cleavage-independent release of cohesin by Wapl phosphorylation', *PLoS Genet,* 15(1), pp. e1007851.

Challa, K., Lee, M. S., Shinohara, M., Kim, K. P. and Shinohara, A. (2016) 'Rad61/Wpl1 (Wapl), a cohesin regulator, controls chromosome compaction during meiosis', *Nucleic Acids Res,* 44(7), pp. 3190-203.

Chan, K. L., Gligoris, T., Upcher, W., Kato, Y., Shirahige, K., Nasmyth, K. and Beckouet, F. (2013) 'Pds5 promotes and protects cohesin acetylation', *Proc Natl Acad Sci U S A,* 110(32), pp. 13020-5.

Chan, K. L., Roig, M. B., Hu, B., Beckouet, F., Metson, J. and Nasmyth, K. (2012) 'Cohesin's DNA exit gate is distinct from its entrance gate and is regulated by acetylation', *Cell,* 150(5), pp. 961-74.

Cheeseman, I. M., Anderson, S., Jwa, M., Green, E. M., Kang, J., Yates, J. R., 3rd, Chan, C. S., Drubin, D. G. and Barnes, G. (2002) 'Phospho-regulation of kinetochore-microtubule attachments by the Aurora kinase Ipl1p', *Cell,* 111(2), pp. 163-72.

Chiang, T., Duncan, F. E., Schindler, K., Schultz, R. M. and Lampson, M. A. (2010) 'Evidence that weakened centromere cohesion is a leading cause of age-related aneuploidy in oocytes', *Curr Biol,* 20(17), pp. 1522-8.

Chunduri, N. K. and Storchova, Z. (2019) 'The diverse consequences of aneuploidy', *Nat Cell Biol,* 21(1), pp. 54-62.

Ciosk, R., Shirayama, M., Shevchenko, A., Tanaka, T., Toth, A. and Nasmyth, K. (2000) 'Cohesin's binding to chromosomes depends on a separate complex consisting of Scc2 and Scc4 proteins', *Mol Cell,* 5(2), pp. 243-54.

Ciosk, R., Zachariae, W., Michaelis, C., Shevchenko, A., Mann, M. and Nasmyth, K. (1998) 'An ESP1/PDS1 complex regulates loss of sister chromatid cohesion at the metaphase to anaphase transition in yeast', *Cell,* 93(6), pp. 1067-76.

Clarke, A. S., Tang, T. T., Ooi, D. L. and Orr-Weaver, T. L. (2005) 'POLO kinase regulates the Drosophila centromere cohesion protein MEI-S332', *Dev Cell,* 8(1), pp. 53-64.

Clift, Bizzari, F. and Marston, A. L. (2009) 'Shugoshin prevents cohesin cleavage by PP2A(Cdc55)-dependent inhibition of separase', *Genes Dev,* 23(6), pp. 766-80.

Cohen-Fix, O., Peters, J. M., Kirschner, M. W. and Koshland, D. (1996) 'Anaphase initiation in Saccharomyces cerevisiae is controlled by the APC-dependent degradation of the anaphase inhibitor Pds1p', *Genes Dev,* 10(24), pp. 3081-93.

Cooper, K. F., Mallory, M. J., Egeland, D. B., Jarnik, M. and Strich, R. (2000) 'Ama1p is a meiosis-specific regulator of the anaphase promoting complex/cyclosome in yeast', *Proc Natl Acad Sci U S A,* 97(26), pp. 14548-53.

Corbett, K. D., Yip, C. K., Ee, L. S., Walz, T., Amon, A. and Harrison, S. C. (2010) 'The monopolin complex crosslinks kinetochore components to regulate chromosome-microtubule attachments', *Cell,* 142(4), pp. 556-67.

Crawley, O., Barroso, C., Testori, S., Ferrandiz, N., Silva, N., Castellano-Pozo, M., Jaso-Tamame, A. L. and Martinez-Perez, E. (2016) 'Cohesin-interacting protein WAPL-1 regulates meiotic chromosome structure and cohesion by antagonizing specific cohesin complexes', *Elife,* 5, pp. e10851.

Cuylen, S. and Haering, C. H. (2011) 'Deciphering condensin action during chromosome segregation', *Trends Cell Biol,* 21(9), pp. 552-9.

D'Ambrosio, C., Schmidt, C. K., Katou, Y., Kelly, G., Itoh, T., Shirahige, K. and Uhlmann, F. (2008) 'Identification of cis-acting sites for condensin loading onto budding yeast chromosomes', *Genes Dev,* 22(16), pp. 2215-27.

Davidson, I. F., Goetz, D., Zaczek, M. P., Molodtsov, M. I., Huis In 't Veld, P. J., Weissmann, F., Litos, G., Cisneros, D. A., Ocampo-Hafalla, M., Ladurner, R., Uhlmann, F., Vaziri, A. and Peters, J. M. (2016) 'Rapid movement and transcriptional re-localization of human cohesin on DNA', *Embo j,* 35(24), pp. 2671-2685.

De, K., Sterle, L., Krueger, L., Yang, X. and Makaroff, C. A. (2014) 'Arabidopsis thaliana WAPL is essential for the prophase removal of cohesin during meiosis', *PLoS Genet,* 10(7), pp. e1004497.

Deardorff, M. A., Bando, M., Nakato, R., Watrin, E., Itoh, T., Minamino, M., Saitoh, K., Komata, M., Katou, Y., Clark, D., Cole, K. E., De Baere, E., Decroos, C., Di Donato, N., Ernst, S., Francey, L. J., Gyftodimou, Y., Hirashima, K., Hullings, M., Ishikawa, Y., Jaulin, C., Kaur, M., Kiyono, T., Lombardi, P. M., Magnaghi-Jaulin, L., Mortier, G. R., Nozaki, N., Petersen, M. B., Seimiya, H., Siu, V. M., Suzuki, Y., Takagaki, K., Wilde, J. J., Willems, P. J., Prigent, C., Gillessen-Kaesbach, G., Christianson, D. W., Kaiser, F. J., Jackson, L. G., Hirota, T., Krantz, I. D. and Shirahige, K. (2012) 'HDAC8 mutations in Cornelia de Lange syndrome affect the cohesin acetylation cycle', *Nature,* 489(7415), pp. 313-7.

Demirel, P. B., Keyes, B. E., Chaterjee, M., Remington, C. E. and Burke, D. J. (2012) 'A redundant function for the N-terminal tail of Ndc80 in kinetochore-microtubule interaction in Saccharomyces cerevisiae', *Genetics,* 192(2), pp. 753-6.

Dreier, M. R., Bekier, M. E., 2nd and Taylor, W. R. (2011) 'Regulation of sororin by Cdk1-mediated phosphorylation', *J Cell Sci,* 124(Pt 17), pp. 2976-87.

Eshleman, H. D. and Morgan, D. O. (2014) 'Sgo1 recruits PP2A to chromosomes to ensure sister chromatid bi-orientation during mitosis', *J Cell Sci,* 127(22), pp. 4974-83.

Fernius, J. and Hardwick, K. G. (2007) 'Bub1 kinase targets Sgo1 to ensure efficient chromosome biorientation in budding yeast mitosis', *PLoS Genet,* 3(11), pp. e213.

Fox, C., Zou, J., Rappsilber, J. and Marston, A. L. (2017) 'Cdc14 phosphatase directs centrosome re-duplication at the meiosis I to meiosis II transition in budding yeast', *Wellcome Open Res,* 2, pp. 2.

Freeman, L., Aragon-Alcaide, L. and Strunnikov, A. (2000) 'The condensin complex governs chromosome condensation and mitotic transmission of rDNA', *J Cell Biol,* 149(4), pp. 811-24.

Fu, G., Hua, S., Ward, T., Ding, X., Yang, Y., Guo, Z. and Yao, X. (2007) 'D-box is required for the degradation of human Shugoshin and chromosome alignment', *Biochem Biophys Res Commun,* 357(3), pp. 672-8.

Fukuda, T. and Hoog, C. (2010) 'The Mouse Cohesin-Associated Protein PDS5B Is Expressed in Testicular Cells and Is Associated with the Meiotic Chromosome Axes', *Genes (Basel),* 1(3), pp. 484-94.

Gandhi, R., Gillespie, P. J. and Hirano, T. (2006) 'Human Wapl is a cohesin-binding protein that promotes sister-chromatid resolution in mitotic prophase', *Curr Biol,* 16(24), pp. 2406-17.

Gerlich, D., Hirota, T., Koch, B., Peters, J. M. and Ellenberg, J. (2006) 'Condensin I stabilizes chromosomes mechanically through a dynamic interaction in live cells', *Curr Biol,* 16(4), pp. 333-44.

Gligoris, T. G., Scheinost, J. C., Burmann, F., Petela, N., Chan, K. L., Uluocak, P., Beckouet, F., Gruber, S., Nasmyth, K. and Lowe, J. (2014) 'Closing the cohesin ring: structure and function of its Smc3-kleisin interface', *Science,* 346(6212), pp. 963-7.

Glotzer, M., Murray, A. W. and Kirschner, M. W. (1991) 'Cyclin is degraded by the ubiquitin pathway', *Nature,* 349(6305), pp. 132-8.

Gomez, R., Felipe-Medina, N., Ruiz-Torres, M., Berenguer, I., Viera, A., Perez, S., Barbero, J. L., Llano, E., Fukuda, T., Alsheimer, M., Pendas, A. M., Losada, A. and Suja, J. A. (2016) 'Sororin loads to the synaptonemal complex central region independently of meiotic cohesin complexes', *EMBO Rep,* 17(5), pp. 695-707.

Gruber, S., Arumugam, P., Katou, Y., Kuglitsch, D., Helmhart, W., Shirahige, K. and Nasmyth, K. (2006) 'Evidence that loading of cohesin onto chromosomes involves opening of its SMC hinge', *Cell,* 127(3), pp. 523-37.

Gruber, S., Haering, C. H. and Nasmyth, K. (2003) 'Chromosomal cohesin forms a ring', *Cell,* 112(6), pp. 765-77.

Guacci, V. and Koshland, D. (2012) 'Cohesin-independent segregation of sister chromatids in budding yeast', *Mol Biol Cell,* 23(4), pp. 729-39.

Guacci, V., Koshland, D. and Strunnikov, A. (1997) 'A direct link between sister chromatid cohesion and chromosome condensation revealed through the analysis of MCD1 in S. cerevisiae', *Cell,* 91(1), pp. 47-57.

Guacci, V., Stricklin, J., Bloom, M. S., Guo, X., Bhatter, M. and Koshland, D. (2015) 'A novel mechanism for the establishment of sister chromatid cohesion by the ECO1 acetyltransferase', *Mol Biol Cell,* 26(1), pp. 117-33.

Haarhuis, J. H., Elbatsh, A. M. and Rowland, B. D. (2014) 'Cohesin and its regulation: on the logic of X-shaped chromosomes', *Dev Cell,* 31(1), pp. 7-18.

Haarhuis, J. H. I., van der Weide, R. H., Blomen, V. A., Yanez-Cuna, J. O., Amendola, M., van Ruiten, M. S., Krijger, P. H. L., Teunissen, H., Medema, R. H., van Steensel, B., Brummelkamp, T. R., de Wit, E. and Rowland, B. D. (2017) 'The Cohesin Release Factor WAPL Restricts Chromatin Loop Extension', *Cell,* 169(4), pp. 693-707.e14.

Haering, C. H., Farcas, A. M., Arumugam, P., Metson, J. and Nasmyth, K. (2008) 'The cohesin ring concatenates sister DNA molecules', *Nature,* 454(7202), pp. 297-301.

Haering, C. H., Lowe, J., Hochwagen, A. and Nasmyth, K. (2002) 'Molecular architecture of SMC proteins and the yeast cohesin complex', *Mol Cell,* 9(4), pp. 773-88.

Hara, K., Zheng, G., Qu, Q., Liu, H., Ouyang, Z., Chen, Z., Tomchick, D. R. and Yu, H. (2014) 'Structure of cohesin subcomplex pinpoints direct shugoshin-Wapl antagonism in centromeric cohesion', *Nat Struct Mol Biol,* 21(10), pp. 864-70.

Harashima, H., Dissmeyer, N. and Schnittger, A. (2013) 'Cell cycle control across the eukaryotic kingdom', *Trends Cell Biol,* 23(7), pp. 345-56.

Hartman, T., Stead, K., Koshland, D. and Guacci, V. (2000) 'Pds5p is an essential chromosomal protein required for both sister chromatid cohesion and condensation in Saccharomyces cerevisiae', *J Cell Biol,* 151(3), pp. 613-26.

Haruki, H., Nishikawa, J. and Laemmli, U. K. (2008) 'The anchor-away technique: rapid, conditional establishment of yeast mutant phenotypes', *Mol Cell,* 31(6), pp. 925-32.

Hasle, H., Clemmensen, I. H. and Mikkelsen, M. (2000) 'Risks of leukaemia and solid tumours in individuals with Down's syndrome', *Lancet,* 355(9199), pp. 165-9.

Hassold, T. and Hunt, P. (2001) 'To err (meiotically) is human: the genesis of human aneuploidy', *Nat Rev Genet,* 2(4), pp. 280-91.

Hauf, S., Roitinger, E., Koch, B., Dittrich, C. M., Mechtler, K. and Peters, J. M. (2005) 'Dissociation of cohesin from chromosome arms and loss of arm cohesion during early mitosis depends on phosphorylation of SA2', *PLoS Biol,* 3(3), pp. e69.

Hauf, S., Waizenegger, I. C. and Peters, J. M. (2001) 'Cohesin cleavage by separase required for anaphase and cytokinesis in human cells', *Science,* 293(5533), pp. 1320-3.

Heidinger-Pauli, J. M., Unal, E., Guacci, V. and Koshland, D. (2008) 'The kleisin subunit of cohesin dictates damage-induced cohesion', *Mol Cell,* 31(1), pp. 47-56.

Heidinger-Pauli, J. M., Unal, E. and Koshland, D. (2009) 'Distinct targets of the Eco1 acetyltransferase modulate cohesion in S phase and in response to DNA damage', *Mol Cell,* 34(3), pp. 311-21.

Hernandez, M. R., Davis, M. B., Jiang, J., Brouhard, E. A., Severson, A. F. and Csankovszki, G. (2018) 'Condensin I protects meiotic cohesin from WAPL-1 mediated removal', *PLoS Genet,* 14(5), pp. e1007382.

Hinshaw, S. M., Makrantoni, V., Harrison, S. C. and Marston, A. L. (2017) 'The Kinetochore Receptor for the Cohesin Loading Complex', *Cell,* 171(1), pp. 72-84.e13.

Hinshaw, S. M., Makrantoni, V., Kerr, A., Marston, A. L. and Harrison, S. C. (2015) 'Structural evidence for Scc4-dependent localization of cohesin loading', *Elife,* 4, pp. e06057.

Hirano, T. (2005) 'Condensins: organizing and segregating the genome', *Curr Biol,* 15(7), pp. R265-75.

Hirano, T., Mitchison, T. J. and Swedlow, J. R. (1995) 'The SMC family: from chromosome condensation to dosage compensation', *Curr Opin Cell Biol,* 7(3), pp. 329-36.

Hnisz, D., Day, D. S. and Young, R. A. (2016) 'Insulated Neighborhoods: Structural and Functional Units of Mammalian Gene Control', *Cell,* 167(5), pp. 1188-1200.

Hong, S., Choi, E. H. and Kim, K. P. (2015) 'Ycs4 is required for efficient double-strand break formation and homologous recombination during meiosis', *J Microbiol Biotechnol*.

Hou, F. and Zou, H. (2005) 'Two human orthologues of Eco1/Ctf7 acetyltransferases are both required for proper sister-chromatid cohesion', *Mol Biol Cell,* 16(8), pp. 3908-18.

Houlard, M., Godwin, J., Metson, J., Lee, J., Hirano, T. and Nasmyth, K. (2015) 'Condensin confers the longitudinal rigidity of chromosomes', *Nat Cell Biol,* 17(6), pp. 771-81.

Hu, B., Itoh, T., Mishra, A., Katoh, Y., Chan, K. L., Upcher, W., Godlee, C., Roig, M. B., Shirahige, K. and Nasmyth, K. (2011) 'ATP hydrolysis is required for relocating cohesin from sites occupied by its Scc2/4 loading complex', *Curr Biol,* 21(1), pp. 12-24.

Huang, C. J., Yuan, Y. F., Wu, D., Khan, F. A., Jiao, X. F. and Huo, L. J. (2017) 'The cohesion stabilizer sororin favors DNA repair and chromosome segregation during mouse oocyte meiosis', *In Vitro Cell Dev Biol Anim,* 53(3), pp. 258-264.

Huang, H., Feng, J., Famulski, J., Rattner, J. B., Liu, S. T., Kao, G. D., Muschel, R., Chan, G. K. and Yen, T. J. (2007) 'Tripin/hSgo2 recruits MCAK to the inner centromere to correct defective kinetochore attachments', *J Cell Biol,* 177(3), pp. 413-24.

Huffaker, T. C., Thomas, J. H. and Botstein, D. (1988) 'Diverse effects of beta-tubulin mutations on microtubule formation and function', *J Cell Biol,* 106(6), pp. 1997-2010.

Hugerat, Y. and Simchen, G. (1993) 'Mixed segregation and recombination of chromosomes and YACs during single-division meiosis in spo13 strains of Saccharomyces cerevisiae', *Genetics,* 135(2), pp. 297-308.

Huis in 't Veld, P. J., Herzog, F., Ladurner, R., Davidson, I. F., Piric, S., Kreidl, E., Bhaskara, V., Aebersold, R. and Peters, J. M. (2014) 'Characterization of a DNA exit gate in the human cohesin ring', *Science,* 346(6212), pp. 968-72.

Indjeian, V. B. and Murray, A. W. (2007) 'Budding yeast mitotic chromosomes have an intrinsic bias to biorient on the spindle', *Curr Biol,* 17(21), pp. 1837-46.

Indjeian, V. B., Stern, B. M. and Murray, A. W. (2005) 'The centromeric protein Sgo1 is required to sense lack of tension on mitotic chromosomes', *Science,* 307(5706), pp. 130-3.

Ishiguro, T., Tanaka, K., Sakuno, T. and Watanabe, Y. (2010) 'Shugoshin-PP2A counteracts casein-kinase-1-dependent cleavage of Rec8 by separase', *Nat Cell Biol,* 12(5), pp. 500-6.

Ivanov, D. and Nasmyth, K. (2005) 'A topological interaction between cohesin rings and a circular minichromosome', *Cell,* 122(6), pp. 849-60.

Ivanov, D., Schleiffer, A., Eisenhaber, F., Mechtler, K., Haering, C. H. and Nasmyth, K. (2002) 'Eco1 is a novel acetyltransferase that can acetylate proteins involved in cohesion', *Curr Biol,* 12(4), pp. 323-8.

Ivanov, M. P., Ladurner, R., Poser, I., Beveridge, R., Rampler, E., Hudecz, O., Novatchkova, M., Heriche, J. K., Wutz, G., van der Lelij, P., Kreidl, E., Hutchins, J. R., Axelsson-Ekker, H., Ellenberg, J., Hyman, A. A., Mechtler, K. and Peters, J. M. (2018) 'The replicative helicase MCM recruits cohesin acetyltransferase ESCO2 to mediate centromeric sister chromatid cohesion', *Embo j,* 37(15).

James, P., Halladay, J. and Craig, E. A. (1996) 'Genomic libraries and a host strain designed for highly efficient two-hybrid selection in yeast', *Genetics,* 144(4), pp. 1425-36.

Johzuka, K. and Horiuchi, T. (2009) 'The cis element and factors required for condensin recruitment to chromosomes', *Mol Cell,* 34(1), pp. 26-35.

Jonak, K., Zagoriy, I., Oz, T., Graf, P., Rojas, J., Mengoli, V. and Zachariae, W. (2017) 'APC/C-Cdc20 mediates deprotection of centromeric cohesin at meiosis II in yeast', *Cell Cycle,* 16(12), pp. 1145-1152.

Jordan, P. W., Eyster, C., Chen, J., Pezza, R. J. and Rankin, S. (2017) 'Sororin is enriched at the central region of synapsed meiotic chromosomes', *Chromosome Res,* 25(2), pp. 115-128.

Kagami, A., Sakuno, T., Yamagishi, Y., Ishiguro, T., Tsukahara, T., Shirahige, K., Tanaka, K. and Watanabe, Y. (2011) 'Acetylation regulates monopolar attachment at multiple levels during meiosis I in fission yeast', *EMBO Rep,* 12(11), pp. 1189-95.

Karamysheva, Z., Diaz-Martinez, L. A., Crow, S. E., Li, B. and Yu, H. (2009) 'Multiple anaphase-promoting complex/cyclosome degrons mediate the degradation of human Sgo1', *J Biol Chem,* 284(3), pp. 1772-80.

Katis, V. L., Galova, M., Rabitsch, K. P., Gregan, J. and Nasmyth, K. (2004a) 'Maintenance of cohesin at centromeres after meiosis I in budding yeast requires a kinetochore-associated protein related to MEI-S332', *Curr Biol,* 14(7), pp. 560-72.

Katis, V. L., Lipp, J. J., Imre, R., Bogdanova, A., Okaz, E., Habermann, B., Mechtler, K., Nasmyth, K. and Zachariae, W. (2010) 'Rec8 phosphorylation by casein kinase 1 and Cdc7-Dbf4 kinase regulates cohesin cleavage by separase during meiosis', *Dev Cell,* 18(3), pp. 397-409.

Katis, V. L., Matos, J., Mori, S., Shirahige, K., Zachariae, W. and Nasmyth, K. (2004b) 'Spo13 facilitates monopolin recruitment to kinetochores and regulates maintenance of centromeric cohesion during yeast meiosis', *Curr Biol,* 14(24), pp. 2183-96.

Kawashima, S. A., Tsukahara, T., Langegger, M., Hauf, S., Kitajima, T. S. and Watanabe, Y. (2007) 'Shugoshin enables tension-generating attachment of kinetochores by loading Aurora to centromeres', *Genes Dev,* 21(4), pp. 420-35.

Kawashima, S. A., Yamagishi, Y., Honda, T., Ishiguro, K. and Watanabe, Y. (2010) 'Phosphorylation of H2A by Bub1 prevents chromosomal instability through localizing shugoshin', *Science,* 327(5962), pp. 172-7.

Kawasumi, R., Abe, T., Arakawa, H., Garre, M., Hirota, K. and Branzei, D. (2017) 'ESCO1/2's roles in chromosome structure and interphase chromatin organization', *Genes Dev,* 31(21), pp. 2136-2150.

Keeney, S., Giroux, C. N. and Kleckner, N. (1997) 'Meiosis-specific DNA double-strand breaks are catalyzed by Spo11, a member of a widely conserved protein family', *Cell,* 88(3), pp. 375-84.

Kerrebrock, A. W., Moore, D. P., Wu, J. S. and Orr-Weaver, T. L. (1995) 'Mei-S332, a Drosophila protein required for sister-chromatid cohesion, can localize to meiotic centromere regions', *Cell,* 83(2), pp. 247-56.

Kiburz, B. M., Amon, A. and Marston, A. L. (2008) 'Shugoshin promotes sister kinetochore biorientation in Saccharomyces cerevisiae', *Mol Biol Cell,* 19(3), pp. 1199-209.

Kiburz, B. M., Reynolds, D. B., Megee, P. C., Marston, A. L., Lee, B. H., Lee, T. I., Levine, S. S., Young, R. A. and Amon, A. (2005) 'The core centromere and Sgo1 establish a 50-kb cohesin-protected domain around centromeres during meiosis I', *Genes Dev,* 19(24), pp. 3017-30.

Kim, J., Ishiguro, K., Nambu, A., Akiyoshi, B., Yokobayashi, S., Kagami, A., Ishiguro, T., Pendas, A. M., Takeda, N., Sakakibara, Y., Kitajima, T. S., Tanno, Y., Sakuno, T. and Watanabe, Y. (2015) 'Meikin is a conserved regulator of meiosis-I-specific kinetochore function', *Nature,* 517(7535), pp. 466-71.

Kitajima, T. S., Hauf, S., Ohsugi, M., Yamamoto, T. and Watanabe, Y. (2005) 'Human Bub1 defines the persistent cohesion site along the mitotic chromosome by affecting Shugoshin localization', *Curr Biol,* 15(4), pp. 353-9.

Kitajima, T. S., Kawashima, S. A. and Watanabe, Y. (2004) 'The conserved kinetochore protein shugoshin protects centromeric cohesion during meiosis', *Nature,* 427(6974), pp. 510-7.

Kitajima, T. S., Sakuno, T., Ishiguro, K., Iemura, S., Natsume, T., Kawashima, S. A. and Watanabe, Y. (2006) 'Shugoshin collaborates with protein phosphatase 2A to protect cohesin', *Nature,* 441(7089), pp. 46-52.

Klapholz, S. and Esposito, R. E. (1980) 'Recombination and chromosome segregation during the single division meiosis in SPO12-1 and SPO13-1 diploids', *Genetics,* 96(3), pp. 589-611.

Klein, F., Mahr, P., Galova, M., Buonomo, S. B., Michaelis, C., Nairz, K. and Nasmyth, K. (1999) 'A central role for cohesins in sister chromatid cohesion, formation of axial elements, and recombination during yeast meiosis', *Cell,* 98(1), pp. 91-103.

Knop, M., Siegers, K., Pereira, G., Zachariae, W., Winsor, B., Nasmyth, K. and Schiebel, E. (1999) 'Epitope tagging of yeast genes using a PCR-based strategy: more tags and improved practical routines', *Yeast,* 15(10b), pp. 963-72.

Krenn, V. and Musacchio, A. (2015) 'The Aurora B Kinase in Chromosome Bi-Orientation and Spindle Checkpoint Signaling', *Front Oncol,* 5, pp. 225.

Kueng, S., Hegemann, B., Peters, B. H., Lipp, J. J., Schleiffer, A., Mechtler, K. and Peters, J. M. (2006) 'Wapl controls the dynamic association of cohesin with chromatin', *Cell,* 127(5), pp. 955-67.

Kuroda, M., Oikawa, K., Ohbayashi, T., Yoshida, K., Yamada, K., Mimura, J., Matsuda, Y., Fujii-Kuriyama, Y. and Mukai, K. (2005) 'A dioxin sensitive gene, mammalian WAPL, is implicated in spermatogenesis', *FEBS Lett,* 579(1), pp. 167-72.

Kuznetsova, A. Y., Seget, K., Moeller, G. K., de Pagter, M. S., de Roos, J. A., Durrbaum, M., Kuffer, C., Muller, S., Zaman, G. J., Kloosterman, W. P. and Storchova, Z. (2015) 'Chromosomal instability, tolerance of mitotic errors and multidrug resistance are promoted by tetraploidization in human cells', *Cell Cycle,* 14(17), pp. 2810-20.

Ladurner, R., Kreidl, E., Ivanov, M. P., Ekker, H., Idarraga-Amado, M. H., Busslinger, G. A., Wutz, G., Cisneros, D. A. and Peters, J. M. (2016) 'Sororin actively maintains sister chromatid cohesion', *Embo j,* 35(6), pp. 635-53.

Lafont, A. L., Song, J. and Rankin, S. (2010) 'Sororin cooperates with the acetyltransferase Eco2 to ensure DNA replication-dependent sister chromatid cohesion', *Proc Natl Acad Sci U S A,* 107(47), pp. 20364-9.

Lavoie, B. D., Hogan, E. and Koshland, D. (2002) 'In vivo dissection of the chromosome condensation machinery: reversibility of condensation distinguishes contributions of condensin and cohesin', *J Cell Biol,* 156(5), pp. 805-15.

Lavoie, B. D., Tuffo, K. M., Oh, S., Koshland, D. and Holm, C. (2000) 'Mitotic chromosome condensation requires Brn1p, the yeast homologue of Barren', *Mol Biol Cell,* 11(4), pp. 1293-304.

Lee, A. J., Endesfelder, D., Rowan, A. J., Walther, A., Birkbak, N. J., Futreal, P. A., Downward, J., Szallasi, Z., Tomlinson, I. P., Howell, M., Kschischo, M. and Swanton, C. (2011) 'Chromosomal instability confers intrinsic multidrug resistance', *Cancer Res,* 71(5), pp. 1858-70.

Lee, B. G., Roig, M. B., Jansma, M., Petela, N., Metson, J., Nasmyth, K. and Lowe, J. (2016) 'Crystal Structure of the Cohesin Gatekeeper Pds5 and in Complex with Kleisin Scc1', *Cell Rep,* 14(9), pp. 2108-2115.

Lee, B. H. and Amon, A. (2003) 'Role of Polo-like kinase CDC5 in programming meiosis I chromosome segregation', *Science,* 300(5618), pp. 482-6.

Lee, B. H., Amon, A. and Prinz, S. (2002) 'Spo13 regulates cohesin cleavage', *Genes Dev,* 16(13), pp. 1672-81.

Lee, B. H., Kiburz, B. M. and Amon, A. (2004) 'Spo13 maintains centromeric cohesion and kinetochore coorientation during meiosis I', *Curr Biol,* 14(24), pp. 2168-82.

Lee, J., Kitajima, T. S., Tanno, Y., Yoshida, K., Morita, T., Miyano, T., Miyake, M. and Watanabe, Y. (2008) 'Unified mode of centromeric protection by shugoshin in mammalian oocytes and somatic cells', *Nat Cell Biol,* 10(1), pp. 42-52.

Lee, N. R., Kim, H. S., Kim, Y. S., Kwon, M. H., Choi, K. S. and Lee, C. W. (2014) 'Regulation of the subcellular shuttling of Sgo1 between centromeres and chromosome arms by Aurora B-mediated phosphorylation', *Biochem Biophys Res Commun,* 454(3), pp. 429-35.

Lehmann, A. R. (2005) 'The role of SMC proteins in the responses to DNA damage', *DNA Repair (Amst),* 4(3), pp. 309-14.

Lengronne, A., Katou, Y., Mori, S., Yokobayashi, S., Kelly, G. P., Itoh, T., Watanabe, Y., Shirahige, K. and Uhlmann, F. (2004) 'Cohesin relocation from sites of chromosomal loading to places of convergent transcription', *Nature,* 430(6999), pp. 573-8.

Lengronne, A., McIntyre, J., Katou, Y., Kanoh, Y., Hopfner, K. P., Shirahige, K. and Uhlmann, F. (2006) 'Establishment of sister chromatid cohesion at the S. cerevisiae replication fork', *Mol Cell,* 23(6), pp. 787-99.

Leonard, J., Sen, N., Torres, R., Sutani, T., Jarmuz, A., Shirahige, K. and Aragon, L. (2015) 'Condensin Relocalization from Centromeres to Chromosome Arms Promotes Top2 Recruitment during Anaphase', *Cell Rep,* 13(11), pp. 2336-2344.

Li, P., Jin, H. and Yu, H. G. (2014) 'Condensin suppresses recombination and regulates double-strand break processing at the repetitive ribosomal DNA array to ensure proper chromosome segregation during meiosis in budding yeast', *Mol Biol Cell,* 25(19), pp. 2934-47.

Li, S., Yue, Z. and Tanaka, T. U. (2017) 'Smc3 Deacetylation by Hos1 Facilitates Efficient Dissolution of Sister Chromatid Cohesion during Early Anaphase', *Mol Cell,* 68(3), pp. 605-614.e4.

Lister, L. M., Kouznetsova, A., Hyslop, L. A., Kalleas, D., Pace, S. L., Barel, J. C., Nathan, A., Floros, V., Adelfalk, C., Watanabe, Y., Jessberger, R., Kirkwood, T. B., Hoog, C. and Herbert, M. (2010) 'Age-related meiotic segregation errors in mammalian oocytes are preceded by depletion of cohesin and Sgo2', *Curr Biol,* 20(17), pp. 1511-21.

Liu, Jia and Yu (2013) 'Phospho-H2A and cohesin specify distinct tension-regulated Sgo1 pools at kinetochores and inner centromeres', *Curr Biol,* 23(19), pp. 1927-33.

Liu, H., Qu, Q., Warrington, R., Rice, A., Cheng, N. and Yu, H. (2015) 'Mitotic Transcription Installs Sgo1 at Centromeres to Coordinate Chromosome Segregation', *Mol Cell,* 59(3), pp. 426-36.

Liu, H., Rankin, S. and Yu, H. (2013) 'Phosphorylation-enabled binding of SGO1-PP2A to cohesin protects sororin and centromeric cohesion during mitosis', *Nat Cell Biol,* 15(1), pp. 40-9.

Liu, J. and Krantz, I. D. (2008) 'Cohesin and human disease', *Annu Rev Genomics Hum Genet,* 9, pp. 303-20.

Llano, E., Gomez, R., Gutierrez-Caballero, C., Herran, Y., Sanchez-Martin, M., Vazquez-Quinones, L., Hernandez, T., de Alava, E., Cuadrado, A., Barbero, J. L., Suja, J. A. and Pendas, A. M. (2008) 'Shugoshin-2 is essential for the completion of meiosis but not for mitotic cell division in mice', *Genes Dev,* 22(17), pp. 2400-13.

Lobanenkov, V. V., Nicolas, R. H., Adler, V. V., Paterson, H., Klenova, E. M., Polotskaja, A. V. and Goodwin, G. H. (1990) 'A novel sequence-specific DNA binding protein which interacts with three regularly spaced direct repeats of the CCCTC-motif in the 5'-flanking sequence of the chicken c-myc gene', *Oncogene,* 5(12), pp. 1743-53.

Longtine, M. S., McKenzie, A., 3rd, Demarini, D. J., Shah, N. G., Wach, A., Brachat, A., Philippsen, P. and Pringle, J. R. (1998) 'Additional modules for versatile and economical PCR-based gene deletion and modification in Saccharomyces cerevisiae', *Yeast,* 14(10), pp. 953-61.

Lopez-Serra, L., Lengronne, A., Borges, V., Kelly, G. and Uhlmann, F. (2013) 'Budding yeast Wapl controls sister chromatid cohesion maintenance and chromosome condensation', *Curr Biol,* 23(1), pp. 64-9.

Losada, A., Hirano, M. and Hirano, T. (1998) 'Identification of Xenopus SMC protein complexes required for sister chromatid cohesion', *Genes Dev,* 12(13), pp. 1986-97.

Losada, A., Hirano, M. and Hirano, T. (2002) 'Cohesin release is required for sister chromatid resolution, but not for condensin-mediated compaction, at the onset of mitosis', *Genes Dev,* 16(23), pp. 3004-16.

Losada, A., Yokochi, T., Kobayashi, R. and Hirano, T. (2000) 'Identification and characterization of SA/Scc3p subunits in the Xenopus and human cohesin complexes', *J Cell Biol,* 150(3), pp. 405-16.

Lowe, J., Cordell, S. C. and van den Ent, F. (2001) 'Crystal structure of the SMC head domain: an ABC ATPase with 900 residues antiparallel coiled-coil inserted', *J Mol Biol,* 306(1), pp. 25-35.

Lu, Y., Dai, X., Zhang, M., Miao, Y., Zhou, C., Cui, Z. and Xiong, B. (2017) 'Cohesin acetyltransferase Esco2 regulates SAC and kinetochore functions via maintaining H4K16 acetylation during mouse oocyte meiosis', *Nucleic Acids Res,* 45(16), pp. 9388-9397.

Lu, Y., Li, S., Cui, Z., Dai, X., Zhang, M., Miao, Y., Zhou, C., Ou, X. and Xiong, B. (2018) 'The cohesion establishment factor Esco1 acetylates alpha-tubulin to ensure proper spindle assembly in oocyte meiosis', *Nucleic Acids Res,* 46(5), pp. 2335-2346.

Lyons, N. A. and Morgan, D. O. (2011) 'Cdk1-dependent destruction of Eco1 prevents cohesion establishment after S phase', *Mol Cell,* 42(3), pp. 378-89.

Markowitz, T. E., Suarez, D., Blitzblau, H. G., Patel, N. J., Markhard, A. L., MacQueen, A. J. and Hochwagen, A. (2017) 'Reduced dosage of the chromosome axis factor Red1 selectively disrupts the meiotic recombination checkpoint in Saccharomyces cerevisiae', *PLoS Genet,* 13(7), pp. e1006928.

Marston, A. L. (2014) 'Chromosome segregation in budding yeast: sister chromatid cohesion and related mechanisms', *Genetics,* 196(1), pp. 31-63.

Marston, A. L. (2015) 'Shugoshins: tension-sensitive pericentromeric adaptors safeguarding chromosome segregation', *Mol Cell Biol,* 35(4), pp. 634-48.

Marston, A. L., Lee, B. H. and Amon, A. (2003) 'The Cdc14 phosphatase and the FEAR network control meiotic spindle disassembly and chromosome segregation', *Dev Cell,* 4(5), pp. 711-26.

Marston, A. L., Tham, W. H., Shah, H. and Amon, A. (2004) 'A genome-wide screen identifies genes required for centromeric cohesion', *Science,* 303(5662), pp. 1367-70.

Matos, J., Lipp, J. J., Bogdanova, A., Guillot, S., Okaz, E., Junqueira, M., Shevchenko, A. and Zachariae, W. (2008) 'Dbf4-dependent CDC7 kinase links DNA replication to the segregation of homologous chromosomes in meiosis I', *Cell,* 135(4), pp. 662-78.

McCarroll, R. M. and Esposito, R. E. (1994) 'SPO13 negatively regulates the progression of mitotic and meiotic nuclear division in Saccharomyces cerevisiae', *Genetics,* 138(1), pp. 47-60.

McGuinness, B. E., Hirota, T., Kudo, N. R., Peters, J. M. and Nasmyth, K. (2005) 'Shugoshin prevents dissociation of cohesin from centromeres during mitosis in vertebrate cells', *PLoS Biol,* 3(3), pp. e86.

Megee, P. C., Mistrot, C., Guacci, V. and Koshland, D. (1999) 'The centromeric sister chromatid cohesion site directs Mcd1p binding to adjacent sequences', *Mol Cell,* 4(3), pp. 445-50.

Mehta, G., Anbalagan, G. K., Bharati, A. P., Gadre, P. and Ghosh, S. K. (2018) 'An interplay between Shugoshin and Spo13 for centromeric cohesin protection and sister kinetochore mono-orientation during meiosis I in Saccharomyces cerevisiae', *Curr Genet*.

Melby, T. E., Ciampaglio, C. N., Briscoe, G. and Erickson, H. P. (1998) 'The symmetrical structure of structural maintenance of chromosomes (SMC) and MukB proteins: long, antiparallel coiled coils, folded at a flexible hinge', *J Cell Biol,* 142(6), pp. 1595-604.

Meyer, R. E., Chuong, H. H., Hild, M., Hansen, C. L., Kinter, M. and Dawson, D. S. (2015) 'Ipl1/Aurora-B is necessary for kinetochore restructuring in meiosis I in Saccharomyces cerevisiae', *Mol Biol Cell*.

Michaelis, C., Ciosk, R. and Nasmyth, K. (1997) 'Cohesins: chromosomal proteins that prevent premature separation of sister chromatids', *Cell,* 91(1), pp. 35-45.

Mishra, P. K., Ciftci-Yilmaz, S., Reynolds, D., Au, W. C., Boeckmann, L., Dittman, L. E., Jowhar, Z., Pachpor, T., Yeh, E., Baker, R. E., Hoyt, M. A., D'Amours, D., Bloom, K. and Basrai, M. A. (2016) 'Polo kinase Cdc5 associates with centromeres to facilitate the removal of centromeric cohesin during mitosis', *Mol Biol Cell,* 27(14), pp. 2286-300.

Moldovan, G. L., Pfander, B. and Jentsch, S. (2006) 'PCNA controls establishment of sister chromatid cohesion during S phase', *Mol Cell,* 23(5), pp. 723-32.

Monje-Casas, F., Prabhu, V. R., Lee, B. H., Boselli, M. and Amon, A. (2007) 'Kinetochore orientation during meiosis is controlled by Aurora B and the monopolin complex', *Cell,* 128(3), pp. 477-90.

Murayama, Y. and Uhlmann, F. (2014) 'Biochemical reconstitution of topological DNA binding by the cohesin ring', *Nature,* 505(7483), pp. 367-71.

Murayama, Y. and Uhlmann, F. (2015) 'DNA Entry into and Exit out of the Cohesin Ring by an Interlocking Gate Mechanism', *Cell,* 163(7), pp. 1628-40.

Musacchio, A. (2015) 'The Molecular Biology of Spindle Assembly Checkpoint Signaling Dynamics', *Curr Biol,* 25(20), pp. R1002-18.

Nagaoka, S. I., Hassold, T. J. and Hunt, P. A. (2012) 'Human aneuploidy: mechanisms and new insights into an age-old problem', *Nat Rev Genet,* 13(7), pp. 493-504.

Nasmyth, K. (1996) 'At the heart of the budding yeast cell cycle', *Trends Genet,* 12(10), pp. 405-12.

Nerusheva, O. O., Galander, S., Fernius, J., Kelly, D. and Marston, A. L. (2014) 'Tension-dependent removal of pericentromeric shugoshin is an indicator of sister chromosome biorientation', *Genes Dev,* 28(12), pp. 1291-309.

Nishiyama, T., Ladurner, R., Schmitz, J., Kreidl, E., Schleiffer, A., Bhaskara, V., Bando, M., Shirahige, K., Hyman, A. A., Mechtler, K. and Peters, J. M. (2010) 'Sororin mediates sister chromatid cohesion by antagonizing Wapl', *Cell,* 143(5), pp. 737-49.

Nishiyama, T., Sykora, M. M., Huis in 't Veld, P. J., Mechtler, K. and Peters, J. M. (2013) 'Aurora B and Cdk1 mediate Wapl activation and release of acetylated cohesin from chromosomes by phosphorylating Sororin', *Proc Natl Acad Sci U S A,* 110(33), pp. 13404-9.

Nogueira, C., Kashevsky, H., Pinto, B., Clarke, A. and Orr-Weaver, T. L. (2014) 'Regulation of Centromere Localization of the Drosophila Shugoshin MEI-S332 and Sister-Chromatid Cohesion in Meiosis', *G3 (Bethesda)*.

O'Donnell, M., Langston, L. and Stillman, B. (2013) 'Principles and concepts of DNA replication in bacteria, archaea, and eukarya', *Cold Spring Harb Perspect Biol,* 5(7).

Okaz, E., Arguello-Miranda, O., Bogdanova, A., Vinod, P. K., Lipp, J. J., Markova, Z., Zagoriy, I., Novak, B. and Zachariae, W. (2012) 'Meiotic prophase requires proteolysis of M phase regulators mediated by the meiosis-specific APC/CAma1', *Cell,* 151(3), pp. 603-18.

Panizza, S., Tanaka, T., Hochwagen, A., Eisenhaber, F. and Nasmyth, K. (2000) 'Pds5 cooperates with cohesin in maintaining sister chromatid cohesion', *Curr Biol,* 10(24), pp. 1557-64.

Parelho, V., Hadjur, S., Spivakov, M., Leleu, M., Sauer, S., Gregson, H. C., Jarmuz, A., Canzonetta, C., Webster, Z., Nesterova, T., Cobb, B. S., Yokomori, K., Dillon, N., Aragon, L., Fisher, A. G. and Merkenschlager, M. (2008) 'Cohesins functionally associate with CTCF on mammalian chromosome arms', *Cell,* 132(3), pp. 422-33.

Peplowska, K., Wallek, A. U. and Storchova, Z. (2014) 'Sgo1 regulates both condensin and Ipl1/Aurora B to promote chromosome biorientation', *PLoS Genet,* 10(6), pp. e1004411.

Petela, N. J., Gligoris, T. G., Metson, J., Lee, B. G., Voulgaris, M., Hu, B., Kikuchi, S., Chapard, C., Chen, W., Rajendra, E., Srinivisan, M., Yu, H., Lowe, J. and Nasmyth, K. A. (2018) 'Scc2 Is a Potent Activator of Cohesin's ATPase that Promotes Loading by Binding Scc1 without Pds5', *Mol Cell,* 70(6), pp. 1134-1148.e7.

Petronczki, M., Matos, J., Mori, S., Gregan, J., Bogdanova, A., Schwickart, M., Mechtler, K., Shirahige, K., Zachariae, W. and Nasmyth, K. (2006) 'Monopolar attachment of sister kinetochores at meiosis I requires casein kinase 1', *Cell,* 126(6), pp. 1049-64.

Pfleger, C. M. and Kirschner, M. W. (2000) 'The KEN box: an APC recognition signal distinct from the D box targeted by Cdh1', *Genes Dev,* 14(6), pp. 655-65.

Pinsky, B. A., Kung, C., Shokat, K. M. and Biggins, S. (2006) 'The Ipl1-Aurora protein kinase activates the spindle checkpoint by creating unattached kinetochores', *Nat Cell Biol,* 8(1), pp. 78-83.

Pinto, B. S. and Orr-Weaver, T. L. (2017) 'Drosophila protein phosphatases 2A B' Wdb and Wrd regulate meiotic centromere localization and function of the MEI-S332 Shugoshin', *Proc Natl Acad Sci U S A,* 114(49), pp. 12988-12993.

Pombo, A. and Dillon, N. (2015) 'Three-dimensional genome architecture: players and mechanisms', *Nat Rev Mol Cell Biol,* 16(4), pp. 245-57.

Potts, P. R. (2009) 'The Yin and Yang of the MMS21-SMC5/6 SUMO ligase complex in homologous recombination', *DNA Repair (Amst),* 8(4), pp. 499-506.

Pouwels, J., Kukkonen, A. M., Lan, W., Daum, J. R., Gorbsky, G. J., Stukenberg, T. and Kallio, M. J. (2007) 'Shugoshin 1 plays a central role in kinetochore assembly and is required for kinetochore targeting of Plk1', *Cell Cycle,* 6(13), pp. 1579-85.

Rabitsch, K. P., Gregan, J., Schleiffer, A., Javerzat, J. P., Eisenhaber, F. and Nasmyth, K. (2004) 'Two fission yeast homologs of Drosophila Mei-S332 are required for chromosome segregation during meiosis I and II', *Curr Biol,* 14(4), pp. 287-301.

Rabitsch, K. P., Petronczki, M., Javerzat, J. P., Genier, S., Chwalla, B., Schleiffer, A., Tanaka, T. U. and Nasmyth, K. (2003) 'Kinetochore recruitment of two nucleolar proteins is required for homolog segregation in meiosis I', *Dev Cell,* 4(4), pp. 535-48.

Rankin, S., Ayad, N. G. and Kirschner, M. W. (2005) 'Sororin, a substrate of the anaphase-promoting complex, is required for sister chromatid cohesion in vertebrates', *Mol Cell,* 18(2), pp. 185-200.

Rao, S. S. P., Huang, S. C., Glenn St Hilaire, B., Engreitz, J. M., Perez, E. M., Kieffer-Kwon, K. R., Sanborn, A. L., Johnstone, S. E., Bascom, G. D., Bochkov, I. D., Huang, X., Shamim, M. S., Shin, J., Turner, D., Ye, Z., Omer, A. D., Robinson, J. T., Schlick, T., Bernstein, B. E., Casellas, R., Lander, E. S. and Aiden, E. L. (2017) 'Cohesin Loss Eliminates All Loop Domains', *Cell,* 171(2), pp. 305-320.e24.

Rappsilber, J. (2011) 'The beginning of a beautiful friendship: cross-linking/mass spectrometry and modelling of proteins and multi-protein complexes', *J Struct Biol,* 173(3), pp. 530-40.

Rattani, A., Ballesteros Mejia, R., Roberts, K., Roig, M. B., Godwin, J., Hopkins, M., Eguren, M., Sanchez-Pulido, L., Okaz, E., Ogushi, S., Wolna, M., Metson, J., Pendas, A. M., Malumbres, M., Novak, B., Herbert, M. and Nasmyth, K. (2017) 'APC/C(Cdh1) Enables Removal of Shugoshin-2 from the Arms of Bivalent Chromosomes by Moderating Cyclin-Dependent Kinase Activity', *Curr Biol,* 27(10), pp. 1462-1476.e5.

Reichmann, J., Dobie, K., Lister, L. M., Best, D., Crichton, J. H., MacLennan, M., Read, D., Raymond, E. S., Hung, C.-C., Boyle, S., Shirahige, K., Cooke, H. J., Bickmore, W. A., Herbert, M. and Adams, I. R. (2017) 'Tex19.1 Regulates Acetylated SMC3 Cohesin and Prevents Aneuploidy in Mouse Oocytes', *bioRxiv*, pp. 102285.

Remus, D. and Diffley, J. F. (2009) 'Eukaryotic DNA replication control: lock and load, then fire', *Curr Opin Cell Biol,* 21(6), pp. 771-7.

Resnick, T. D., Satinover, D. L., MacIsaac, F., Stukenberg, P. T., Earnshaw, W. C., Orr-Weaver, T. L. and Carmena, M. (2006) 'INCENP and Aurora B promote meiotic sister chromatid cohesion through localization of the Shugoshin MEI-S332 in Drosophila', *Dev Cell,* 11(1), pp. 57-68.

Ribeiro, S. A., Gatlin, J. C., Dong, Y., Joglekar, A., Cameron, L., Hudson, D. F., Farr, C. J., McEwen, B. F., Salmon, E. D., Earnshaw, W. C. and Vagnarelli, P. (2009) 'Condensin regulates the stiffness of vertebrate centromeres', *Mol Biol Cell,* 20(9), pp. 2371-80.

Riedel, C. G., Katis, V. L., Katou, Y., Mori, S., Itoh, T., Helmhart, W., Galova, M., Petronczki, M., Gregan, J., Cetin, B., Mudrak, I., Ogris, E., Mechtler, K., Pelletier, L., Buchholz, F., Shirahige, K. and Nasmyth, K. (2006) 'Protein phosphatase 2A protects centromeric sister chromatid cohesion during meiosis I', *Nature,* 441(7089), pp. 53-61.

Rolef Ben-Shahar, T., Heeger, S., Lehane, C., East, P., Flynn, H., Skehel, M. and Uhlmann, F. (2008) 'Eco1-dependent cohesin acetylation during establishment of sister chromatid cohesion', *Science,* 321(5888), pp. 563-6.

Rowland, B. D., Roig, M. B., Nishino, T., Kurze, A., Uluocak, P., Mishra, A., Beckouet, F., Underwood, P., Metson, J., Imre, R., Mechtler, K., Katis, V. L. and Nasmyth, K. (2009) 'Building sister chromatid cohesion: smc3 acetylation counteracts an antiestablishment activity', *Mol Cell,* 33(6), pp. 763-74.

Salah, S. M. and Nasmyth, K. (2000) 'Destruction of the securin Pds1p occurs at the onset of anaphase during both meiotic divisions in yeast', *Chromosoma,* 109(1-2), pp. 27-34.

Salic, A., Waters, J. C. and Mitchison, T. J. (2004) 'Vertebrate shugoshin links sister centromere cohesion and kinetochore microtubule stability in mitosis', *Cell,* 118(5), pp. 567-78.

Sansregret, L. and Swanton, C. (2017) 'The Role of Aneuploidy in Cancer Evolution', *Cold Spring Harb Perspect Med,* 7(1).

Sarangapani, K. K., Duro, E., Deng, Y., Alves Fde, L., Ye, Q., Opoku, K. N., Ceto, S., Rappsilber, J., Corbett, K. D., Biggins, S., Marston, A. L. and Asbury, C. L. (2014) 'Sister kinetochores are mechanically fused during meiosis I in yeast', *Science,* 346(6206), pp. 248-51.

Schmitz, J., Watrin, E., Lenart, P., Mechtler, K. and Peters, J. M. (2007) 'Sororin is required for stable binding of cohesin to chromatin and for sister chromatid cohesion in interphase', *Curr Biol,* 17(7), pp. 630-6.

Shintomi, K. and Hirano, T. (2009) 'Releasing cohesin from chromosome arms in early mitosis: opposing actions of Wapl-Pds5 and Sgo1', *Genes Dev,* 23(18), pp. 2224-36.

Shonn, M. A., McCarroll, R. and Murray, A. W. (2002) 'Spo13 protects meiotic cohesin at centromeres in meiosis I', *Genes Dev,* 16(13), pp. 1659-71.

Skibbens, R. V., Corson, L. B., Koshland, D. and Hieter, P. (1999) 'Ctf7p is essential for sister chromatid cohesion and links mitotic chromosome structure to the DNA replication machinery', *Genes Dev,* 13(3), pp. 307-19.

Solomon, D. A., Kim, T., Diaz-Martinez, L. A., Fair, J., Elkahloun, A. G., Harris, B. T., Toretsky, J. A., Rosenberg, S. A., Shukla, N., Ladanyi, M., Samuels, Y., James, C. D., Yu, H., Kim, J. S. and Waldman, T. (2011) 'Mutational inactivation of STAG2 causes aneuploidy in human cancer', *Science,* 333(6045), pp. 1039-43.

Song, J., Lafont, A., Chen, J., Wu, F. M., Shirahige, K. and Rankin, S. (2012) 'Cohesin acetylation promotes sister chromatid cohesion only in association with the replication machinery', *J Biol Chem,* 287(41), pp. 34325-36.

Stephens, A. D., Haase, J., Vicci, L., Taylor, R. M., 2nd and Bloom, K. (2011) 'Cohesin, condensin, and the intramolecular centromere loop together generate the mitotic chromatin spring', *J Cell Biol,* 193(7), pp. 1167-80.

Storchova, Z., Becker, J. S., Talarek, N., Kogelsberger, S. and Pellman, D. (2011) 'Bub1, Sgo1, and Mps1 mediate a distinct pathway for chromosome biorientation in budding yeast', *Mol Biol Cell,* 22(9), pp. 1473-85.

Strom, L., Karlsson, C., Lindroos, H. B., Wedahl, S., Katou, Y., Shirahige, K. and Sjogren, C. (2007) 'Postreplicative formation of cohesion is required for repair and induced by a single DNA break', *Science,* 317(5835), pp. 242-5.

Strom, L., Lindroos, H. B., Shirahige, K. and Sjogren, C. (2004) 'Postreplicative recruitment of cohesin to double-strand breaks is required for DNA repair', *Mol Cell,* 16(6), pp. 1003-15.

Strunnikov, A. V., Hogan, E. and Koshland, D. (1995) 'SMC2, a Saccharomyces cerevisiae gene essential for chromosome segregation and condensation, defines a subgroup within the SMC family', *Genes Dev,* 9(5), pp. 587-99.

Strunnikov, A. V., Larionov, V. L. and Koshland, D. (1993) 'SMC1: an essential yeast gene encoding a putative head-rod-tail protein is required for nuclear division and defines a new ubiquitous protein family', *J Cell Biol,* 123(6 Pt 2), pp. 1635-48.

Sullivan, M., Hornig, N. C., Porstmann, T. and Uhlmann, F. (2004) 'Studies on substrate recognition by the budding yeast separase', *J Biol Chem,* 279(2), pp. 1191-6.

Sullivan, M. and Morgan, D. O. (2007) 'A novel destruction sequence targets the meiotic regulator Spo13 for anaphase-promoting complex-dependent degradation in anaphase I', *J Biol Chem,* 282(27), pp. 19710-5.

Sumara, I., Vorlaufer, E., Gieffers, C., Peters, B. H. and Peters, J. M. (2000) 'Characterization of vertebrate cohesin complexes and their regulation in prophase', *J Cell Biol,* 151(4), pp. 749-62.

Sumara, I., Vorlaufer, E., Stukenberg, P. T., Kelm, O., Redemann, N., Nigg, E. A. and Peters, J. M. (2002) 'The dissociation of cohesin from chromosomes in prophase is regulated by Polo-like kinase', *Mol Cell,* 9(3), pp. 515-25.

Sutani, T., Kawaguchi, T., Kanno, R., Itoh, T. and Shirahige, K. (2009) 'Budding yeast Wpl1(Rad61)-Pds5 complex counteracts sister chromatid cohesion-establishing reaction', *Curr Biol,* 19(6), pp. 492-7.

Tachibana-Konwalski, K., Godwin, J., van der Weyden, L., Champion, L., Kudo, N. R., Adams, D. J. and Nasmyth, K. (2010) 'Rec8-containing cohesin maintains bivalents without turnover during the growing phase of mouse oocytes', *Genes Dev,* 24(22), pp. 2505-16.

Tada, K., Susumu, H., Sakuno, T. and Watanabe, Y. (2011) 'Condensin association with histone H2A shapes mitotic chromosomes', *Nature,* 474(7352), pp. 477-83.

Tanaka, T., Cosma, M. P., Wirth, K. and Nasmyth, K. (1999) 'Identification of cohesin association sites at centromeres and along chromosome arms', *Cell,* 98(6), pp. 847-58.

Tanaka, T., Fuchs, J., Loidl, J. and Nasmyth, K. (2000) 'Cohesin ensures bipolar attachment of microtubules to sister centromeres and resists their precocious separation', *Nat Cell Biol,* 2(8), pp. 492-9.

Tang, Z., Shu, H., Qi, W., Mahmood, N. A., Mumby, M. C. and Yu, H. (2006) 'PP2A is required for centromeric localization of Sgo1 and proper chromosome segregation', *Dev Cell,* 10(5), pp. 575-85.

Tang, Z., Sun, Y., Harley, S. E., Zou, H. and Yu, H. (2004) 'Human Bub1 protects centromeric sister-chromatid cohesion through Shugoshin during mitosis', *Proc Natl Acad Sci U S A,* 101(52), pp. 18012-7.

Tanno, Y., Kitajima, T. S., Honda, T., Ando, Y., Ishiguro, K. and Watanabe, Y. (2010) 'Phosphorylation of mammalian Sgo2 by Aurora B recruits PP2A and MCAK to centromeres', *Genes Dev,* 24(19), pp. 2169-79.

Tong, K. and Skibbens, R. V. (2014) 'Cohesin without cohesion: a novel role for Pds5 in Saccharomyces cerevisiae', *PLoS One,* 9(6), pp. e100470.

Tonkin, E. T., Wang, T. J., Lisgo, S., Bamshad, M. J. and Strachan, T. (2004) 'NIPBL, encoding a homolog of fungal Scc2-type sister chromatid cohesion proteins and fly Nipped-B, is mutated in Cornelia de Lange syndrome', *Nat Genet,* 36(6), pp. 636-41.

Toth, A., Ciosk, R., Uhlmann, F., Galova, M., Schleiffer, A. and Nasmyth, K. (1999) 'Yeast cohesin complex requires a conserved protein, Eco1p(Ctf7), to establish cohesion between sister chromatids during DNA replication', *Genes Dev,* 13(3), pp. 320-33.

Toth, A., Rabitsch, K. P., Galova, M., Schleiffer, A., Buonomo, S. B. and Nasmyth, K. (2000) 'Functional genomics identifies monopolin: a kinetochore protein required for segregation of homologs during meiosis i', *Cell,* 103(7), pp. 1155-68.

Uhlmann, F., Lottspeich, F. and Nasmyth, K. (1999) 'Sister-chromatid separation at anaphase onset is promoted by cleavage of the cohesin subunit Scc1', *Nature,* 400(6739), pp. 37-42.

Uhlmann, F., Wernic, D., Poupart, M. A., Koonin, E. V. and Nasmyth, K. (2000) 'Cleavage of cohesin by the CD clan protease separin triggers anaphase in yeast', *Cell,* 103(3), pp. 375-86.

Unal, E., Arbel-Eden, A., Sattler, U., Shroff, R., Lichten, M., Haber, J. E. and Koshland, D. (2004) 'DNA damage response pathway uses histone modification to assemble a double-strand break-specific cohesin domain', *Mol Cell,* 16(6), pp. 991-1002.

Unal, E., Heidinger-Pauli, J. M., Kim, W., Guacci, V., Onn, I., Gygi, S. P. and Koshland, D. E. (2008) 'A molecular determinant for the establishment of sister chromatid cohesion', *Science,* 321(5888), pp. 566-9.

Unal, E., Heidinger-Pauli, J. M. and Koshland, D. (2007) 'DNA double-strand breaks trigger genome-wide sister-chromatid cohesion through Eco1 (Ctf7)', *Science,* 317(5835), pp. 245-8.

van Ruiten, M. S. and Rowland, B. D. (2018) 'SMC Complexes: Universal DNA Looping Machines with Distinct Regulators', *Trends Genet,* 34(6), pp. 477-487.

Vanoosthuyse, V., Prykhozhij, S. and Hardwick, K. G. (2007) 'Shugoshin 2 regulates localization of the chromosomal passenger proteins in fission yeast mitosis', *Mol Biol Cell,* 18(5), pp. 1657-69.

Vaur, S., Cubizolles, F., Plane, G., Genier, S., Rabitsch, P. K., Gregan, J., Nasmyth, K., Vanoosthuyse, V., Hardwick, K. G. and Javerzat, J. P. (2005) 'Control of Shugoshin function during fission-yeast meiosis', *Curr Biol,* 15(24), pp. 2263-70.

Vega, H., Waisfisz, Q., Gordillo, M., Sakai, N., Yanagihara, I., Yamada, M., van Gosliga, D., Kayserili, H., Xu, C., Ozono, K., Jabs, E. W., Inui, K. and Joenje, H. (2005) 'Roberts syndrome is caused by mutations in ESCO2, a human homolog of yeast ECO1 that is essential for the establishment of sister chromatid cohesion', *Nat Genet,* 37(5), pp. 468-70.

Verzijlbergen, K. F., Nerusheva, O. O., Kelly, D., Kerr, A., Clift, D., de Lima Alves, F., Rappsilber, J. and Marston, A. L. (2014) 'Shugoshin biases chromosomes for biorientation through condensin recruitment to the pericentromere', *Elife,* 3, pp. e01374.

Vincenten, N., Kuhl, L. M., Lam, I., Oke, A., Kerr, A. R., Hochwagen, A., Fung, J., Keeney, S., Vader, G. and Marston, A. L. (2015) 'The kinetochore prevents centromere-proximal crossover recombination during meiosis', *Elife,* 4.

Waizenegger, I. C., Hauf, S., Meinke, A. and Peters, J. M. (2000) 'Two distinct pathways remove mammalian cohesin from chromosome arms in prophase and from centromeres in anaphase', *Cell,* 103(3), pp. 399-410.

Wang, B. D., Eyre, D., Basrai, M., Lichten, M. and Strunnikov, A. (2005) 'Condensin binding at distinct and specific chromosomal sites in the Saccharomyces cerevisiae genome', *Mol Cell Biol,* 25(16), pp. 7216-25.

Wang, H. T., Frackman, S., Kowalisyn, J., Esposito, R. E. and Elder, R. (1987) 'Developmental regulation of SPO13, a gene required for separation of homologous chromosomes at meiosis I', *Mol Cell Biol,* 7(4), pp. 1425-35.

Watanabe, Y. and Nurse, P. (1999) 'Cohesin Rec8 is required for reductional chromosome segregation at meiosis', *Nature,* 400(6743), pp. 461-4.

Watrin, E., Schleiffer, A., Tanaka, K., Eisenhaber, F., Nasmyth, K. and Peters, J. M. (2006) 'Human Scc4 is required for cohesin binding to chromatin, sister-chromatid cohesion, and mitotic progression', *Curr Biol,* 16(9), pp. 863-74.

Weijerman, M. E. and de Winter, J. P. (2010) 'Clinical practice. The care of children with Down syndrome', *Eur J Pediatr,* 169(12), pp. 1445-52.

Weitzer, S., Lehane, C. and Uhlmann, F. (2003) 'A model for ATP hydrolysis-dependent binding of cohesin to DNA', *Curr Biol,* 13(22), pp. 1930-40.

Wendt, K. S., Yoshida, K., Itoh, T., Bando, M., Koch, B., Schirghuber, E., Tsutsumi, S., Nagae, G., Ishihara, K., Mishiro, T., Yahata, K., Imamoto, F., Aburatani, H., Nakao, M., Imamoto, N., Maeshima, K., Shirahige, K. and Peters, J. M. (2008) 'Cohesin mediates transcriptional insulation by CCCTC-binding factor', *Nature,* 451(7180), pp. 796-801.

Wolf, P. G., Cuba Ramos, A., Kenzel, J., Neumann, B. and Stemmann, O. (2018) 'Studying meiotic cohesin in somatic cells reveals that Rec8-containing cohesin requires Stag3 to function and is regulated by Wapl and sororin', *J Cell Sci,* 131(11).

Wu, N. and Yu, H. (2012) 'The Smc complexes in DNA damage response', *Cell Biosci,* 2, pp. 5.

Wutz, G., Varnai, C., Nagasaka, K., Cisneros, D. A., Stocsits, R. R., Tang, W., Schoenfelder, S., Jessberger, G., Muhar, M., Hossain, M. J., Walther, N., Koch, B., Kueblbeck, M., Ellenberg, J., Zuber, J., Fraser, P. and Peters, J. M. (2017) 'Topologically associating domains and chromatin loops depend on cohesin and are regulated by CTCF, WAPL, and PDS5 proteins', *Embo j,* 36(24), pp. 3573-3599.

Xiong, B., Lu, S. and Gerton, J. L. (2010) 'Hos1 is a lysine deacetylase for the Smc3 subunit of cohesin', *Curr Biol,* 20(18), pp. 1660-5.

Xu, L., Ajimura, M., Padmore, R., Klein, C. and Kleckner, N. (1995) 'NDT80, a meiosis-specific gene required for exit from pachytene in Saccharomyces cerevisiae', *Mol Cell Biol,* 15(12), pp. 6572-81.

Xu, Z., Cetin, B., Anger, M., Cho, U. S., Helmhart, W., Nasmyth, K. and Xu, W. (2009) 'Structure and function of the PP2A-shugoshin interaction', *Mol Cell,* 35(4), pp. 426-41.

Yamamoto, A., Guacci, V. and Koshland, D. (1996) 'Pds1p, an inhibitor of anaphase in budding yeast, plays a critical role in the APC and checkpoint pathway(s)', *J Cell Biol,* 133(1), pp. 99-110.

Yong-Gonzalez, V., Wang, B. D., Butylin, P., Ouspenski, I. and Strunnikov, A. (2007) 'Condensin function at centromere chromatin facilitates proper kinetochore tension and ensures correct mitotic segregation of sister chromatids', *Genes Cells,* 12(9), pp. 1075-90.

Yu, H. G. and Koshland, D. (2005) 'Chromosome morphogenesis: condensin-dependent cohesin removal during meiosis', *Cell,* 123(3), pp. 397-407.

Yu, H. G. and Koshland, D. (2007) 'The Aurora kinase Ipl1 maintains the centromeric localization of PP2A to protect cohesin during meiosis', *J Cell Biol,* 176(7), pp. 911-8.

Yu, H. G. and Koshland, D. E. (2003) 'Meiotic condensin is required for proper chromosome compaction, SC assembly, and resolution of recombination-dependent chromosome linkages', *J Cell Biol,* 163(5), pp. 937-47.

Zhang, J., Hakansson, H., Kuroda, M. and Yuan, L. (2008a) 'Wapl localization on the synaptonemal complex, a meiosis-specific proteinaceous structure that binds homologous chromosomes, in the female mouse', *Reprod Domest Anim,* 43(1), pp. 124-6.

Zhang, J., Shi, X., Li, Y., Kim, B. J., Jia, J., Huang, Z., Yang, T., Fu, X., Jung, S. Y., Wang, Y., Zhang, P., Kim, S. T., Pan, X. and Qin, J. (2008b) 'Acetylation of Smc3 by Eco1 is required for S phase sister chromatid cohesion in both human and yeast', *Mol Cell,* 31(1), pp. 143-51.

Zhao, P. A., Rivera-Mulia, J. C. and Gilbert, D. M. (2017) 'Replication Domains: Genome Compartmentalization into Functional Replication Units', *Adv Exp Med Biol,* 1042, pp. 229-257.